UNIVERSITAT DE BARCELONA

Molecular retention mechanisms of the G1 cyclin/Cdk complex in budding yeast

Galal Yahya Abd El Rahim Metwally

Molecular retention mechanisms of the G1 cyclin/Cdk complex in budding yeast

Galal Yahya Abd El Rahim Metwally

PhD Thesis

University of Barcelona
2015

Molecular retention mechanisms of the G1 cyclin/Cdk complex in budding yeast

Galal Yahya Abd El Rahim Metwally

PhD Thesis

University of Barcelona
2015

PhD Thesis presented by Galal Yahya Abd El Rahim Metwally and supervised by Dr. Martí Aldea to obtain the Doctor title from the University of Barcelona

Department of Cell Biology
Molecular Biology Institute of Barcelona - CSIC

Faculty of Pharmacy
University of Barcelona

Biomedicine PhD Program
2010-2015

Acknowledgments

I am completely indebted to Professors Martí Aldea and Carme Gallego, for their continuous guidance and for many stimulating discussions. Their original insights and approach to science have contributed greatly to my scientific maturity and will continue to inspire me in the future. Besides taking care of me actually I consider them very simply like my family.

My PhD study in Aldea's lab gave me a big family of previous and current lab mates whom I consider like brothers and sisters and the words of acknowledgment fail to describe how helpful and kind they are especially , David Moreno, Raul Ortíz , Eva Parisi, Sara Gutierrez (the master of kinase assays) and Neus Pedraza (previous Postdoc of Carme).

David helped me a lot in the writing beside his help in microscopy, Raul was my honest guide in Barcelona, Sara helped me with the kinase assay, Eva helped me with experiments and Neus was our reference for western blot.

My PhD and all our work was not going to be achieved without the help of Alba Cornadó, our lab manager and research technician.

I want to thank Maya Georgieva (former Postdoc of Carme) for her discussions during the weekly meetings of the group.

I would like also to thank all the CYC group of Lleida University UDL, Professors Jordi Torres-Rosell , Eloi Garí, Neus Colomina and Paco Ferrezuelo.

I cannot forget my lab mates of UDL Marcelino Bermúdez-López, Seba Almedawar, Marta Rafel, Irene Pociño-Merino and Sonia Rius.

Marcelino Bermúdez (Previous PhD student of Jordi and currently a postdoc in Luis Aragon lab) and Seba Almedawar were more than friends in Lleida they helped me a lot with learning the techniques and the courses of the DEA. I appreciate a lot the help of Marcelino and Seba.

Another person I want to mention in my acknowledgment is Mr. Josep Rafel, the father of Marta and my landlord in Barcelona, for being so nice person and helpful.

My special appreciation to all my teachers through all stages of education in Egypt, in particular my professors and my friends of the Pharmacy degree in Zagazig University.

Finally no words can explain my gratitude towards my family in Egypt, my parents, my uncle (Dr. Kamel Metwally) , my grandparents, my wife and my lovely son Mohammed.

الْحَمْدُ لِلَّهِ الَّذِي هَدَانَا لِهَٰذَا وَمَا كُنَّا لِنَهْتَدِيَ لَوْلَا أَنْ هَدَانَا اللَّهُ

صدق الله العظيم سورة الأعراف - الآية ٤٣

اتقدم بخالص الشكر و التقدير لكل من ساعدني في استكمال هذه الرسالة العلمية و كل من ساهم في نجاحي في دراسة الدكتوراة في جامعة برشلونة باسبانيا والحمد لله الذي توج هذا المجهود العظيم وكلله بالنجاح في الدراسة العلمية

كما اتقدم باسمى ايات العرفان لاسرتي الكريمة واسأل الله لهم الصحة والعافية وجزاهم الله عني خيرا

ولا استطيع ان انسى فضل كل من علمني حرفاً في جميع مراحل التعليم المختلفة جعله الله زخراً لهم في الدنيا والاخرة

كما اشكر كل الزملاء والسادة اعضاء هيئة التدريس بكلية الصيدلة جامعة الزقازيق واخص بالشكر قسم الميكروبيولوجي والمناعة بكلية الصيدلة الذي اتشرف بالانتماء اليه

اسأل الله الامن والامان لمصرنا الغالية

واتمنى من الله أن أكون قد تركت صوره طيبه عن المسلمين لكل من تعامل معي و تعاملت معه

إِنْ أُرِيدُ إِلاّ الإِصْلاَحَ مَا اسْتَطَعْتُ وَمَا تَوْفِيقِيَ إِلاّ بِاللّهِ عَلَيْهِ تَوَكّلْتُ وَإِلَيْهِ أُنِيبُ

صدق الله العظيم سورة هود - الآية ٨٨

Index

Summary

Budding yeast (*Saccharomyces cerevisiae)* cells coordinate cell growth and cell cycle progression essentially during G1, where they must reach a critical cell size to traverse Start and enter the cell cycle. The most upstream activator of Start is Cln3, a G1 cyclin that together with the cyclin-dependent kinase Cdc28 triggers a transcriptional wave that drives cell cycle entry. The Cln3 cyclin is a low abundant and very unstable protein whose levels respond very rapidly to nutritional changes by different regulatory mechanisms, allowing the cell to adjust proliferation requirements to growth capabilities very efficiently in changing environments. However, Cln3 expression is not sharply regulated through the cell cycle and it is already present in early G1 cells. Notably, most Cln3 is retained bound to the ER in early G1 with the assistance of Whi3, an RNA-binding protein that binds the *CLN3* mRNA, and it is released in late G1 by Ydj1, a J-chaperone that might transmit growth capacity information to the cell cycle machinery. However, little is known on the molecular mechanisms that retain the Cdc28-Cln3 complex in the cytoplasm and how do these mechanisms transmit information of cell size to coordinate cell proliferation with cell growth. As Cdc28 is important for proper retention of Cln3 at the ER, we hypothesized that mutations weakening interactions to unknown ER retention factors would cause premature release of the Cdc28-Cln3 complex and, hence, a smaller cell size.

This thesis describes the isolation and characterization of a *CDC28* quintuple mutant, which causes premature entry into the cell cycle and a small cell size and we refer to as *CDC28*^{wee}. Next we used isobaric tags for relative and absolute quantitation (iTRAQ) to identify direct interactors with lower affinities for mutant Cdc28^{wee}, aiming at the identification of proteins with key regulatory roles in the retention mechanism. Among the identified proteins we found Srl3, a protein of unknown function, here renamed as Whi7. Here we show that Whi7 acts as an inhibitor of Start, associates to the ER and contributes to efficient retention of the Cln3 cyclin, thus preventing its unscheduled accumulation in the nucleus. Our results demonstrate that Whi7 acts in a positive feedback loop to release the G1 Cdk-cyclin complex and trigger Start once a critical size has been reached, thus uncovering a key nonlinear mechanism at the earliest known events of cell cycle entry.

In addition to Whi7 we also identified Whi8, renamed here as Whi8, which is an RNA-binding protein present in both stress granules (SGs) and P bodies (PBs) with unknown

biological function. We have found that Whi8 interacts with Cdc28 *in vivo*, binds and colocalizes with the *CLN3* mRNA, and interacts with Whi3 in an RNA-dependent manner. Whi8-deficient cells showed a smaller budding cell size while, on the other hand, overexpression of Whi8 increased the budding volume. Cells lacking Whi8 were not capable of accumulating the *CLN3* mRNA in SGs under stress conditions, and Cln3 synthesis remained high under glucose and nitrogen starvation, two environmental stress conditions that dramatically decrease Cln3 levels in the cell. Whi8 accumulation in SGs depended on an intrinsically disordered domain (IDD) identified at C-terminus of Whi8 and specific PKA phophosites. Our results suggest that Whi8 acts under stress as a safeguard that limits the influx of newly synthesized Cln3 (and likely other proteins) into the cell cycle machinery, by trapping the *CLN3* mRNA in mRNA granules. Thus, we have found a unique target for signaling pathways that directly links stress response and cell cycle entry.

Introduction

"'*The first thing I've got to do*,' said Alice to herself, as she wandered about in the wood, '*is to grow to my right* ***size*** *again*…'" – Lewis Carroll, Alice's Adventures in Wonderland (1865).

The word "cell" comes from the Latin word "cella" which means small room (Simpson, 1977). The size of living eukaryotic cells can range from 10 microns, which is the diameter of budding yeast *S. cerevisiae* (Forsburg & Nurse, 1991), to around 30 microns, the diameter of human keratinocytes (Sun & Green, 1976), and up to 1300 microns, the diameter of *Xenopus laevis* frog oocytes (Dumont, 1972). A cell's size is a fundamental attribute that contributes to function in the context of multicellular organisms and to fitness in the context of unicellular organisms. Size imposes constraints on cellular design. For instance, as cells grow larger, passive diffusion may limit intracellular transport and the decreased surface area to volume ratio may make nutrient uptake limiting for cell growth.

The first insights into cell size control were made around 100 years ago, when Boveri, Hertwig, and their colleagues (Wilson, 1925) observed a fundamental correlation between ploidy and cell volume. Here, in this study, we provide new insights about spatial regulation of cell size trying to answer how size homeostasis is achieved in proliferating cells during the G1 phase of the cell cycle in *S. cerevisiae*, our working model. It is clear that coordination between growth and proliferation is an active process in a great variety of unicellular organisms ranging from bacteria to protists. Indeed, the highly diverged budding and fission yeasts each possess specific regulatory networks dedicated to converting the accrual of sufficient biomass into a stimulus for cell cycle progression. Just how cells convert steady increases in size into a switch-like decision to enter the cell cycle is a fascinating question in biological engineering. While it is clear that cell growth and division must be correlated in metazoans, it remains a contentious issue whether such cells actively and cell-autonomously couple growth and division. Size control has inspired much research over the past century, yet, relative to other aspects of cell biology, this problem has been recalcitrant to conventional genetics and biochemistry. In thinking about cell size control, it is important to distinguish cell growth, the cell cycle, and the mechanisms that coordinate the two either in direct or indirect manners.

1. The cell cycle

Nucleated cells destined to grow and reproduce have to go through a cyclic process that includes growth, DNA duplication, nuclear division (mitosis) and cellular division (cytokinesis). During interphase cells take their time to grow (G1 and G2), replicate their DNA (S phase), repair DNA damage, and make sure that cells are ready to divide in the proceeding stage (M phase). M phase is composed of two major events, mitosis and cytokinesis. During mitosis sister chromatids are attached to microtubules coming from opposite poles of the spindle, and are aligned in the middle of the cell forming the metaphase plate. Once all sister chromatids are correctly bi-oriented, sister chromatid cohesion is destroyed resulting in their separation and retraction towards opposite ends of the cell during anaphase. Mitosis ends with nuclear cleavage (telophase), and is followed by cytokinesis, which results in two daughter cells each with identical chromosome number to that of the original cell. To ensure the correct order of events, the cell contains a complex regulatory network called the cell cycle control system. Cyclin dependent kinases (Cdks) are the central components of this system, which catalyze the covalent attachment of phosphate groups derived from ATP to protein substrates. Cdks are activated by binding to different cyclins, which trigger different cell cycle events. The different cyclin/Cdk complexes can be classified into G1-Cdk, G1/S-Cdk, S-Cdk, and M-Cdk. Each cyclin/Cdk complex promotes the activation of the next in sequence, thus ensuring that the cycle progresses in an orderly manner. The cell cycle control system drives progression through the cell cycle at regulatory transitions called checkpoints. The first checkpoint is called Start or G1/S checkpoint. When conditions are ideal for cell proliferation, the levels of G1/S cyclin increase, promotes the formation of G1/S-Cdk complex (Figure 1). These complexes activate S-Cdk, resulting in phosphorylation of proteins that initiate DNA replication and S-phase entry.

Eventually, G1/S- and S-Cdk complexes promote the activation of M-Cdk complexes, which drive progression through the second major checkpoint at the entry into mitosis (G2/M checkpoint). M-Cdk complexes phosphorylate proteins that promote spindle assembly, bringing the cell to metaphase. Progression through the last checkpoint (spindle assembly checkpoint, SAC) at the metaphase to anaphase transition, occurs when M-Cdk stimulates the anaphase promoting complex (APC) which triggers anaphase by destruction of a protein called securin. In addition, APC causes the

proteolytic destruction of cyclins to close the cell cycle. If conditions are not appropriate for cell proliferation, cells arrest cell cycle progression at these checkpoints until they are satisfied and the conditions are favorable again to continue. Arrest at the early stages of the cell cycle occurs at the Start checkpoint by inhibiting the activation of S-Cdks. Similarly, failure to complete DNA replication blocks entry into mitosis by inhibiting M-Cdk activation. The proteolytic activity of the APC is also inhibited at the metaphase to anaphase transition when there is a delay in the spindle assembly, which prevents sister chromatid segregation until the spindle is ready (Peters, 2006; Woodbury & Morgan, 2007) .

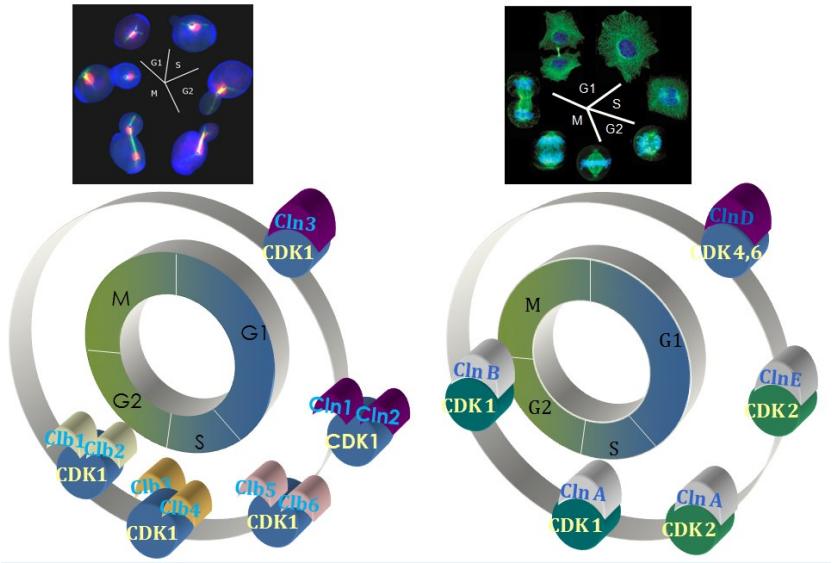

Figure 1: Overwiew of the Cell Cycle

Overview of the cell cycle in budding yeast (on the left) and mammalian cells (on the right).

2. The cell cycle control system

The regulatory network regulating the order and timing of cell cycle is called the cell cycle control system. The fundamental G1/S transition regulatory pathways of the cell cycle are conserved from yeast to humans. These systems-level properties are conserved across eukaryotes despite frequent lack of protein sequence homology, and share cyclins, CDKs, transcription factors and other regulators of the cell cycle. A list of functional orthologues between yeast and humans of G1/S phase transcriptional regulators and cyclin-CDKs are indicated in Table 1. Although the functional orthologues

of cyclins and CDKs share significant sequence homology, there is a total lack of sequence homology between yeast and the higher eukaryotic G1/S transcriptional regulators.

Regulator type	*Saccharomyces cerevisiae*	*Schizosaccharomyces pombe*	*Drosophila melanogaster*	*Homo sapiens*
G1–S transcriptional regulators				
Activators	SBF (Swi6–Swi4)	MBF (Cdc10–Res1–Res2)	E2f1	E2F1, E2F2, E2F3
Repressors	MBF (Swi6–Mbp1)		E2f2	E2F4, E2F5, E2F6, E2F7, E2F8
Inhibitors	Whi5	Possibly Whi5	Rbf1	RB
Co-repressors	Nrm1	Nrm1, Yox1	Rbf2	p107, p130
Cyclin–CDK				
G1 phase regulator	Cdc28–Cln3	Cdc2–Puc1	Cdk4–cyclin D	CDK4–cyclin D, CDK6–cyclin D
G1–S phase regulator	Cdc28–Cln1, Cdc28–Cln2	Cdc2–Puc1 Cdc2–Cig1	Cdk2–cyclin E	CDK2—cyclin E
S phase regulator	Cdc28– Clb5, Cdc28–Clb6	Cdc2– Cig1, Cdc2– Cig2	Cdk2–cyclin E, Cdk1–cyclin A, Cdk2–cyclin A	CDK2—cyclin E, CDK1–cyclin A, CDK2–cyclin A
M phase regulator	Cdc28– Clb1, Cdc28–Clb2, Cdc28–Clb3, Cdc28–Clb4	Cdc2–Cdc13	Cdk1–cyclin B	CDK1–cyclin B
Checkpoint protein kinases				
Sensor and/or transducer	Mec1	Rad3	ATR	ATR
	Tel1	Tel1	ATM	ATM
Effector	Chk1	Cds1	Chk1	CHK1
	Rad53	Chk1	Chk2	CHK2

Table1: Functional orthologues between yeast and humans of G1–S phase transcriptional regulators and cyclin-CDKs.

Adapted from Bertoli et al. (2013)

There are three major regulatory checkpoints of the cell cycle: Start, which describes the cell cycle entry in late G1; the G2/M checkpoint, that describes how entry into mitosis is controlled; and finally the metaphase-to-anaphase transition, where the final events of mitosis and cytokinesis are initiated. The central components of this control system are the cyclin-dependent kinases (Cdks). As the cell progresses through the cycle, abrupt changes or oscillations in the enzymatic activity of these kinases lead to changes in the phosphorylation state, and thus the activation state, of the Cdk protein substrates that control cell cycle events. Cdk protein concentrations are constant throughout the cell cycle; oscillations in their activity depend primarily on oscillations in the levels of other regulatory subunits tightly bound to Cdks called cyclins that stimulate the Cdks catalytic activity. Different cyclin-Cdk complexes exist during different cell cycle stages. These complexes G1-, G1/S-, S- and M-Cdks control the passage through the three major regulatory checkpoints (Figure 2). Each cyclin-Cdk complex activates the next one in a series, and this ensures the cell cycle progression in an ordered fashion.

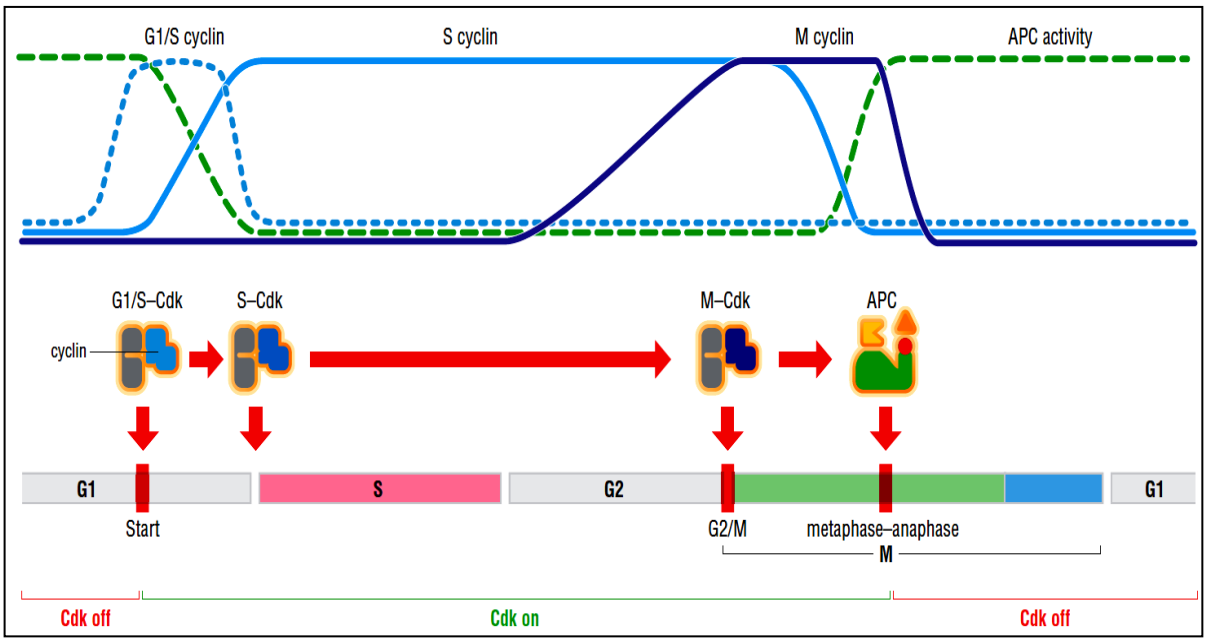

Figure 2: A simplified overview of the cell cycle control system

Levels of the three major cyclin types oscillate during the cell cycle (top), providing the basis for oscillations in the cyclin-Cdk complexes that drive cell cycle events (bottom). In general, Cdk levels are constant and in large excess over cyclin levels; thus, cyclin-Cdk complexes form in parallel with cyclin levels. The enzymatic activities of cyclin-Cdk complexes also tend to rise and fall in parallel with cyclin levels, although in some cases Cdk inhibitor proteins or phosphorylation introduce a delay between the formation and activation of cyclin-Cdk complexes. Formation of active G1/S-Cdk complexes commits the cell to a new division cycle at the Start checkpoint in late G1. G1/S-Cdks then activate the S-Cdk complexes that initiate DNA replication at the beginning of S phase. M-Cdk activation occurs after the completion of S phase, resulting in progression through the G2/M checkpoint and assembly of the mitotic spindle. APC activation then triggers sister-chromatid separation at the metaphase-to-anaphase transition. APC activity also causes the destruction of S and M cyclins and thus the inactivation of Cdks, which promotes the completion of mitosis and cytokinesis. APC activity is maintained in G1 until G1/S-Cdk activity rises again and commits the cell to the next cycle. This scheme serves only as a general guide and does not apply to all cell types. Adapted from Morgan (2007).

The activity of cyclin-Cdk complexes is governed by multiple regulatory mechanisms including cyclin concentrations which are a function of combination of changes in cyclin gene expression and rates of cyclin degradation ,the addition or removal of inhibitory phosphorylation, and finally by changes in the levels of Cdk inhibitor proteins. The G1/S-, S- and M-Cdks are inactive in G1 due to lack of expression of those cyclin genes by inhibitory gene regulatory proteins, high rates of cyclin degradation through the activation of an E3 ubiquiting ligase complex called the anaphase-promoting complex or AP, which specifically targets the S and M cyclins (but not the G1/S cyclins) for proteolysis and degradation (Figure 2), and finally the presence of high concentrations of Cdk inhibitors in G1.

Cell cycle entry begins when the cell receives extracellular signals (mitogens, for example) and intracellular (systems monitoring cell growth, for example) trigger a combination of events that promote G1/S- and S-cyclin gene expression consequently activation of G1/S-Cdks. G1/S-Cdk activity peaks immediately because in one hand the G1/S cyclins are not targeted by the APC and on the other hand because the Cdk inhibitor proteins either do not act on G1/S-Cdks (in yeast and flies) or are removed from G1/S-Cdks (in mammals). The G1/S-Cdks directly initiate some early cell cycle steps and more importantly activate the S-Cdks by triggering the destruction of Cdk inhibitor proteins and the inactivation of the APC, the two major inhibitors of S-Cdk activity in G1. S-Cdks then phosphorylate specific proteins that initiate chromosome duplication (spindle pole body in yeast), thereby launching S phase. Toward the end of S phase, M-cyclin gene expression is switched on and M-cyclin concentration rises, leading to the accumulation and activation of M-Cdk complexes during G2. In most cell types, these M-Cdk complexes are initially held inactive by inhibitory phosphorylation of the Cdk subunit. At the onset of mitosis, the abrupt removal of this inhibitory phosphorylation by phosphatases leads to the activation of all M-Cdks and those are responsible for deriving the cycle progression through the G2/M checkpoint. The consequence of mitotic events begins with spindle assembly and other early mitotic events lead to the alignment of duplicated sister chromatids on the mitotic spindle in metaphase. In addition to driving the cell to metaphase, M-Cdks finally stimulate activation of the APC, which triggers the metaphase to anaphase transition and mitotic exit. A major function of the APC at the metaphase to anaphase checkpoint is to stimulate the destruction of proteins that hold the sister chromatids together. The APC also causes destruction of S and M cyclins, resulting in the inactivation of all major Cdk activities in late mitosis. Decreased S- and M-cyclin gene expression and increased production of Cdk inhibitor proteins also occurs in late mitosis. The resulting inactivation of Cdks allows dephosphorylation of their mitotic targets, spindle disassembly and the completion of M phase. Low levels of Cdk activity then maintained until late in the following G1 of the next cycle, when rising G1/S-Cdk activities again commit the cell to a new cycle. The cell cycle control system is simply summarized in (Figure 2).

The cyclin-Cdk complexes and other cell cycle regulators are assembled into a highly interconnected unidirectional regulatory system whose effectiveness is enhanced by a number of important features including. First, feedback loops and other regulatory interactions that lead to irreversible, switch-like activation and inactivation of cyclin-Cdk complexes, and this allow cell cycle to be triggered in an all-or-none fashion, to avoid the damage that might result from partial initiation. Second, regulatory interactions between the different cyclin-Cdk switches ensure order and coordination between each others. Third, the robust activation and inactivation of every cyclin-Cdk switch due to control by multiple mechanisms, and this helps the system to operate well and display adaptation against a variety of conditions and regulatory inputs from various intracellular and extracellular factors (Morgan, 2007).

Cyclin-dependent kinases

The cyclin-dependent kinases (Cdks) are a family of serine/threonine protein kinases whose small MW (~34-40 kDa). All Cdks require the binding of a regulatory cyclin subunit for their enzymatic activation. In most cases, full activation also requires phosphorylation of a threonine residue near the kinase active site. In the fission yeast *S. pombe* and the budding yeast *S. cerevisiae*, all cell cycle events are controlled by a single essential Cdk called Cdk1 (Table 2), on the other hand cell cycle in higher eukaryotes are controlled by at least two Cdks, known as Cdk1 and Cdk2, which operate primarily in M phase and S phase, respectively. Animal cells also contain two more Cdks (Cdk4 and Cdk6) that are important in regulating G1 and cell cycle entry (Table 2).

Cyclin-Dependent Kinases				
Species	**Name**	**Original name**	**Size (amino acids)**	**Function**
S. cerevisiae	Cdk1	Cdc28	298	all cell cycle stages
S. pombe	Cdk1	Cdc2	297	all cell cycle stages
H. sapiens	Cdk1	Cdc2	297	M phase
	Cdk2		298	G1/S, S, possibly M phases
	Cdk4		303	G1 phase
	Cdk6		326	G1 phase

Table 2: Table of cyclin –dependent kinases that control the cell cycle in yeast and *H. sapiens*

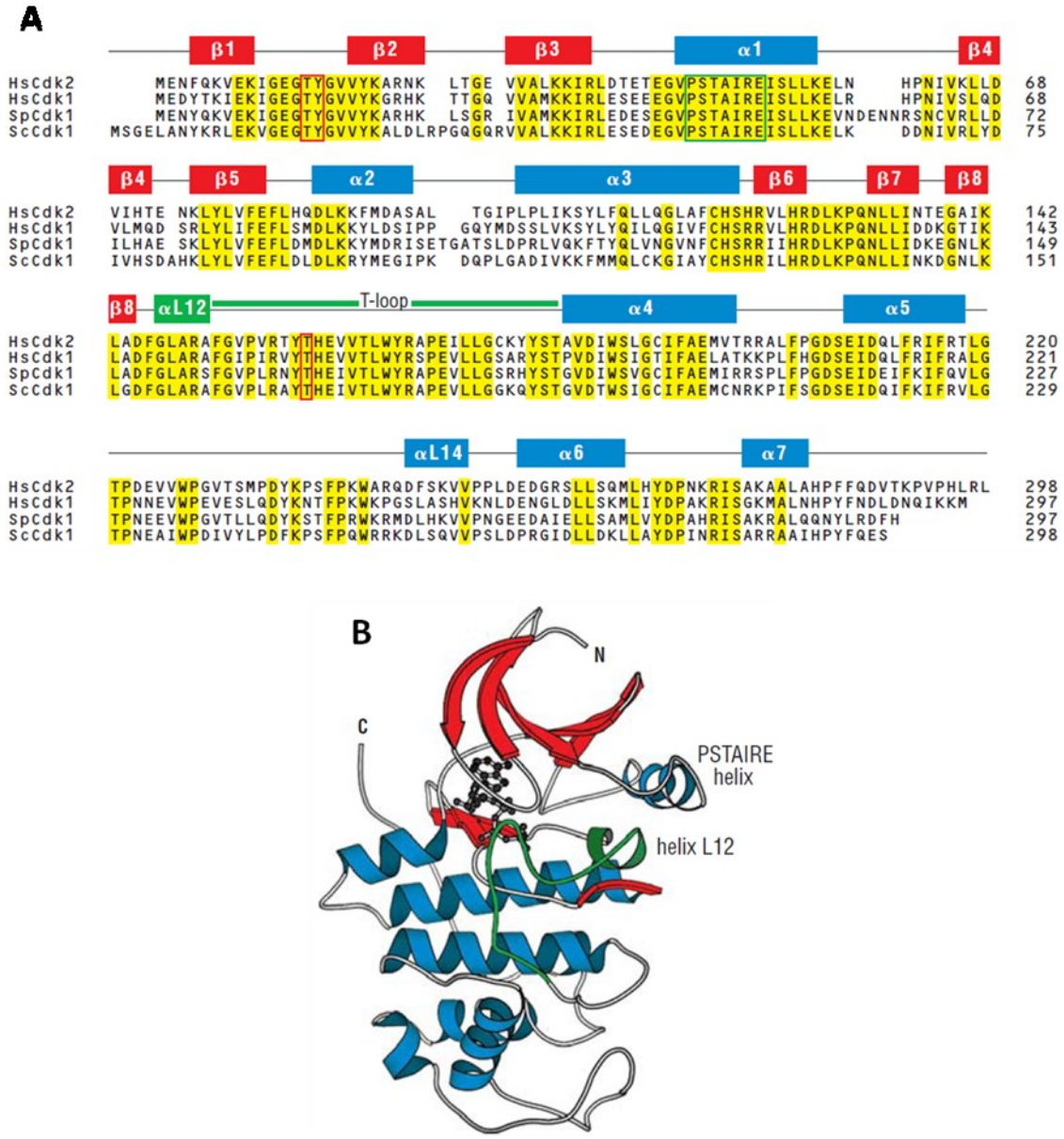

Figure 3: Cyclin-dependent kinase structure

(A) Amino-acid sequences of major Cdks controlling the cell cycle in humans (*H. sapiens* (Hs) Cdk1 and Cdk2) and yeast (*S. pombe* (Sp) Cdk1 and *S. cerevisiae* (Sc) Cdk1). Yellow residues are identical in all four kinases. Above the alignment, secondary structure elements in human Cdk2 are shown for comparison with the tertiary structure in panel (b). Key landmarks are highlighted, including the PSTAIRE or α1 helix, the inhibitory phosphorylation sites Thr 14 and Tyr 15, the activating phosphorylation site (Thr 160 in human Cdk2) and the T-loop or activation loop where Thr 160 is found.
(B) Tertiary structure of human Cdk2, determined by X-ray crystallography. Like other protein kinases, Cdk2 is composed of two lobes: a smaller amino-terminal lobe (top) that is composed primarily of beta sheet and the PSTAIRE helix, and a large carboxy-terminal lobe (bottom) that is primarily made up of alpha helices. The ATP substrate is shown as a ball-and-stick model, located deep within the active-site cleft between the two lobes. The phosphates are oriented outward, toward the mouth of the cleft, which is blocked in this structure by the T-loop (highlighted in green). Adapted from Morgan (2007).

Cdks phosphorylate a large number of protein substrates in the cell during cell cycle. These Cdk substrates are phosphorylated at serine or threonine residues in a specific sequence context where the target serine (S) or threonine (T) residue is followed by a proline (P); it is also highly favorable for the target residue to have a basic amino acid two positions after the target residue. The typical phosphorylation amino acid consensus sequence for Cdks is [S/T*]PX[K/R], where S/T* indicates the phosphorylated serine or threonine, X represents any amino acid and K/R represents the basic amino acid lysine (K) or arginine (R) (Morgan, 2007).

Like all protein kinases, Cdks have a two-lobed tertiary structure comprising a small N-terminal lobe and a larger C-terminal lobe. ATP fits snugly in the cleft between the lobes, in such a way that the phosphates are oriented toward the mouth of the cleft. The protein substrate binds at the entrance of the cleft, interacting mainly with the surface of the C-terminal lobe. Nearby residues catalyze the transfer of the terminal γ-phosphate of ATP to hydroxyl oxygen in a serine or threonine residues within the protein substrate.

There are two structural modifications revealed by detailed crystallographic studies of the structure of human Cdk2, those two modifications explain why Cdks hold inactive in the absence of cyclin. First, a large, flexible loop (the T-loop or activation loop) rises from the C-terminal lobe to block the binding of protein substrate at the entrance of the active site cleft. Second, in the inactive Cdk several important amino-acid side chains in the active site are incorrectly positioned, so that the phosphates of ATP are not ideally oriented for the kinase reaction. Therefore activation of Cdk requires extensive structural changes in the Cdk active site. Two α-helices exert a particularly important contribution to the Cdk activity control upon cyclin binding. The highly conserved PSTAIRE helix of the upper kinase lobe (also known as the α1 helix) interacts directly with cyclin and moves inward, causing the reorientation of residues that interact with the phosphates of ATP. The small L12 helix, just before the T-loop in the primary sequence, changes structure to become a beta strand, also contributing to reconfiguration of the active site and T-loop (Johnson et al., 2002, Morgan, 1997; Ubersax et al., 2003) (Figure3A and 3B).

Cyclins

Cyclins are the Cdk partners; they bind and activate Cdks. They are called cyclins because of displaying cyclical changes in concentration during the cell cycle, which help to generate the oscillations in Cdk activity consequently cell cycle control. The regulation of cyclin concentration is driven by changes in cyclin gene expression (transcriptiona) and destruction of cyclins (proteolysis). Cyclins can be divided into four classes, based primarily on the phase of their expression and their functions during the cell cycle.

The G1/S cyclins, S cyclins and M cyclins which are directly involved in the control of cell cycle events (Table3). The fourth class, the G1 cyclins, contributes to the control of cell cycle entry in response to extracellular factors.

Cyclin class (with Cdk partner)				
Species	**G1**	**G1/S**	**S**	**M**
S. cerevisiae	Cln3 (Cdk1)	Cln1,2 (Cdk1)	Clb5,6 (Cdk1)	Clb1,2,3,4 (Cdk1)
S. pombe	Puc1 (Cdk1)	Cig1 (Cdk1)	Cig2 (Cdk1)	Cdc13 (Cdk1)
H. sapiens	Cyclin D1,D2,D3 (Cdk4,6)	Cyclin E (Cdk2)	Cyclin A (Cdk2,1)	Cyclin B (Cdk1)

Table 3: Table of major cyclin classes involved in cell cycle control

The G1/S cyclins oscillate during the cell cycle (peak in late G1 and fall in early S phase). The primary function of G1/S cyclin-Cdk complexes is to trigger progression through Start, initiate the pre steps of DNA replication, and finally G1/S cyclins also initiate other early cell cycle events, such as centrosome duplication in vertebrates (the spindle pole body, in yeast). The S cyclins, which form S cyclin-Cdk complexes, their levels remain high throughout S phase, G2 and early mitosis; they are directly responsible for stimulating DNA replication. Finally, M cyclins appear and their concentration rising as the cell approaches mitosis (peak in metaphase and fall in anaphase). M cyclin-Cdk complexes derive the mitotic phase events like assembly of the mitotic spindle and the alignment of sister-chromatid pairs on the spindle at metaphase. M cyclins destruction in anaphase allows the cell to commit mitotic exit and cytokinesis. Beside activation of the associated Cdk subunit, cyclins direct their Cdk partner to specific substrates, either directly by binding the substrate itself or by taking the Cdk to a subcellular compartment where the substrate is found, in fact some cyclins contain sequence information that targets them and

their Cdk partners to specific subcellular locations (NLS of Cln3 for example), providing another mechanism by which a cyclin can direct its catalytic partner to the right substrates all this helps to explain the molecular basis of cyclin specificity (Morgan, 2007).

3. Cdk regulation

Cyclin binding alone is not enough to fully activate Cdks, complete activation of a Cdk also requires phosphorylation of a threonine residue adjacent to the kinase active site beside conformational changes in the Cdk structure itself. In the next sections, other structure activity requirements of Cdk are going to be discussed in more details.

Control of Cdk activity by phosphorylation

Complete activation of a Cdk, also requires phosphorylation of a threonine residue adjacent to the kinase active site by enzymes called Cdk-activating kinases (CAKs). CAK activity is maintained at a constant high level throughout the cell cycle and is not regulated by any known cell cycle control pathway (Espinoza et al., 1996; Kaldis, 1999; Kaldis et al., 1998; Lolli & Johnson, 2005; Morgan, 2007; Sutton & Freiman, 1997).

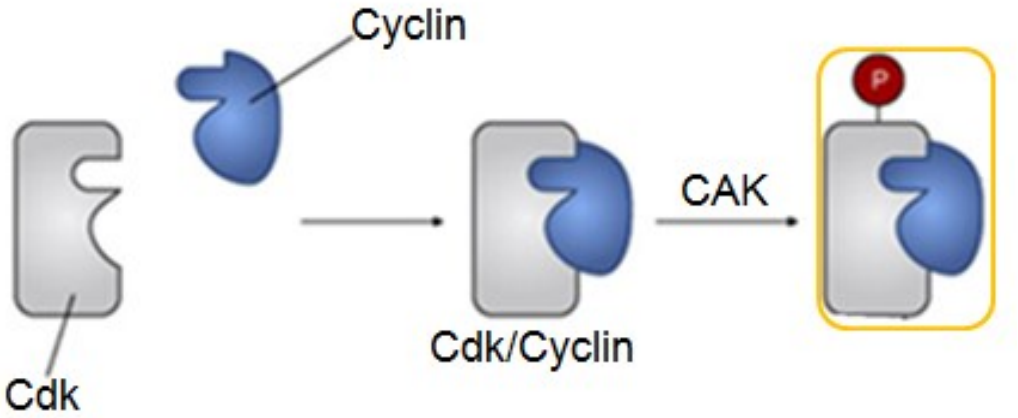

Figure 4: Two steps in Cdk activation

Cyclin binding alone causes partial activation of Cdks, but complete activation also requires activating phosphorylation by CAK. In animal cells, CAK phosphorylates the Cdk subunit only after cyclin binding, and so the two steps in Cdk activation are usually ordered as shown here, with cyclin binding occurring first. Budding yeast contains a different version of CAK that can phosphorylate the Cdk even in the absence of cyclin, and so the two activation steps can occur in either order. In all cases, CAK tends to be in constant excess in the cell, so that cyclin binding is the rate-limiting step in Cdk activation. Adapted from Morgan (2007).

In addition, in mammalian cells, phosphorylation can occur only after cyclin binding, whereas in budding yeast cells phosphorylation occurs before cyclin binding (Ross et al., 2000). In both cases, however, cyclin binding and not CAK phosphorylation is the highly regulated, rate limiting step in Cdk activation (Morgan, 2007). Simply this activating phosphorylation of Cdk can therefore be considered as a post-translational modification that is required for enzyme activity (Figure 4).

Control of Cdk activity by inhibitory phosphorylation

Besides the activating phosphorylation of Cdks by CAK, two other inhibitory phosphorylations do have important functions in the regulation of Cdk activity. One is at a conserved tyrosine residue (Tyr15 in human Cdks) that is found in all major Cdks. In animal cells, additional phosphorylation of an adjacent threonine residue (Thr14) further blocks Cdk activity. Thr14 and Tyr15 are located in the roof of the kinase ATP-binding site and their phosphorylation probably inhibits activity by interfering with the orientation of ATP phosphates (Booherl et al., 1993; Lim et al., 1996; Morgan, 1997; Morgan, 2007). Changes in the phosphorylation of these sites are particularly important in the activation of M-Cdks at the onset of mitosis, and they are also thought to influence the timing of G1/S- and S-phase Cdk activation (Nurse, 1990). The phosphorylation state of Tyr15 and Thr14 is controlled by the balance of opposing kinase and phosphatase activities acting at these sites (Morgan, 2007). One enzyme responsible for Tyr15 phosphorylation is Wee1, which is present (under various names) in all eukaryotes (Table 4).

Wee1 & Cdc25 family		
Species	**Wee1 enzymes**	**Cdc25 enzymes**
S. cerevisiae	Swe1	Mih1
S. pombe	Wee1	Cdc25
	Mik1	
vertebrates	Wee1: phosphorylates Tyr 15	Cdc25A: control of G1/S &G2/M
	Myt1:phosphorylates Thr 14& Tyr 15	Cdc25B: control of G2/M
		Cdc25C: control of G2/M

Table 4: Table of Wee1 and Cdc25 family

Dephosphorylation of inhibitory sites is carried out by Cdc25 phosphatases (Russell et al., 1989), (Table 4). The actions of these enzymes are shown in (Figure 5). Fission yeast contains two kinases, that both contribute to Tyr15 phosphorylation, Wee1 and Mik1. A second protein kinase, Myt1, related to Wee1, phosphorylates both of Thr14 and Tyr15 in vertebrates. The counterbalance of Wee1 and Cdc25 activity provides the basis for the switch-like character of M-Cdk activation, which allows abrupt and irreversible entry into mitosis. Both enzymes are regulated by their mitotic substrate: phosphorylation of Wee1 by M-Cdk inhibits Wee1 and on the contrary activates Cdc25. Thus, M-Cdk activates its own activator and inhibits its inhibitor, and the resulting feedback loops are thought to generate switch-like Cdk activation during early mitosis (Angeli et al., 2004; Kim & Ferrell, 2007; King et al., 2013; Watanabe et al., 2004). Wee1 and Cdc25 are also important targets for regulation of Cdk activity in response to DNA damage (Rhind & Russell, 2001).

Figure 5: Control of Cdk activity by inhibitory phosphorylation

The fully active cyclin-Cdk complex (center) can be inhibited by further phosphorylation at one or two sites in the active site of the enzyme. Phosphorylation of Tyr 15 by Wee1, or phosphorylation of both Thr 14 and Tyr 15 by Myt1 inactivates the cyclin-Cdk complex. Dephosphorylation by the phosphatase Cdc25 leads to reactivation. Adapted from(Morgan 2007).

The structural basis of Cdk activation

The structural basis of Cdk activation is understood from X-ray crystallographic studies of human Cdk2 in various states of activity (Figure 6). As described earlier, the active site of Cdk2 is located in a cleft between the two lobes of the kinase (Figure 6a). ATP, with its phosphates oriented outward, binds deep within the cleft. The protein substrate would normally interact with the entrance of the active-site cleft, but this region is blocked by the T-loop in the inactive Cdk2 monomer (Brown et al., 1999; Russo et al., 1996; Takaki et al., 2009). Key residues in the ATP-binding site are also misoriented in the Cdk2 monomer, suppressing its activity.

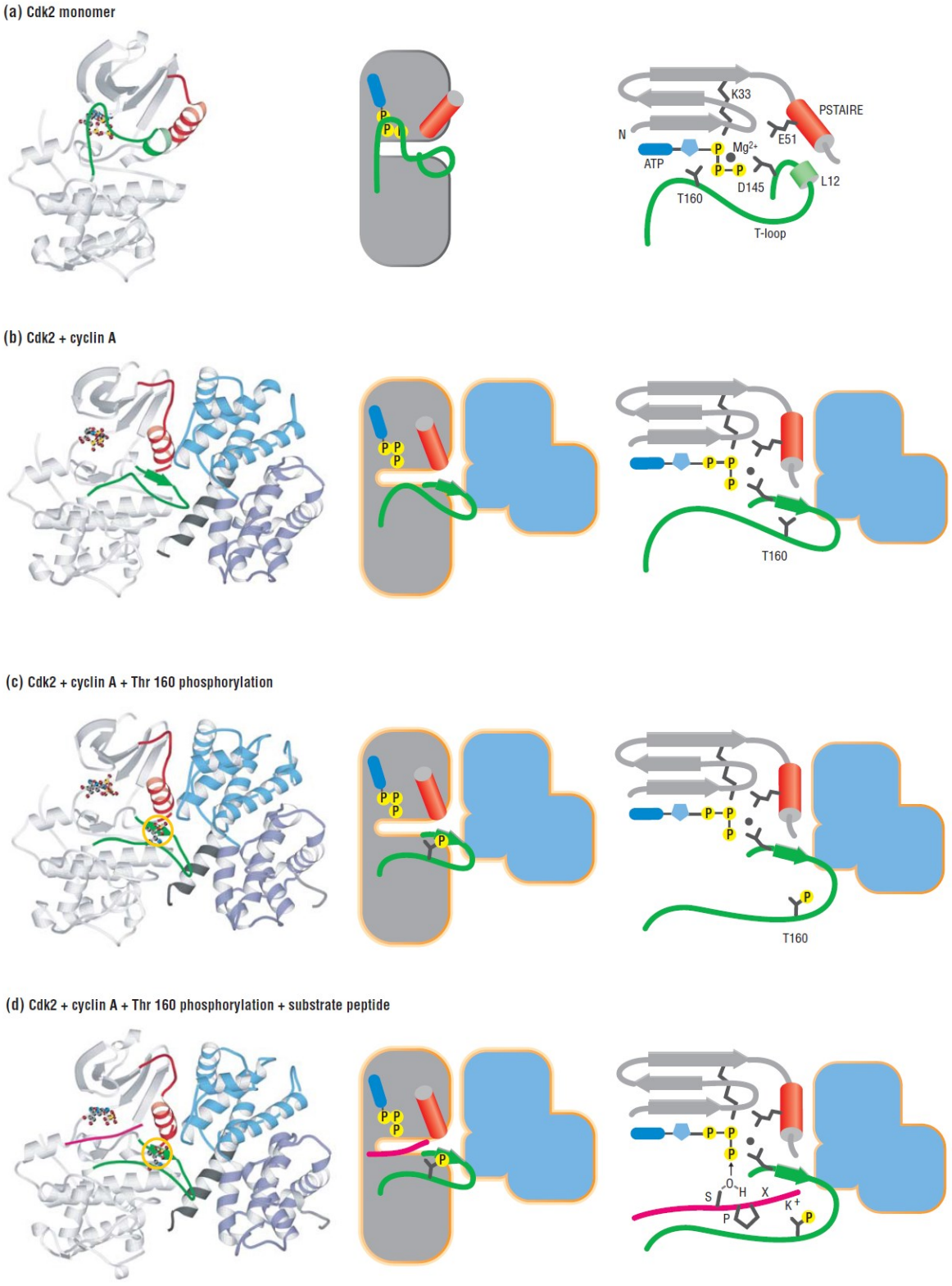

Figure 6: The structural basis of Cdk activation

These diagrams illustrate the structure of human Cdk2 in various states of activity. In each case, the complete structure is represented in the left column (PDB 1hck, 1fin, 1jst, 1gy3), while the right columns provide schematic views that emphasize key substructures, including the ATP in the active site, the T-loop (green) and the PSTAIRE helix (red).

(a) In the inactive Cdk2 monomer, the small L12 helix next to the T-loop pushes out the large PSTAIRE helix, which contains glutamate 51 (E51), a residue important in positioning the ATP phosphates. The T-loop also blocks the active-site cleft.
(b) When cyclin A binds, the PSTAIRE helix moves inward and the L12 helix changes structure to form a small beta strand;as a result, E51 moves inward to interact with lysine 33 (K33), while aspartate 145 (D145) also shifts position. These changes lead to the correct orientation of the ATP phosphates. The T-loop is also shifted out of the active-site entrance.
(c) The phosphorylation of threonine160 (T160) in the T-loop (yellow circle in left column) then causes the T-loop to flatten and interact more extensively with cyclin A.
(d) Phosphorylation allows the T-loop to interact effectively with a protein substrate containing the SPXK consensus sequence (pink). The proline at the second position in this sequence interacts with the backbone of the T-loop, while the positively charged lysine residue at the fourth position (K^+) interacts, in part, with the negatively charged phosphate on T160. The hydroxyl oxygen of the serine residue (S) in the substrate is now positioned for nucleophilic attack on the γ-phosphate. Adapted from Morgan (2007).

Cyclin A binding has a major impact on the Cdk2 active site conformation (Figure 6b). Several helices in the cyclin box contact both lobes of Cdk2 in the region adjacent to the active site cleft, resulting in extensive conformational changes in Cdk2. The most obvious change occurs in the T-loop, in which the L12 helix has been changed into a beta strand, so no longer block the binding site for the protein substrate but lies almost flat at the entrance of the cleft. Major changes also occur in the ATP-binding site, leading to the correct positioning of the ATP phosphates to allow phosphate transfer. Although cyclin A structure is unaffected by Cdk2 binding, it provides a rigid framework against which the pliable Cdk2 subunit is molded. The T-loop of Cdk2 contains Thr160, the threonine residue whose phosphorylation by the Cdk-activating kinase (CAK) further increases the activity of the cyclin A-Cdk2 complex. After phosphorylation, the phosphate on Thr160 is inserted in a cationic pocket and acts as the central node for a network of hydrogen bonds spreading outward to stabilize neighboring interactions in both the Cdk and cyclin. The T-loop is flattened and moves closer to cyclin A (Figure 6c and 6d), and this region serves as a key part of the binding site for protein substrates containing the [S/T*] PX [K/R] consensus phosphorylation site. Crystallographic studies of Cdk activation on human Cdk2 and its partner cyclin A serves as a good representative for the entire Cdk family, but the details of Cdk activation seem to be different in some complexes. It is likely that different cyclins do not induce precisely the same conformational changes in the associated Cdk subunit, for example, the same Cdk, when bound by different cyclins, displays different amounts of kinase activity toward the [S/T*] PX [K/R] sequence.

Cdk regulation by inhibitory subunits

During G1, most Cdk activity in dividing cells is suppressed, this creates a transition period during which cell growth and other extracellular factors can regulate entry into the next cycle, there are three mechanisms that suppress Cdk activity during G1, increased cyclin destruction by proteolysis, decreased cyclin gene expression and the inhibition of Cdk activity by Cdk inhibitor proteins (CKIs) that bind and inactivate cyclin-Cdk complexes. Another function of CKIs is promoting the cell cycle arrest in G1 in response to unfavorable extracellular conditions or intracellular signals like DNA damage. Most, if not all, eukaryotic organisms possess a CKI that contributes to the establishment of a stable G1: these include Sic1 in budding yeast, Rum1 in fission yeast (Labib & Moreno, 1996; Mendenhall et al., 1995; Moreno et al., 1994; Schwob et al., 1994). Although these proteins do not show significant sequence homology, they share several important functional features. First, all of them are potent inhibitors of the major S- and M-Cdk complexes, and all are expressed at high levels in G1 cells to inhibit S- or M-Cdk activity in those cells (Mendenhall, 1993; Weinreich et al., 2001). Second, these proteins have no effect on G1/S-Cdks; as a result, they have no inhibitory effect on the activity these kinases at Start (Mendenhall, 1993; Weinreich et al., 2001). Finally, these inhibitors are all targeted for destruction by proteolysis when phosphorylated by Cdks (Borg et al., 2007; Nash et al., 2001; Verma et al., 1997). In late G1, G1/S-Cdk activity increases therefore leads to destruction of these inhibitors turning on S-Cdk activation at the beginning of S phase. Given the clear importance of Sic1 and Rum1 in yeast, it is perhaps surprising that a clear functional homolog of these proteins has not been identified in mammalian cells. However, animal cells do possess another CKI protein called p27 in mammals that helps govern Cdk activity in G1, although by mechanisms that are somewhat distinct from those used by yeast Sic1 (Barberis et al., 2005; Brocca et al., 2009). Most importantly, p27 inhibits G1/S-Cdks (cyclin E-Cdk2) as well as the S-Cdk cyclin A-Cdk2, but has relatively little effect on the M-Cdk cyclin B-Cdk1. Thus, in mammals the rise of G1/S-Cdks in late G1 requires the removal of p27, which is achieved by a combination of mechanisms. First, the G1-Cdks (cyclin D-Cdk4) remove p27 from G1/S-Cdks. Second, p27 is destroyed in late G1 as a result of phosphorylation by multiple protein kinases, including the G1/S-Cdks themselves (Sherr & Roberts, 1999). Other CKIs help promote G1 arrest in response to specific inhibitory signals. Far1 in budding yeast (Peter et al., 1993; Peter & Herskowitz, 1994) and the INK4 proteins of

mammals inhibit G1-Cdk activity when cells encounter anti-proliferative signals in the environment (Hirai et al., 1995). The p21 protein from mammals blocks G1/S- and S-Cdks, and thus cell cycle entry, in response to DNA damage, giving the cell time to repair the damage before starting to replicate its DNA.

The CKIs of animal cells are grouped into two major families, based on their structures, CDK targets and mechanism of Cdk inhibition (Table 5). The first class includes the INK4 proteins (inhibitors of CDK4), so named for their ability to specifically inhibit the catalytic subunits of CDK4 and CDK6. Four such proteins [$p16^{INK4a}$ (Serrano et al., 1993), $p15^{INK4b}$ (Hannon & Beach, 1994), $p18^{INK4c}$ (Guan et al., 1994; Hirai et al., 1995), and $p19^{INK4d}$ (Chan et al., 1995; Hirai et al., 1995)] are composed of multiple ankyrin repeats and bind only to CDK4 and CDK6 but not to other CDKs or to D-type cyclins. The second class includes the Cip/Kip family whose actions affect the activities of cyclin D-, E-, and A-dependent kinases. The latter class includes $p21^{Cip1}$ (Dulić et al., 1994; el-Deiry et al., 1993; Gu et al., 1993; Harper et al., 1993; Noda et al., 1994; Xiong et al., 1993), $p27^{Kip1}$ (Polyak et al., 1994a; Polyak et al., 1994b; Toyoshima & Hunter, 1994), and $p57^{Kip2}$ (Lee et al., 1995; Matsuoka et al., 1995), all of which contain characteristic motifs within their N-terminal moieties that enable them to bind both to cyclin and CDK subunits (Chen et al., 1995; Chen et al., 1996; Lin et al., 1996; Nakanishi et al., 1995; Russo et al., 1996; Warbrick et al., 1995). The N-terminal half of the mammalian Cip/Kip proteins p21 and p27 is responsible for their Cdk inhibitory function and is composed of two key subregions: a short segment containing an RXL motif for cyclin binding, and a longer segment for Cdk binding. The structure of the Cdk2-cyclin A-p27 complex reveals the Cdk-binding region of p27. These interactions completely disrupt the catalytic function of the Cdk enzyme through partial distortion of the structure of the kinase N-terminal lobe above the active site, and also through direct blocking of the ATP-binding site, In contrast to Cip/Kip proteins, members of the INK4 family are inhibitors of only Cdk4 and Cdk6, binding preferentially to the Cdk monomer. Crystallographic structural studies indicate that these inhibitors bind both N-terminal and C-terminal lobes of the Cdk on the side opposite the cyclin-binding site, disrupting the binding and orientation of ATP. The INK4 protein also twists the upper lobe of the kinase into an orientation that is incompatible with cyclin binding.

Cdk Inhibitors				
Species	**Name**	**Alternatives**	**Relatives**	**Targets, function**
S. cerevisiae	Sic1		Rum1	inhibits S– and M–Cdks, suppresses Cdk activity in G1
	Far1		no relatives	inhibits G1/S–Cdk in response to mating pheromone
S. pombe	Rum1		Sic1	inhibits S– and M–Cdks, suppresses Cdk activity in G1
H. sapiens	p21	Cip1/Waf1	Cip/Kip	inhibits G1/S– and S–Cdks, activates cyclin D–Cdk4
	p27	Kip1	Cip/Kip	inhibits G1/S– and S–Cdks, activates cyclin D–Cdk4
	p57	Kip2	Cip/Kip	inhibits G1/S– and S–Cdks, activates cyclin D–Cdk4
	$p15^{INK4b}$		INK4	inhibits Cdk4, Cdk6
	$p16^{INK4a}$		INK4	inhibits Cdk4, Cdk6
	$p18^{INK4c}$		INK4	inhibits Cdk4, Cdk6
	$p19^{INK4d}$		INK4	inhibits Cdk4, Cdk6

Table 5: Cdk Inhibitors the cell cycle in yeast and *H. sapiens*
Adapted from Morgan (2007)

Switch-like activation of Cdk

The activation of G1/S-, S- and M-Cdks all display switch-like behavior based on ultrasensitive and feedback mechanisms. In budding yeast, a major consequence of the initiation of G1/S gene expression is the increased production of both G1/S cyclins and S cyclins. The G1/S cyclins Cln1 and Cln2 immediately form active complexes with Cdk1. The S cyclins Clb5 and Clb6 also bind Cdk1, but these S-Cdks are held in the inactive state by the Cdk inhibitor Sic1, which is abundant in G1 cells and specifically inhibits Clb-Cdk1 complexes but not Cln-Cdk1 complexes.

The major function of the G1/S-Cdks is to trigger the activation of the S-Cdks by promoting the destruction of Sic1. Because of the high levels of Sic1 in G1, a stockpile of inactive S-Cdk1-Sic1complexes accumulates as the cell approaches S phase (Figure 7). Sic1 is then phosphorylated at multiple sites by the rising wave of Cln1,2-Cdk1 activity. Phosphorylation of Sic1 triggers its destruction, thereby unleashing the Clb5,6-Cdk1 complexes and triggering the onset of chromosome duplication. Clb5,6-Cdk1 complexes exert a positive feedback loop through Sic1phosphorylation, so Clb5,6-Cdk1 complexes promote their own activation through inhibiting their own inhibitor Sic1, the destruction of phosphorylated Sic1 depends on its ubiquitination by SCF, a ubiquitin-protein ligase that collaborates with the ubiquitin-conjugating enzyme Cdc34 to promote the destruction of several cell cycle regulatory proteins (Harper, 2002; Kõivomägi et al., 2011; Nash et al., 2001; Verma et al., 2001). Phosphorylated Sic1p is bound by Cdc4p, which is the substrate recognition subunit of the E3 ligase, SCF-Cdc4

(Deshaies & Ferrell, 2001; Skowyra et al., 1997). In conjunction with the E2 enzyme Cdc34p, SCF-Cdc4 polyubiquitinates Sic1p on N-terminal residues (Feldman et al., 1997; Petroski & Deshaies, 2003; Sadowski et al., 2010; Verma et al., 1997).The activation of cyclin B-Cdk1, a vertebrate M-Cdk that triggers spindle assembly and other early events at the onset of mitosis is the best understood example of a biochemical switch in cell cycle control (Figure 8). In eukaryotes, mitosis is driven by the cyclin B1-Cdk1 complex (Morgan, 2007).

The enzymatic activity of cyclin B1-Cdk1 depends upon the phosphorylation state of Cdk1: a conserved threonine residue in the activation loop (Thr 161 in human Cdk1) must be phosphorylated, and two sites in the ATP binding pocket (Thr14 and Tyr15 in human Cdk1) must be dephosphorylated. Kinases of the Wee1/Myt1 family phosphorylate Thr14 and Tyr15 (Booher et al., 1997; Fattaey & Booher, 1997; Heald et al., 1993; Liu et al., 1997; McGowan & Russell, 1993; Mueller et al., 1995; Parker & Piwnica-Worms, 1992). Phosphatases of the Cdc25 family dephosphorylate both of these sites (Millar et al., 1991; Strausfeld et al., 1991). Thus Cdc25 phosphatase is an activator of Cdk1, and Wee1 and Myt1 are inactivators. Wee1 and Cdc25 not only regulate Cdk1, they are also regulated in turn by Cdk1. The same is true of Myt1 protein (Booher et al., 1997; Fattaey & Booher, 1997; Liu et al., 1997; Mueller et al., 1995; Palmer et al., 1998); Cdk1 phosphorylates and activates Cdc25 (Hoffmann et al., 1993; Kumagai & Dunphy, 1992; Solomon et al., 1990), on the contrary Cdk1 phosphorylates and inhibits Wee1 (McGowan & Russell, 1995; Mueller et al., 1995).

The addition of Wee1 and Cdc25 to the system creates a switch-like Cdk1 activation, because Cdk1 activity inhibits Wee1 and stimulates Cdc25, resulting in a positive feedback, where the Cdk1/Wee1/Cdc25 system can be viewed as two interlocking, mirror-image feedback loops (Figure 8).

4. Cell cycle transcriptional regulation

Oscillations in Cdk activity during the cell cycle are driven not only by mechanisms involving protein phosphorylation, subunit binding and regulated proteolysis, but also by changes in the transcription of regulatory genes.

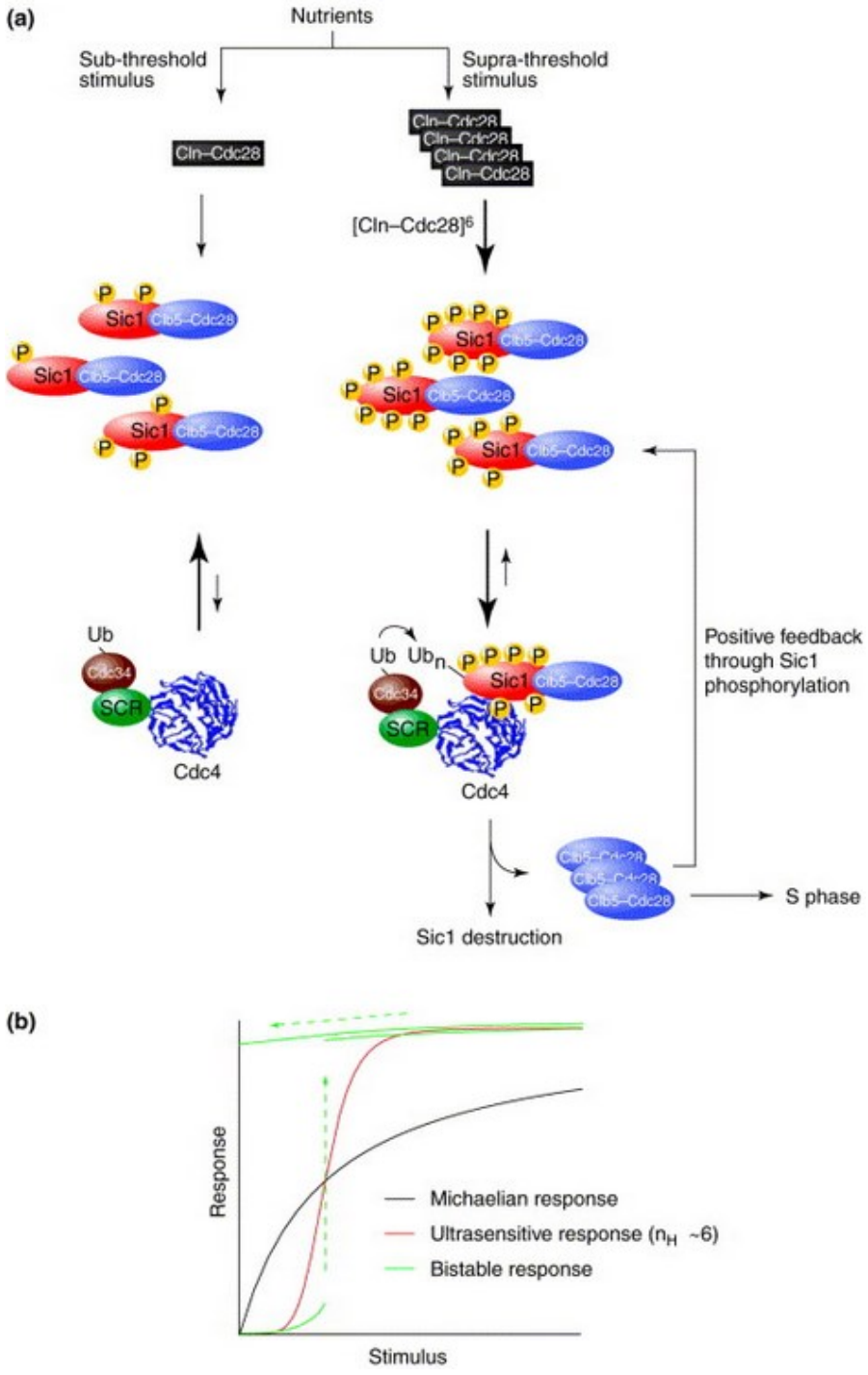

Figure 7: Multisite phosphorylation of Sic1 results in an ultrasensitive response

(a) Nutrient levels determine the extent of Cln–Cdc28 kinase activity. At sub-threshold level of nutrients, Sic1 is poorly phosphorylated on suboptimal Cdc4 phospho-degron (CPD) motifs. In the presence of sufficient Cln–Cdc28, Sic1 is phosphorylated on many sites, which supports ubiquitination by increasing the probability of a productive interaction between Sic1 and the E3 ubiquitin ligase SCF^{Cdc4}. The requirement for multiple phosphorylated sites produces an ultrasensitive stimulus–response profile. Activation of Clb5–Cdc28 upon Sic1 degradation allows further phosphorylation of Sic1 to further steepen the ultrasensitivity profile.

(b) Theoretical sensitivity plots for Sic1-CPD (Michaelian), Sic1 without positive feedback from Clb5–Cdc28 [Hill coefficient (n_H) ~6], and a bi-stable system generated by the combination of ultrasensitivity and positive feedback. Adapted from Harper (2002).

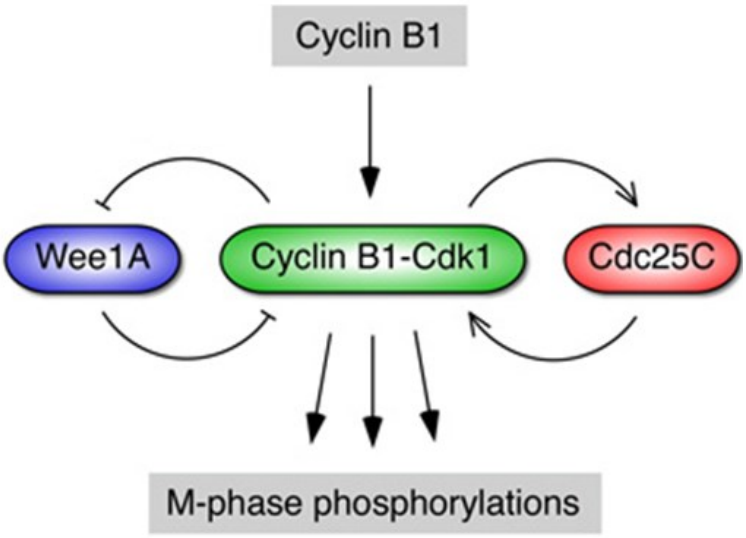

Figure 8: Schematic view of the regulation of cyclin B1-Cdk1 activity by cyclin B1, Wee1, and Cdc25C

Functions for Wee1 and Cdc25C account for the bistability of the mitotic trigger. Adapted from Trunnell et al. (2011).

Regulation of gene transcription is particularly important in controlling synthesis of the cyclins, in *S. cerevisiae*, a significant fraction of genes (>10%) are transcribed with cell cycle periodicity (Cho et al., 1998; Spellman et al., 1998). These genes encode critical cell cycle regulators as well as proteins with no direct connection to cell cycle functions. These genes can be organized into clusters exhibiting similar patterns of periodic transcription, which are achieved via both repressive and activating mechanisms, and are ruled by CDKs and a network of transcription factors that has an oscillatory property by itself (Orlando et al., 2008; Wittenberg & Reed, 2005). The main transcriptional control clusters are the G1, the S-phase, the Clb2 and the M-G1 clusters.

The G1 gene cluster

The G1-gene cluster is triggered at Start and the consequence is transcriptional activation of greater than 200 genes, many of which associated with cell cycle progression (Cho et al., 1998; Spellman et al., 1998). The G1-specific gene cluster are targeted by two heterodimeric transcription factors comprised of unique DNA-binding components, Swi4 (SBF) or Mbp1 (MBF), and a common component, Swi6, that works as

transcription cofactor. The binding site for MBF is called MCB (Mlu Cell cycle Box), due to the presence of an *Mlu*I restriction site in the consensus sequence, and that for SBF is SCB (Swi4 Cell cycle Box).The target genes for SBF and MBF have been traditionally defined by the presence of redundant SCB and MCB sequences in their promoters. Functionally, SBF and MBF targets, respectively, fall roughly into two classes. MBF targets include those involved in the control or execution of DNA replication and repair (*POL2*, *CDC2*, *RNR1*, *CLB5/6*), whereas SBF targets include those involved in cell morphogenesis, spindle pole body duplication and other growth-related functions (*CLN1/2*, *PCL1/2*, *GIN4*, *FKS1/2*) (Koch et al., 1993; Nasmyth & Dirick, 1991; Slansky & Farnham, 1996).

Cln3-Cdc28 is the primary activator of G1-specific transcription under physiological conditions (Dirick et al., 1995; Stuart & Wittenberg, 1995; Tyers et al., 1993). Later on it was shown that any of the three G1 cyclins (Cln1, Cln2, or Cln3) in conjunction with Cdc28 were sufficient to initiate Cdk1-dependent activation of G1-specific transcription (Cross & Tinkelenberg, 1991; Dirick et al., 1995). In late G1, the activity of the G1-Cdk, Cln3-Cdk1, promotes the inhibitory phosphorylation of Whi5, thereby unleashing active SBF and MBF (Costanzo et al., 2004; De Bruin et al., 2004) results in the increased expression of a large group of G1/S genes, including the genes encoding G1/S and S-cyclins. Thus, the activation of SBF and MBF promotes G1/S- and S-phase Cdk activities, and Cln1,2-Cdc28 activities further reinforce SBF and MBF activation through a positive feedback loop that involves phosphorylation of Whi5 (Cross & Tinkelenberg, 1991; Dirick & Nasmyth, 1991; Skotheim et al., 2008) to ensure coherent activation (Figure 9a and 9c).

Analysis of the transcriptional machinery regulating the G1/S gene clusters of yeast and mammals reveals strong conservation of the transcriptional machinery regulating the G1/S gene clusters (Figure 9b and 9c). Despite the high degree of conservation of the topology of these regulatory circuits, the transcription factors exhibit little or no relatedness in terms of either amino acid sequence or structure (Bertoli et al., 2013).

The S-phase gene clusters

The G1/S transition, characterized by the initiation of DNA replication, is accompanied by the activation of two clusters of S phase genes. One cluster represents the genes

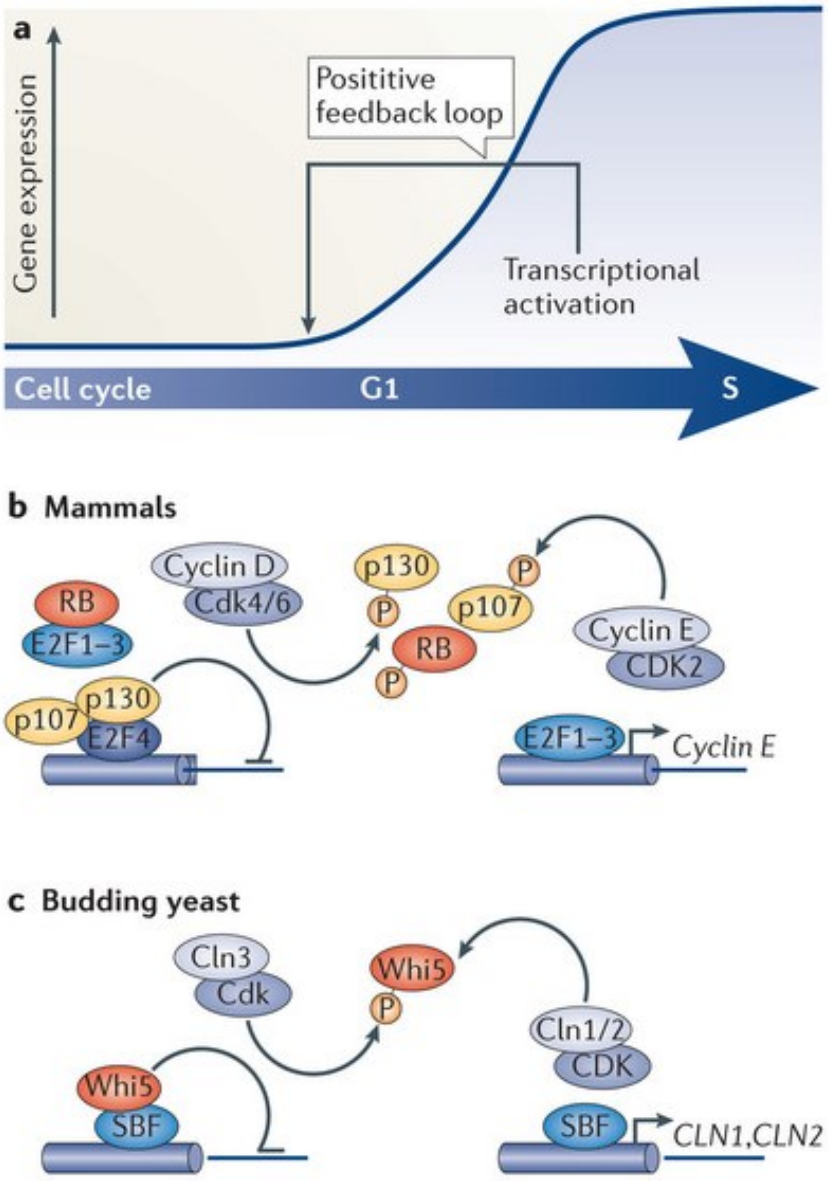

Figure 9: Conservation of the G1/S transcriptional activation in yeast and mammals

(a) Schematic showing how the G1–S transcriptional program, once initiated, is reinforced by a positive feedback loop.

(b) In mammalian cells, the transcriptional repressors RB, p107 and p130 (collectively known as pocket proteins) are bound to E2F transcription factors to repress expression during early G1. Pocket proteins either prevent activator E2F proteins (such as E2F1, E2F2 and E2F3) to activate transcription or function as co-repressors for repressor E2F proteins (such as E2F4). Phosphorylation of pocket proteins by cyclin D– cyclin-dependent kinase 4 (CDK4) and cyclin D–CDK6 probably releases them from the E2F transcription factors. This induces the transcription of G1–S target gene; including the gene encoding cyclin E. Cyclin E–CDK2 phosphorylates pocket proteins, thereby providing a positive feedback loop.

(c) Model depicting G1–S transcriptional activation in budding yeast. In early G1, transcription is inhibited by Whi5 binding to the SBF (SCB-binding factor) complex at target promoters. Cln3–Cdk relieves transcriptional inhibition by phosphorylating Whi5, which induces its nuclear export and thereby G1–S transcription. Activation of transcription results in the accumulation of Cln1 and Cln2, which in complex with Cdk, further inactivate Whi5 through phosphorylation. This provides positive feedback that results in cell cycle commitment. Adapted from Bertoli et al. (2013)

encoding the histones, which make up the nucleosomes that package newly replicated DNA and the S phase cluster that represents the other genes expressed during S phase.
Histone genes are regulated by, as yet, poorly understood transcriptional regulatory mechanism involving SBF/MBF, Spt10, histone chaperones, and other factors. The S phase cluster, the second, much larger cluster, is regulated by Hcm1. Major bursts of cell cycle-regulated gene expression, Hcm1 plays a central role in that regulatory circuitry. It is one of four members of the forkhead family of transcription factors found in budding yeast (Hcm1, Fkh1, Fkh2, and Fhl1 (Forkhead-like) (Murakami et al., 2010). Like the other members of that family, which include mammalian Fox transcription factors, Hcm1 binds DNA directly via a winged helix DNA-binding motif. Hcm1 found to be phosphorylated by Clb/Cdk1 *in vitro* due to the presence of putative CDK phosphorylation sites in Hcm1, this suggests Hcm1 a likely target of the Cdk1 protein kinase (Ubersax et al., 2003).
The Hcm1 transcription factor appears to regulate ~180 genes based upon the timing of their expression and the presence of the Hcm1-binding site in their promoters (Pramila et al., 2006). However, only a small fraction of those genes were found to bind Hcm1 by genome wide chromatin immunoprecipitation (Horak et al., 2002).

The Clb2 cluster

Also called G2/M gene cluster is accompanied by activation of a family of ~35 genes falling into the G2/M cluster (Cho et al., 1998; Spellman et al., 1998), This set of genes has been termed the 'Clb2 cluster' based on the *CLB2* mitotic cyclin gene, which had previously been shown to exhibit these mRNA kinetics (Ghiara et al., 1991; Surana et al., 1991). Other members of this family include *CLB1* (another M cyclin gene), *CDC5* (the yeast polo-like kinase homolog), *CDC20* (a mitotic specificity factor for the APC protein–ubiquitin ligase), and *SWI5* and *ACE2* (transcription factors required for late M-early G1-specific gene expression). Interestingly, it was through analysis of the *SWI5* promoter that insight into regulation of this gene cluster was first obtained. A protein complex known as Swi5 factor (SFF) was shown to be capable of binding to specific elements in the *SWI5* promoter (Lydall et al., 1991). More recent work on *SWI5* and other cluster genes, notably *CLB2*, has revealed that SFF sites are binding sites for members of the forkhead transcription factors (Kumar et al., 2000; Pic et al., 2000). The primary regulator of this gene cluster is the MADS box transcription factor Mcm1, in conjunction

with the forkhead family member Fkh2 and the coactivatorNdd1, both members of the S phase gene cluster regulated by Hcm1 (Kumar et al., 2000; Loy et al., 1999). The collaboration of Mcm1with Fkh2 in the context of transcriptional regulation of the G2/M cluster is, in part, a consequence of the occurrence of adjacent Mcm1- and Fkh2-binding sites in G2/M cluster promoters (Boros et al., 2003; Lydall et al., 1991). The association of that heterodimer with the adjacent binding sites on those genes opens the way for associations of the coactivator Ndd1 to activate gene expression. Whereas other forkhead family members possess the capacity to bind to the DNA via their conserved winged helix motif, only Fkh2 can also associate directly with Mcm1 and thereby exert its effect on gene expression in that context. Interestingly, this binding interface has been conserved sufficiently for Fkh2 to bind to the human serum response factor (SRF), the homolog of Mcm1 (Boros et al., 2003). Fkh1, which lacks the Mcm1 interaction domain of Fkh2, binds to the same DNA motif as Fkh2 at *CLB2* cluster promoters, but only in the absence of Mcm1 (Hollenhorst et al., 2001; Koranda et al., 2000). Phosphorylation of Ndd1by both Clb2/Cdk1 and Cdc5 polo-like kinase appears necessary for efficient recruitment to the Fkh2 FHA domain and robust activation of Clb2 cluster genes (Darieva et al., 2006, 2012; Pic-Taylor et al., 2004; Reynolds et al., 2003). The requirement for Ndd1 phosphorylation constitutes a positive feedback loop, wherein both Clb2 and Cdc5, when expressed as G2/M cluster genes, activate and loop over their own gene expression

The M to early G1 cluster

A large number of yeast genes required for G1 functions like MCM proteins involved in prereplication complex assembly, transcription factors required for *G1* gene expression and proteins involved in the yeast mating response, which occurs during G1 are expressed from M phase to early G1 (Cho et al., 1998; Spellman et al., 1998). However, some other non G1-specific function proteins (e.g., genes of the PHO regulon) also follow the same expression pattern (Cho et al., 1998; Spellman et al., 1998).

The largest group of M-G1 genes periodicity are those driven by the Mcm1 (Nurrish & Treisman, 1995; Shore & Sharrocks, 1995). Unlike the Clb2 cluster of genes that also require Mcm1 binding, the so-called MCM cluster genes do not contain sites for Fkh1/2 binding. This explains why deletion of *FKH1* and *FKH2* has no effect on these genes (Zhu et al., 2000). Instead, most of these genes contain a site for binding the homeodomain

repressors Yox1 and Yhp1 (Pramila et al., 2002) in close proximity to a palindromic site capable of binding an Mcm1 dimer, known as an ECB (early cell cycle box) (McInerny et al., 1997). In addition, Yox1 and Yhp1 can bind directly to Mcm1 (Pramila et al., 2002), presumably promoting cooperativity. It is the occupancy of these repressive sites that blocks Mcm1-mediated transcription through most of the cell cycle, and it is the periodic transcription of the genes encoding these presumably unstable repressors that determines their functional interval. Yox1 is expressed in mid-G1 through early S phase (Horak et al., 2002; Pramila et al., 2002; Spellman et al., 1998), whereas Yhp1 appears to be expressed later in the cell cycle (Cho et al., 1998; Spellman et al., 1998), leaving an interval from M phase to early G1 without occupation by repressors. So, Mcm1 can apparently drive transcription of these genes without DNA binding of additional activating proteins during this window. The second class of M-G1 expressed genes is the Sic1 cluster (the G1-Cdk inhibitor). Deletion of *FKH1* and *FKH2* affects periodic expression of these genes (Zhu et al., 2000). Yet, Fkh1 and Fkh2 do not bind the promoters of these genes. The basis for the indirect requirement for *FKH* genes is the assignment of transcription factors Swi5 and Ace2 to the Clb2 cluster (Nasmyth et al., 1987; Spellman et al., 1998). Genes of the Sic1 cluster contain related consensus sites that bind Ace2 and Swi5 (Zhu et al., 2000). The relationship between Ace2 and Swi5, however, is complex. Although both transcription factors recognize the same set of sites on target genes, their effect on such genes can vary from activation to repression (Dohrmann et al., 1996; McBride et al., 1999). The ability of these factors to bind co-activators and co-repressors targeted to the Sic1 genes cluster could explain for this differential behavior.

A third group of M-G1 activated genes are those that are normally induced by mating pheromone, the MAT cluster (Spellman et al., 1998). It has been shown that the periodic expression of these genes depends on a DNA sequence known as PRE (pheromone response element) and a PRE-binding transcription factor, Ste12 (Oehlen et al., 1996). Upon receptor-mediated activation of the pheromone response pathway, the MAP kinase homolog Fus3 activates Ste12 in one hand by direct phosphorylation of Ste12 and indirectly by inactivating Dig1 and Dig2 two co-repressors of Ste12 (Bardwell et al., 1998; Breitkreutz et al., 2003; Kusari et al., 2004; van Drogen et al., 2001).

5. Ubiquitination and proteolysis during cell cycle

Unidirectional and irreversible transitions from one phase to the next during cell cycle are achieved in one hand through mechanisms that provide all-or-none, irreversible Cdk activation and on the other hand by the proteolytic destruction of regulatory proteins. Proteolysis is particularly critical at the metaphase-to-anaphase transition, where sister-chromatid separation and mitotic exit are triggered by the irreversible destruction of M cyclins and proteins that control sister-chromatid cohesion. Destruction of cyclins also helps establish the state of low Cdk activity in G1. In addition, at the end of G1, where the destruction of Cdk inhibitor proteins helps drive the irreversible activation of S-Cdks. Cyclins, Cdk inhibitor proteins and other cell cycle regulators are targeted for degradation by the attachment of multiple copies of the small protein ubiquitin, in a process known as ubiquitination (Hershko & Ciechanover, 1998).

Ubiquitinated proteins are recognized and destroyed by giant protease complexes called proteasomes. Ubiquitination is carried out in a series of reactions, in the first step, ubiquitin activation; ubiquitin is covalently attached through its carboxyl terminus to the sulfhydryl group of a cysteine in the active site of the ubiquitin-activating enzyme (E1). This reaction is powered by ATP hydrolysis. The E1-ubiquitin conjugate then interacts with a ubiquitin-conjugating enzyme (E2) that catalyzes the transfer of the ubiquitin to an active-site cysteine in E2. The final step is the transfer of the ubiquitin to the target protein. This depends on a third enzyme, the ubiquitin-protein ligase (E3), which helps catalyze transfer of ubiquitin from the E2-ubiquitin conjugate, to the amino group of a lysine side chain in the target protein. Remarkably, a single ubiquitin-protein ligase molecule bound to the target protein can catalyze the successive transfer of several ubiquitin molecules, resulting in the ubiquitination of multiple lysines in the target. In addition, ubiquitin-protein ligases catalyze the attachment of ubiquitin to lysine residues within ubiquitin itself, resulting in the formation of long polyubiquitin chains on the target. These are recognized by receptors on the proteasome, which then binds the target protein and destroys it by proteolysis (Figure 10).

The SCF complex

The SCF (Skp1–Cullin–F-box protein) and SCF-like complexes are the largest family of ubiquitin–protein ligases and ubiquitinate a broad range of proteins involved in cell

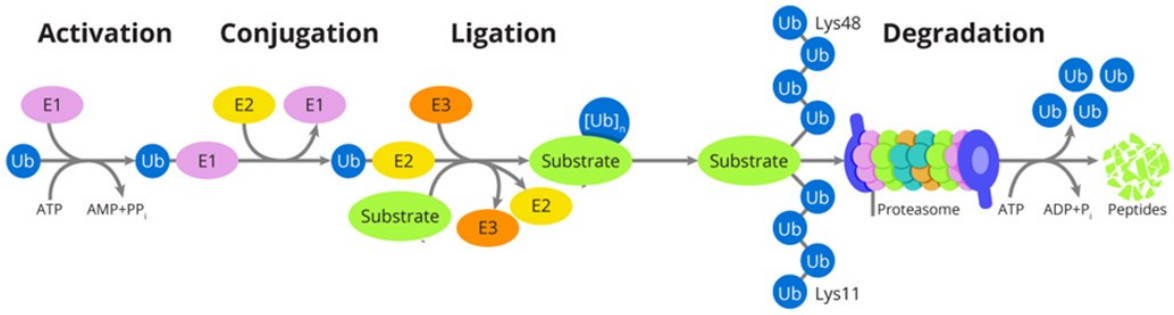

Figure 10: Schematic diagram of the ubiquitination system

Two large, multisubunit ubiquitin-protein ligases are crucial for the G1/S and metaphase-to-anaphase transitions. For the ubiquitination and proteolysis of targets such as Cdk inhibitors at the G1/S transition, the key ubiquitin-protein ligase is an enzyme called SCF. The anaphase-promoting complex (APC) or cyclosome that promotes metaphase-to-anaphase transition, APC is turned off on S phase and switched on during anaphase to exit from mitosis (DeSalle & Pagano, 2001; Zachariae & Nasmyth, 1999).

cycle progression, signal transduction and transcription (Deshaies, 1999; Koepp et al., 1999). In budding yeast SCF complex contains three core subunits: F-box binding protein Skp1, a scaffold protein Cullin or Cdc53 and interchangeable F-box protein. SCF complexes are composed of several shared subunits including Skp1, an adaptor protein that binds and recruits a variety of F-box containing proteins (Bai et al., 1996; Skowyra et al., 1997); Cdc53, a cullin family member that recruits the ubiquitin conjugating enzyme Cdc34 to Skp1/F-box proteins (Mathias et al., 1996; Patton et al., 1998; Willems et al., 1996); Hrt1, a RING-H2 domain protein that stimulates ubiquitin ligase activity (Ohta et al., 1999; Seol et al., 1999); and Cdc34, a ubiquitin-conjugating enzyme that catalyzes the transfer of activated ubiquitin to the target protein (Goebl et al., 1988; Seol et al., 1999; Skowyra et al., 1997). In addition, to these shared subunits, SCF complexes also contain one of several unique F-box motif containing proteins, including Cdc4, Grr1, Met30, Dia2, or Saf1, that function as substrate specific adaptors or specificity determinants recruiting multiply phosphorylated substrates to the SCF core complex (Craig & Tyers, 1999; Patton et al., 1998; Willems et al., 1999). SCF promotes the G1/S transition and G2/M phase transitions of the mitotic cell cycle, SCF ubiquitinates and degrades G1 cyclins Cln1 & Cln2 (Barral et al., 1995; Willems et al., 1996), S -phase cyclins Clb6 (Jackson et al., 2006), CDK inhibitors Sic1& Far1 (Blondel et al., 2000;

Feldman et al., 1997; Henchoz et al., 1997; Skowyra et al., 1997), Swe1(Wee1 homolog in budding yeast) (Kaiser et al., 1998) and proteins involved in DNA replication like Cdc6 (Drury et al., 1997; Sánchez et al., 1999).

SCF is active throughout the cell cycle and the degradation of its substrates is controlled at the level of phosphorylation, which in many cases is mediated by Cdk activity (Nash et al., 2001).

The APC complex

The anaphase-promoting complex (APC): an E3 ubiquitin ligase in the ubiquitin-mediated proteolysis pathway (Zachariae & Nasmyth, 1999). The APC regulates the metaphase/anaphase transition and exit from mitosis/G1 entry through ubiquitination of various substrates including M phase cyclins, the sister chromatid separation inhibitor Pds1(Securin), the Kip1 and Cin8 motor proteins, Cdc5p, and the spindle disassembly factor, Ase1 (Cohen-Fix et al., 1996; Gordon & Roof, 2001; Juang et al., 1997; Shirayama et al., 1998). Ubiquitination by the APC is controlled by activator subunits that bind the APC core at different stages of the cell cycle. Two conserved activators, Cdc20 and Cdh1, are particularly important regulates the activity and substrate specificity of the APC.

Cdc20 activates the APC at the metaphase-to-anaphase transition to allow sister-chromatid segregation and to initiate the exit from mitosis (Visintin et al., 1997). The levels of Cdc20 are cell cycle regulated accumulating in S phase, peak in mitosis due to transcriptional upregulations by Clb-Cdk and finally drop in G1 due to degradation by APC^{Cdh1} (Pesin & Orr-Weaver, 2008; Prinz et al., 1998).

At metaphase, APC is activated through phosphorylation of APC core subunits by M-Cdks and also Cdc5 polo like kinase (Rudner & Murray, 2000), which enhances Cdc20 binding. APC^{Cdc20} then targets Pds1 and the M cyclins for destruction, thereby inactivating M-Cdks. Thus, M-Cdks initiate the chain of events that lead to their eventual destruction, resulting in a negative feedback loop. APC activation and cyclin destruction follow M-Cdk activation only after a delay, so that premature destruction of cyclins does not occur early in mitosis. Because APC activation by Cdc20 depends on phosphorylation of the enzyme by, M-Cdk inactivation leads to decreased phosphorylation of the APC, dissociation of Cdc20 and the consequent inactivation of the APC. Thus APC^{Cdc20}, like M-Cdk, promotes its own inactivation. By the end of mitosis, APC^{Cdc20} is no longer active.

Cdh1, another APC activator, is a homolog of CDC20 then activates the APC in late mitosis and early G1 to maintain cyclin destruction until entry into the next cell cycle (Visintin et al., 1997; Zachariae & Nasmyth, 1999). Unlike Cdc20, does not require the APC to be phosphorylated in order to bind, Cdh1 is expressed throughout cell cycle and is held inactive by Clb-Cdc28-dependent phosphorylation from S phase to metaphase. The active APC^{Cdh1} complex therefore forms only when Cdks are inactivated by APC^{Cdc20} at the metaphase-to-anaphase transition, allowing Cdh1 to be dephosphorylated by Cdc14, upon activation of the Mitotic Exit Network (MEN) (Jaspersen et al., 1999; Zachariae & Nasmyth, 1999). APC^{Cdh1} activity remains high throughout G1, ensuring that S and M cyclin destruction and therefore S- and M-Cdk inactivity continues until the cell is committed to another cell cycle. G1/S cyclins, however, are not recognized by APC^{Cdh1}. Thus the activity of G1/S-Cdks rises unopposed in late G1 and they phosphorylate Cdh1, thereby inactivating the APC until the next metaphase (Figure 11).

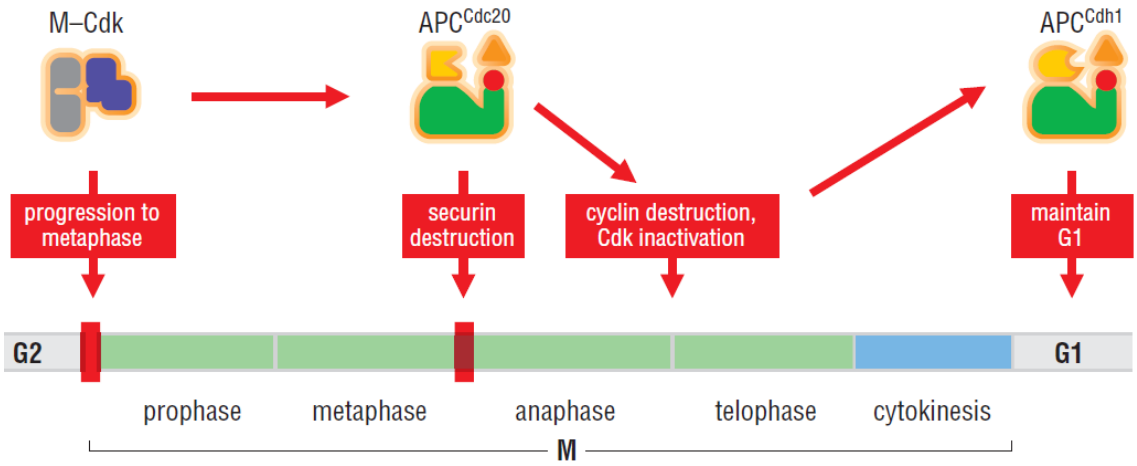

Figure 11: Control of late mitotic events by the APC

M-Cdk activity promotes early mitotic events, resulting in the metaphase alignment of sister chromatids on the spindle. M-Cdk activity also promotes the activation of APC^{Cdc20}, which triggers anaphase and mitotic exit by stimulating the destruction of regulatory proteins, such as securin and cyclins that govern these events. By promoting cyclin destruction and thus Cdk inactivation, APC^{Cdc20} also triggers activation of APC^{Cdh1}, thereby ensuring continued APC activity in G1. Adapted from Morgan (2007)

6. Start execution in *S. cerevisiae*

Cell size can be considered as the outcome of complex parallel and interconnected processes that convey different sorts of intrinsic and extrinsic information. Of all these processes, cell growth and cell cycle are particularly relevant as they likely apply to all organisms, and their efficient and precise coordination is a fundamental biological

problem (Baserga, 2007; Cook & Tyers, 2007; Cooper, 2004; Donachie & Blakely, 2003; Grebien et al., 2005; Mitchison, 2003; Zaritsky et al., 2007). As a unicellular eukaryote, *S. cerevisiae* has been widely used to study the mechanisms that determine cell size, mainly because this budding yeast displays two of the most universal properties regarding cell size control, a constant mass/ploidy ratio (Mortimer, 1958) and a critical size threshold for cell cycle progression (Hartwell & Unger, 1977; Johnston et al., 1977), which is mainly exerted at Start, a key event in late G1. Two heteromeric transcription factors (Nasmyth, 1996), SBF (Swi6–Swi4) and MBF (Mbp1–Swi6), drive a transcriptional wave of ~200 genes (Futcher, 2002) at Start to initiate budding and trigger S-phase entry. The most upstream activator of Start is a complex formed by Cln3 (Cross, 1988; Dirick et al., 1995; Nash et al., 1988; Sudbery et al., 1980), a G1 cyclin, and Cdc28 (Mendenhall & Hodge, 1998), the cyclin-dependent kinase that controls the cell cycle in budding yeast. The Cdc28–Cln3 complex phosphorylates Whi5 (and presumably Swi6) at multiple residues to activate SBF- and MBF-dependent transcription (De Bruin et al., 2004). Two other G1 cyclins, Cln1 and Cln2, are upregulated by SBF and have a key role with Cdc28 in a positive feedback loop essential for coherent and irreversible execution of Start (Dirick & Nasmyth, 1991; Skotheim et al., 2008). The Cln3 cyclin is present at constant levels throughout G1 (Tyers et al., 1993) and it is regulated by a retention/release mechanism that prevents its unscheduled accumulation in the nucleus (Aldea, 2007). Whi3, first identified as a negative regulator of Cln3 activity (Nash et al., 2001), binds the *CLN3* mRNA and recruits Cdc28 to help retain newly formed Cdc28–Cln3 complexes at the endoplasmic reticulum (ER) during early and mid G1 (Wang et al., 2004). In late G1, the Ydj1 chaperone has an essential role in releasing Cln3 or the Cdc28–Cln3 complex from the ER (Vergés et al., 2007), which allows its accumulation in the nucleus to phosphorylate Whi5 and trigger Start (Figure 12). On the other hand, and in addition to its role at Start, Ydj1 is heavily involved in protein translocation across the ER membrane (Caplan et al., 1992), a key process for cell growth.

These lines of evidence suggest that the critical size could be set by mechanisms intimately linked to cell growth (Aldea, 2007). Although it is generally accepted that budding yeast cells must grow to reach a critical size before cell cycle entry (Hartwell & Unger, 1977; Johnston et al., 1977; Jorgensen & Tyers, 2004), cell volume at Start displays a very large variability under constant conditions (Lord & Wheals, 1981), which strongly argues against the existence of a deterministic mode of cell size control. This

key question has been analysed recently at a single-cell level, and it was proposed that cell size variability at Start is mainly due to molecular noise intrinsic to the mechanisms that activate the G1/S regulon (Di Talia et al., 2007), or due to variability at the volume growth rate in G1 (Ferrezuelo et al., 2012), but still the molecular mechanisms behind size control a hot topic for discussion and research and here we try to characterize new regulators of cell size during early stages of cell cycle in *S. cerevisiae* .

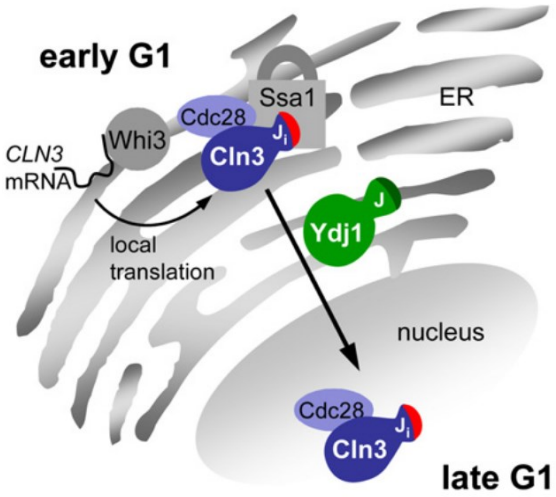

Figure 12: Cln3 retention at the ER is modulated during G1 by the J_i domain and the Ydj1 chaperone

G1 cyclin Cln3 retention at the ER is modulated during G1 by the J_i domain and the Ydj1 chaperone. By inhibiting the Hsp70 conformational cycle, the J_i domain would lock Ssa1,2 chaperones into a tightly associated ER complex with Cdc28 in early G1, thus preventing unscheduled nuclear import of Cln3. In late G1, once a relative surplus of Ydj1 (and most likely other folding activities) is achieved, ATPase activation by Ydj1 would unlock the Ssa1,2 complex and trigger ER release and nuclear accumulation of Cln3 to initiate cell cycle entry. Adapted from Vergés et al. (2007).

7. *Wee* and *whi* mutants

Working with the fission yeast *S. pombe* in the 1970s, Paul Nurse and colleagues identified mutants that divided at an abnormally small size and called them “wee” after the Scottish word for small. Analysis of these mutants was instrumental in elucidating regulation of the cell cycle in fission yeast by the cyclin-dependent kinase (Cdk) encoded by the cdc2 gene (Nurse, 1990). Later, small-size mutants were discovered in *S. cerevisiae*, and were promptly given the moniker whi, pronounced “wee”.

Mutations that accelerate cell division relative to cell growth result in a small cell size, referred to as a Wee or Whi phenotype in fission yeast and budding yeast, respectively. Such mutants have provided key insights into cell cycle control (Cross, 1988; Garí et al., 2001; Nash et al., 1988; Nurse, 1975; Sudbery et al., 1980). *WHI1-1*is a hypermorphic allele of *CLN3*, which encodes the cyclin that activates the cyclin-dependent kinase Cdc28 to cue events at Start (Cross, 1988; Nash et al., 1988; Sudbery et al., 1980; Tyers et al., 1993), whereas Whi3 is an RNA binding protein that sequesters the *CLN3 mRNA* transcript into an inactive state (Garí et al., 2001; Nash et al., 2001) and Whi5 is the G1 transcriptional repressor that binds to the SCB binding factor (SBF) at SCB target promoters in early G1 and then phosphorylated in late G1 by Cln3-Cdc28 complex to relieve repression and activate Start (Costanzo et al., 2004; De Bruin et al., 2004). A list of identified Whi mutants of budding yeast are indicated in (Table 6), that includes *WHI7* (*SRL3*) characterized in this thesis and published online (Yahya et al., 2014) and Whi8 (YGR250c), another Whi mutant characterized in this study and still unpublished. Screens for small cell size mutants have not only identified key proteins of the Start network, such as Cln3, Whi3 and Whi5, but also central regulators of ribosome biogenesis (Jorgensen et al., 2002), namely Sfp1 and Sch9, indicating a close functional interaction between the machineries that control growth and proliferation (Jorgensen & Tyers, 2004).

Systematic name	Gene name	Alias(es)	Description
YAL040C	CLN3	cyclin CLN3, WHI1, FUN10, DAF1	G1 cyclin involved in cell cycle progression
YOR043W	WHI2		Protein required for full activation of the general stress response
YNL197C	WHI3		RNA binding protein that sequesters CLN3 mRNA in cytoplasmic foci
YDL224C	WHI4		Putative RNA binding protein
YOR083W	WHI5		Repressor of G1 transcription
YKR020W	VPS51	VPS67, API3, WHI6	Component of the GARP (Golgi-associated retrograde protein) complex
YKR091W	SRL3	WHI7	GTB motif (G1/S transcription factor binding) containing protein

Table 6: List of Whi mutants identified and characterized in *S. cerevisiae.*

This thesis describes the isolation and characterization of a *CDC28* quintuple mutant, which we refer to as *CDC28*^{wee}, that causes premature entry into the cell cycle and a small cell size. Next we used isobaric tags for relative and absolute quantitation (iTRAQ) to identify direct interactors with lower affinities for mutant Cdc28^{wee}, aiming at the identification of proteins with key regulatory roles in the retention mechanism. Among the identified proteins we found Srl3, a protein of unknown function, here renamed as Whi7. Here we show that Whi7 acts as an inhibitor of Start, associates to the ER and contributes to efficient retention of the Cln3 cyclin, thus preventing its unscheduled accumulation in the nucleus. Our results demonstrate that Whi7 acts in a positive feedback loop to release the G1 Cdk-cyclin complex and trigger Start once a critical size has been reached (Figure 13), thus uncovering a key nonlinear mechanism at the earliest known events of cell cycle entry.

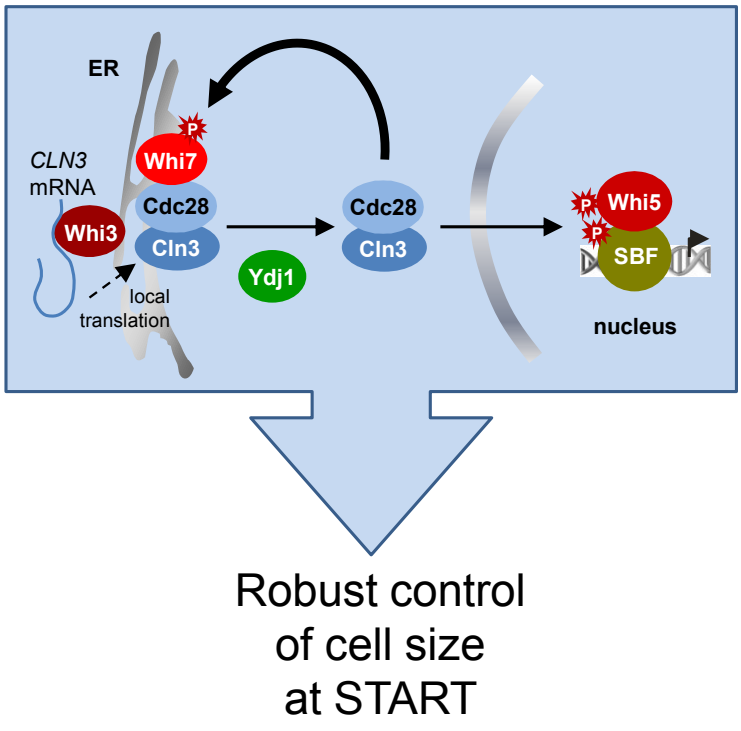

Figure 13: Proposed model for Whi7 role at Start

In addition to Whi7 we also identified Whi8, an RNA-binding protein present in both stress granules (SGs) and P bodies (PBs) with unknown biological function. We have found that Whi8 interacts with Cdc28 *in vivo*, binds and colocalizes with the *CLN3*

mRNA, and interacts with Whi3 in an RNA-dependent manner. Whi8-deficient cells showed a smaller budding cell size while, on the other hand, overexpression of Whi8 increased the budding volume. Cells lacking Whi8 were not capable of accumulating the *CLN3* mRNA in SGs under stress conditions, and Cln3 synthesis remained high under glucose and nitrogen starvation, two environmental stress conditions that dramatically decrease Cln3 levels in the cell. Whi8 accumulation in SGs depended on an intrinsically disordered domain (IDD) identified at C-terminus of Whi8 and specific PKA phophosites. Our results suggest that Whi8 acts under stress as a safeguard that limits the influx of newly synthesized Cln3 (and likely other proteins) into the cell cycle machinery, by trapping the *CLN3* mRNA in mRNA granules. Thus, we have found a unique target for signaling pathways that directly links stress response and cell cycle entry.

Objectives

This thesis aimed at reaching the following objectives:

- Genetic screen, isolation and characterization of *CDC28 ^{wee}* mutants able to subvert ER sequestration of the Cdc28-Cln3 complex
- Subproteomic analysis of interactors of wild type and *wee* mutant Cdc28 proteins using iTRAQ to pinpoint G1 regulators
- Functional analysis of the identified candidates as regulators of cell size and cell cycle entry
- Characterization of their role in the molecular mechanism of retention of the G1 Cdk-cyclin complex

Materials and Methods

1. Construction of yeast strains

Epitope tagging of genes and deletions was performed as described (Janke et al., 2004). Lists of the strains, plasmids, and primers used in this study are provided in Supplementary Table 2, Supplementary Table 3, and Supplementary Table 4.

All PCRs were done using MyCycler™ PCR system from Bio-Rad. The polymerase "iProof™ High-Fidelity DNA Polymerase" from Bio-Rad was used for epitope tagging and deletions of genes. To check gene integrations in yeast we used; colony PCR using SupraTherm™ Taq DNA polymerase (Gene Craft). Amplification of yeast genes or Epitope-tags was usually done in a 50-100µl PCR reaction using 0.5µM primer1, 0.5µM primer2, 0.2mM of dNTPs, 1x iProof HF buffer, 0.5mM MgCl2, 0.5µl genomic DNA or 1µl 1:20 diluted plasmid Mini prep and 1µl iProof™ polymerase (2U/µl) in case of amplicons that have high GC content we use 1x iProof GC buffer and add DMSO up to 3% to the PCR mix. In general, the following amplification protocol was used: 30s 98°C, [20s 98°C, 30s at the respective °C, 1min / 1000bp 72°C], 35cycles, 10min 72°C.

In case of Random mutagenesis to prepare mutant library of *CDC28* gene we used an error prone protocol for the PCR where MgCl2 increased to 7mM, dCTPs and dTTPs to 1mM and MnCl2 0.5mM is added immediately before The Taq DNA polymerase SupraTherm™ Taq DNA polymerase (Gene Craft) using this amplification protocol 5min 94°C, [1min 94°C, 1min at the respective °C, 1min / 1000bp 72°C], 35 cycles, 7min 72°C.

Yeast cells transformation

50ml of yeast were grown to an optical density of 0.5 to 0.8OD_{600} and harvested by centrifugation for 3min at 3600rpm using a ROTINA 380R centrifuge (Hettich). After washing with 10ml H2O, the pellet was resuspended in 500µl of solution I (10mM Tris-HCl, pH 7.5, 1mM EDTA & 100mM Li-acetate). After centrifugation, the pellet was resuspended in a mix of 40µl DNA of interest in 1xTE (10mM Tris-HCl, pH 8.0, 1mM EDTA, pH 8.0), 5µl of ssDNA (DNA of salmon or herring testis,2 mg/ml), and 5µl of 1M Li-acetate finally,300µl of solution II (10mM Tris-HCl, pH 7.5,1mM EDTA, 100mM Li-acetate & 40% PEG-4000) was added and the mixture was incubated for 30min at 30°C in a dry bath incubator of Elite major science . Transformations were then heat-shocked for 15min at 42°C in a dry bath incubator of Elite major science, followed by 3min incubation on ice. 1ml of H2O was added and centrifuged. The pellet was resuspended in 50µl H2O and plated on selective plates. For genomic integrations of a galactose

promoter, epitope tagging or a disruption cassette that require expression of drug resistance genes, the pellets were resuspended in 4ml YPD or YPG and incubated for 4h at room temperature prior to plating.

Colony PCR from yeast

A yeast colony was resuspended in 15µl of Milli-Q (Millipore) water and patched in appropriate selection plate. Next, a small spoon of glass beads (SIGMA) was added, and cells were boiled at 95°C for 2minutes. Then, cells were broken for 30seconds at power 5.5 using the FastPrep (FP120, Bio101 Thermosavant). Finally, after spinning at 10krpm for 1minute, 2µl of supernatant were taken for the PCR reaction. The following amplification protocol was used: 30s 94°C, [20s 94°C, 30s at the respective °C, 1min / 1000 bp 72°C], 35cycles, 10min 72°C.

Genomic DNA preparation of yeast cells

4ml of an overnight culture with an OD_{600}> 1 were centrifuged (3min, 3600rpm) and washed with 10ml H2O. The cells were resuspended in 500µl H2Oand 200µl lysis buffer (2% Triton X-100, 1% SDS, 100mM NaCl, 10mM Tris-HCl, pH8.0,1mM-EDTA).300µl glass beads and 300µl phenol:chloroform:isoamylalcohol (25:24:1) were added and the mixture was vortexed for 3min. After a centrifugation for 10min at 16,000g the upper phase was removed and extracted with an equal volume of chloroform. Genomic DNA was precipitated using 1.2ml 100% ethanol and incubation of the solution for 10min at -20°C. After a centrifugation for 30min at 4°C and 16,000g, the pellet was dried and resuspended in 400µl TE (10 mM Tris-HCl, pH 8.0, 1 mM EDTA, pH 8.0). To destroy RNA, 20µl RNaseA (10 mg/ml) were added and incubated for 40min at 37°C. Genomic DNA was precipitated by addition of 40µl 3M Na-acetate, pH 5.2 and 800µl 100% ethanol and incubation of the mixture for 10min at – 20°C. After centrifugation (16,000g, 4°C, 30min) the pellet was washed with 80% ethanol, dried and resuspended in 30µl TE.

2. Gene cloning and plasmid construction

PCR purification was done using QIAquick PCR purification kit from Qiagen. Dephosphorylation and ligation were done using the Rapid DNA Dephos & Ligation Kit from Roche. Site-directed mutagenesis was performed using the Quickchange

mutagenesis kit from Agilent Technologies. Plasmid extraction was done using GenElute Plasmid Miniprep Kit (SIGMA) according to manufacture guide. Newly constructed plasmids were checked by either plasmid jet preps and restriction digestion, or *E.coli* colony PCR. Detection of DNA was done by loading on 0.8 to 1.5% SeaKem® LE Agarose (LONZA) gel prepared with the running buffer 1xTAE (from 50x; Tris-HCL, EDTA-Na2 pH 8.5). DNA was then stained by incubating the agarose gel for 15 minutes in ethidium bromide bath with a final concentration of 0.5µg/ml. Detection was done by exposing the gel to UV light source (Alpha Inno Tech), image capture by Olympus camera, and analysis with AlphaDigiDoc software.

E. coli DH5α competent cells transformation

For plasmid transformation, 50µl of Subcloning Efficiency™ DH5α™ Competent Cells from Invitrogen were thawed on ice and 1-5µl of DNA was added with gentle mixing. Next, they were incubated on ice for 30minutes, at 42°C for 20seconds (heat shock) and on ice again for 2minutes. 1ml of prewarmed LB was added to the transformation tube, and cells were then incubated at 37°C for one hour to allow expression of the antibiotic (ampicillin for example) resistance gene. After incubation, cells were pelleted at 6000rpm for 5minutes, and 950µl of the supernatant was removed, while the pellet was resuspended with the 50µl left and plated on LB+Antibiotic plate.

Colony PCR from *E. coli*

Colonies were picked with toothpicks and swirled into 25µl of Milli-Q water. The same toothpick was used to make a patch on LB-Ampicillin plate. The suspended colonies were then boiled for 2minutes, and centrifuged at 13000rpm for 2minutes. 20µl of the supernatant were transferred to a new tube, from which 1µl was used as template for the PCR. This procedure allows rapid screening for the presence of the insert in its correct orientation.

Jet preps

Colonies that were previously picked on LB-Ampicillin plate were resuspended in 500µl of LB-Ampicillin liquid medium and then pelleted by centrifugation for 30 seconds at 13000rpm. Next, 50µl of BT (2%Triton X-100/NaOH pH 12.4) were added to the pellet without resuspension. Then, 50µl of phenol/chloroform were added and the tubes where shaken vigorously for 30seconds. After centrifugation for 5minutes at 13000rpm,

5µl were combined with loading buffer (5x FLB, 100 µg/ml RNase). To analyze with restriction digestion, 40µl of the supernatant were taken and chromatin was precipitated by adding 4µl of 2% acetic acid 4µl of 3M NaOAc pH 8, and 100µl of ethanol, and centrifugation at 13000 rpm for 5minutes. The pellet was then washed with 1ml 70% ethanol, and resuspended with10 µl Milli-Q water. 5µl of the resuspended chromatin was used in 10µl digestion reaction. The digested plasmids were combined with loading buffer (5x FLB, 100 µg/ml RNase) and loaded into an agarose gel along with the undigested ones.

3. Growth media, serial dilution and generation time measurements

Yeast cells were grown in YP (Yeast extract, peptone) supplemented with different sugars (2%), glucose, galactose and raffinose. A final concentration of 200µg/ml of genetecin (DUCHEFA), 300µg/ml of hygromycin B (Sigma), and 200µg/ml of nourseothricin (Werner BioAgents) antibiotics, was used to select for gene tagging and deletions that confer antibiotic resistance. SC medium (YNB, drop-out) was used to select for plasmid auxotrophies, which include; tryptophan (40µg/ml), leucine (120µg/ml), histidine (20µg/ml) and uracil (20µg/ml). In case of glucose starvation cells were grown exponentially for 14-16hours until $OD6_{00}$ 0.3-0.4 in SDC or YPD media then collected by filtration and after a quick wash, resuspended at the same cellular concentration in pre-wormed SC or YP media. In case of nitrogen starvation, Yeast nitrogen base without ammonium sulfate was used as recommended by the manufacturer (Difco) to prepare SD media without the nitrogen source, and the required amino acids were added to the following final concentrations: 15µg/ml leucine, 5µg/ml histidine and 10µg/ml tryptophan according to (Gallego et al., 1997). Nitrogen deprivation experiments were done with cells growing exponentially for 14–16hours until OD_{600} = 0.3–0.4, which were then collected by filtration and, after a quick wash, resuspended at the same cellular concentration in pre-warmed medium lacking the nitrogen source.. LB was used to grow bacterial *E.coli* DH5α and BL21. A final concentration of 50µg/ml of Ampicillin (ROCHE) was added to select for cloned plasmids.

For serial dilution and replica plating of yeast cells, around one colony was resuspended in 400µl of the appropriate growth medium. Then, the OD_{600} was measured and cells were diluted in 200µl to OD_{600} 0.3 inside 96well plate. Four 10X serial dilutions or five 5x serial dilutions were made by carrying 20µl from the first dilution to the next. Replica plating on different media was done by 48pin stamp.

For generation time measurements cells were grown overnight in YP plus raffinose. The next day, cultures were diluted to the same OD_{600} and split in to two; in one of the two the sugar raffinose was substituted with galactose to allow the expression of the fusions under the *GAL* promoter. The OD_{600} was measured every hour for 8hours. The ln of the OD_{600} was calculated in an excel table and plotted on a graph as a function of time. The slope was used to calculate the generation time by dividing the natural logarithm of 2 (ln2) over the slope. *GAL1p*-driven gene expression was induced by addition of 2% galactose to cultures grown in 2% raffinose at OD_{600} = 0.5. When stated, 10µM β-estradiol was used to induce the *GAL1* promoter in strains expressing the Gal4-hER-VP16 (GEV) transactivator (Louvion et al., 1993).

4. Protein techniques

Post-alkaline extraction

Post-alkaline extraction was mainly used to check correct tagging of transformation colonies. Yeast cells, obtained from colony patches on plates, were resuspended in 200µl 0.1M NaOH, and incubated for 5minutes at room temperature. After incubation, the alkaline supernatant was removed by spinning at 13.000rpm for 15seconds, and the pellets were resuspended with 1xSSR and boiled at 95°C for protein elution. Next, samples were loaded on SDS-PAGE gels and analyzed by western blot. 4xSS (20% sucrose, 0.05% bromophenol blue, 0.1% NaAZ) and 4xSR (8%SDS in 0.5 M Tris-HCl pH 6.8) are used at equal volumes, along with 2% β-mercaptoethanol, to prepare the loading buffer 2xSSR.

Urea extraction

Urea extraction was mainly used to quantitatively check the levels of expression of proteins. 10ODs of exponentially growing cultures were collected and processed by adding 30µl of 5M urea and boiling at 95°C for 2minutes. Next, two small spatulefull of

glass beads were added, and cells were broken using the FastPrep for 30seconds power 6. Then, 100µl of 1xSR were added and cell extracts were boiled at 95°C for 2minutes. Finally, the protein extracts in the supernatant were obtained after centrifugation at high speed for 5minutes. Protein concentration was checked using BIO-RAD Micro DC protein assay. Equal concentrations of proteins were loaded on SDS-PAGE gels after boiling at 95°C with loading buffer (1xSS and 2%β-mercaptoethanol) for 2minutes.

Western Blot

The running gel was prepared at different percentages from 30% acrylamide/Bis-acrylamide with 0.375M Tris-HCl pH 8.8, 0.1% SDS, 0.08% Ammonium persulfate, and 0.1% TEMED. 5% stacking gel was prepared from 30% acrylamide/ Bis-acrylamide, with 0.125MTris-HCl pH 6.8, 0.1% SDS, 0.066% Ammonium persulfate, and 0.1% TEMED. After loading, proteins were allowed to migrate at 20mA/gel for around 90minutes. The Mini-PROTEAN® Tetra cell for hand cast gels and PowerPac™ HC power supply along with casting stands, casting frames, and glass plates from BIO-RAD.

PVDF membrane (Millipore) was prepared by wetting with methanol then rehydrating with water and then transfer buffer. 20% methanol transfer buffer was used for transfer small proteins while 10% was used for larger ones. The gel and the membrane were assembled with transfer paper (GE Health care) as directed in the Semi-Dry transfer machine Trans-Blot® (BIO-RAD), and proteins were transferred at 60mA/gel for one hour.

Blocking was done with 5% milk PBST (8g of NaCl, 0.2g of KCl, 1.44g of Na_2HPO_4, 0.24g of KH_2PO_4&0.1% Tween-20) for one hour at room temperature. The primary antibody was added and left for 2hours at room temperature or overnight at 4°C. The antibodies used for western blot analysis are shown in (Supplementary Table 1).

The membrane was washed three times with PBST for 5minutes each, and once with 0.025% milk PBST or 10minutes then incubated with the secondary antibody in 0.025% milk,0.02%SDS- PBST for one hour at room temperature. After washing three times with PBST, the membrane was incubated with Clarity™ Western ECL Substrate from BIO-RAD for 5minutes. The signal was detected using Amersham Pharmacia Biotech Hyperprocessor imaging system from Amersham.

ER spin

Collect 50OD_{600} by filtration using 0.45µm Nitrocellulose MF™ membrane filters (Millipore) in a filter cassette from NALGENE®, resuspend in 1ml cold water, spin 1 minute at 5krpm and shock freeze pellet with liquid nitrogen (keep at -70°C if needed).

Thaw the pellet at 37°C for 10seconds (exactly), and resuspend in cold 200µl STE10. Transfer to a new precooled tube with 0.5ml glass beads. Break cells for 30seconds at power 5 with the Fast Prep in the cold room.

Add 500µl STE10, vortex for 5seconds, and keep 50µl extract in 50µl 2xSSR (T).

Roll the remaining extract for 15minutes at 4°C. Spin at 1.8krpm for 2minutes at 4°C in Microcentrifuge 5417R (Eppendorf), take 0.5ml supernatant to a clean tube, and keep 50µl in 50µl 2xSSR (S).

Spin at 13.2krpm for 30minutes at 4°C. Keep 100µl supernatant in 100µl 2xSSR (S13). Carefully remove all the supernatant and resuspend the pellet in 200µl 1xSSR (P13).

STE10 (for 8 samples)

60% sucrose	1.0ml
Q water	4.7ml
2M Tris-HCl pH 7.5	30µl
0.5M MgCl2	24µl
0.1M DTT	60µl
25x PPI	60µl
100x PIA	60µl
200x PIB	30µl
200mM PMSF	30µl

Gradient fractionation of yeast cell extracts

Collect 50OD_{600} by filtration, resuspend in 1ml cold water, spin 1minute at 5krpm and shock freeze pellet with liquid nitrogen (keep at -70°C if needed)

Thaw the pellet at 37°C for 10seconds (exactly), and resuspend in cold 200µl STE10. Transfer to a new precooled tube with 0.5 ml glass beads. Break cells for 30seconds at power 5 with the Fast Prep in the cold room.

Add 500µl STE10, vortex for 5seconds. Roll the remaining extract for 5minutes at 4°C. Spin at 1.8krpm for 2minutes, take 0.5ml supernatant to a clean tube, and keep 50µl in 50µl 2xSSR as soluble extract (S).

Load 0.4ml onto a 20-60% sucrose gradient prepared in Polyallomer centrifuge tubes (13X51mm) from Beckman Coulter® the night before and spin at 40krpm for 6hours at 4°C in Optima™L-90K µltracentrifuge (Beckman) using SW55 TI rotor (Beckman).
Take 12 x 0.45ml fractions from the top with a 1ml Gilson and add to 0.65ml cold 0.02% DOC (Sigma). Mix and add 0.1ml 72% (saturated) TCA (Sigma) .Mix and let on ice for one hour.
Spin at 12krpm for 10minutes, drain, add 1ml cold acetone (VWR). You may leave tubes overnight at -20°C. Spin at 12krpm for 2minutes.
Speed-vacuum for 10minutes in Concentrator 5301 (Eppendorf) and add 50µl 1xSR sample buffer and 5µl 1M Tris base (Sigma) to the pellets. Vortex for 5seconds and incubates at 65°C for 10minutes. Repeat this step twice before samples are boiled and loaded onto SDS-PAGE gels.

2 gradients	**STE60**	**STE20**	**STE10**
60% sucrose	5.0ml	1.67ml	0.33ml
Q water	- ml	3.33ml	1.67ml
2M Tris-HCl pH 7.5	25µl	25µl	10µl
0.5M MgCl2	20µl	20µl	8µl
0.1M DTT	50µl	50µl	20µl
25x PPI	25µl	25µl	10µl
100x PIA	50µl	50µl	40µl
200x PIB	25µl	25µl	20µl
200mM PMSF	25µl	25µl	10µl

Gradient steps	**60%**	**50%**	**40%**	**30%**	**20%**
STE60	2.0ml	1.5ml	1.0ml	0.5ml	- ml
STE20	- ml	0.5ml	1.0ml	1.5ml	2.0ml
Vol. in 5ml Beckman tube	0.95ml	0.95ml	0.95ml	0.95ml	0.95ml

Purification of GST-Whi8 fusion protein

Transform BL21 *E.coli* background with the required GST-fusion construct Prepare a preculture of 10ml shaking overnight at 250–300rpm at 37°C in LB supplemented with 100µg/ml ampicillin till Saturation. Dilute 1/50 in 50ml LB Amp keep shaking at 37°C wait 2hours (OD600=0.25). Induce with IPTG to a final concentration of 1.5mM final concentration and incubate at 30°C shaking at 250–300rpm for 5-6hours. Harvest cells by centrifugation at 3000rpm for 15min at 4°C in 50ml centrifuge tube. Decant the supernatant, Cell pellet may be frozen for up to several months at −80°C.

Resuspend the pelleted *E. coli* cells in 1ml cold lysis buffer (cells might be freshly prepared or thawed frozen cell pellets), rotate for 30minutes at 4°C. Lyse cells by sonication on ice (~4times for 30sec at force 6 each with 1min rest between bursts to minimize sample heating). Spin at 16000g for 15minutes at 4°C, carefully transfer the supernatant to a clean 1ml tube and keep aside 20µl as your **input** to verify the level of expression of your fusion protein by SDS-PAGE

On the other hand prepare the GST beads (GST-Sepharose beads) wash 100µl GST beads 4 to 5times with 1 ml cold buffer **B** to remove the storage solution

Mix the supernatant we got before with the washed GST beads and rotate for 1 hour at 4°C. Collect the GST beads by centrifugation at 3000rpm for 10seconds and carefully remove the supernatant without losing beads

Wash the beads 4times with cold buffer **B** by rotation at 4°C for 5minutes

Finally resuspend the GST beads in the suitable kinase buffer to be ready for the kinase assay and keep 10µl of the GST beads to verify the binding and purification efficiency.

Buffer B	**Stock**
1xPBS	10x
1mM DTT	1M
0.1% TRITON-X100	10%
2x PIA	100x
200x PIB	200x
200mM PMSF	200x
1mg/ml lysozyme	10mg/ml to prepare lysis buffer

In Vitro protein kinase assay

GST-Whi8 protein was affinity-purified using GST-Sepharose 4B beads (Amersham Biosciences) and finally resuspended in a suitable kinase buffer according to the manufacturer's instructions. The GST-fused Whi8 on the beads were mixed in 50µl of kinase buffer containing 0.5µCi of [γ-^{32}P] ATP, 100µm ATP, and 10mm $MgCl_2$ with Protein Kinase A Catalytic Subunit from bovine heart (Sigma) and incubated at 30°C for 30min. After the beads had been washed with the kinase buffer, the proteins were eluted by boiling the beads in SDS sample buffer for 5min. The eluted proteins were resolved by SDS-PAGE and detected by autoradiography.

Protein immunoprecipitation (IP)

Collect 50O.D_{600} of cells (500ml $OD6_{00}$ =1) by centrifugation at 5000rpm at 4°C for 3minutes. Wash the pellet by cold water 3 times by centrifugation (5000rpm at 4°C for 3minutes).You can freeze the pellet in liquid nitrogen and keep at -80°C.

Add 150µl of buffer AI and resuspend the pellet then add glass beads up to 1mm from the meniscus. Break the cell using the fast prep machine power 4 for 40seconds. Test the breaking efficiency under the microscope if less than 50% repeat breaking using the same settings. Add 150µl of buffer AI then add 60µl of KCl 2M and 60µl of TRITON 10% and mix by inversion 3-5times. Spin the extract you get at 12000rpm for 1minute at 4°C then transfer the supernatant to a new clean 1ml tube. Spin again for 5minutes at 12000rpm at 4°C and carefully transfer the supernatant to a new dry clean 1ml tube without taking the upper fatty layer neither the pellet

Mix 20µl of the cell extract of the supernatant with 20µl of 2xSSR and keep aside this will be the WCE

On the other hand prepare 50µl of αFLAG M2 affinity gel beads from Sigma (100µl slurry) for IP by washing 3times with cold buffer A (500µl each wash) finally resuspend in 50µl buffer AI and the add the supernatant and rotate at 4°C for 2hours then collect the beads by spinning at 1000rpm for 30seconds and remove the supernatant with 29G MYJECTOR® 1ml insulin syringe.

Wash 3times by buffer IPP150 (500µl each wash) and collect the beads by spinning at 1000rpm for 30seconds and remove the supernatant with insulin syringe. Elute with 50µl of 1xSR and incubate at 37°C for 5minutes. Collect the eluate by centrifugation at 1000rpm for 60 seconds and collect the eluate carefully with the tip of the pipette without collecting any beads mix with loading buffer (1xSS and 2% β-mercaptoethanol) and boil at 95°C for 2minutes.

The immunoprecipitated proteins were loaded together with the input in SDS-PAGE, and detected using western blot analysis. The antibodies used for western blot analysis were α-FLAG and α-HA (Supplementary Table 1).

Buffer A	**Stock**
10 mM HEPES-Na pH7.5	10x
0.5mM DTT	1M
1.5mM MgCl2	1M
10mM KCl	2M
Q-H2O	to 10ml

25X Protease inhibitors cocktail EDTA free from Roche and 10XPPI (25mM Sodium Fluoride, 25mM β-glycerophosphate, 25mM EGTA, 125mM sodium pyrophosphate) add to Buffer A to prepare Buffer AI

Buffer IPP150	**Stock**
10mM Tris-HCl pH8.0	2M
150mM NaCl	5M
0.1% TRITON	10%
Q-H2O	to 10 ml

For large scale immunoprecipitations of Cdc28-3FLAG for iTRAQ analysis 3-l YPD cultures of cells with either wild-type or *wee CDC28-3FLAG* strains were grown at 30°C to OD_{600} = 5–6 to enrich for G1 cells, then cells pellets were collected by centrifugation in 250ml NALGENE® centrifuge bottles using Avanti™J-25 centrifuge (Beckman) and JA-10 rotor (Beckman) at 5Krpm for 5min at 4°C, pellets then washed twice with cold water and finally resuspended in 50ml lysis buffer and disrupted using Constant Cell Disruption System at 4°C after preparation of cell extracts the supernatant is obtained the same way then rotated with 1ml αFLAG M2 affinity gel beads from Sigma at 4°C for 2hours then loaded on Poly-Prep® Chromatography columns (BIO-RAD) to collect and wash the beads by draining at 4°C finally elute the beads using 500µl of 1% SDS and keep samples for western blot and ruby staining. The iTRAQ analysis was done at the BIDMC Proteomics Core Center (Harvard University), essentially as described by (Afkarian et al., 2010). A set of four pairs of immunoprecipitates from either wild-type or *wee CDC28* cells were digested with trypsin, labeled with eight isobaric tags, pooled, and separated by two dimensional liquid chromatography into 15fractions. Each fraction was analyzed in an 8-plex run using an AB/Sciex 4800 MALDI-TOF/TOF mass spectrometer.

5. RNA techniques

RNA immunoprecipitation (RIP)

50ml OD_{600} = 1 of exponentially growing cells expressing protein of interest fused to 6FLAG epitope were collected and then lysed as described under protein immunoprecipitation section with the exception of adding to the lysis buffer 40units/µl RNaseOUT ™ (Invitrogen) beside phosphatase and protease inhibitors mixture (Roche

Applied Science). Extracts then rotated with 50µl αFLAG M2 affinity gel beads from Sigma for 2hours at 4°C. The beads were then washed four times with wash buffer (IPP150) RNAs were extracted according to standard protocols of (E.Z.N.A. total RNA Kit I; Omega Bio-Tek).

RT-qPCR

After RNA extraction, First-Strand cDNA Synthesis Using SuperScript™ II RT (Invitrogen) was performed according to standard protocol (Invitrogen life technologies) Reactions were carried out according to the manufacturer's instructions in a total volume of 20µl using MyCycler™ PCR system from Bio-Rad. Obtained cDNA levels were determined by quantitative real-time PCR using TaqMan probes against mRNAs of interest from Sigma. PCRs were run and analyzed with an iCycler iQ real-time detection system (Bio-Rad). The probes and primers used for RT-qPCR are shown in (Supplementary Table 5)

6. Cell biology methods

Cln3-3HA immunofluorescence

Take 5ml of cells (YPD with uracil and/or adenine if needed, OD_{600}=0.5-1), add 0.6 ml 37% Formaldehyde (10% methanol), and rotate for 50min.

Spin cells at 2krpm for 3min, wash once with 1ml PB (0.1M KH_2PO_4 pH 7.4), and resuspend in 1ml PB.

Take 0.2ml of cells, add 1µl β-mercaptoethanol and 2µl Zymolyase Z100T (Seikagaku Biobusiness Corporation), and incubate 20min at 30°C (cells get dull gray).Place cells on ice for 5min, spin at 3krpm for 2min, and resuspend in 0.1ml PBS. Samples can be kept overnight on ice at this stage, but not longer.

Treat slides (Delta lab) with 20µl/well 0.1% Poly-L-Lysine (Sigma) for 10min, and wash twice with 50µl/well Q-water. Place cells (20µl/well), let stand for 10min at RT, and remove most of the liquid by gentle aspiration.

Place in ice-cold methanol for 6min (carefully plunge slide into a 50ml tube placed on ice 1h ahead).Wash in PBS (50ml tube) for 1min at RT.

Add 50µl/well BS and block for 30min at RT. Add 20µl/well primary Ab mix and incubate for 1-2hours at RT. Wash three times with PBS.

Add 20μl/well secondary Ab mix and incubate for 30min at RT in the dark. Wash three times with PBS. Add 20μl/well second secondary Ab mix and incubate for 30min at RT in the dark. Wash three times with PBS.

Let dry for 10min and mount with 50% glycerol-PB (keep at 4°C in the dark in a humid chamber).

Clear all solutions at 12krpm for 2min before addition to wells.

PBS – same as in (Sambrook, Fritsch, & Maniatis, 1989) (prepare as a 20x stock)

BS - 3% BSA in PBS

BS/10 – 0.3% BSA in PBS

Z100T – 10mg/ml Zymolyase 100T in 50% glycerol-PB. Roll it for 15min at 4°C. Keep aliquots at -70°C.

50% glycerol-PB – 50% glycerol 10 mM KH_2PO_4 pH 7.4

Slides (black print) – Leave in hot 0.5% Mistol (90-95°C) for 15min, rub the printed slide with foam, rinse three times with tap water, three times with deionized water, twice with Q-water and once with ethanol. Dry and keep

Primary antibody mix (200μl): 1μl of 0.1μg/μl rat 3F10 α-HA in 200μl BS/10.

Secondary antibody mix (200μl): 0.2μl 2μg/μl Alexa488 goat α-rat in 200μl BS/10.

Second Secondary antibody mix (200μl): 0.2μl 2μg/μl Alexa488 rabbit α-goat in 200μl BS/10 (Supplementary Table1).

Bright field, DAPI images of the nuclei and immunofluorescence images of Cln3-3HA were captured using Upright Microscope Nikon E600.

For colocalization of Whi7 and Whi8 to the ER marker Ole1-GFP by immunofluorescence methanol permeabilization was omitted, in order not to disturb the ER structure and GFP signal was intensified with a rabbit α-GFP Alexa 488-labeled antibody (Molecular Probes). Z-stack images were captured using Spectral Confocal Microscope Zeiss LSM780.

Semiautomated quantification of Cln3-3HA levels

Briefly, we have developed N2CJ as a plugin for ImageJ that uses bright-field and DAPI-staining images to determine in a semiautomated manner both cellular (yellow) and nuclear (magenta) limits and quantify levels in both compartments (Figure 14).

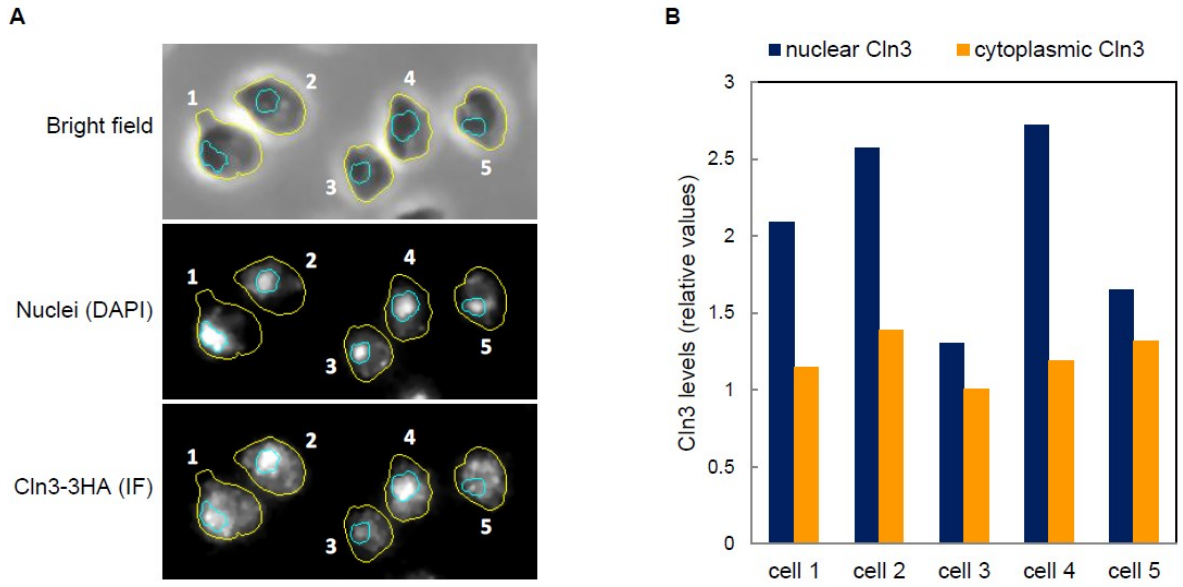

Figure 14: Semiautomated Quantification of Cln3-3HA Levels in both Nuclear and Cytoplasmic Compartments by Immunofluorescence

(A) A sample stack of late G1-arrested cells by α-factor treatment. Briefly, we have developed N2CJ as a plugin for ImageJ that uses bright-field and DAPI-staining images to determine in a semiautomated manner both cellular (yellow) and nuclear (magenta) limits and quantify immunofluorescence levels in both compartments.
(B) Quantification of nuclear (blue bars) and cytoplasmic (yellow bars) levels of Cln3-3HA from indicated cells in (A).

Stress granules imaging in live cells

Cells (BY4741 background) were grown to an OD_{600} of 0.3-0.35 in the appropriate medium. For observation, cells were washed twice and resuspended in SC plus amino acids supplemented with glucose. For glucose depletion, cells were washed in SC supplemented with appropriate amino acids without glucose and resuspended in the same medium prewarmed to 42°C and incubated at 42°C for 15min before imaging. To prepare cells for microscopy, concentrated cell culture was mounted onto Concanavalin A from Sigma (0.2mg/ml) treated slides and pictures were taken immediately after the glucose starvation or the heat shock treatment. Z-stack images were captured using Spectral Confocal Microscope Zeiss LSM780. To visualize RNA localization, cells cotransformed with a plasmid containing NLS-MS2-GFP or NLS-MS2-mCherry which binds specifically to MS2 binding sites in RNA and another plasmid that carries 6 copies of the MS2 binding sites integrated between the ORF and the 3′UTR of the mRNA by the method developed by (Haim, Zipor, Aronov, & Gerst, 2007) (Figure 15).

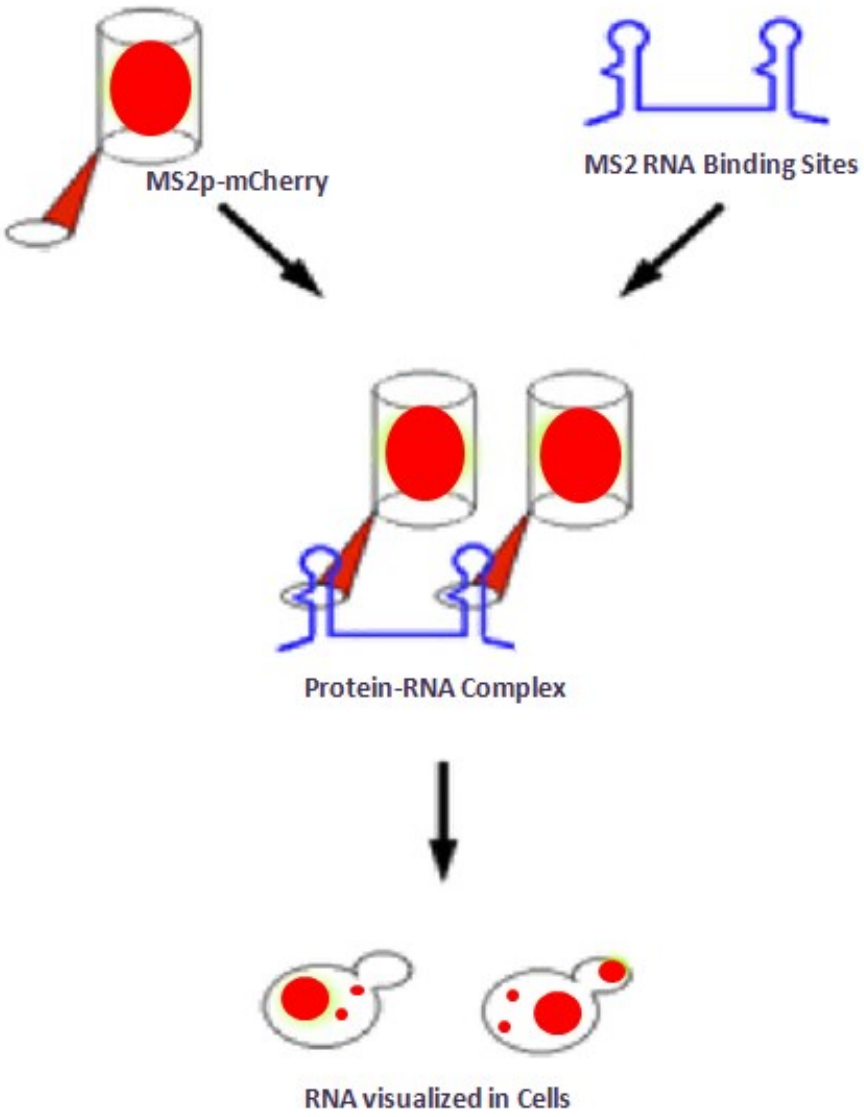

Figure 15: RNA visualization by MS2 system

7. Screen for Cdk *wee* mutants

We adapt the main procedures from (Nash et al., 2001). Yeast strain CML128 with endogenous *CDC28* gene under the control of the regulatable *GAL1p* promoter, and transformed with a plasmid library containing randomly mutagenized *CDC28* copies. Transformants were spread on 5SDC-leu plates at ~1000cells per plate. Plates were incubated at 30°C for 5days. Colonies were pooled with 1 ml YPD. A sample from the pooled cells was used to inoculate 100ml culture in YPD at OD_{600} 0.005, a glucose medium in which wt *CDC28* allele expression was repressed shaking at 30°C overnight.

Early exponential cells OD_{600} 0.5 were harvested, sonicated, and ~10^9 cells were layered onto a 30ml 2.0–10% (w/v) sorbitol gradient prepared in sterile polypropylene 50ml Falcon centrifuge tube (Fisher brand®) in a "stay-put," which separates cells according to size. Larger cells fall through the gradient faster than smaller ones. After 6hr of sedimentation, fractions (0.5ml per fraction up to 15 fractions) were collected from the top. Cell size was analyzed using a Coulter (Hialeah, FL) channelyzer. Fractions containing the smallest 5% of cells were pooled and used to reinoculate YPD culture. The size enrichment procedure was repeated two more times (Figure 16). After the third size enrichment, the smallest 5% of cells (almost the 7 top fractions) were spread on YEPD plates. Individual colonies were chosen and inoculated in 96well plate and left to grow at 30°C overnight without shaking then diluted 5 times in 0.5ml YPD in 24 well plates and grown at 30°C for 8 hours shaking at 180 rpm. Cell volume distributions were obtained with a Coulter channelyzer.

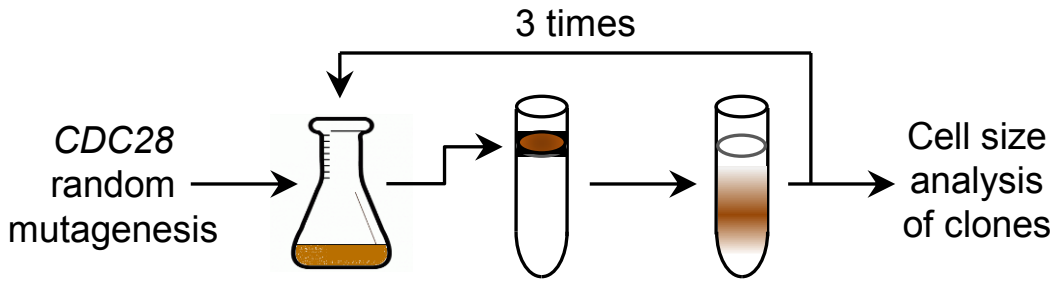

Figure 16: Screen of for small-cell-size mutants of Cdc28

Diagram of small cell size *CDC28* mutant screen. A plasmid-borne *CDC28* mutant library was transformed into a *GAL1p-CDC28* strain, and pooled transformants were subject to three rounds of enrichment in small cells by differential sedimentation

Results

1. A Whi7- anchored loop controls the G1 Cdk-cyclin complex at start

Cells commit to a new cell cycle at Start by activation of the G1 Cdk-cyclin complex which, in turn, triggers a genome-wide transcriptional wave that drives the G1/S transition. In budding yeast, the Cdc28-Cln3 complex is regulated by an ER-retention mechanism that is important for proper cell size control. We have isolated *wee* Cdc28 mutants showing impaired retention at the ER and premature accumulation of the Cln3 cyclin in the nucleus. The differential interactome of a quintuple Cdc28^{wee} mutant pinpointed Whi7, a Whi5 paralog that is a target of Cdc28 and associates to the ER in a phosphorylation-dependent manner. Our results demonstrate that the Cln3 cyclin and Whi7 act in a feedforward loop to release the G1 Cdk-cyclin complex and trigger Start once a critical size has been reached, thus uncovering a key non-linear mechanism at the earliest known events of cell cycle entry.

Critical size variability: growth-independent sources and the Start network

We have recently shown that budding yeast cells set the critical size at a single-cell level as a function of the growth rate during G1 (Ferrezuelo et al., 2012), which explains the principal component of variation observed in the critical size (Di Talia et al., 2007; L H Hartwell & Unger, 1977; Johnston et al., 1977). Once the growth-rate component is excluded, wild-type cells only display a small residual cell-to-cell variation (Ferrezuelo et al., 2012), indicating the existence of a precise and robust size control in budding yeast. Thus, we asked whether the robustness of this mechanism would depend on the different components of the Start network, and to what extent it does so (Figure 17A). As expected, cells lacking the two G1/S cyclins (Cln1 and Cln2) or any of the transcription factors (Swi4 or Swi6) involved in the transcriptional feedback loop showed an increased residual noise in cell volume at Start compared to wild-type cells (Figure 17B). Cln3, the upstream G1 cyclin that triggers the feedback loop, is assumed not to be important once *CLN1* and *CLN2* transcription has been activated and, consequently, would not play a significant role in providing Start with coherence and robustness.

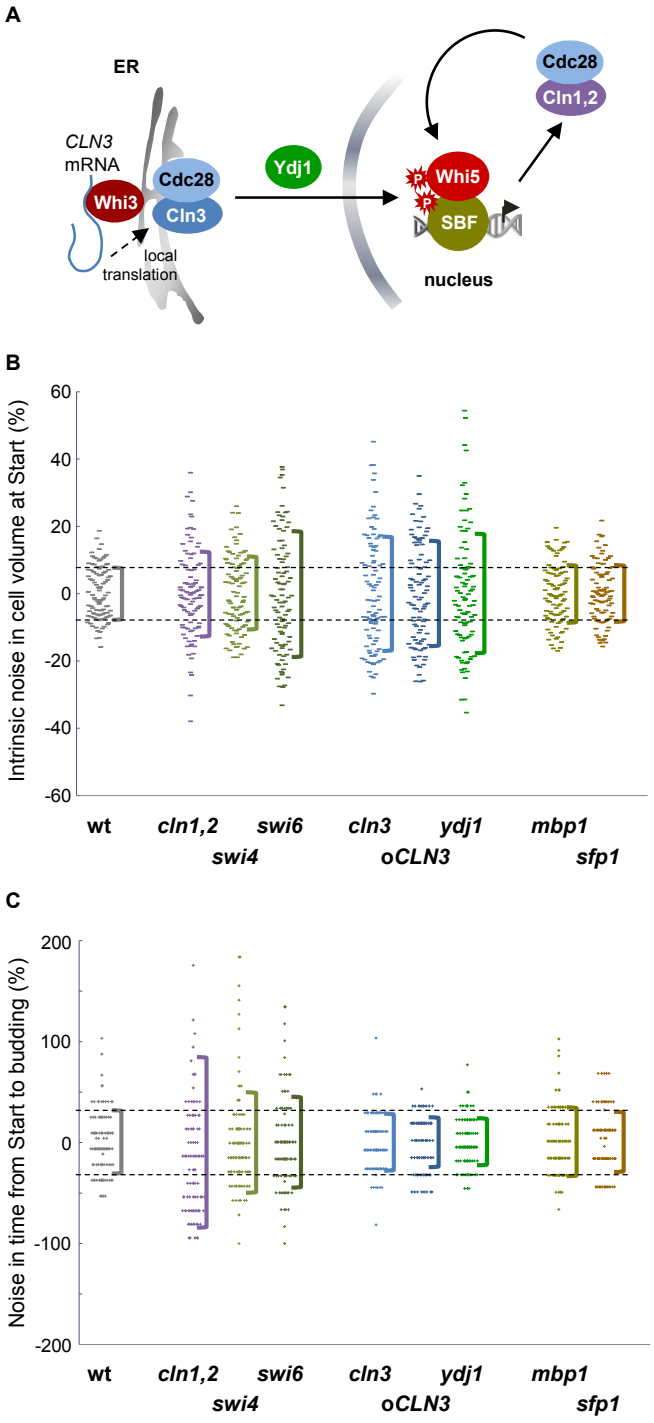

Figure 17: Residual noise in the critical size and the Start network

(A) Scheme of the Start network. Briefly, the G1 Cdk-cyclin complex formed by Cln3 and Cdc28 phosphorylates Whi5 and activates SBF (Swi6-Swi4) and MBF (Swi6-Mbp1) transcription factors to induce the G1/S regulon. Whi3 binds the *CLN3* mRNA and recruits Cdc28 to help retain newly formed Cdc28-Cln3 complexes at the ER in early G1. In late G1 the Ydj1 chaperone releases Cln3 from the ER and allows its accumulation in the nucleus to trigger Start. Cln1 and Cln2 cyclins generate a positive feedback loop for coherent and irreversible SBF and MBF activation.

(B) Percentage differences of volume at Start to that predicted by growth rate in G1 are plotted for 100 cells of the referred genotypes. Brackets indicate SD.

(C) Percentage differences of budding time (Start to budding) to population average are plotted for 100 cells of the referred genotypes. Brackets indicate SD.

However, we observed a clear increase of residual noise in the critical size of cells lacking Cln3. Notably, overexpression of Cln3 also increased the level of residual noise in cell size at Start.

Ydj1 is a chaperone that drives ER release and nuclear accumulation of Cln3 in late G1 (Vergés et al., 2007) and is also important in keeping a low cell-to-cell variation of cell size at Start (Figure 17B). In contrast, loss of Mbp1 did not modify residual noise levels in the critical size, a result consistent with the fact that this G1/S transcription factor is not involved in the G1/S-cyclin feedback loop. Cells lacking Sfp1, a master activator of ribosome biogenesis that has a profound effect on cell size control (Jorgensen et al., 2004), showed wild-type levels of residual noise in cell size at Start, which is in accordance with the idea that Sfp1 acts upstream of the Start network to set growth rate and, as a consequence, the critical size (Ferrezuelo et al., 2012). Finally, Cln3 and Ydj1 did not seem to play an important role in the robustness of the G1/S transition as deduced from noise levels in the time period from Start to budding (Figure 17C). All these data point to the notion that Cln3 and Ydj1 are important in triggering Start in a robust manner as a function of growth rate and suggest the existence of nonlinear processes driving chaperone-dependent release of the Cdc28-Cln3 complex from the ER.

A screen for Cdk wee mutants

Binding to Cdc28 is important for proper retention of the Cln3 cyclin at the ER until late G1 (Vergés et al., 2007), which suggests that this Cdk is acting as a bridge to unknown ER-associated proteins. Thus, mutations in Cdc28 that would weaken these interactions might cause premature release of the Cdc28-Cln3 complex and, hence, a smaller cell size. To perform this mutant screen we first placed the endogenous *CDC28* gene under the control of the regulatable *GAL1p* promoter, and transformed the resulting strain with a plasmid library containing randomly mutagenized *CDC28* copies. These transformants where then subject to three rounds of enrichment for small cell size mutants and more than 900 isolated clones where analyzed by their cell size distribution and Cln3 nuclear accumulation to end up with 6 independent *CDC28* mutants that have relatively small size and more nuclear accumulation of Cln3 compared to wild type *CDC28* carrying background (Figure 18A and 18B).

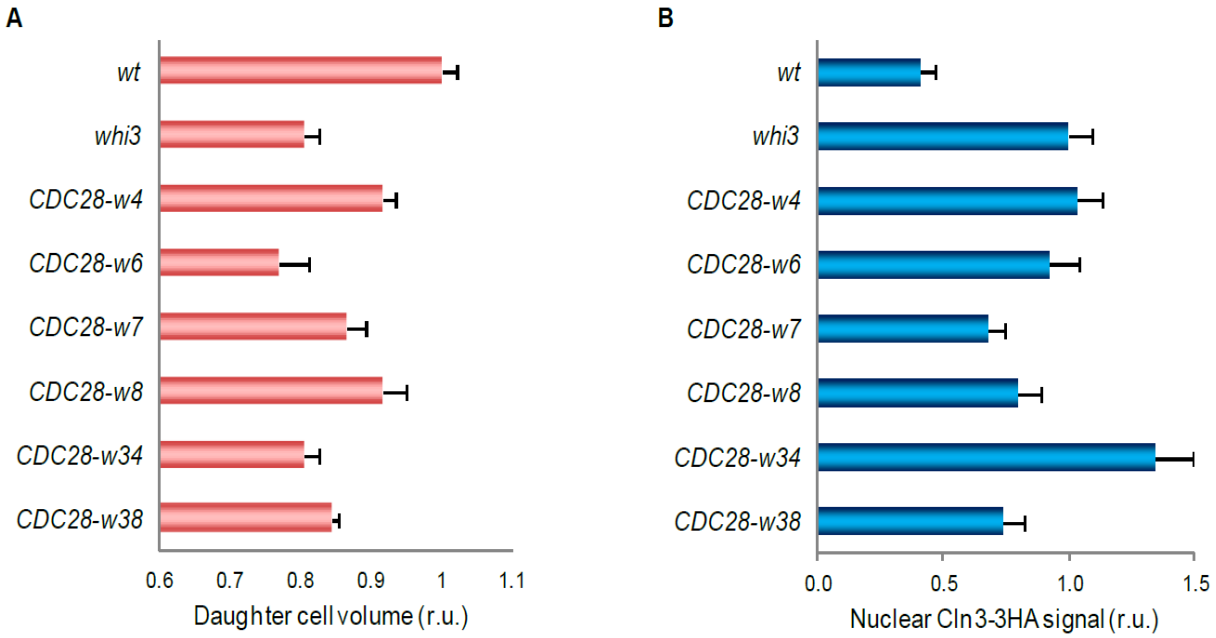

Figure 18: Cell volume and nuclear accumulation of Cln3-3HA in small cell size *CDC28* mutants

(A) Daughter cell volume deduced from Coulter-counter distributions as described by (Jorgensen et al., 2002) for wild-type (wt), Whi3-deficient (*whi3*) and the following mutant strains: *CDC28-w4 (*K24R, D80N, R97G, S213G), *CDC28-w6 (*S2G, S46G, K96T, K187N, K274R), *CDC28-w7 (*S46C, K96I, Q251L), *CDC28-w8 (*K223N, R288G), *CDC28-w34* (Y23H, L61I, H130Y) and *CDC28-w38 (*I56L, K209E). Relative mean values from triplicate distributions and confidence limits (α=0.05) for the mean are plotted.
(B) Nuclear Cln3-3HA levels for wild-type (wt), Whi3-deficient (*whi3*) and the indicated *CDC28* mutant strains were measured as in Figure 3A. Relative mean values and confidence limits (α=0.05) for the mean (N>200) are plotted.

Cdc28 *wee* mutations are found in two clusters

By sequencing, the identified mutants contained a total of 11 amino acid substitutions distributed in two regions of the Cdc28 molecule (Figure 19A). A group of 5 mutations were found in or in the vicinity of the cyclin-binding domain, suggesting that these variants could display a stronger interaction to Cln3 or be more susceptible to activation by Cln3. One of them affected S46, a CK2 target previously involved in cell size control by others (Russo et al., 2001). Notably, the remaining substitutions were found at five positions clustered at an opposite region in the C-terminal lobe of Cdc28, and mostly affected basic amino acids with likely exposed side chains (Figure 19B). As we were particularly interested in Cdc28 domains different from the cyclin-binding region, we decided to characterize these mutations further and to build a quintuple mutant that we will refer to as *CDC28^{wee}*.

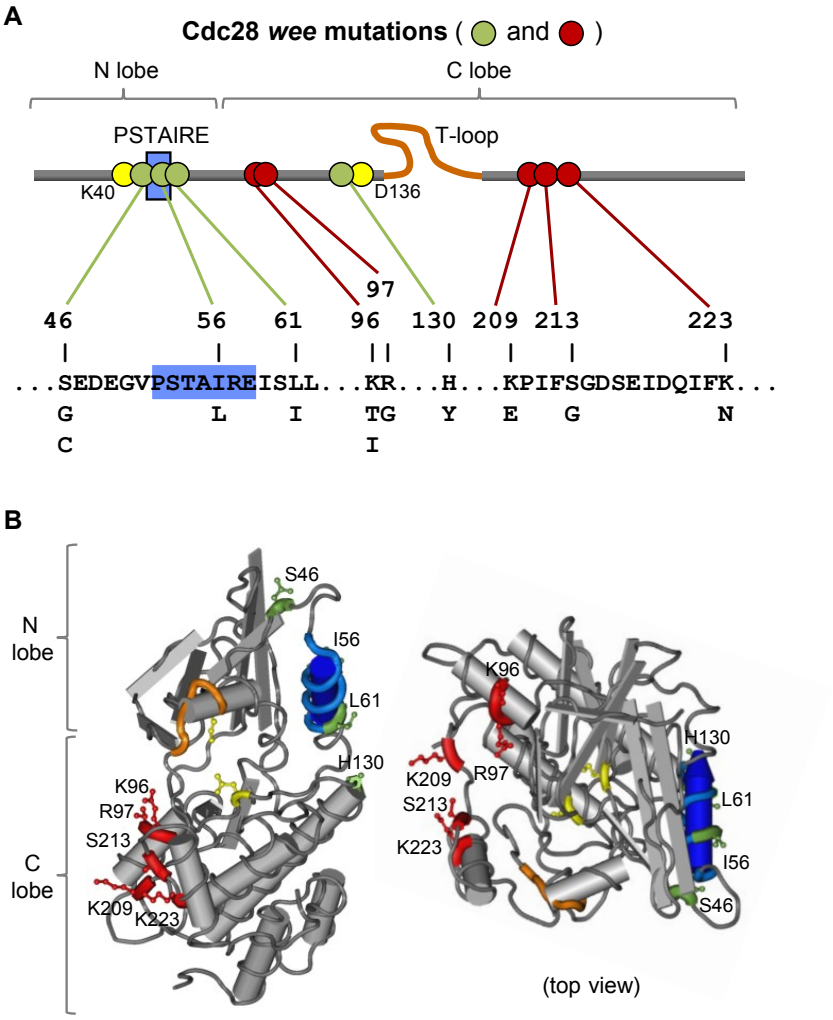

Figure 19: Cdc28 *wee* mutations found in two clusters

(A) Scheme of the Cdc28 polypeptide indicating the two sets of amino acid substitutions found in small-cell-size mutants, one of them including four positions (green) lying at the N lobe and the other set with five positions (red) at the C lobe. The regulatory T-loop (orange) and the PSTAIRE helix (blue) that interacts with cyclins are also indicated.
(B) Cdk4-based structural representation of Cdc28 showing the position of the two sets of amino acid substitutions indicated in (A).

Phenotype of *CDC28*^{wee} mutant

In agreement with the phenotypes of the single mutations, the quintuple *CDC28*^{wee} mutant displayed a strong shift in the overall distribution towards small cell sizes that was strictly dependent on the presence of Cln3 since a *cln3* deletion masked the size effect of the *CDC28*^{wee} compared to the wild type allele (Figure 20A). In contrast, effects of *CDC28*^{wee} on budding size (Figure 20B) were additive to the *whi3* deletion, suggesting

that both alterations affect related but independent components of the mechanisms that control cell size in budding yeast. *CDC28*^{wee} cells showed a higher mean level of nuclear Cln3 (Figure 20C) and, more important, a strong increase in the proportion of cells displaying a nuclear signal of Cln3 above a certain threshold (Figure 20C).

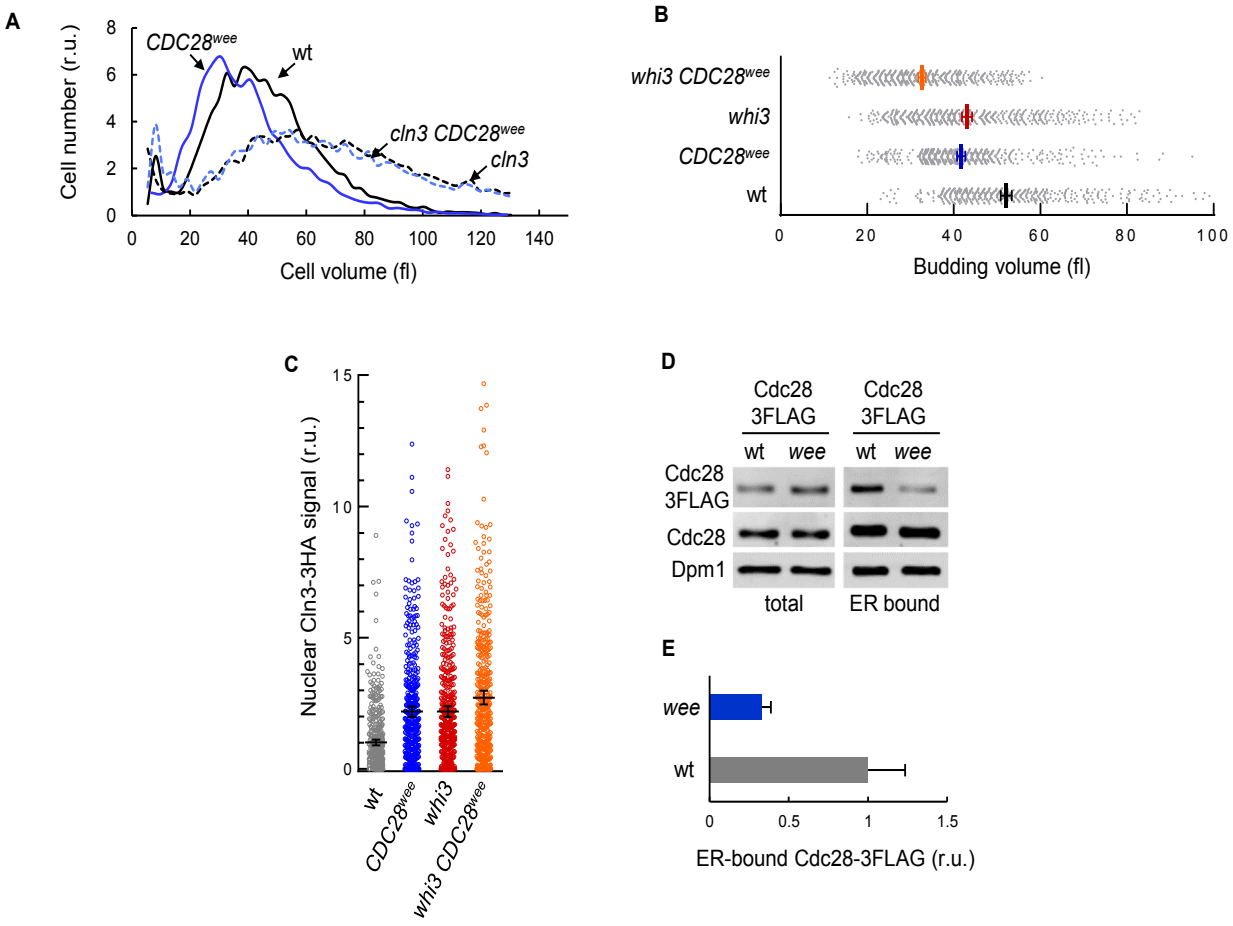

Figure 20: Phenotype of *CDC28*^{wee} mutant

(A) Coulter counter cell volume distributions for the indicated strains are shown.

(B) Cell volumes at budding of individual cells (n > 500) with indicated genotypes are plotted. Mean values (thick vertical lines) and confidence limits (α = 0.05, thin vertical lines) for the mean are also shown.

(C) Nuclear accumulation of Cln3-3HA in asynchronous individual cells (n > 450) with indicated genotypes as measured by semiautomated quantification of immunofluorescence levels in both nuclear and cytoplasmic compartments. Values were made relative to the average obtained from wild-type (WT) cells. Mean values (thick horizontal lines) and confidence limits (α = 0.05, thin horizontal lines) for the mean are shown.

(D) Total extracts and ER-bound fractions from WT cells expressing an additional *CDC28-3FLAG* or *CDC28*^{wee}*-3FLAG* construct were analyzed by western to detect endogenous and 3FLAG-tagged Cdc28 proteins. Dpm1 is shown as ER marker.

(E) Chemiluminescent quantification of Cdc28-3FLAG and Cdc28^{wee}-3FLAG protein levels analyzed in (D) are plotted relative to the endogenous chromosome-borne Cdc28 protein levels. Mean values from triplicate samples and confidence limits (α = 0.05) for the mean are shown.

The effects caused by *CDC28*^{wee} were comparable to the *whi3* deletion and, similarly to effects on cell size, both alterations behaved in an additive manner with regard to nuclear accumulation of Cln3 (Figure 20C). Finally, Cdc28^{wee} levels in ER-enriched fractions were lower compared to the wild-type Cdc28 protein (Figures 20D and 20E), which suggested that the mutated residues at the C-terminal lobe of the yeast Cdk could have a prominent role in retaining the G1 Cdk-cyclin complex at the ER. The low abundance of Cdc28^{wee} in ER-enriched fractions was also a key finding to go further into a proteomic analysis to uncover the components of the retention device behind ER-sequestration of Cdc28.

Identification of differentially weakened interactions of Cdc28^{wee}

Once its effects on cell size control, Cln3 localization and low abundance in ER-enriched fractions had been clearly established, we decided to use the quintuple Cdc28^{wee} mutant to identify interactors of Cdc28 that could have a direct role in the retention of the G1 Cdk-cyclin complex at the ER during G1 phase. To detect changes in the Cdc28 interactome we used iTRAQ to analyze four independent pairs of FLAG-tagged wild-type and *wee* Cdc28 immunoprecipitates from G1 cells (Figures 21A and 21B).

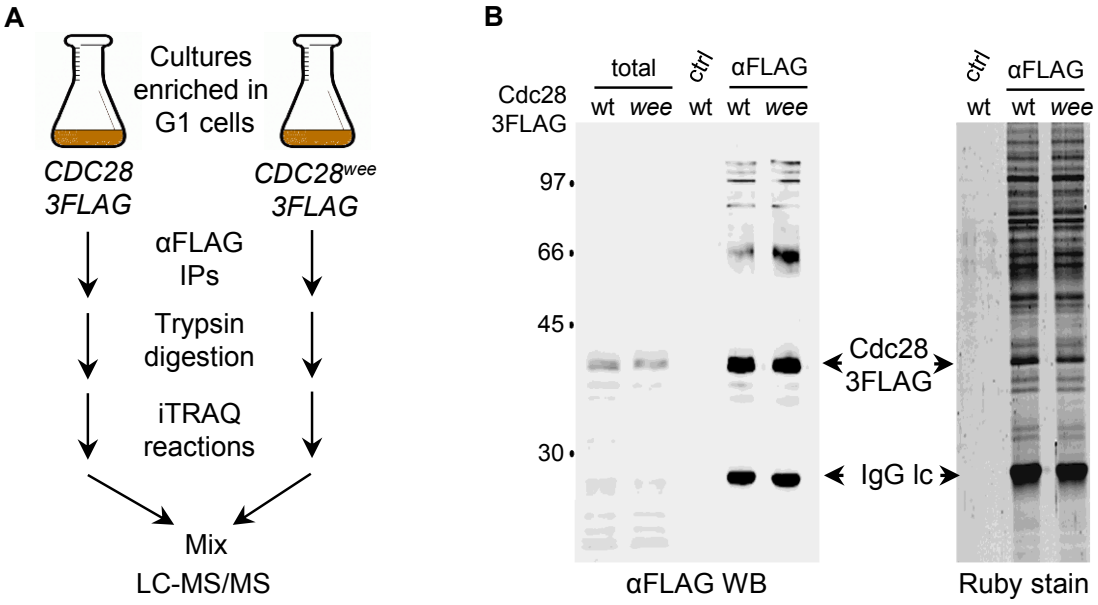

Figure 21: iTRAQ analysis of differential interactors of Cdc28^{wee}

(A) Schematic of the iTRAQ comparative analysis of Cdc28^{wee} and Cdc28 interactors.
(B) Western analysis (left) and ruby-stained gel (right), showing total cell extracts, and αFLAG or control immunoprecipitates of WT and mutant (*wee*) 3FLAG-tagged Cdc28 proteins, used in the iTRAQ analysis. The positions of Cdc28-3FLAG proteins and IgG light chains are indicated.

Qualitative assessment of iTRAQ data

After filtering the data to consider only those proteins identified at a 95% confidence level (Figure 22A), our data were consistent with previous high-throughput studies of Cdc28 interactors using affinity capture-MS approaches (Breitkreutz et al., 2010; Collins et al., 2007; Gavin et al., 2002, 2006; Ho et al., 2002) (Figure 22B).

A

Unused score	Proteins detected	Distinct peptides
>2.0	146	1972
>1.3 (95%)	176	2261
>0.47	287	3136
>0.05	822	5218
After filtering*	770	Nd

* Non yeast, ribosomal and transposon-encoded proteins

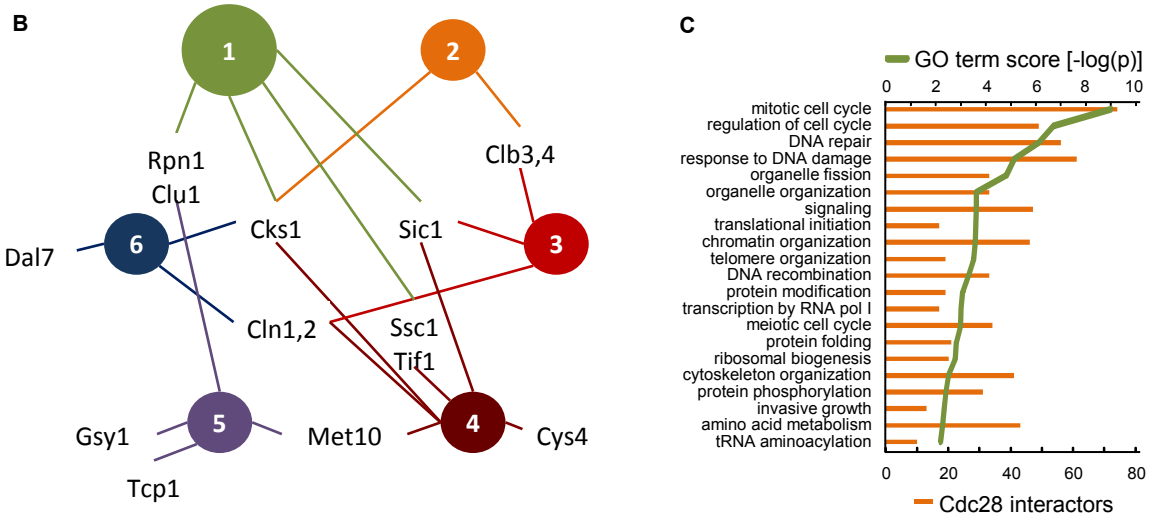

Figure 22: Qualitative assessment of Cdc28 interactors obtained from iTRAQ

(A) A table indicating the unused score of Cdc28 interactors identified in the iTRAQ analysis (Unused ProtScore reflects the amount of total, unique peptide evidence related to a given protein ProtScore = -log (1 - (PercentConfidence/100))

(B) Cdc28 Interactors Identified by High-Throughput Affinity Capture-MS Approaches The diagram shows the Cdc28 interactors identified in our iTRAQ analysis at 95%confidence (1: our iTRAQ data) that have been also identified by other affinity capture-MS approaches (2: Breitkreutz et al., 2010; 3: Collins et al., 2007; 4: Gavin et al., 2006; 5: Ho et al., 2002; 6: Gavin et al., 2002). The absence of cyclins at sufficient levels for univocal identification in our iTRAQ analysis is likely due to the fact that we used cultures highly enriched in G1 cells.

(C) GO term frequencies and –log (p) scores of identified Cdc28 interactors by iTRAQ analysis.

The absence of cyclins at sufficient levels for unambiguous identification in our iTRAQ analysis is likely due to the fact that we used cultures highly enriched in G1 cells. On the

other hand, the most frequent functional categories among the 816 proteins above a low cutoff value were related to cell cycle control (Figure 22C).

Discrimination of candidates with lower affinity for Cdc28

The variability in the levels of a total of 219 proteins in immunoprecipitates was analyzed as a Q score for Cdc28^{wee} interactors and an S score for Cdc28^{wt} interactors. From every interactor we obtained 4 pairs of Q scores and 4 pairs of S scores, which were used to analyze the existence of unexpected biases in the two immunoprecipitates.

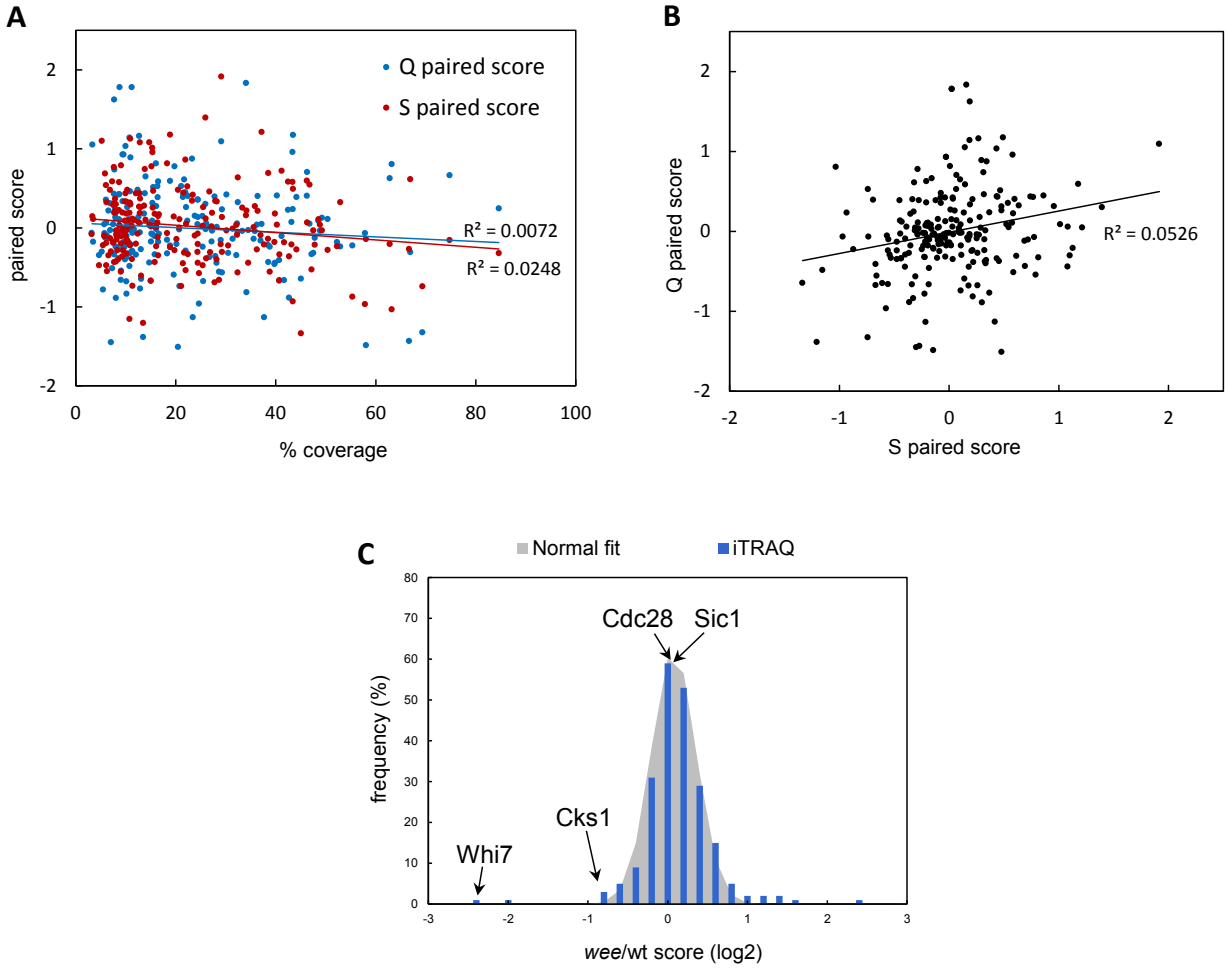

Figure 23: Quantitative analysis of iTRAQ data

(A) Scatter plot displaying paired score (Q and S) against the coverage% of the proteins identified (calculated as the percentage of the residues in each protein sequence that have been identified). R^2 represents the coefficient of determination that describes fit consistency.
(B) Scatter plot displaying Q paired scores against S paired scores of the iTRAQ identified proteins.
(C) Frequency distribution (blue bars) of Cdc28 interactors by a *wee*/wt score that indicates their relative presence in mutant Cdc28^{wee} and WT Cdc28 immunoprecipitates. A normal fit distribution (gray area) is also shown, and the positions of Cdc28, Sic1, Cks1, and Whi7 proteins are indicated.

Both of Q and S scores show an internal variability that is independent of the the peptide coverage percentage of the proteins identified (Figure 23A). In addition, the internal variability within Q scores shows no correlation with the internal variability within S scores (Figure 23B). Thus, no unexpected biases for protein enrichments in the two immunoprecipitates were found. Finally, an average Q/S score was obtained as $\log_2$ (*wee*/wt) to compare the relative immunoprecipitation efficiencies of each candidate interactor to *wee* and wild-type Cdc28 proteins (Supplementary Table 6). Figure 23C shows the distribution of these candidate interactors by their Q/S score. As a proof-of-principle Cdc28 offered a score not significantly different from 0, and the same lack of depletion in *wee* versus wild-type Cdc28 immunoprecipitates was observed for Sic1, which suggests that the interaction of these two proteins does not involve the residues mutated in Cdc28^{wee}.

Whi7 interacts with Cdc28

Of particular importance to our present purpose, the candidate interactor with the lowest Q/S score was Srl3 (YKR091W), a protein of unknown function that had been isolated as a suppressor of Rad53-lethality (Desany et al., 1998), and identified as a phosphorylation target of Cdc28 (Ubersax et al., 2003). Here we show that this protein is an inhibitor of cell cycle entry that plays a key role in regulating the correct localization of the Cln3 cyclin during G1 phase.

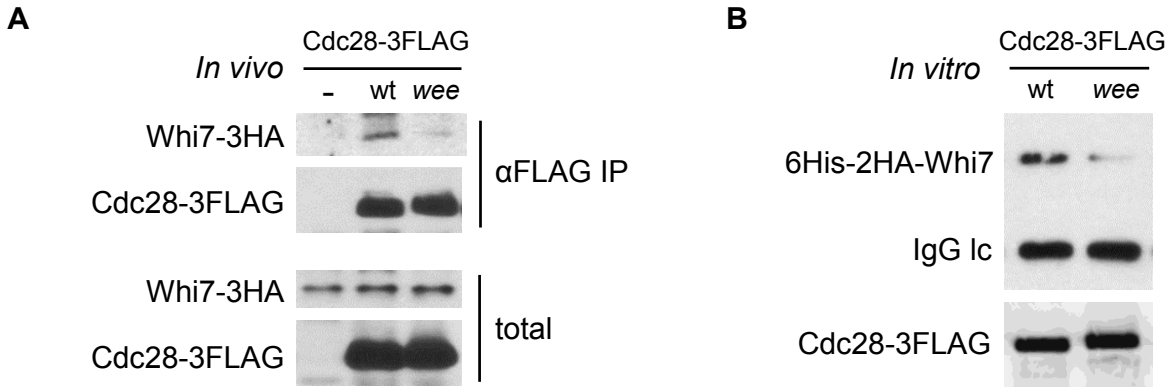

Figure 24: Whi7 interaction with Cdc28

(A) In vivo Cdc28-Whi7 interaction assay. Western analysis of cell extracts (total) and αFLAG immunoprecipitates (αFLAG IP) of *3HA-WHI7* cells expressing WT or mutant (*wee*) Cdc28-3FLAG proteins. **(B)** In vitro Cdc28-Whi7 interaction assay. Purified 6His-2HA-Whi7 was added to αFLAG immunoprecipitates (αFLAG IP) of cells expressing WT or mutant (*wee*) Cdc28-3FLAG proteins, and the bound fraction was analyzed by western. The position of IgG light chains is indicated.

We therefore propose renaming it as Whi7. Confirming the weakened interaction of Whi7 to Cdc28^{wee} observed by iTRAQ analysis, we found lower levels of a 3HA-tagged Whi7 protein in Cdc28^{wee} immunoprecipitates from yeast cells compared to wild-type Cdc28 (Figure 24A). Furthermore, bacterially expressed Whi7 bound Cdc28^{wee} with a lower efficiency compared to wild-type Cdc28 in vitro (Figure 24B).

Whi7 is strikingly similar to Whi5, the nuclear Cdc28 target

Whi7 was described as a Whi5 paralog (Byrne & Wolfe, 2005). Whi7 and Whi5 share significant similarities at the sequence level (Figure 25A), particularly at domains where phosphorylation of Whi5 by Cdc28 takes place (Wagner et al., 2009).

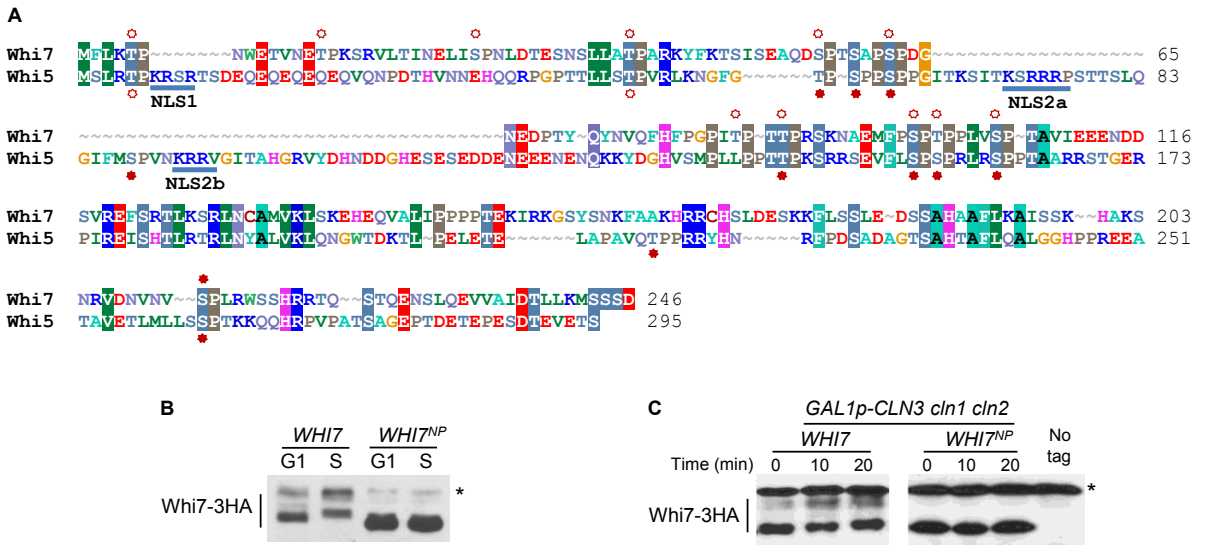

Figure 25: Whi7, a Whi5-related protein, is phosphorylated upon cell cycle entry

(A) Whi7 (amino acids 55–225) and Whi5 (amino acids 109–275) display 31% identity and 46% similarity ($p = 3.4 \times 10^{-11}$). Nuclear localization sequences NLS1 and bipartite NLS2 (Taberner et al., 2009) are underlined, and experimentally demonstrated (Wagner et al., 2009) and putative Cdk phosphorylation sites are indicated by filled and open symbols, respectively.
(B) Cells expressing 3HA-tagged wild-type (*WHI7*) or nonphosphorylatable (*WHI7^{NP}*) Whi7 proteins were arrested in late G1 (G1) with α factor and released into S phase (S) to prepare cell extracts for western analysis. An αHA crossreacting band is indicated (*).
(C) *GAL1p-CLN3 cln1 cln2* cells expressing 3HA-tagged wild-type (*WHI7*) or nonphosphorylatable (*WHI7^{NP}*) Whi7 were arrested in G1 by growth in 2% raffinose for 4 hr. Two percent galactose was added to induce expression of *GAL1p-CLN3*, and samples were collected at the indicated times for western analysis. HA-untagged cell extracts were used as control (right lane). An αHA crossreacting band is indicated (*).

Whi7 is also phosphorylated when cells execute the G1/S transition (Figure 25B) or after induction of Cln3 expression (Figure 25C), which suggests that Whi7, in a similar manner to Whi5, could be regulated by Cdc28-dependent hyperphosphorylation during

cell cycle entry. However, Whi7 lacks the Whi5 sequences responsible for its regulated nuclear localization during the cell cycle (Costanzo et al., 2004; Taberner et al., 2009; Wagner et al., 2009).

Whi7 interacts with Cks1

Whi7 has been shown to interact with Cks1 (Gavin et al., 2002), an important subunit of Cdc28 (Harper, 2001), but levels of Cks1 were only slightly reduced in Cdc28^{wee} immunoprecipitates (Figure 26A), suggesting that the interaction between Whi7 and Cdc28 is not mediated by Cks1 alone.

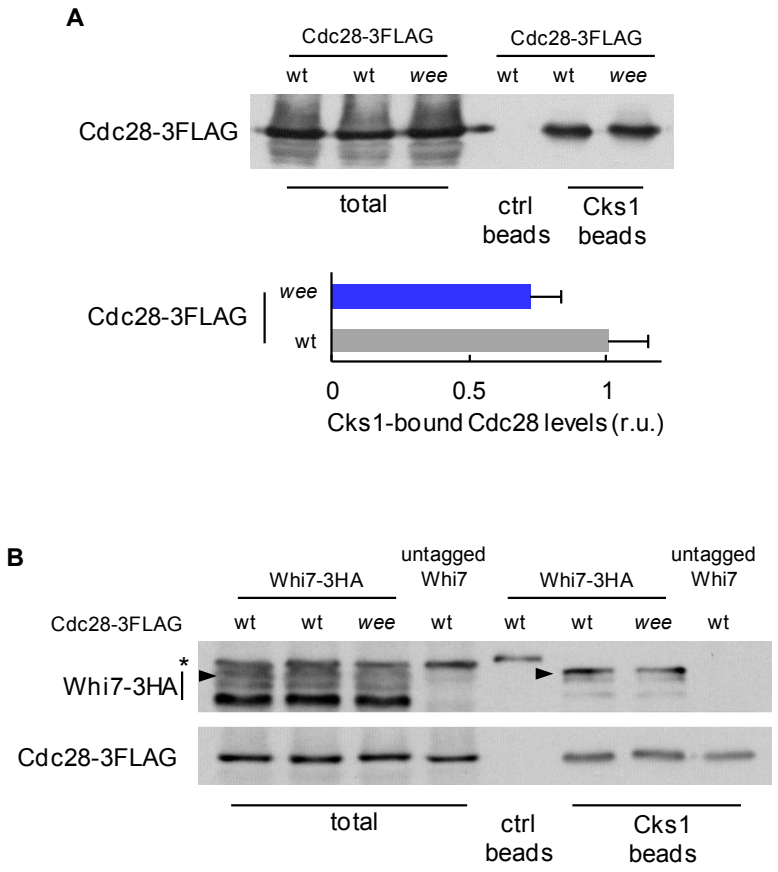

Figure 26: Cks1 interactions with Cdc28 and Whi7

(A) Cdc28-Cks1 interaction assay. Extracts (total) of cells expressing wild-type (wt) or mutant (*wee*) Cdc28-3FLAG proteins were used in pull-down assays with control (ctrl) or *S. pombe* Suc1 (Cks1) beads and samples were analyzed by western. Relative levels of Cdc28-3FLAG proteins in Cks1 pull-down samples are plotted at the bottom.

(B) Cdc28-Whi7-Cks1 interaction assay. Extracts (total) of cells expressing Whi7-3HA and wild-type (wt) or mutant (*wee*) Cdc28-3FLAG proteins were used in pull-down assays with control (ctrl) or *S. pombe* Suc1 (Cks1) beads and samples were analyzed by western. Slow-migrating forms of phosphorylated Whi7 are indicated (arrowhead). An αHA crossreacting band is also indicated (*).

Notably, we found that phosphorylated forms of Whi7 display an increased affinity for Cks1 (Figure 26B), suggesting that basic-charge driven Cks1 interaction could play a key role in Whi8 multiphosphorylation.

Whi7 localizes to the ER

Available immunofluorescence data suggest that Whi7 localizes to cytoplasmic patches (Kumar et al., 2002). Preliminary confocal microscopy images showed a pattern reminiscent of proteins belonging to ER-associated compartments, and coexpression with Ole1-GFP as ER marker confirmed that Whi7-3HA staining produces a punctate pattern closely associated to the ER network (Figure 27A and 27B). Confirming this association, we found that a fraction of Whi7 cosediments with Dpm1, another ER marker, in sucrose gradients (Figure 27C) Furthermore, while the Whi7^{NP} mutant protein was present at higher levels than the wild-type protein in the dense, ER-containing fractions of sucrose gradients, phosphorylated Whi7 was enriched more than 4-fold in the soluble fractions (Figure 27C). Notably, this behavior is similar to that of Cdc28, a fraction of which is found in dense ER-containing fractions (Vergés et al., 2007). Similarly to cyclin Cln3 (Vergés et al., 2007), association of Whi7 to the ER was sensitive to alkaline pH (Figure 27D). However, the Whi7^{NP} mutant protein was more resistant to alkaline dissociation, indicating that the nonphosphorylatable Whi7 mutant is more tightly bound to the ER.

Whi7 is a negative regulator of Start

Next we decided to test whether Whi7 is an inhibitor of cell cycle entry and plays a key role in regulating the correct localization of the Cln3 cyclin during G1 phase. The *whi7* disruption caused a clear reduction in cell volume at budding (Figure 28A), suggesting a role in the pathways that control the critical size in budding yeast. Cell size at Start is a growth rate-dependent parameter (Jorgensen & Tyers, 2004), and each single cell sets the critical size in a very robust manner as a function of its individual growth rate during G1 (Ferrezuelo et al., 2012). As *whi7* cells showed no population differences in growth rate compared to wild-type cells, we concluded that Whi7 is a negative regulator of Start that acts independently of the growth rate-sensing mechanism, most likely as a Cdc28 interactor that contributes to retaining the G1 Cdk-cyclin complex at the ER.

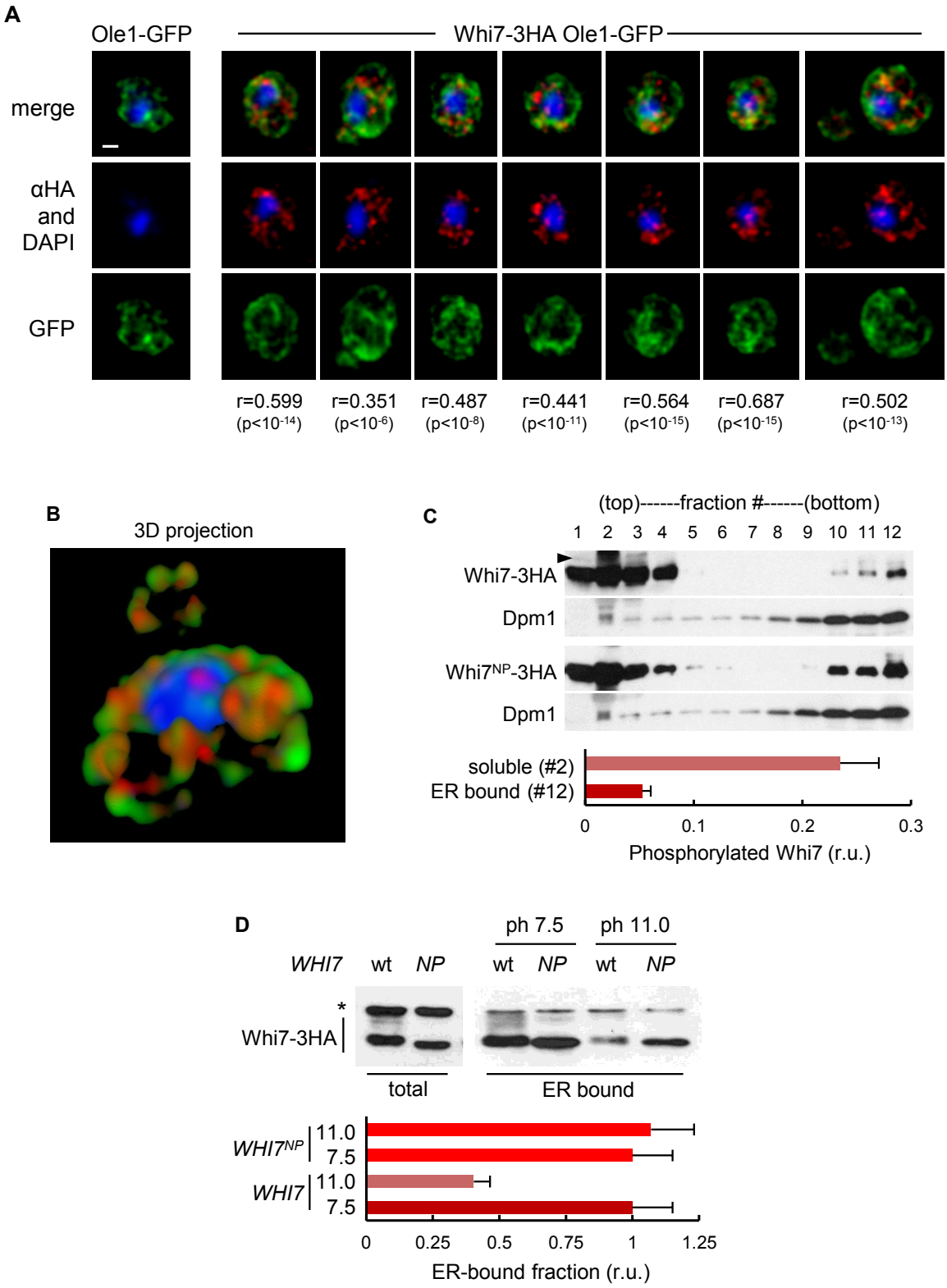

Figure 27: Whi7 is found associated to the ER in a phosphorylation-dependent manner

(A) Confocal images of WT cells expressing Whi7-3HA at endogenous levels and Ole1-GFP as ER marker. Nuclei were detected by DAPI staining, and HA-untagged cells were analyzed as control (left panels). An overlaid stack of 20 0.34μm deconvolved sections is shown for each image. Bar indicates 2μm. The Pearson's coefficient of colocalization of Whi7-3HA and Ole1-GFP signals and the corresponding p value obtained by Costes' randomization are shown at the bottom of each image set.

(B) 3D projection of the merged stack corresponding to cell in right panel (D).
(C) Western analysis of the distribution of Whi7-3HA and nonphosphorylatable Whi7^{NP}-3HA in sucrose gradients. Dpm1 is shown as ER marker. Relative levels of slow-migrating forms of phosphorylated Whi7 (arrowhead) in soluble (#2) and ER-containing (#12) fractions are plotted at the bottom.
(D) Whi7 and Whi7NP Associate to the ER with Different Efficiencies .Total extracts from cells expressing Whi7-3HA or non-phosphorylatable Whi7NP-3HA proteins were either untreated (pH 7.5) or subject to 0.1 M Na2CO3 (pH 11.0) before separation of ER-bound proteins for western analysis. An αHA crossreacting band is indicated (*). Whi7-3HA and Whi7NP-3HA relative protein levels in the ER-bound fraction are plotted at the bottom. Mean values from triplicate samples and confidence limits (α=0.05) for the mean are shown.

Contrary to the *whi7* deletion, the presence of the nonphosphorylatable mutant of Whi7 (Whi7^{NP}) caused an increase in cell volume at budding (Figure 28A), suggesting that phosphorylation at Cdk-consensus sites would counteract its activity as a negative regulator of Start. In addition, overexpression of *WHI7* from a regulatable promoter (Figure 28B) that mimics induction levels caused by and ER-stress agent delayed cell budding and caused a rapid and marked increase in cell size at budding (Figure 28C-28E).

Whi7 overexpression strongly affects Cln3 nuclear accumulation

The Cln3 cyclin accumulates in the nucleus at Start (Wang et al., 2004), and alteration of the mechanisms that help retain the G1 Cdk-cyclin complex at the ER cause unscheduled accumulation of Cln3 in the nucleus (Vergés et al., 2007). Therefore we decided to test whether Whi7 acts as a regulator of Cln3 localization. Whi7-deficient cells showed an increase in the average level of nuclear Cln3 and, more important, an increase in the proportion of cells displaying a high level of Cln3 in the nucleus (Figure 29A) in both asynchronous cultures and late G1 arrested cells. Moreover, *WHI7* overexpression caused a rapid reduction in the average level of nuclear Cln3, the decrease being even faster when the nonphosphorylatable Whi7^{NP} was overproduced (Figure 29A).

Notably, *WHI7* overexpression reduced to undetectable levels the presence of Cln3 in the lighter fractions of sucrose gradients (Figure 29B), which contain soluble protein complexes and are enriched in Cln3 cyclin when its nuclear accumulation is maximal (Vergés et al., 2007). Taken together, these data support the notion that Whi7 is a component of the mechanism that retains the Cln3 cyclin at the ER and prevents its unscheduled accumulation in the nucleus.

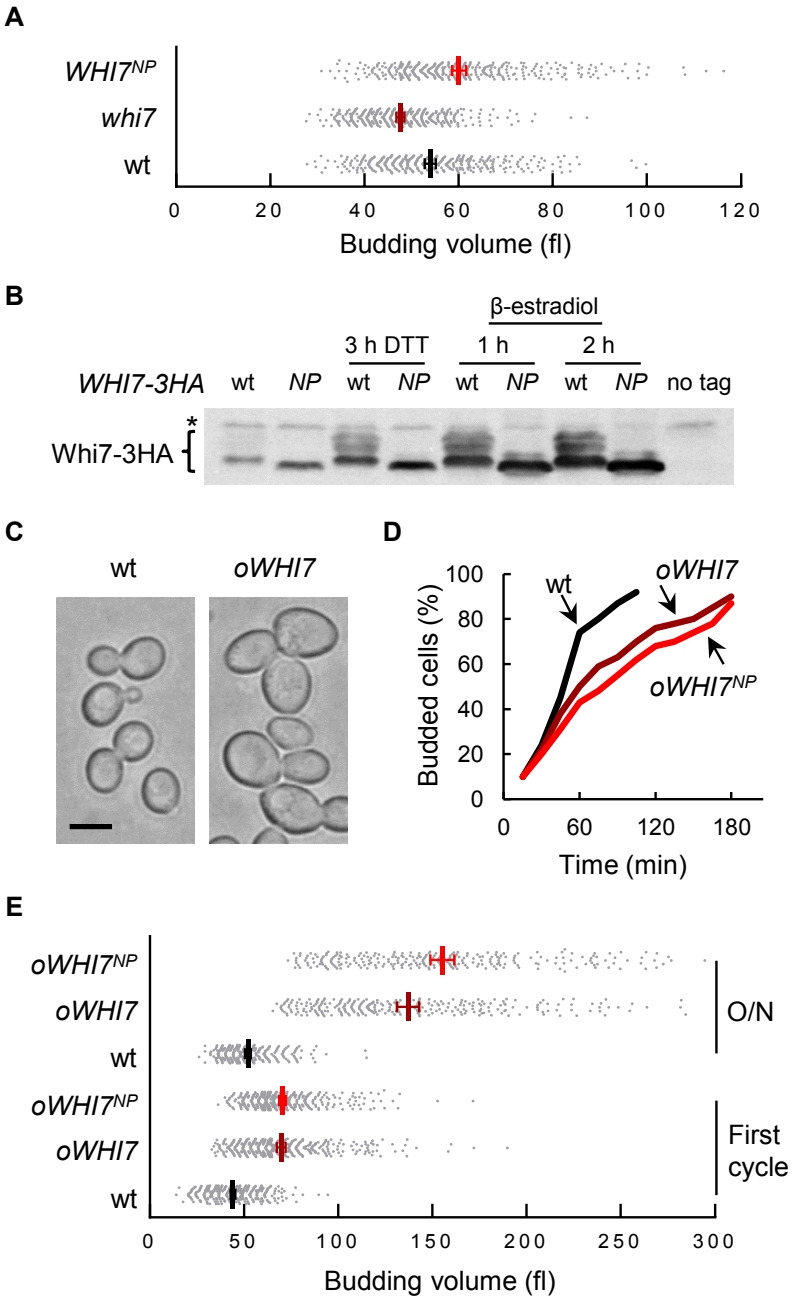

Figure 28: Whi7 is a negative regulator of cell cycle entry

(A) Individual cell volumes at budding of WT, *whi7*, or *WHI7^{NP}* cells (n > 350) with indicated genotypes are plotted. Mean values (thick vertical lines) and confidence limits (α = 0.05, thin vertical lines) for the mean are also shown.

(B) Western analysis of total cell extracts of WT and nonphosphorylatable (*NP*) *WHI7-3HA* cells left untreated or subject to 5mM DTT for 3hr. β-estradiol was used to induce for the indicated times expression of WT and nonphosphorylatable mutant (*NP*) *GAL1p-WHI7-3HA* cells. HA-untagged cell extracts were analyzed as control (right lane). An αHA crossreacting band is indicated (*).

(C) Bright-field images of asynchronous WT and *WHI7* overexpressing (*oWHI7*). Bar indicates 5µm.

(D) Early G1 WT cells overexpressing either wild-type (*oWHI7*) or nonphosphorylatable (*oWHI7^{NP}*) *WHI7* were used to determine budding index as an indicator of cell cycle entry.

(E) Early G1 cells, as in (D), were induced with β-estradiol, and individual cell volumes at budding were determined thereafter (first cycle, n> 400) or after overnight growth (O/N, n > 250). Mean values (thick vertical lines) and confidence limits (α = 0.05, thin vertical lines) for the mean are also shown.

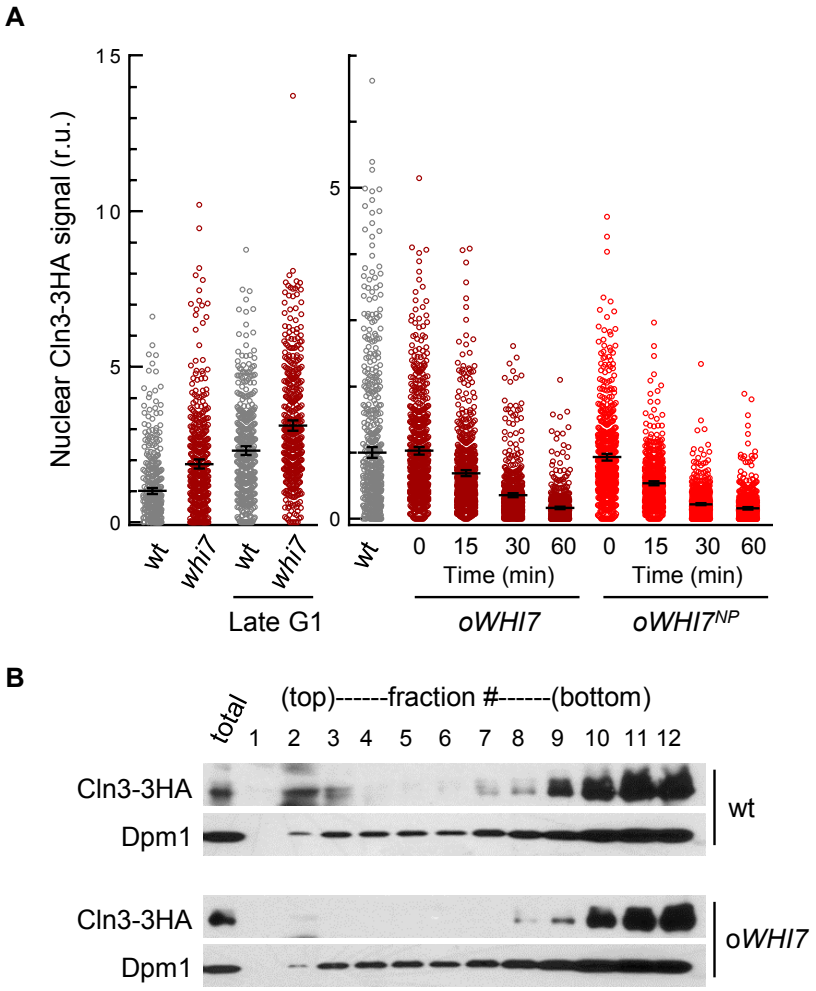

Figure 29: Whi7 plays an important role in retention of Cln3 at the ER

(A) Nuclear accumulation of Cln3-3HA in asynchronous and late G1-arrested cells (n > 600) of WT and Whi7-deficient (*whi7*) *CLN3-3HA* strains. Cells overexpressing either wild-type (*oWHI7*) or nonphosphorylatable (*oWHI7*^{NP}) *WHI7* were induced with β-estradiol, and samples were taken at indicated times. Mean values (thick horizontal lines) and confidence limits (α = 0.05, thin horizontal lines) for the mean are shown.

(B) Extracts (total) from *CLN3-3HA* WT or overexpressing *WHI7* (*oWHI7*) cells were used to analyze, by western, the distribution of Cln3-3HA in sucrose gradients. Dpm1 is shown as ER marker.

Whi7 and chaperones play a related role in the Cln3 retention mechanism

As mentioned in the introduction, the Ydj1 chaperone plays a key role in releasing the Cln3 cyclin from the ER to allow its nuclear accumulation in late G1 (Vergés et al., 2007) We found that moderate chaperone overexpression also increased nuclear levels of Cln3

even in the presence of Whi7^{NP} (Figure 30A and 30B), indicating that Whi7 and chaperones play related roles in the retention-release mechanism that regulates Cln3 localization.

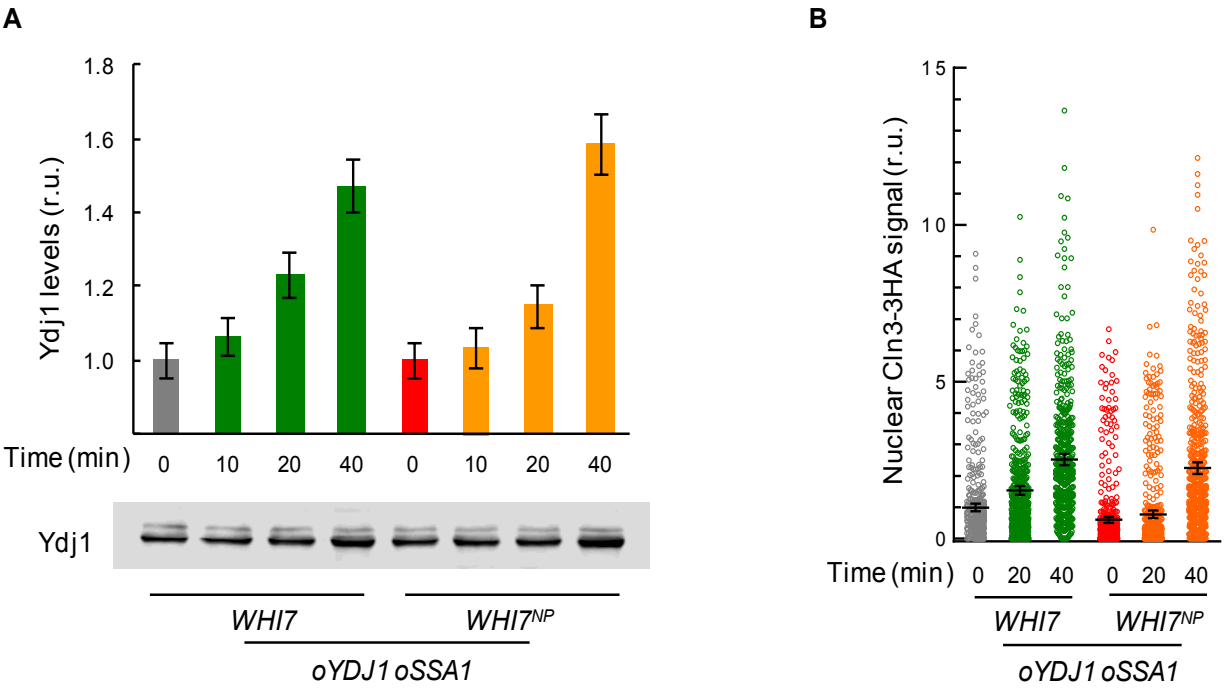

Figure 30: Ydj1 and Ssa1 chaperones are able to counteract the inhibitory effects of Whi7^{NP} on Cln3 nuclear accumulation

(A) Wild-type (*WHI7*) and non-phosphorylatable Whi7 (*WHI7NP*) *CLN3-3HA GAL1p-YDJ1 GAL10p-SSA1* cells were induced with β-estradiol and samples were taken at the indicated times for western analysis of Ydj1 levels, which are plotted at the top as relative values. Mean values from triplicate samples and confidence limits (α=0.05) for the mean are shown.
(B) Nuclear levels of Cln3-3HA in cells (N>500) as in (A). Mean values (thick horizontal lines) and confidence limits (α=0.05, thin horizontal lines) for the mean are shown.

Whi7 acts in a positive feedback loop to release the G1 Cdk1-Cyclin complex

Whi7 acts as an inhibitor of Start and, at the same time, is also a target of the Cdk under its regulation, which suggests that Whi7 could be a central component of a positive feedback loop in releasing the G1 Cdk-cyclin complex in late G1. Whi7 is important for proper retention of Cdc28-Cln3 complexes, and, once partly released by chaperone activity, these complexes could phosphorylate Whi7 and decrease its retention functions to facilitate further release of the Cdc28-Cln3 complex in a positive feedback loop.

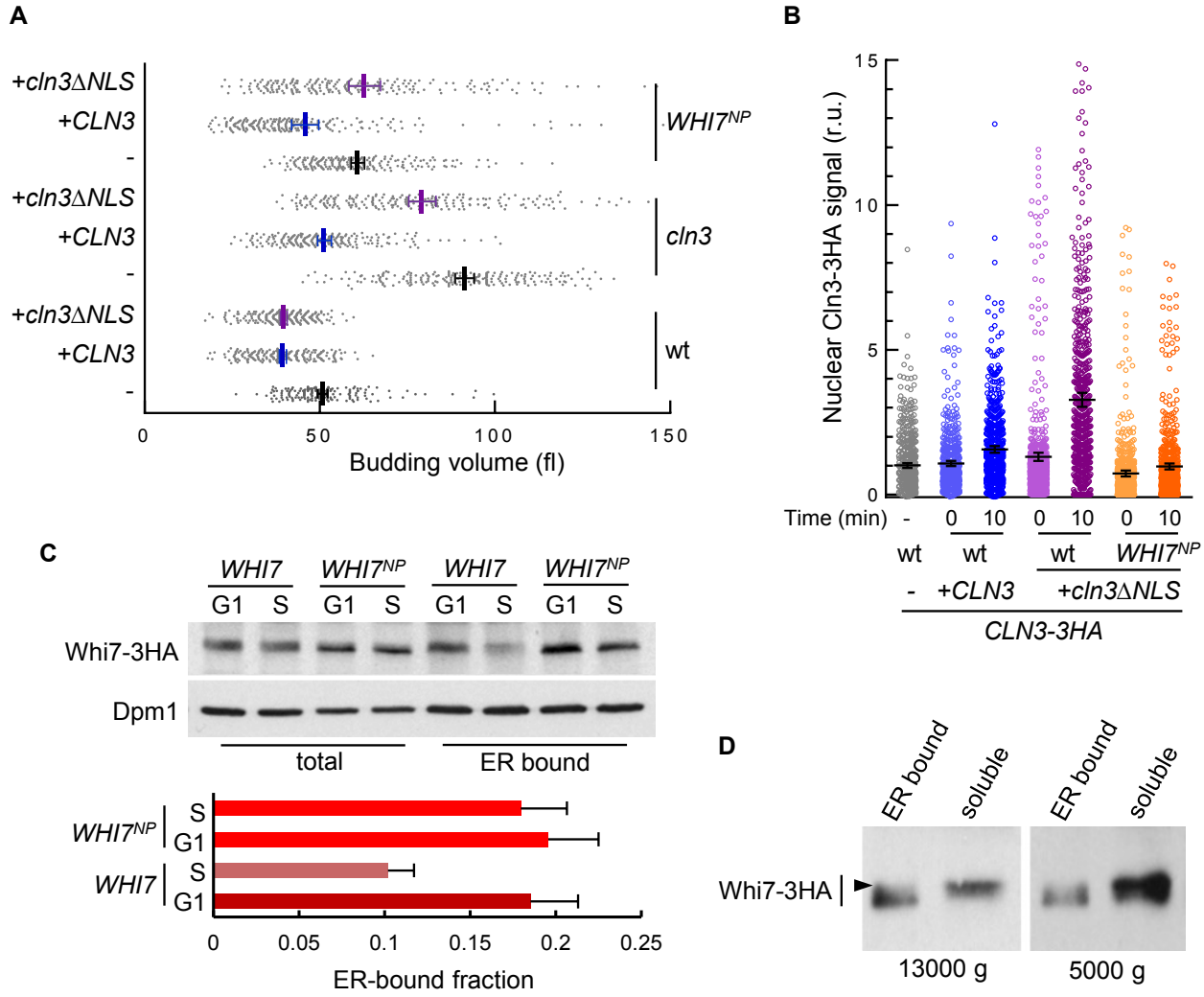

Figure 31: Whi7, Cdc28, and Cln3 participate in a positive feedback loop to release the Cdc28-Cln3 complex in late G1

(A) Individual cell volumes at budding of WT, Cln3-deficient (*cln3*), or expressing nonphosphorylatable Whi7 (*WHI7^{NP}*) cells (n > 400) with an additional copy of *CLN3* or *cln3ΔNLS* alleles are plotted. Mean values (thick vertical lines) and confidence limits (α = 0.05, thin vertical lines) for the mean are shown.
(B) Nuclear accumulation of Cln3-3HA in WT or nonphosphorylatable *WHI7* (*WHI7^{NP}*) *CLN3-3HA* cells (n > 600). Expression of additional wild-type (*+CLN3*) or cytoplasmic (*+cln3ΔNLS*) *CLN3* alleles was induced with β-estradiol, and samples were taken at indicated times. Mean values (thick horizontal lines) and confidence limits (α = 0.05, thin horizontal lines) for the mean are shown.
(C) Cells expressing Whi7-3HA or nonphosphorylatable Whi7^{NP}-3HA proteins were arrested in late G1 with α factor (G1) and released into S phase (S) to prepare total extracts and ER-bound fractions for western analysis. Dpm1 is shown as ER marker. Whi7-3HA and Whi7^{NP}-3HA relative protein levels in the ER-bound fraction are plotted. Mean values from triplicate samples and confidence limits (α = 0.05) for the mean are shown.
(D) *GAL1p-CLN3 cln1 cln2* cells expressing Whi7-3HA were arrested in G1 by growth in 2% raffinose for 4hr. Two percent galactose was added to induce expression of *GAL1p-CLN3* for 20min, and samples were taken to separate ER-bound proteins from soluble proteins by centrifugation for 30min at either 13,000 × *g* or 5,000 × *g*. A western analysis of Whi7-3HA is shown, and slow-migrating forms of phosphorylated Whi7 are indicated (arrowhead).

This hypothesis predicts that the Cdc28-Cln3 complex ought to have a cytoplasmic function or, in other words, that a *cln3ΔNLS* construct that cannot complement Cln3-deficient cells (Edgington & Futcher, 2001; Miller & Cross, 2001); and Figure 31A) should advance Start when added in *trans* to wild-type cells. Indeed, an additional copy of the *cln3ΔNLS* allele produced a decrease in budding cell size as noteworthy as that produced by a second wild-type *CLN3* allele (Figure 31A). Furthermore, expression of *cln3ΔNLS* caused a rapid increase in the nuclear accumulation of a chromosome-borne Cln3-3HA protein (Figure 31B), this effect being even more pronounced than that produced by a second wild-type *CLN3* gene. Notably, these hyperactivity effects of *cln3ΔNLS* were completely suppressed by the presence of the nonphosphorylatable Whi7^{NP} protein (Figures 31A and 31B), suggesting that the cytoplasmic function of the Cdc28-Cln3 complex is to modulate Whi7 association to the ER by phosphorylation. To test this idea, we analyzed the distribution of Whi7 in ER-bound and soluble fractions after induction of Cln3 expression and found that phosphorylated Whi7 forms were clearly enriched in the soluble fraction (Figure 31C). Finally, while ER-associated Whi7 levels decreased in S phase compared to G1-arrested cells, Whi7^{NP} levels remained unaffected (Figure 31D). These results reinforce the notion that phosphorylation of Whi7 modulates its association to the ER. Although most Whi7 is found in soluble fractions, we estimate that Whi7 levels are 100-times higher compared to Cln3, which suggests that only a small fraction of Whi7 would be involved in controlling the G1 Cdk-cyclin complex.

The kinase activity of Cdc28 is required for the positive feedback loop

To test whether the cytoplasmic role of Cln3 requires the kinase activity of Cdc28, we designed a Cdc28-Cln3 chimera (Coudreuse & Nurse, 2010) that would allow us to combine the *cln3ΔNLS* allele and a kinase-dead *cdc28^{KD}* mutation. The *CDC28-CLN3* fusion under the *CLN3* promoter produced similar protein levels compared to the wild-type *CLN3* gene and associated to the ER as wild-type Cln3 (Figure 32C). The *CDC28-CLN3* chimera was able to complement a *cln3* deletion (Figure 32A), causing a reduction in the budding cell size in wild-type cells (Figures 32A and 32D). Accordingly, the Cdc28-Cln3 chimera accumulated in the nucleus at higher levels compared to Cln3 (Figure 32F).

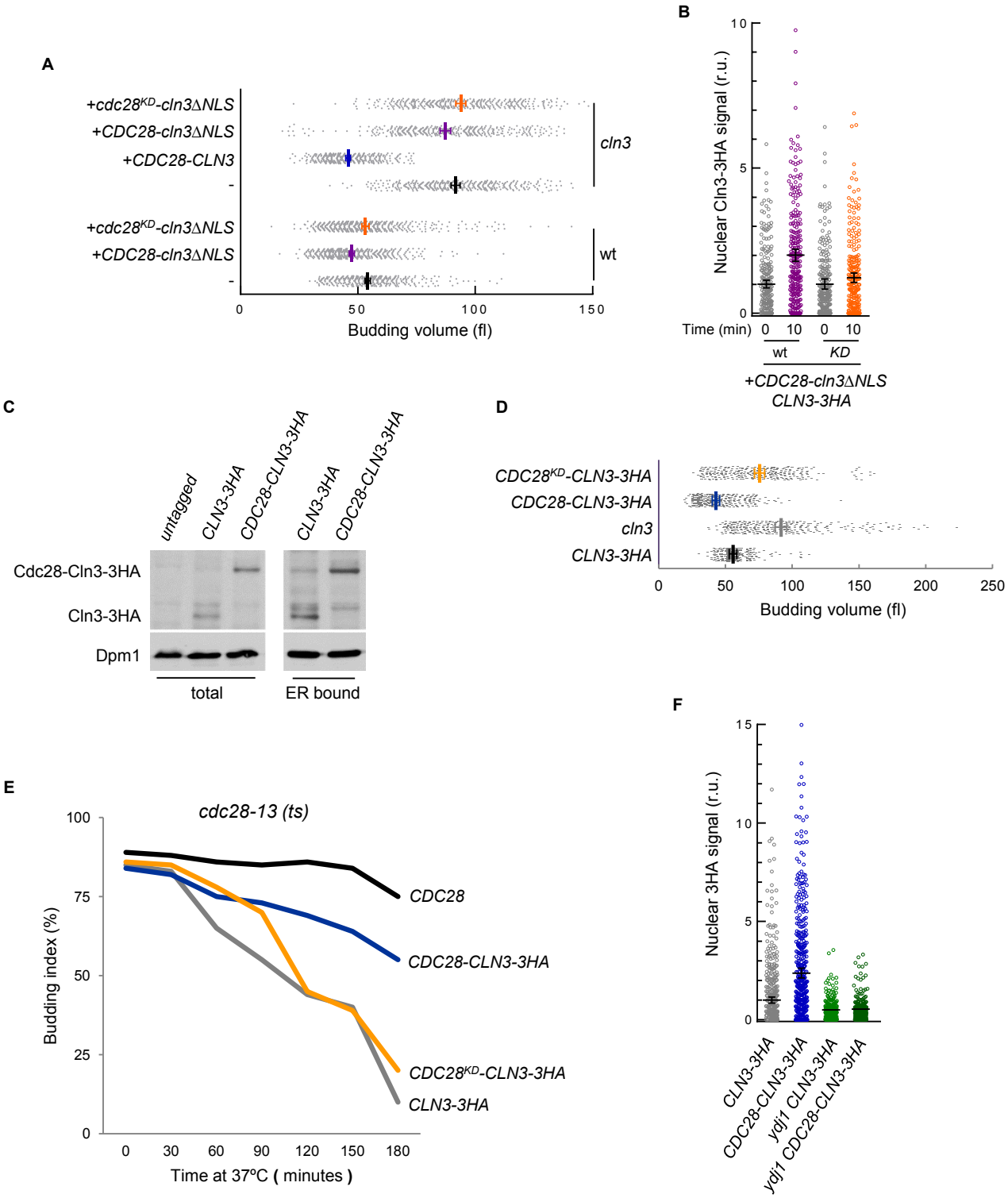

Figure 32: A *CDC28-CLN3* Chimera is fully functional and recapitulates chaperone-dependent Cln3 nuclear accumulation

(A) Individual cell volumes at budding of WT and Cln3-deficient (*cln3*) cells (n > 400) with an additional copy of *CDC28-CLN3*, *CDC28-cln3ΔNLS*, or *cdc28^{KD}-cln3ΔNLS* chimeras are plotted. Mean values (thick vertical lines) and confidence limits (α = 0.05, thin vertical lines) for the mean are also shown.
(follows in next page)

(B) Nuclear accumulation of Cln3-3HA in WT or nonphosphorylatable *WHI7* (*WHI7^{NP}*) *CLN3-3HA* cells (n > 250). Expression of either WT or kinase-dead (*KD*) *CDC28-cln3ΔNLS* chimeras was induced with β-estradiol, and samples were taken at indicated times. Mean values (thick horizontal lines) and confidence limits (α = 0.05, thin horizontal lines) for the mean are shown.
(C) Total extracts and ER-bound fractions from wild-type cells expressing *CLN3-3HA* or the *CDC28-CLN3-3HA* chimera were analyzed by western. Untagged cells were used as control. Dpm1 is shown as ER marker.
(D) Individual cell volumes at budding of wild-type cells (N=200) expressing *CLN3-3HA, CDC28-CLN3-3HA* or *CDC28KD-CLN3-3HA* are plotted. Mean values (thick vertical lines) and confidence limits (α=0.05, thin vertical lines) for the mean are also shown.
(E) Thermosensitive *cdc28-13* cells expressing either *CDC28, CDC28-CLN3-3HA, CDC28KD-CLN3-3HA* or *CLN3-3HA* were shifted at the restrictive temperature (37ºC) at time 0, and the percentage of budding was determined thereafter.
(F) Nuclear accumulation of Cln3-3HA and Cdc28-Cln3-3HA in wild-type (wt) or Ydj1- deficient (*ydj1*) cells (N>250) as in Figure 2F. Mean values (thick horizontal lines) and confidence limits (α=0.05, thin horizontal lines) for the mean are shown.

More importantly, the Cdc28-Cln3 chimera recapitulated the Ydj1-dependence for nuclear accumulation of wild-type Cln3 (Figure 32F). Confirming the hyperactivity observed in *trans* with *cln3ΔNLS*, a *CDC28-cln3ΔNLS* construct caused a reduction in the budding cell size only if a wild-type copy of *CLN3* was present (Figure 32A) and increased accumulation in the nucleus of a chromosome-borne Cln3-3HA protein (Figure 32B). However, a kinase-dead *cdc28^{KD}-cln3ΔNLS* chimera (Figures 32D and 32E) did not affect either budding size or nuclear levels of the chromosome-borne Cln3-3HA protein (Figures 32A and 32B), indicating that the cytoplasmic contribution of Cln3 to its own release requires the kinase activity of Cdc28.

2. Whi8 as a new regulator of the G1-Cdk in budding yeast

The differential interactome of a quintuple Cdc28^{wee} mutant pinpointed Whi8 as one of the proteins that were more abundant in the wild type Cdc28 proteome compared to the mutant *wee* one. Whi8, renamed in this work as Whi8, had no known biological function, but it contains RNA-binding domains and has been observed in both SGs and PBs. We have found that Whi8 interacts with Cdc28 *in vivo*, binds and colocalizes with the *CLN3* mRNA, and interacts with Whi3, an RNA-binding protein that binds specifically to *CLN3* mRNA. Most important, Whi8 deficient cells display show much higher levels of Cln3 under glucose and nitrogen starvation, which are two acute stress conditions, and we found by life microscopy that *whi8* cells were unable to accumulate the *CLN3* mRNA in stress granules. Finally, Whi8 accumulation in SGs depends on PKA and the presence of specific phophosites within Whi8. Thus, we have found a unique target of stress signaling that creates a direct link between stress response and G1 progression.

Whi8 interacts with Cdc28

Whi8 one of the candidates that were more abundant in the wild type Cdc28 proteome compared to Cdc28^{wee} (lower log2 *wee*/wt) according to our iTRAQ data. Table 7 shows the candidate interactors with P-value $p \leq 0.05$ (threshold p-value) by their *wee*/wt score.

As mentioned in Table 7 Whi8 has unknown biological function, it is an RNA-binding protein and exists in both SGs and PBs (Buchan et al., 2008). Confirming the weakened interaction of Whi8 to Cdc28^{wee} observed by iTRAQ analysis, we found lower levels of a 3HA-tagged Whi8 protein in Cdc28^{wee} immunoprecipitates from yeast cells compared to wild-type Cdc28 (Figure 33).

Phenotype of *whi8* and overexpression of *WHI8*

The *whi8* deletion caused a clear reduction in cell volume at budding (Figure 34A), suggesting a role in the pathways that control the critical size in budding yeast. As *whi8* cells showed no population differences in growth rate compared to wild-type cells, we concluded that Whi8 is a negative regulator of Start that acts independently of the growth rate-sensing mechanism, most likely as a Cdc28 interactor that contributes to retaining the G1 Cdk-cyclin complex at the ER.

Name		wee/wt score (log2)	p value
Srl3 / Whi7	Potential Cdc28p substrate, interacts with Cks1	-3.288	3.0E-23
Hsp60	Heat shock protein 60, mitochondrial	-3.288	3.1E-23
YCR087C-A	Nucleolar protein of unknown function	-1.830	5.6E-08
Krs1	Lysyl-tRNA synthetase, cytoplasmic	-1.499	9.7E-06
Efb1	Elongation factor 1B	-1.340	8.0E-05
Rpa34	DNA-directed RNA polymerase I subunit	-1.329	9.1E-05
YGR250C	RNA-binding protein, localizes to stress granules	-1.304	1.2E-04
Yef3	Elongation factor 3A	-1.224	3.2E-04
Leo1	RNA polymerase-associated protein	-1.147	7.6E-04
Ssa2	Hsp70-type major chaperone	-1.093	1.3E-03
Cks1	Cyclin-dependent kinase regulatory subunit	-1.070	1.7E-03
Fpr4	Peptidyl-prolyl cis-trans isomerase	-0.981	4.0E-03
Stm1	Protein involved in TOR signaling	-0.966	4.6E-03
Sic1	Cyclin-dependent kinase inhibitor	-0.925	6.6E-03
Nsr1	Nuclear localization sequence-binding protein	-0.887	9.1E-03
Ste20	S/T-protein kinase, potential Cdc28p substrate	-0.873	1.0E-02
Bfr1	Nuclear segregation protein	-0.864	1.1E-02
Cne1	Calnexin homolog, ER chaperone	-0.845	1.3E-02

Table 7: A list of the top candidates ($p \leq 0.05$) according to the best Q/S score

The best Q/S score is the mean calculated after excluding the outlier of the 4 scores in *wee* or wt (log2 *wee*/wt). Proteins with p value >0.05 are shown ranked in ascending order. Whi7 and Whi8 (YGR250c) appear in the top 10 of the list (green arrowheads).

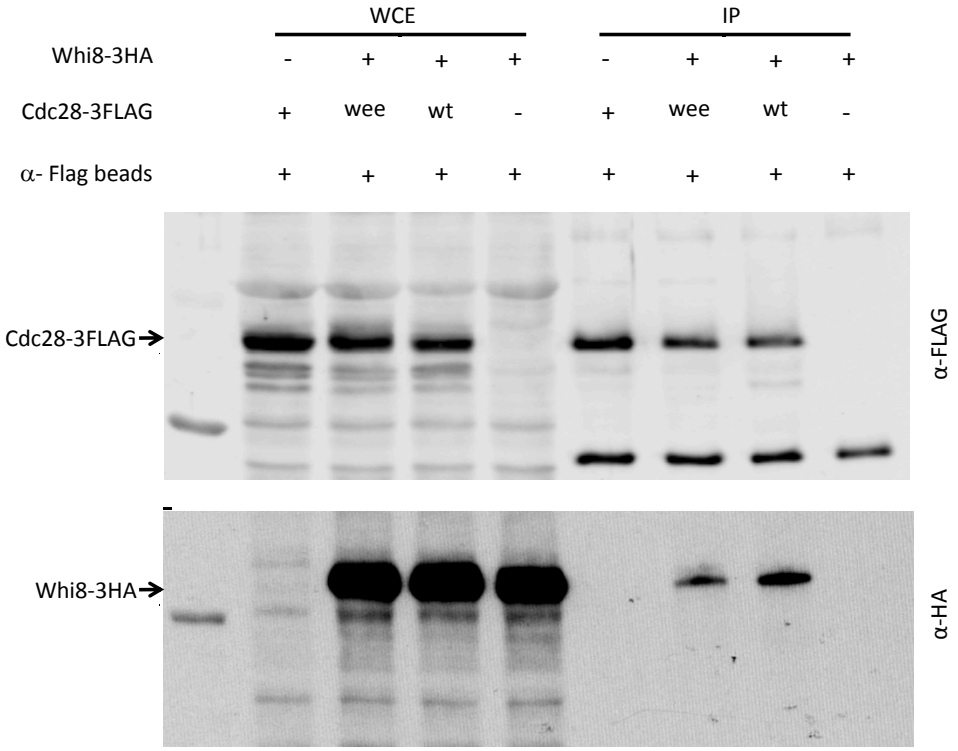

Figure 33: Whi8 interaction with Cdc28

In vivo Cdc28-Whi8 interaction assay. Western analysis of cell extracts (total) and αFLAG immunoprecipitates (αFLAG IP) of *WHI8-3HA* cells expressing WT or mutant (*wee*) Cdc28-3FLAG proteins.

The *whi8* deletion effect on budding size was strictly dependent on the presence of Cln3 since *cln3* deletion mask the size effect of the *whi8* deletion compared to the wild type (Figure 34A). In contrast, effects of *whi8* deletion on budding size were additive to the *whi3* deletion (Figure 34A), suggesting that both alterations affect related but independent components of the mechanisms that control cell size in budding yeast. Whi8-deficient cells showed a higher mean level of nuclear Cln3 and, more important, a strong increase in the proportion of cells displaying a nuclear signal of Cln3 above a certain threshold (Figure 34B). In addition, overexpression of *WHI8* from a regulatable promoter caused a rapid and marked increase in cell size at budding (Figure 34C), and a time-dependent reduction of the nuclear signal of Cln3 (Figure 34D).

Whi8 interacts with Whi3 in an RNA-dependent manner

WHI3 was isolated as a gene involved in cell size regulation that exerts a negative role on Cln3 (R. S. Nash et al., 2001). Whi3 contains an RNA-binding domain that binds the *CLN3* mRNA and confines its translation to a distinct molecular environment (Garí et al., 2001) and also recruits the Cdc28 kinase preventing unscheduled nuclear accumulation of Cdc28-Cln3 complexes (Wang et al., 2004) by an unknown mechanism. Whi3 interacts with Cdc28 *in vivo*, suggesting that the interaction between Whi3 and Cdc28 is part of a cytoplasmic retention mechanism with an important role in regulating G1 events (Wang et al., 2004). Thus, Whi3 was proposed to be an anchor for Cdc28-Cln3 complexes. However Whi3 and Cdc28 do not interact *in vitro*, suggesting that other proteins would mediate their association *in vivo* (Wang et al., 2004). Indeed, Whi8 interacts *in vivo* with Whi3 and, more interestingly, this interaction was mostly lost upon treatment with RNase, strongly suggesting this interaction is mediated by common target mRNAs (Figure 35).

Whi8 localizes to the ER

Preliminary confocal microscopy images showed a pattern reminiscent of proteins belonging to ER-associated compartments, and coexpression with Ole1-GFP as ER marker confirmed that Whi8-3HA staining produces a punctate pattern closely associated or adjacent to the ER network (Figure 36A and 36B). Confirming this association, we found that a fraction of Whi8 cosediments with Dpm1, another ER marker, in sucrose gradients (Figure 36C). This behavior is similar to that of Whi7 and

Cdc28, a fraction of which is found in dense ER-containing fractions (Vergés et al., 2007).

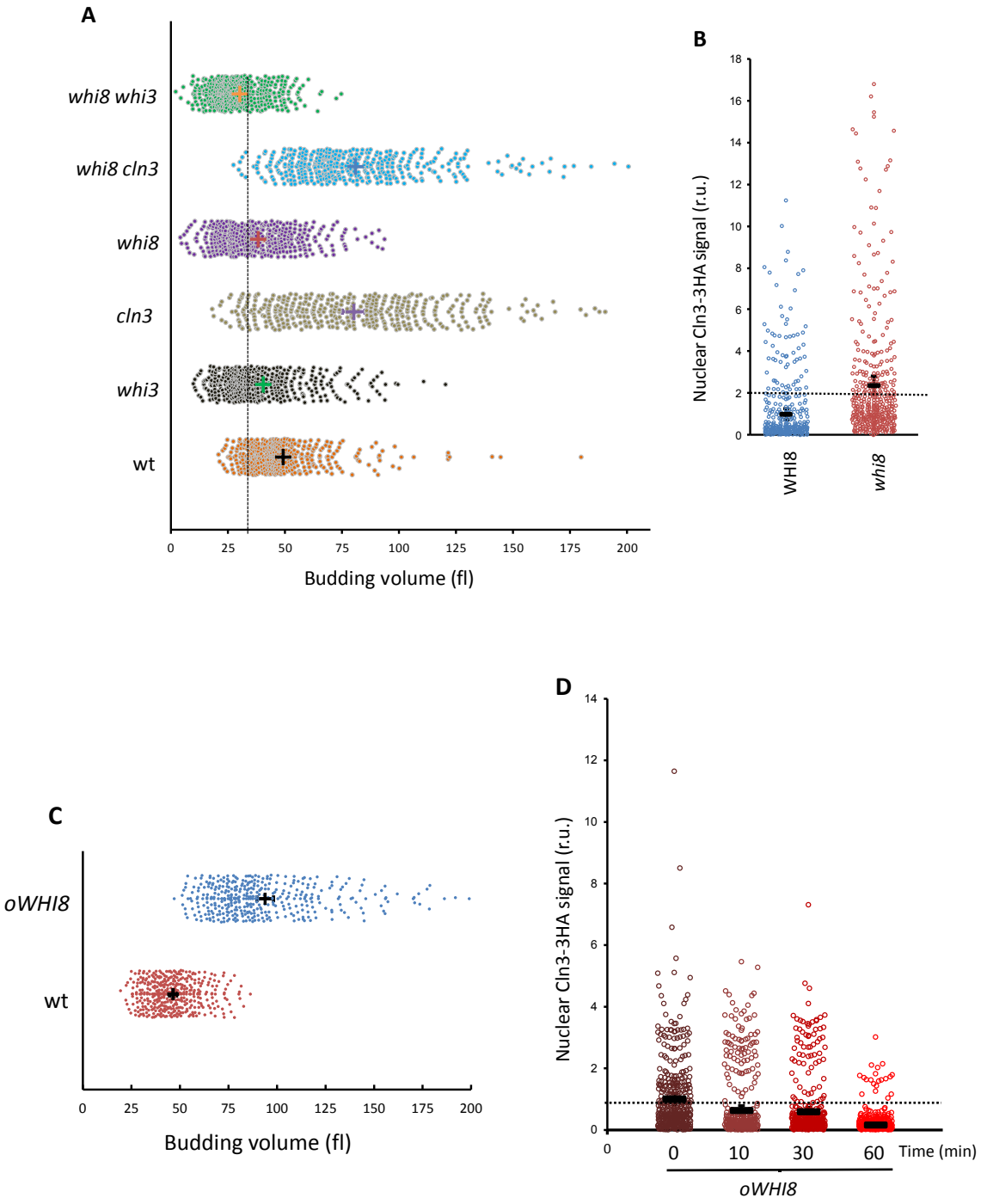

Figure 34: Phenotype of *whi8* and *oWHI8* cells

(A) Cell volumes at budding of individual cells (n > 500) with indicated genotypes are plotted. Mean values (vertical lines) and confidence limits (α = 0.05, thin vertical lines) for the mean are also shown.

(B) Nuclear accumulation of Cln3-3HA in asynchronous individual cells (n > 450) of wild-type (wt) or Whi8- deficient (*whi8*) as measured by semiautomated quantification of immunofluorescence levels in both nuclear and cytoplasmic compartments. Values were made relative to the average obtained from wild-type (wt) cells. Mean values and confidence limits (α = 0.05) for the mean are shown.
(C) Individual cell volumes at budding were determined thereafter (first cycle, n> 400) of cells overexpressing an empty vector or overexpressing *WHI8* (O/N, n > 250). Mean values (thick vertical lines) and confidence limits (α = 0.05, thin vertical lines) for the mean are also shown.
(D) Nuclear accumulation of Cln3-3HA in asynchronous cells (n > 600) overexpressing *WHI8.* Cells overexpressing *WHI8* were induced with β-estradiol, and samples were taken at indicated times. Mean values (thick horizontal lines) and confidence limits (α = 0.05, thin horizontal lines) for the mean are shown.

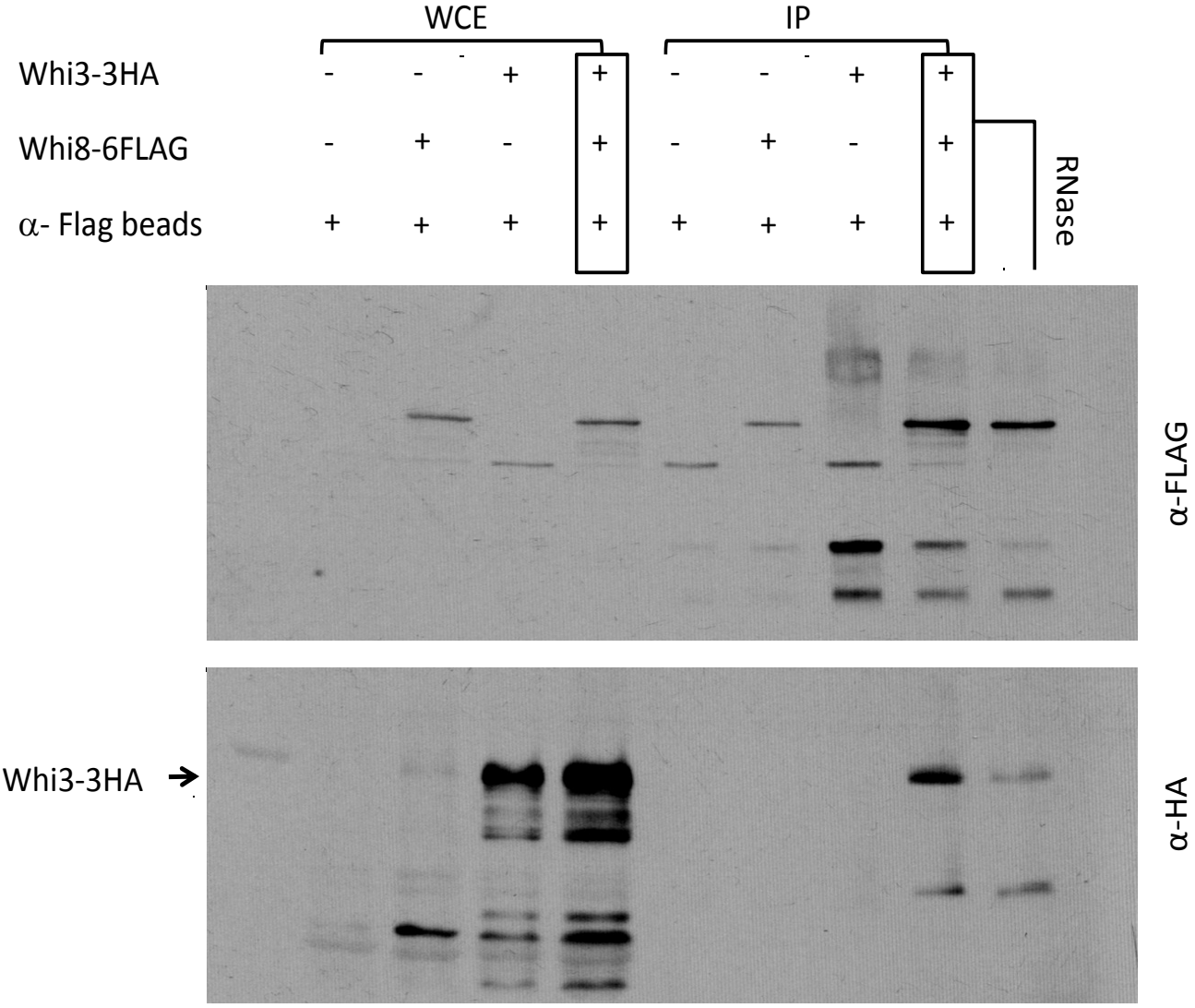

Figure 35: Whi8 interaction with Whi3

Western analysis of cell extracts (total) and αFLAG immunoprecipitates (αFLAG IP) of cells expressing Whi8-6FLAG and/or Whi3-3HA proteins with or without RNase treatment.

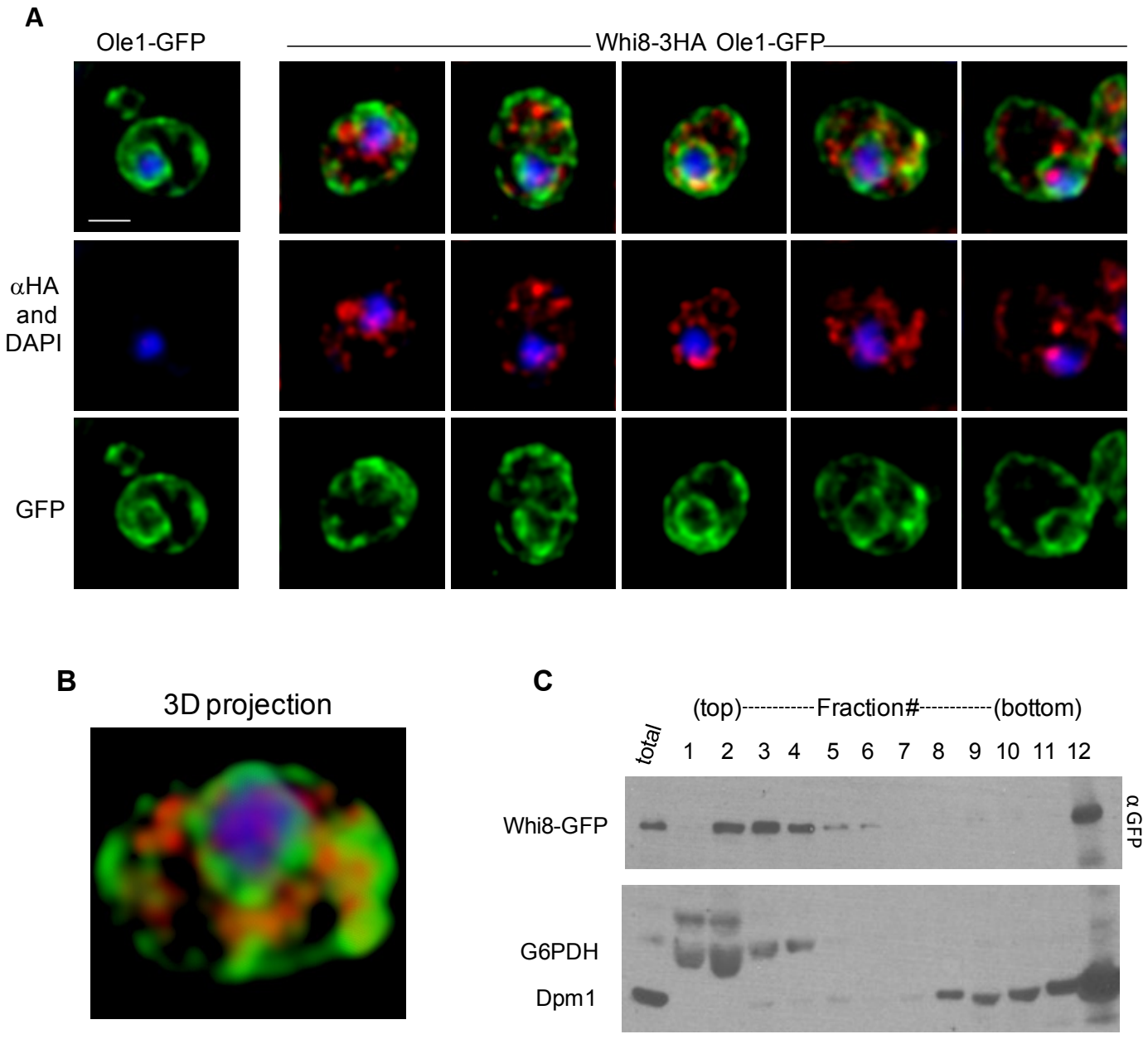

Figure 36: Whi8 is associated to the ER

(A) Confocal images of WT cells expressing Whi8-3HA at endogenous levels and Ole1-GFP as ER marker. Nuclei were detected by DAPI staining, and HA-untagged cells were analyzed as control (left panels). An overlaid stack of 20 0.34µm deconvolved sections is shown for each image. Bar indicates 2µm.
(B) 3D projection of the merged stack corresponding to a cell in right panel (A).
(C) Western analysis of the distribution of Whi8-GFP in sucrose gradients. GAPDH is shown as cytoplasmic marker and Dpm1 as ER marker.

Whi8 interacts with mRNAs involved in cell cycle regulation

Both Whi3 and Whi8 are RNA-binding proteins and we have shown that the interaction between Whi3 and Whi8 requires RNA. In addition to the *CLN3* mRNA (Garí et al., 2001), Whi3 binds a large number of mRNAs encoding for membrane and exocytic proteins involved in processes such as transport and cell wall biogenesis (Colomina et al., 2008).

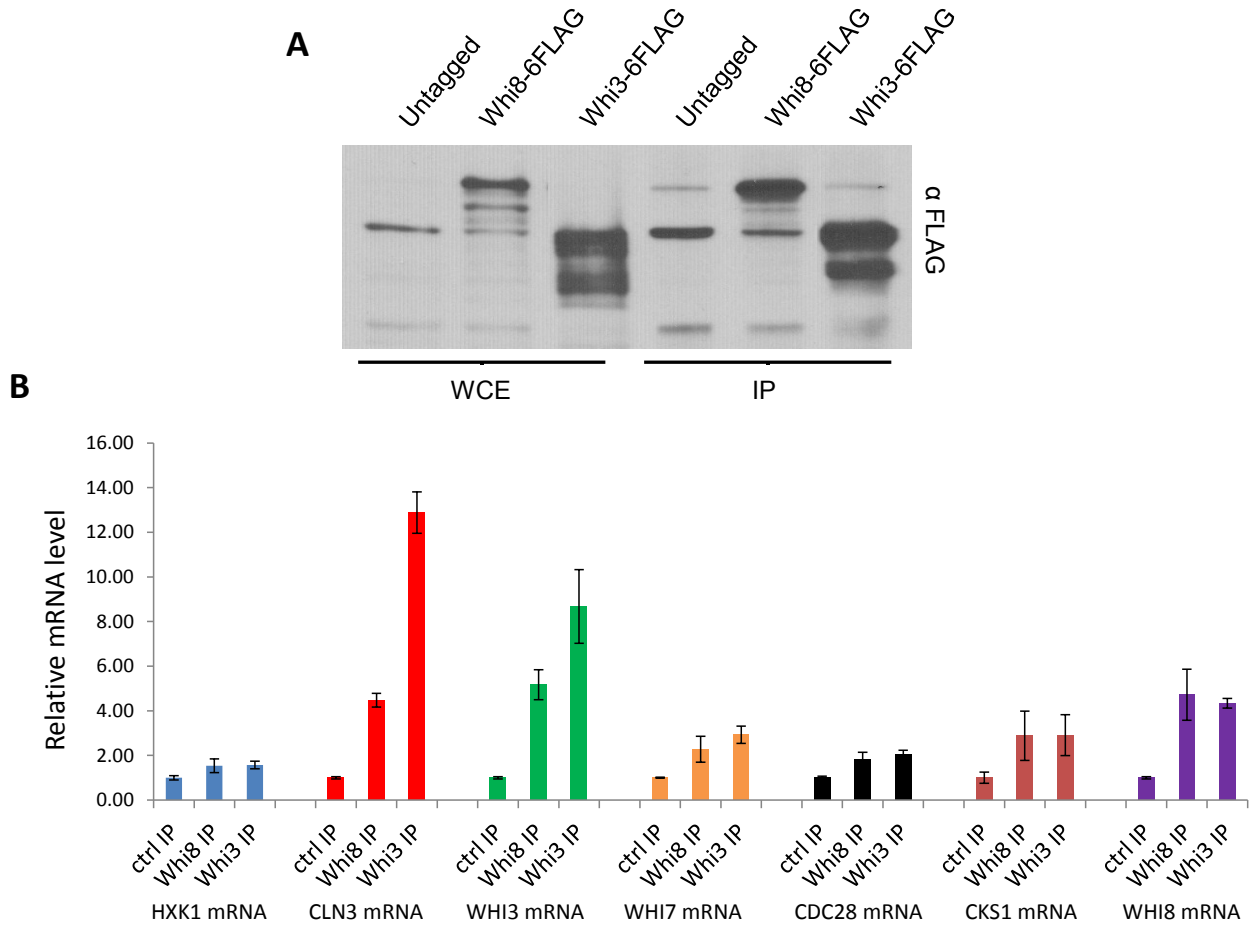

Figure 37: Whi8 associates with *CLN3*, *WHI3* and *WHI8* mRNAs

(A) Western analysis of cell extracts (total) and αFLAG immunoprecipitates (αFLAG IP) using anti-FLAG M2 agarose beads (Sigma) of cells expressing Whi8-6FLAG or Whi3-6FLAG or no epitope (negative IP); total RNAs were extracted from the immunoprecipitates and analyzed by by real-time RT-PCR.
(B) Relative levels of mRNAs found in αFLAG IPs shown in panel A. IPs with αFLAG shown in panel A were used to quantify the relative levels of the indicated mRNAs by real-time RT-PCR. Gene symbols are as follows: *HXK1* (housekeeping mRNA), *CLN3*, *WHI3*, *WHI7* (*SRL3*), *CDC28*, *CKS1* and *WHI8* mRNA. The mean values from three independent immunoprecipitation experiments and respective confidence limits (α = 0.05) were plotted.

Here we focused upon specific mRNAs that are functionally related to cell cycle regulation. We performed an IP for Whi3 or Whi8 fused to 6FLAG (Figure 37A) and we extracted the RNA. We found that both Whi3 and Whi8 bind mRNAs functionally related to the cytoplasmic retention device as *CLN3*, *WHI3*, *WHI7* and *WHI8* mRNAs with different affinities and, similar to the behavior of Whi3, Whi8 binds its own mRNA, perhaps to locally direct its own translation to specific ER-associated sites (Figure 37B).

Whi8 colocalizes with the *CLN3* mRNA *in vivo* under stress

Whi3 and *CLN3* mRNA localize to stress granules in response to glucose deprivation or heat shock (Cai & Futcher, 2013; Holmes et al., 2013). However, the colocalization of *CLN3* mRNA and stress granules was preserved in *whi3* and *whi3 whi4* double mutants, suggesting the existence of other proteins with essential roles in mRNA sequestration in stress granules. As Whi8 had been observed in both SGs and PBs (Buchan et al., 2008), we decided to test the colocalization of *CLN3* mRNA and Whi8 granules formed under stress conditions. To test this hypothesis, we examined the *in vivo* localization of *CLN3* mRNA using the MS2 system (Gu et al., 2004; Haim et al., 2007). We constructed a strain carrying the *CLN3* ORF with no ATG fused to 6 copies of MS2 binding sites (MS2bs) under *GAL1p* promoter and an ectopically expressed NLS-MS2-mCherry fusion, which binds specifically to the MS2 loops. The NLS in MS2-mCherry sequesters the unbound MS2-mCherry in the nucleus so that the GFP background signal becomes very low in the cytoplasm. In cells carrying *CLN3-MS2bs*, but not in control cells with *CLN3* lacking MS2bs, one or two bright mCherry foci (and sometimes additional less bright foci) were observed in the cytoplasm. The much larger, brighter red spots are nuclei, which contain unbound NLS-MS2-GFP. Then we coexpressed a GFP-Whi8 fusion and observed that, when cells are grown in glucose, Whi8-GFP is somewhat unevenly spread throughout the cytoplasm. Although its distribution is not completely homogeneous, it does not appear lumpy, or to be in distinct foci with one or two bright mCherry foci of *CLN3*. Notably, under glucose starvation the mCherry foci containing *CLN3* mRNA colocalized with Whi8-GFP foci as cytoplasmic aggregates, suggesting that the *CLN3* mRNA was localized to Whi8 granules (Figure 38).

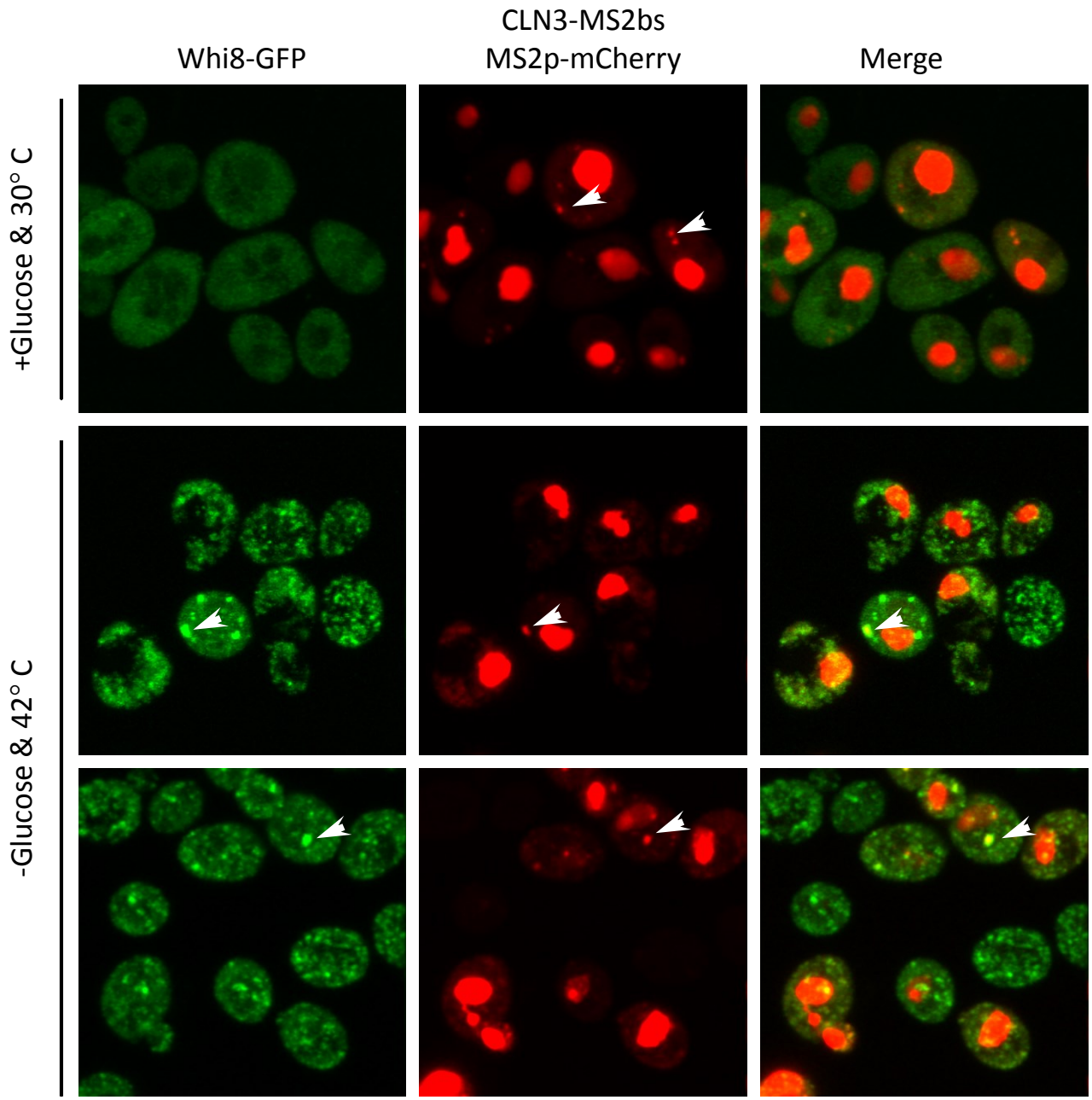

Figure 38: Under stress, *CLN3* mRNA colocalizes with Whi8 granules.

Cells with WHI8-GFP (BY4741) were cotransformed with *CLN3-MS2bs* and NLS-MS2-mCherry for co-localization of Whi8-GFP and *CLN3* mRNA. Cells were starved of glucose and shaked at 42°C for 15min before analyzed under the microscope. Whi8 is shown in green and MS2-mCherry is shown in red. Excess NLS-MS2-mCherry appears as large red lumps in the nucleus. Small red foci indicate *CLN3* mRNA and green foci represent Whi8 granules (white arrow head). Images are shown as a projection of z-stacks. At higher contrast and brightness, additional *CLN3* foci can be seen in some cells. Control cells grown at 30°C without starvation show no cytoplasmic GFP foci of Whi8.

CLN3 mRNA localization to stress granules requires Whi8

Since Whi3 is not required for *CLN3* mRNA localization to stress granules (Cai & Futcher, 2013; Holmes et al., 2013), we wanted to know whether Whi8 would have an essential role. To test the *in vivo* localization of *CLN3* mRNA with stress granules in *whi8* or *whi3 whi8* double deletion background, we co-expressed a Pub1-mCherry fusion together with NLS-MS2-GFP and *CLN3-MS2bs*.

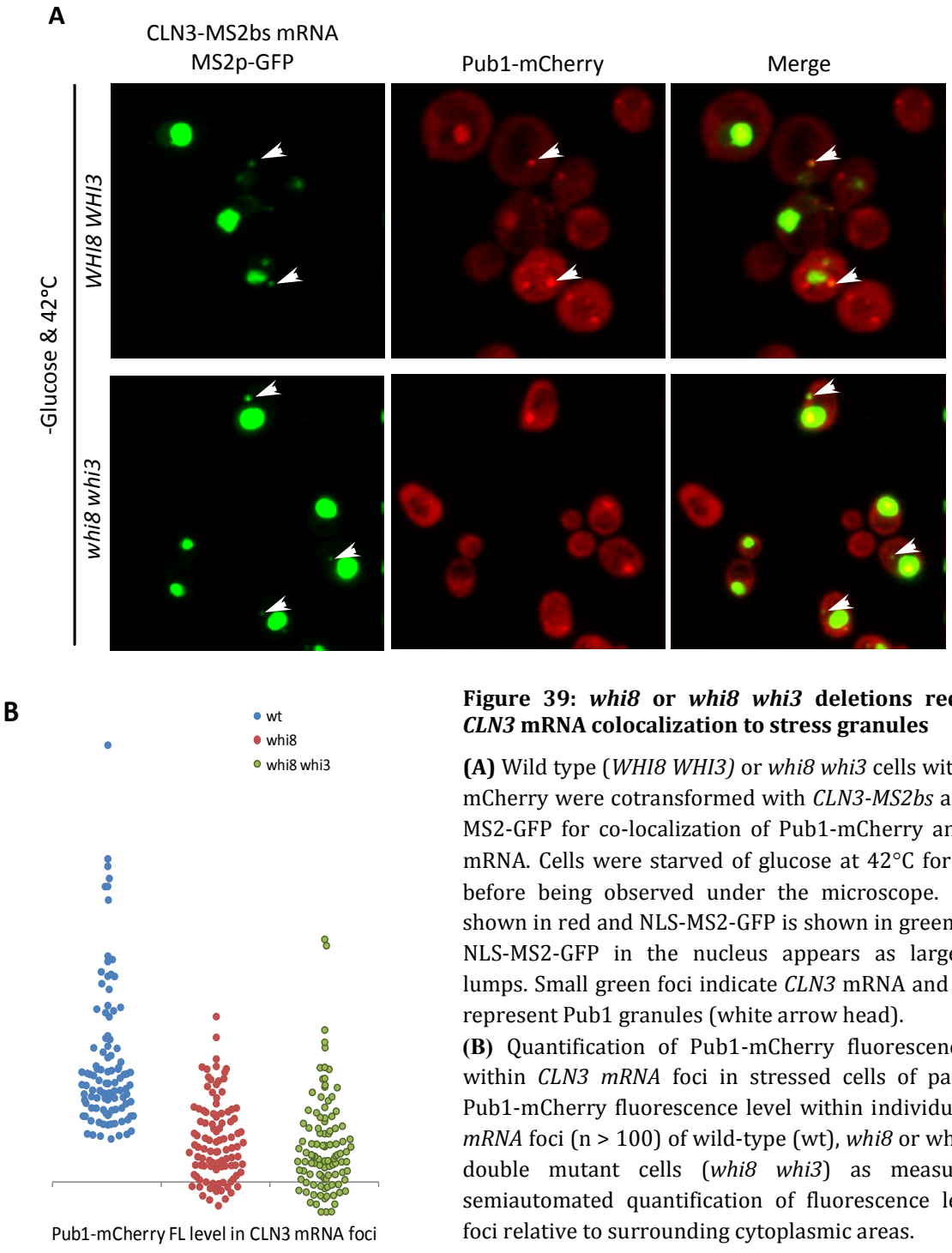

Figure 39: *whi8* or *whi8 whi3* deletions reduce *CLN3* mRNA colocalization to stress granules

(A) Wild type (*WHI8 WHI3)* or *whi8 whi3* cells with Pub1-mCherry were cotransformed with *CLN3-MS2bs* and NLS-MS2-GFP for co-localization of Pub1-mCherry and *CLN3* mRNA. Cells were starved of glucose at 42°C for 15 min before being observed under the microscope. Pub1 is shown in red and NLS-MS2-GFP is shown in green. Excess NLS-MS2-GFP in the nucleus appears as large green lumps. Small green foci indicate *CLN3* mRNA and red foci represent Pub1 granules (white arrow head).
(B) Quantification of Pub1-mCherry fluorescence level within *CLN3 mRNA* foci in stressed cells of panel (A)**.** Pub1-mCherry fluorescence level within individual *CLN3 mRNA* foci (n > 100) of wild-type (wt), *whi8* or whi8 whi3 double mutant cells (*whi8 whi3*) as measured by semiautomated quantification of fluorescence levels in foci relative to surrounding cytoplasmic areas.

As already found by others (Cai & Futcher, 2013) we observed that, under glucose starvation, the GFP foci containing *CLN3* mRNA co-localized with Pub1-mCherry foci in otherwise wild type or Whi3-deficient cells. However, colocalization of *CLN3* mRNA and the stress granule marker Pub1 dramatically decreased in *whi8* or *whi3 whi8* double deletion background. Moreover the Pub1-mCherry fluorescence level in the *CLN3* mRNA foci was strongly reduced in *whi8* or *whi3 whi8* mutant cells (Figure 39A and 39B).

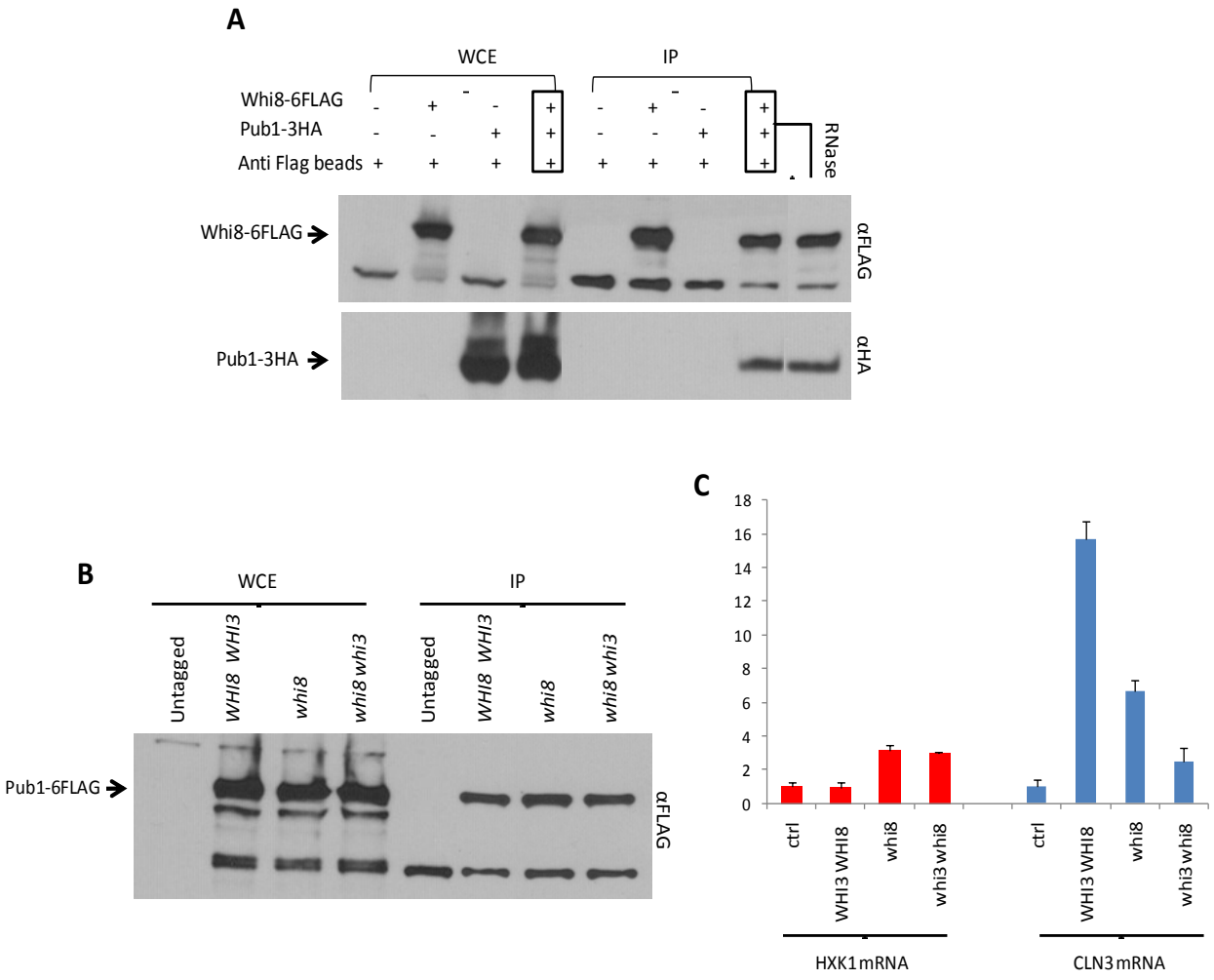

Figure 40: Whi8 interaction with components of the stress granules

(A) Western analysis of cell extracts (total) and αFLAG immunoprecipitates (αFLAG IP) of cells expressing Whi8-6FLAG and Pub1-3HA proteins, for negative IP we use a background expressing one or none of the two epitopes. For RNase treatment, the immunoprecipitate from a background expressing the two epitopes was incubated in lysis buffer with 10mg/ml RNase at 4°C for 15 minutes prior to washing.
(B) Western analysis of cell extracts (total) and αFLAG immunoprecipitates (αFLAG IP) of cells expressing Pub1-6FLAG in wild-type (wt), *whi8* or *whi8 whi3* double deletion mutant.
(C) Relative levels of *CLN3* mRNA found in Pub1 αFLAG IPs shown in panel B. Total RNAs were extracted from αFLAG IPs shown in panel B then analyzed by qualitative real-time RT-PCR. The relative levels of mRNAs in every IP for *HXK1* (housekeeping mRNA) and *CLN3* mRNA. The mean values from three independent immunoprecipitation experiments and respective confidence limits (α = 0.05) were plotted.

To further test the interaction between Whi8 and Pub1 we performed an IP of Whi8-6FLAG and we measured Pub1-3HA levels by western blot. We found that Whi8 and Pub1 clearly interact and, more interestingly, the interaction between Whi8 and Pub1 did not require RNA as it was the case between Whi8 and Whi3 (Figure 40A). Then we analyzed the ability of Pub1 to bind the *CLN3* mRNA under stress in wt, *whi8* or *whi3 whi8* double mutant cells. We performed RNA-IP (RIP) of Pub1-6FLAG from the different strain backgrounds under stress and extracted the RNA to analyze *CLN3* mRNA levels by RT-qPCR. We found a clear decrease in the level of detectable *CLN3* mRNA in IPs of Pub1-6FLAG from *whi8* or *whi3 whi8* double mutant cells (Figure 40B and 40C).

CLN3 mRNA translation is inhibited by Whi8 upon stress

CLN3 mRNA levels are induced by glucose, and *CLN3* mRNA translation is also positively regulated by nitrogen sources (Parviz & Heideman, 1998; Gallego et al., 1997). Thus, Cln3 protein levels are highest in glucose and lower in poorer carbon sources (Hall et al., 1998), and translation of the *CLN3* mRNA is repressed approximately 8-fold under nitrogen deprivation by unknown mechanisms (Gallego et al., 1997). On the other hand, the functional significance of the assembly of mRNPs into SGs remains unclear. Although several factors that are involved in SG formation are translational repressors, there is a lack of clear evidence that the assembly of mRNPs into SGs in itself is important for translational repression (Buchan et al., 2008; Fujimura et al., 2008; Kwon et al., 2007; Loschi et al., 2009; Mokas et al., 2009; Ohn et al., 2008). An alternative idea that has been put forth is that mRNPs that are assembled into SGs remain poised to re-enter translation as soon as stress is relieved (Buchan & Parker, 2009). Consistent with this, several studies have presented evidence that the ability to form SGs is correlated with the survival of cells exposed to stress (Buchan & Parker, 2009). We reasoned that recruiting *CLN3* mRNA by Whi8 into stress granules under glucose starvation may be important for translational repression in order to arrest cell cycle in G1 under stress. Thus, we decided to compare the level of Cln3 protein in wild type and Whi8-deficient cells during a time course experiment under starvation. As already described, we observed a rapid drop in Cln3 protein level within 10 min under glucose starvation. Interestingly, Cln3 protein levels remained much higher in the *whi8* mutant cells in both starvation regimes (Figure 41).

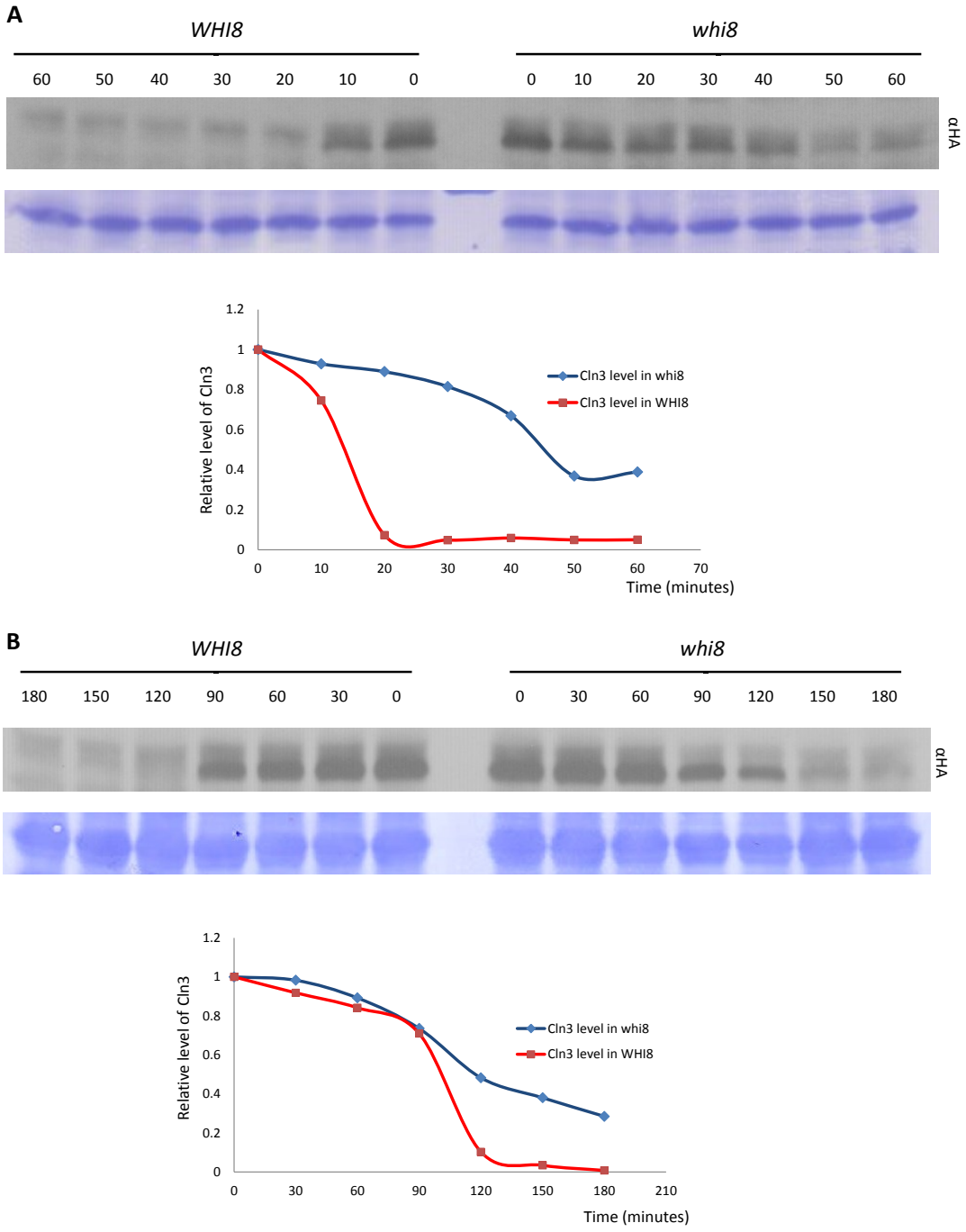

Figure 41: Whi8 is important to decrease Cln3 levels upon starvation

(A) Western analysis of cell extracts (total) of *WHI8* or *whi8* cells carrying Cln3-3HA-tagged proteins. Cells were deprived of glucose up to 60minutes and samples were taken at the indicated time points for western blot analysis with the α-HA 12CA5 monoclonal antibody. Coomassie Blue stained membrane shown as a loading control and the relative Cln3-3HA protein levels obtained by Western blot analysis (insert) were quantified as values relative to time 0.

(B) Western analysis of cell extracts (total) of *WHI8* or *whi8* cells carrying Cln3-3HA-tagged proteins. Cells were deprived of nitrogen up to 180minutes and samples were taken at the indicated time points for western blot analysis with the α-HA 12CA5 monoclonal antibody. Coomassie Blue stained membrane shown as a loading control and the relative Cln3-3HA protein levels obtained by Western blot analysis (insert) were quantified as values relative to time 0.

The IDD of Whi8 is essential for self-aggregation

Whi8 contains sequences sharing many features with intrinsically disordered domains (IDD) which, in turn, have been shown to mediate the assembly of proteins into stress granules (Gilks et al., 2004). Thus, we decided to test whether the Whi8 IDD is important for recruitment into stress granules. A truncation mutant of Whi8 lacking the IDD (Whi8-1) dramatically lost the spontaneous aggregation assembly and strongly impaired its ability to form granules under stress (Figure 42A). The truncation of Whi8 had no effect on its overall protein levels but decreased its proportion bound to the endoplasmic reticulum under stress compared to wild type Whi8 (Figure 42B and 42C).

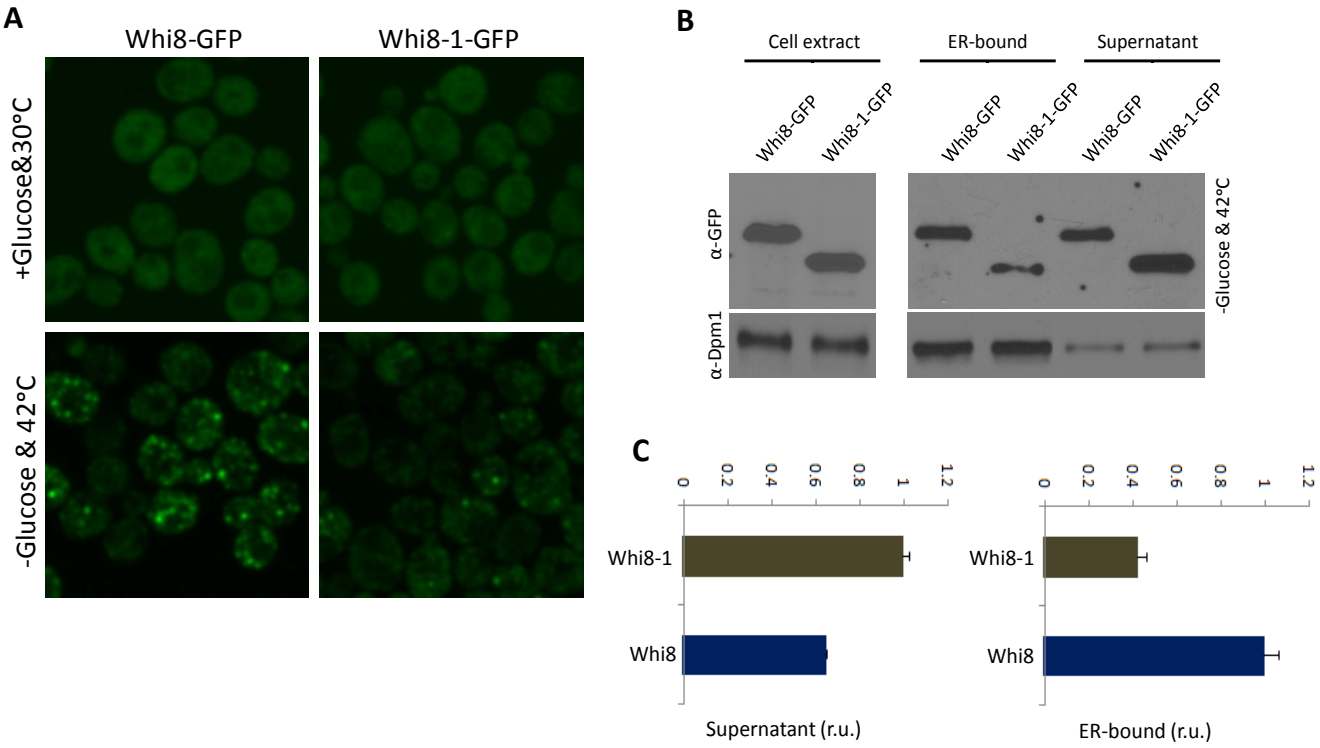

Figure 42: Intrinsically disordered domain at C-terminus of Whi8 promote spontaneous aggregation under stress

(A) Whi8-GFP and Whi8-1-GFP (IDD lacking mutant) cells grown to mid-log phase and then transferred to a medium lacking glucose for 15min at 42°C. Representative fluorescence microscopy images of Whi8-GFP foci are shown.

(B) Western analysis of total extracts, ER-bound and supernatant fractions from cells expressing Whi8-GFP and Whi8-1-GFP. Dpm1 is shown as ER marker.

(C) Chemiluminescent quantification of Whi8-GFP and Whi8-1-GFP protein levels analyzed in (B) are plotted relative to the endogenous Dpm1 protein levels. Mean values from triplicate samples and confidence limits ($\alpha = 0.05$) for the mean are shown.

Whi8 is phosphorylated by PKA *in vitro*

The Ras/cAMP-dependent protein kinase (PKA) pathway in yeast has been implicated in numerous cellular processes, including carbon storage, stress response, growth, differentiation, and life span (Hall et al., 1998; Santangelo et al., 2006; Tamaki et al., 2007; Thevelein & De Winde, 1999). Over, PKA has been implicated in cell size control by nutritional conditions, and decreased PKA signaling results in decreased cell size, whereas hyperactive PKA signaling leads to increased cell size (Baroni et al., 1989; Tokiwa et al., 1994) indicating that PKA is a positive regulator of cell size control.

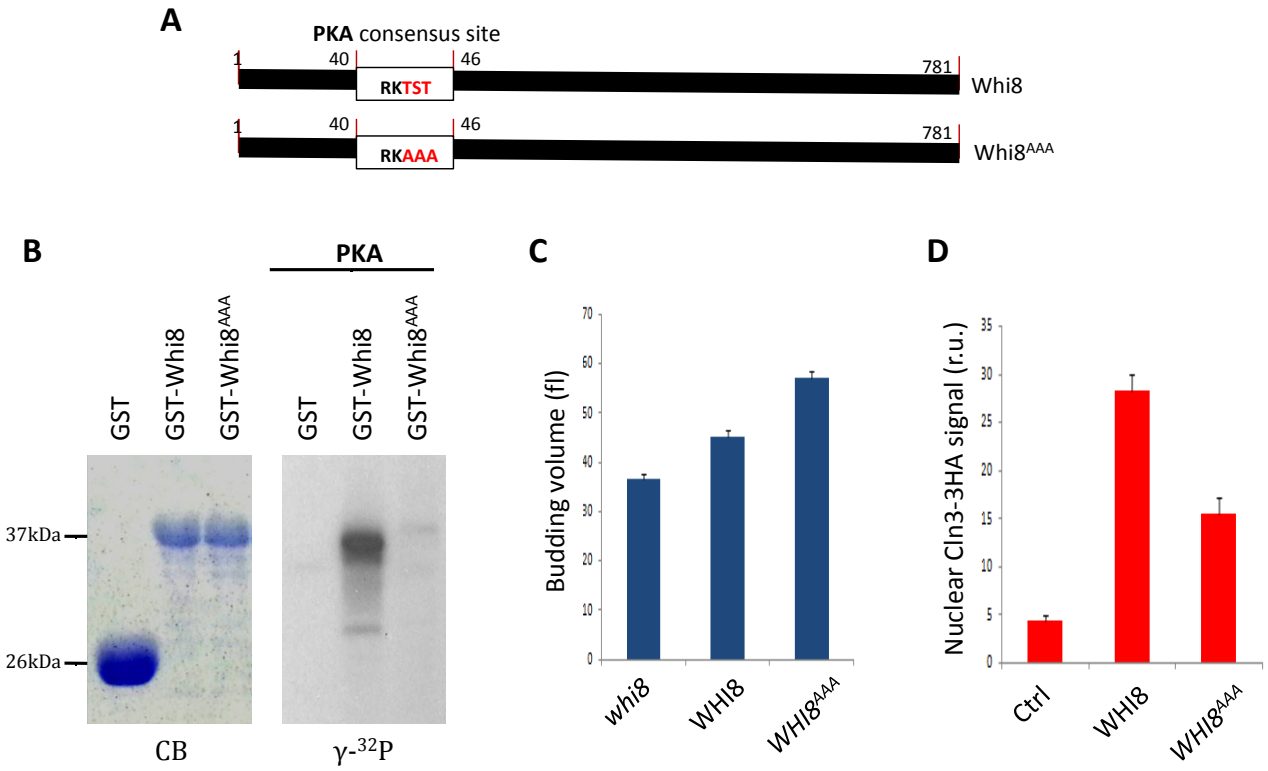

Figure 43: Whi8 phosphorylation by PKA

(A) Schematic representation of full-length Whi8. The location of the PKA consensus phosphorylation site at Ser-44 according to (Ptacek et al., 2005) we mutate also the two threonines after and before Ser-44 and we name this non-phosphorylatable mutant *WHI8^{AAA}* .

(B) Recombinant GST (control), GST-Whi8 (1-100) or GST-Whi8^{AAA} (1-100) were purified from *E. coli* and incubated with Protein Kinase A Catalytic Subunit from bovine heart (Sigma) in the presence of [γ-^{32}P] ATP (γ-*^{32}P*). Phosphorylated Whi8 was separated by SDS-PAGE and detected by autoradiography.

(C) Cell volumes at budding with indicated genotypes are plotted. Mean values and confidence limits (α = 0.05, error bars) for the mean are also shown.

(D) Nuclear accumulation of Cln3-3HA in asynchronous individual cells (n > 450) of untagged, *WHI8-CLN3-3HA* (*wt*) or *WHI8^{AAA}-CLN3-3HA* as measured by semiautomated quantification of immunofluorescence levels in both nuclear and cytoplasmic compartments. Mean values and confidence limits (α = 0.05, error bars) for the mean are shown.

Whi3 is phosphorylated by the Ras/cAMP-dependent protein kinase (PKA) and phosphorylation of Ser568 in Whi3 by PKA plays an inhibitory role in Whi3 function (Mizunuma et al., 2013). According to previously identified substrates of PKA (Kreegipuu et al., 1999; Ptacek et al., 2005; Zhu et al., 2000) Whi8 contains a typical consensus site at position 44 (Figure 43A), with a serine surrounded by threonines. In order to build a non-phosphorylatable mutant of Whi8 we mutated the TST sequence to three alanines. Next we purified recombinant Whi8 and Whi8^{AAA} fused to GST and we performed a kinase assay using bovine heart PKA. We found that PKA efficiently phosphorylated Whi8 but not the Whi8^{AAA} mutant (Figure 43B). Notably, Whi8^{AAA} cells displayed a larger cell volume and lower Cln3 nuclear level compared to wild type cells (Figure 43C and 43D).

Phosphorylation by PKA modulates RNA binding and aggregation of Whi8

Phosphorylation of Whi3 by PKA decreases its interaction with the *CLN3* mRNA and it is important for the promotion of G1/S progression (Mizunuma et al., 2013). The phenotypes of the Whi8^{AAA} cells (see above) suggested that PKA phosphorylation could have an inhibitory effect on Whi8 (Mizunuma et al., 2013). Thus, we performed a RIP assay followed by RT-qPCR analysis to test the PKA phosphorylation effects on the RNA binding affinity of Whi8, and found that Whi8^{AAA} binds its target mRNAs more avidly than wild type Whi8 (Figure 44A and 44B).

The PKA pathway has a general role in the regulation of P body foci formation as mutants with constitutive PKA signaling are defective in P body assembly (Ramachandran et al., 2011; Shah et al., 2013). To further characterize the role of PKA phosphorylation in stress granule assembly and test the participation of Whi8, we decided to test the aggregation assembly of GFP-tagged Whi8 or Whi8^{AAA} when starved of glucose under constitutive PKA signaling, which was attained by doing the analysis in cells lacking Bcy1, an inhibitory subunit of PKA (Cannon & Tatchell, 1987; Toda et al., 1987). We found that, while high PKA activity dramatically suppressed aggregation of Whi8-GFP but not that of Whi8^{AAA}. These data suggest that the inhibition of Whi8 foci formation by PKA is due, at least in part, to the direct phosphorylation of Whi8 (Figure 44C).

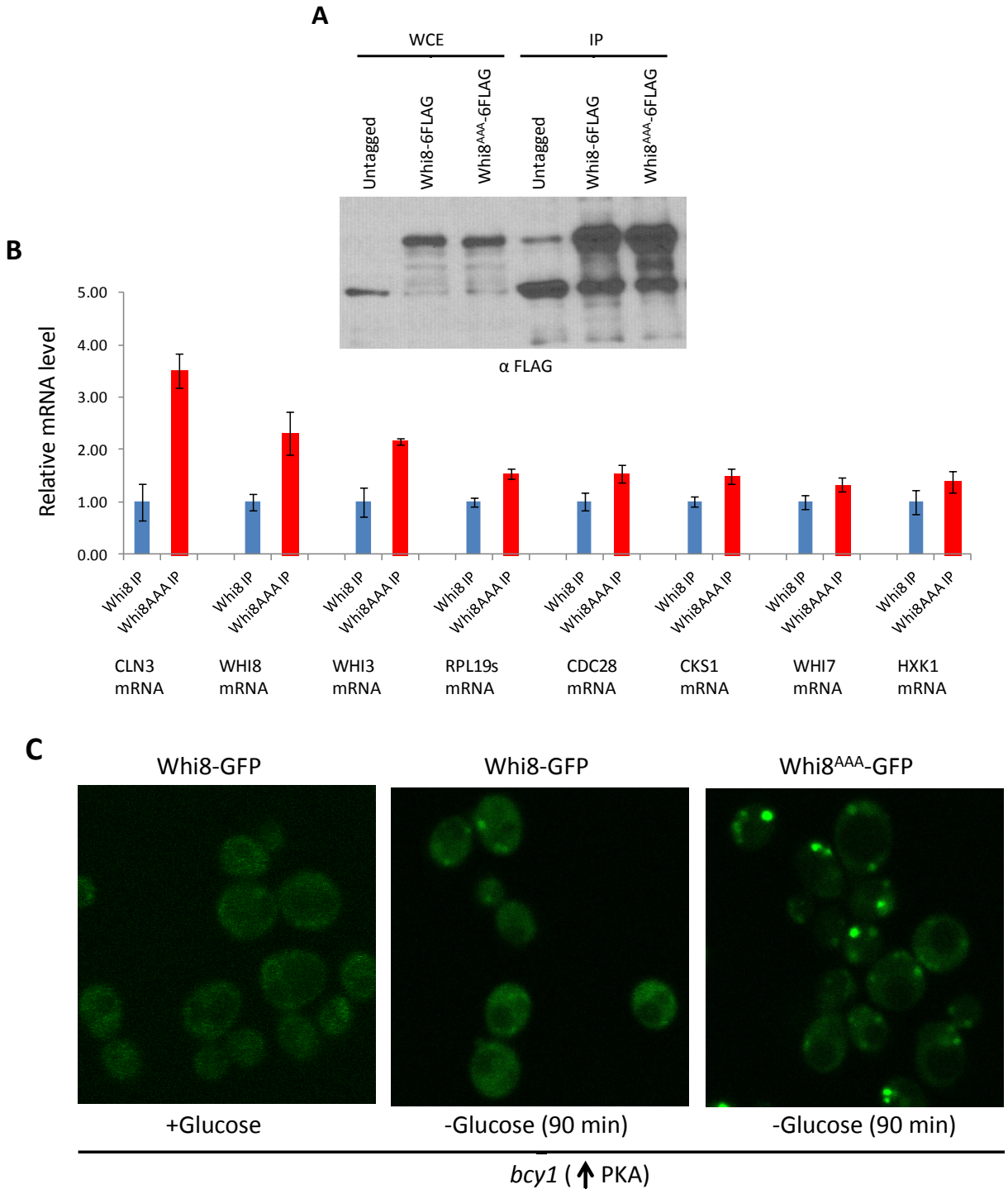

Figure 44: PKA phosphorylation modulates Whi8 RNA binding and aggregation.

(A) Western analysis of cell extracts (total) and αFLAG immunoprecipitates (αFLAG IP) from cells expressing Whi8-6FLAG , Whi8^{AAA}-6FLAG or no epitope (negative IP).

(B) Relative levels of mRNAs found in αFLAG IPs shown in panel A. Relative levels of the indicated mRNAs were quantified by RT-qPCR. Gene symbols are as follows: *CLN3*, *WHI8*, *WHI3*, *RPL19S*, *CDC28*, *CKS1*, *WHI7* (*SRL3*) and *HXK1* (housekeeping mRNA). Mean values from three independent immunoprecipitation experiments and respective confidence limits (α = 0.05) are plotted.

(C) Wild-type and *bcy1* cells expressing the indicated GFP-tagged Whi8 proteins were grown to mid-log phase and then transferred to a medium lacking glucose for 90 min. Representative fluorescence microscopy images are shown.

Discussion

Cln3, the most upstream activator of Start, is present already in early G1 but only accumulates in the nucleus in late G1. In early G1 cells most Cln3 is retained bound to the ER, being specifically released in late G1 to trigger the Start transition (Aldea et al., 2007). Association to the ER depends on the counteracting activities of a J-like domain in Cln3 itself and the J-chaperone Ydj1, which plays a key role in ER release and nuclear accumulation of Cln3 in late G1 cells. Moreover, Ydj1 is limiting for release of Cln3 from the ER and cell cycle entry, and it was proposed that chaperone availability may transmit growth capacity information to the cell cycle machinery (Vergés et al., 2007). However, little is known on the molecular mechanisms that retain the Cdc28-Cln3 complex in the cytoplasm and how do these mechanisms transmit information of cell size to coordinate cell proliferation with cell growth. In mouse cells, the Hsc70 chaperone associates to newly synthesized cyclin D1 polypeptides in extremely high molecular weight complexes (Diehl et al., 2003), suggesting that protein hijacking mechanisms (Traven et al., 2004) may also regulate cell cycle entry in metazoans as well.

Whi3 had been identified as a putative RNA-binding protein involved in cell size regulation (Nash et al., 2001). In addition, Whi3 binds the *CLN3* mRNA and plays an important negative role in all functional aspects of Cln3 activity, that is regulation of G1 length, and modulation of cell fate options such as mating, meiosis and filamentous growth (Garí et al., 2001). Whi3 recruits Cdc28 and contributes to keep Cln3–Cdc28 complexes in the cytoplasm during G1. Whi3 was detected in complexes with Cln3, showing that these multimeric complexes do exist, although perhaps only transiently (Wang et al., 2004).

Binding to Cdc28 is important for proper retention of the Cln3 cyclin at the ER until late G1 (Vergés et al., 2007). Remarkably, a fraction of the cyclin-dependent kinase Cdc28 also behaved as being associated to the ER and, more interestingly, the association of Cdc28 to the ER is independent of Cln3 binding (Vergés et al., 2007; Wittenberg et al., 1987). These previous data suggested that interaction to Cdc28 could be an important element in the association of Cln3 to the ER. In other words, Cdc28 would work like a bridge or an adaptor in the association of Cln3 to unknown ER-associated proteins.

As the Cdk-cyclin interaction was essential for retention at the ER, we reasoned that Cdc28 could act as a link to unknown ER-associated proteins and, hence, Cdc28 mutants with a weakened interaction with the ER should produce a small-cell-size phenotype (*wee* phenotype). To understand the molecular basis of the sequestration mechanism better, we decided to perform a genetic screen to isolate *CDC28* mutants able to subvert the sequestration of the Cdc28/Cln3 complex. Although the screen was initially intended for dominant mutations, it was performed in a strain where expression of the endogenous *CDC28* ORF is driven by a *GAL1p* regulatable promoter. From this genetic screen we isolated 6 independent *CDC28*^{wee} mutants that showed a consistent reduction in cell size compared to wild type and a clear increase in the nuclear levels of Cln3-3HA. A *cln3* deletion was epistatic to these *CDC28*^{wee} mutations, while a *whi3* deletion displayed additive effects on cell size, suggesting the existence of Cdc28 interactors that could regulate the activity of the Cdc28-Cln3 complex at Start.

1. Cdc28^{wee} as a tool to identify ER-associated interactors

The identified mutants contained a total of 11amino acid substitutions distributed in two regions of the Cdc28 molecule. A group of 5 mutations were found in or in the vicinity of the cyclin-binding domain, suggesting that these variants could display a stronger interaction to Cln3 or be more susceptible to activation by Cln3. One of them affected S46, a CK2 target previously involved in cell size control by others (Russo et al., 1996). Notably, the remaining substitutions were found at five positions clustered at an opposite region in the C-terminal lobe of Cdc28 in a region adjacent to the interface to the Cks1 subunit (Bourne et al., 1996), and mostly affected basic amino acids with likely exposed side chains. As we were particularly interested in Cdc28 domains different from the cyclin-binding region, we decided to characterize these mutations further and to build a quintuple mutant that we refer to as *CDC28*^{wee}.

CDC28^{wee} cells showed up to a 35% reduction in the daughter cell volume compared to wild type, an increased nuclear accumulation of Cln3, and lower Cdc28 levels in the ER-dense fraction. These data propelled us to perform a differential proteomic analysis of Cdc28 and Cdc28^{wee} interactors, aiming at the identification of yet uncovered proteins having key roles in cell cycle entry, specifically at holding the Cdc28-Cln3 complex at the ER and preventing premature execution of Start.

2. Whi7, an inhibitor of Start that contributes to ER retention of the G1 Cdk

Our iTRAQ analysis of the Cdc28^{wee} differential interactome identified a protein of unknown function that had been initially isolated as a suppressor of Rad53-lethality (Srl3; (Desany et al., 1998), here renamed as Whi7. We have found that Whi7 interacts directly with Cdc28 and plays an inhibitory role at Start. Notably, Whi7 has been defined as a paralog of Whi5 (Byrne & Wolfe, 2005), one of the key nuclear targets of the G1 Cdk-cyclin complex (Costanzo et al., 2004; De Bruin et al., 2004). Sequence similarity between Whi7 and Whi5 is particularly high at the Cdk-phosphorylated regions (Wagner et al., 2009). However, Whi7 lacks the sequences that direct nuclear import in Whi5 (Taberner et al., 2009; Wagner et al., 2009), and our immunofluorescence and biochemical data indicate that a fraction of Whi7 is associated to the ER. We have found that Whi7 is an inhibitor of Start that contributes to efficient association of the Cln3 cyclin to the ER and prevents its unscheduled accumulation in the nucleus. Cks1 (Gavin et al., 2002) and the Cln2 cyclin (Archambault et al., 2004) have been shown to interact with Whi7, pointing to the existence of quaternary complexes involving Whi7, Cks1, Cdc28, and a G1 cyclin. Whi7 is phosphorylated by Cdc28 (Ubersax et al., 2003), and we have found that phosphorylated forms of Whi7 display an increased affinity for Cks1. Cks1 contributes to full activation of Cdc28-Cln3 *in vitro* (Reynard et al., 2000) and directs processive hyperphosphorylation of target proteins thanks to an exposed cationic pocket (Bourne et al., 1996; Kõivomägi et al., 2011, 2013). Whi7 is upregulated in a number of stress situations (Berry & Gasch, 2008; Gasch et al., 2000), underscoring its role as an inhibitor of Start. We have found that increasing Whi7 expression to levels similar to those caused by ER stress is sufficient to prevent nuclear accumulation of Cln3 and delay cell cycle entry. Furthermore, Whi7 is upregulated by α factor (Roberts et al., 2000), and here we show that Whi7 is also important in restraining nuclear accumulation of Cln3 in α factor-arrested cells. Finally, inhibition of the TOR pathway by rapamycin causes a strong upregulation of Whi7 (Huang et al., 2004), suggesting that nutrients may withhold Whi7 to promote cell cycle entry. Thus, Whi7 may play an important role by connecting different environmental signals to the cell cycle machinery.

3. Whi7 establishes a positive feedback loop at the earliest known steps of Start

Irreversible transitions are often executed by mechanisms operating as bistable systems to stabilize the new situation. Different mechanisms have been identified that create bistable devices and, among them, the positive feedback loop is perhaps the best characterized one (Ferrell et al., 2002; Novak et al., 2010). While Cln3 determines G1 length and triggers Start when a critical size has been reached, Cln1 and Cln2 cyclins act in a nuclear feedback loop to ensure coherent and irreversible activation of the G1/S regulon (Charvin et al., 2010; Cross & Tinkelenberg , 1991; Dirick & Nasmyth, 1991; Skotheim et al., 2008). We have recently shown that budding yeast cells set the critical size at a single-cell level as a function of the individual growth rate (Ferrezuelo et al., 2012). Once the growth-rate component is excluded, wild-type cells only display a small residual cell-to-cell variation, indicating the existence of a precise and robust size control in budding yeast. Here we show that Cln3 and Ydj1 are as important as the two G1/S cyclins (Cln1 and Cln2) or transcription factors (Swi4 and Swi6) involved in the nuclear feedback loop in attaining a robust cell size control at Start, suggesting the existence of nonlinear activating mechanisms to trigger Start prior to transcriptional upregulation of *CLN1* and *CLN2*. We have identified an unexpected cytoplasmic function of cyclin Cln3 acting in a positive feedback loop on its own release from the ER. This function requires the kinase activity of Cdc28, and it is completely abolished in the presence of the nonphosphorylatable Whi7^{NP} mutant, indicating that the positive loop also involves Cdc28 and Whi7. Since Whi7 is important for correct retention of cyclin Cln3, we propose that, once primed by the Ydj1 chaperone, initial low levels of free Cdc28-Cln3 complexes would phosphorylate Whi7 to inhibit its retention role and accelerate release of further G1 Cdk-cyclin complexes (Figure 45). Whereas Whi7^{NP} is more tightly associated to the ER compared to wild-type, phosphorylation of Whi7 decreases its association to the ER. These observations suggest that phosphorylation of Whi7 would play a key role in releasing the G1 Cdk-cyclin complex from the ER at Start. Release of Cln3 by a positive feedback loop would be expected to act as a switch-like mechanism. Although we did not observe bimodal distributions of nuclear levels of Cln3, they displayed a high level of positive skewness, which could suggest the existence of two subpopulations overlapped by experimental and inherent sources of variation.

In this regard, variability in Cln3 nuclear import and export rates in the cell population would also contribute to the observed continuous distributions of nuclear levels of Cln3. Concerted Ydj1 and Ssa1 overexpression is able to suppress the inhibitory effects of the nonphosphorylatable Whi7^{NP} mutant, thus arguing against chaperones acting only downstream from Whi7 and suggesting that Ydj1 and Ssa1 would also belong to the positive feedback loop. The increased affinity of Cks1 for phosphorylated proteins could strengthen the interaction of the Cdc28-Cln3 complex to soluble phosphorylated Whi7, thus contributing to the positive feedback loop. In summary, while the transcriptional loop driven by Cln1 and Cln2 would make Start a coherent and irreversible process, the upstream Cln3-driven loop would be the key decision-making mechanism to enter the cell cycle and provide cells with a robust size control (Figure 45).

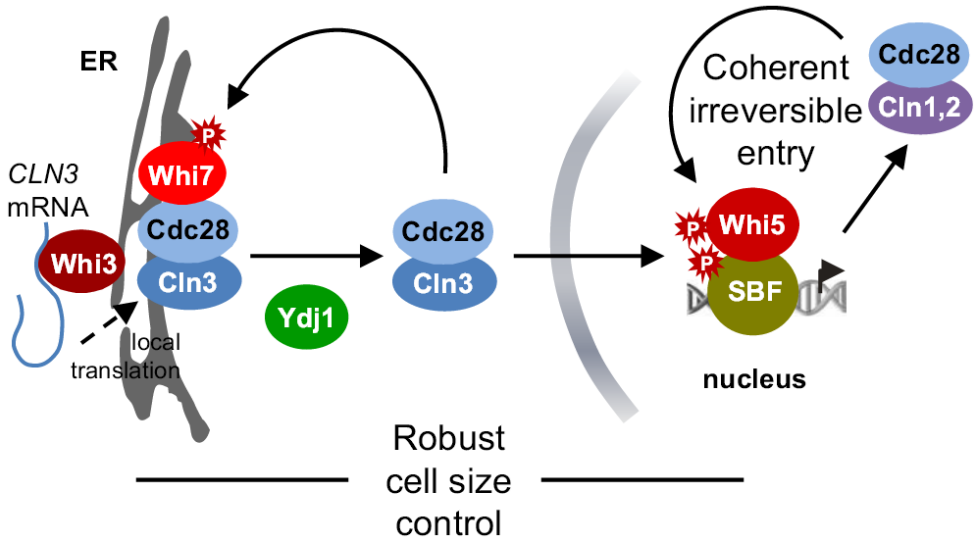

Figure 45: Whi7 establishes a Cln3-driven loop at the earliest steps of Start

Cln3 acts in a positive feedback loop on its own release from the ER. While being dependent on the kinase activity of Cdc28, this function is completely abolished by a nonphosphorylatable Whi7^{NP} protein, which indicates that the positive loop also involves Cdc28 and Whi7. Whi7 is also required for proper retention of cyclin Cln3, and we propose that initially released levels of Cdc28-Cln3 complexes by the Ydj1 chaperone would phosphorylate Whi7, inhibiting its retention role and accelerating release of further G1 Cdk-cyclin complexes. Thus, while a Cln1,2-driven loop in the nucleus inactivates Whi5 to attain coherent and irreversible activation of the G1/S regulon, an earlier Cln3-directed loop in the cytoplasm would inactivate Whi7, triggering Start in a switch-like manner for robust cell-size control.

5. Whi8, a novel Cdc28 interactor that binds the *CLN3* mRNA

Our iTRAQ analysis also identified YGR250c as another interesting *whi* candidate, which we have renamed as Whi8. Whi8 is a protein of unknown biological function that contains RNA-binding domains and has been observed in both SGs and PBs (Buchan et al., 2008). We have found that Whi8 interacts with Cdc28 *in vivo* confirming our iTRAQ data. Importantly, Whi8 interacts with Whi3 in an RNA-dependent manner and colocalizes with the *CLN3* mRNA and other mRNAs encoding cell cycle regulators. Cells lacking Whi8 show a clear small size while, on the other hand, overexpression of *WHI8* dramatically increases cell size. The effect of *whi8* deletion or *WHI8* overexpression on cell size was found to be epistatic to *CLN3* and affected Cln3 accumulation in the nucleus. Accordingly to a role in the retention device, Whi8 was found associated to the ER in a similar pattern to Whi7 and Cdc28 itself. We propose that Whi8 is the missing piece between Whi3 and Cdc28 (Wang et al., 2004), having a key role in linking cell cycle progression to stress conditions.

6. Whi8 halts *CLN3* mRNA translation under stress

CLN3 mRNA and Whi3 localize to stress granules in response to glucose deprivation or heat shock (Cai & Futcher, 2013; Holmes et al., 2013). However, Whi3 is totally dispensable for recruiting the *CLN3* mRNA to SGs, suggesting the participation of additional factors with key roles in the assembly of specific mRNAs into SGs. We found that *CLN3* mRNA colocalizes with Whi8 in SGs. While localization of the *CLN3* mRNA in SGs was preserved in *whi3* and *whi3 whi4* double mutants, it sharply decreased in both *whi8* and *whi8 whi3* mutants. These data establish a predominant role for Whi8 in targeting the *CLN3* mRNA to SGs. Regarding the functional consequences of the aggregation of Whi8 and the *CLN3* mRNA into SGs, we have found that Cln3 levels remained much higher under glucose and nitrogen starvation in Whi8-deficient cells. Thus, cells would regulate G1 progression under stress by halting *CLN3* mRNA translation in SGs, thereby limiting the influx of newly synthesized Cln3 into the cell cycle machinery. We propose Whi8 as a unique target of stress signaling pathways that sequesters the *CLN3* mRNA (and likely other mRNAs) in SGs to repress its translation under stress. Moreover, once stress is relieved SG disassembly would rapidly unleash the stored pool of *CLN3* mRNA to resume G1 progression as fast as possible (Figure 46).

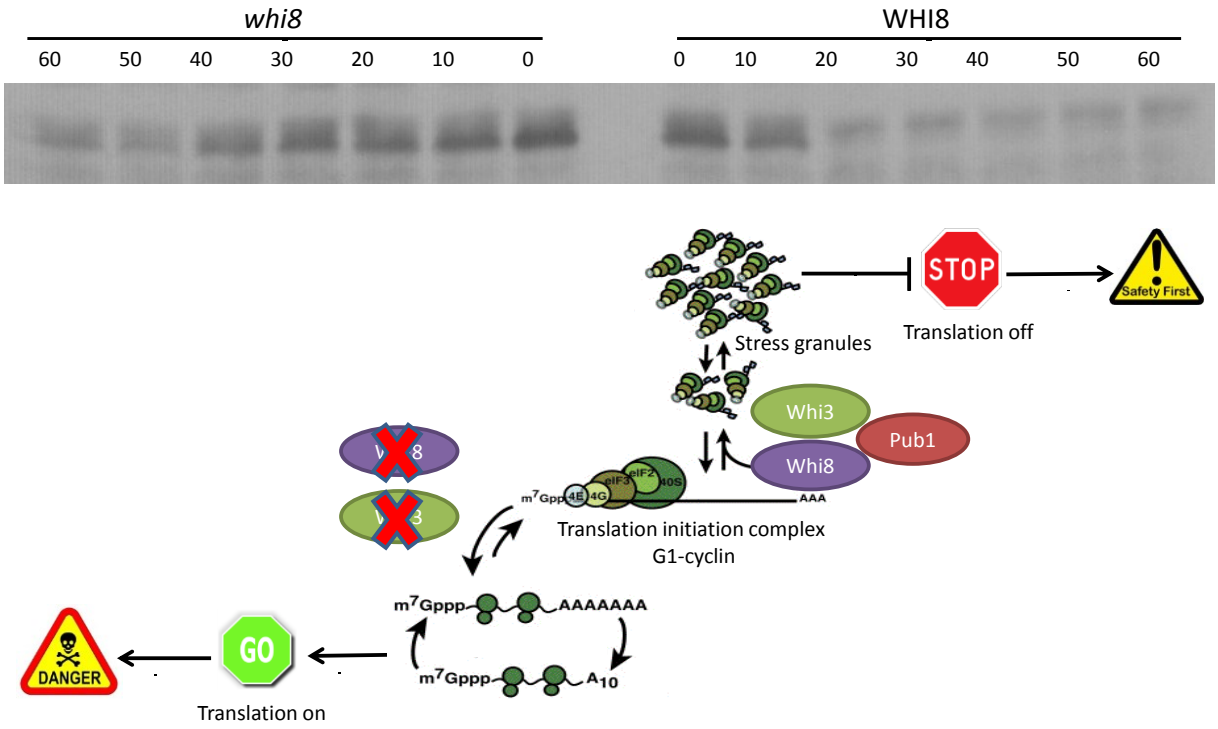

Figure 46: Whi8 works as a safeguard that limits the influx of newly synthesized Cln3 under stress

According to our observations, *CLN3* mRNA would be recruited by Whi8 and Whi3 into stress granules under nutrient starvation to shut down translation and limit the influx of newly synthesized Cln3 into the cell cycle machinery.

7. PKA phosphorylation modulates Whi8 aggregation and RNA binding capacity

We have found that Whi8 aggregation and RNA-binding capacity are both negatively regulated by PKA, and we have identified a specific phosphosite responsible for this regulatory behavior. Importantly, we have also demonstrated that PKA phosphorylation is essential and sufficient to prevent Whi8 assembly into SGs.

Besides modulating the aggregation of Whi8, PKA phosphorylation seems to influence the RNA-binding capacity of Whi8. This is based on the observation that Whi8^{AAA} shows increased binding affinity for the same sets of mRNAs compared to Whi8. Indeed, this phosphorylation would indirectly influence the association between Whi3 and Whi8. Accordingly, Whi8^{AAA} cells show larger cell size and reduced nuclear signal of Cln3. In summary, these results suggest that PKA appears to act as a negative regulator of Whi8 and that phosphorylation by PKA also contributes to down-regulation of Whi8 function, thus linking nutrient availability to G1 progression and Start execution (Figure 47).

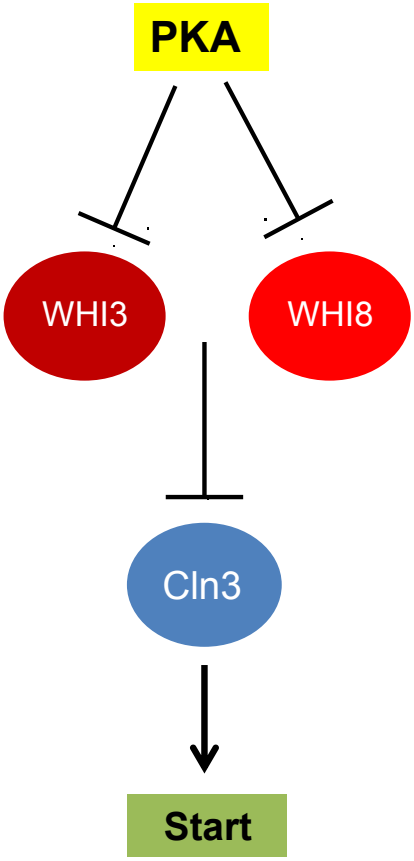

Figure 47: PKA inhibitory effect of Whi3 and Whi8

PKA phosphorylation of Whi8 (and Whi3) unleashes the *CLN3* mRNA and allows chaperones to release the Cdc28-Cln3 complex from the ER to trigger Start.

8. The C-terminal IDD of Whi8 is a structural determinant of Whi8 aggregation

Another effector of Whi8 aggregation is a structural determinant of Whi8 itself, an intrinsically disordered domain (IDD) at its C-terminus that we have found essential to modulate its subcellular localization into SGs. Previously it had been shown that prion like aggregation of TIA-1 drives its assembly into SGs (Gilks et al., 2004). In the same context, RNA binding domains are also essential for SG assembly. The RNA recognition motifs (RRMs) are required to recruit RNA into SGs, whereas IDDs favor their aggregation into macromolecular assemblies (Gilks et al., 2004). In case of Whi3, deletion of the prion related domain (the glutamine rich domains) did not affect co-localization of Whi3 with P-bodies or stress granules. On the other hand, deletion of the RRM largely but not entirely disrupted Whi3 accumulation in granules. Deletion of both the RRM and the glutamine rich domain was required to prevent completely formation

of Whi3 foci (Cai & Futcher, 2013). Deletion of the C- terminal IDD of Whi8 caused a strong reduction in Whi8 foci formation, which suggests that the two proteins use different molecular interactions for their recruitment into SGs.

9. Anatomy of the ER retention device

After adding the new factors identified in this study, in particular Whi7 and Whi8, we can recast the ER-retention device of the G1 Cyclin/Cdk Complex in budding yeast during G1 to accommodate the new findings and fill the gaps in the first proposed model of the retention device published more than ten years ago (Wang et al., 2004).

First, Whi3 and Whi8 would retain the *CLN3* mRNA at specific ER sites to confine newly synthesized Cln3 polypeptides in the same environment where a fraction of Cdc28 exists due to direct interaction with Whi8 and Whi7. Newly formed Cdc28-Cln3 complexes would be retained until a fraction of this complex is released by chaperone activity, which would multiphosphorylate Whi7 to create a positive feedback loop and trigger Start (Figure 48).

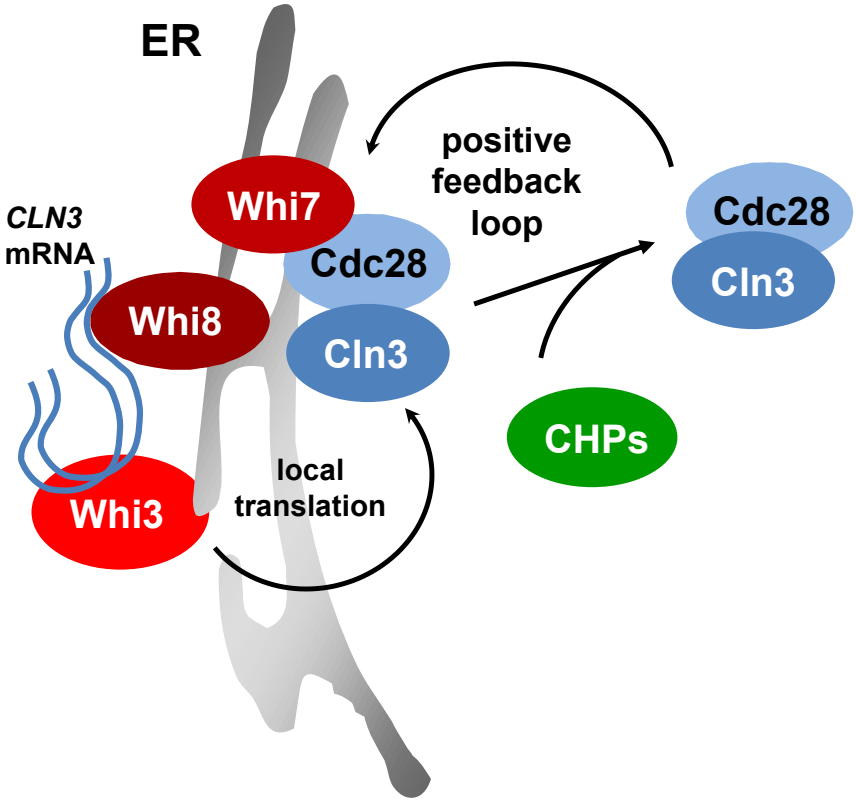

Figure 48: The ER-retention device including Whi7 and Whi8

A final proposed model of the ER-retention device including Whi7 and Whi8 identified in our study

Conclusions

This thesis has reached the following main conclusions:

- A genetic screen of randomly mutagenized *CDC28* clones give rise to a quintuple mutant referred as *CDC28 ^{wee}* that shows a consistent reduction in the budding cell volume, increased nuclear accumulation of Cln3 and a low proportion of the encoded Cdc28^{wee} protein within the ER-dense fraction compared to wild type Cdc28.
- The Cdc28^{wee} differential interactome identified Whi7 and Whi8 as new Cdc28 interactors with a negative function at Start.
- Whi7 is associated to the ER and it is strikingly similar to Whi5, interacts with Cks1, Cln2 and Cdc28 and is phosphorylated by Cln3-Cdc28 complex in late G1.
- Whi7 is important for retention of the Cln3-Cdc28 complex and establishes a positive feedback loop in late G1 to ensure coherent release and robust cell size control.
- Whi8 interacts *in vivo* with Cdc28, binds Whi3 in an RNA dependent manner and associates mRNAs encoding for of cell cycle regulators as *CLN3*, *WHI3, and WHI8* itself.
- Whi8 is important to recruit the *CLN3 mRNA* in stress granules and inhibit its translation upon stress.
- Whi8 spontaneous aggregation in granules depends on an intrinsically disordered domain at its C-terminus.
- Whi8 is phosphorylated in vitro by PKA and this phosphorylation event decreases both its RNA binding affinity and its aggregation capacity, linking a nutrient sensing pathway to cell cycle entry under stress conditions.

Supplementary tables

Antibodies used in western blot analysis and immunofluorescence

Primary antibody	Source	Conditions	Secondary antibody	Source	Conditions
12CA5Mouse Monoclonal (αHA)	Roche	2hours at room temp.1: 500 ,0.25%TBST Milk	ECL α-Mouse IgG (from sheep) horse reddish peroxidase linked	GE healthcare	1hour at room temperature, 1:10,000, ,0.25%PBST- Milk 0.02% SDS
3F10Rat Monoclonal (αHA)	Roche	1hours at room temp.1: 500 ,0.5%BSA in 1xPBS	Goat α -rat IgG Alexa Fluor® 568 labeled antibodies	Invitrogen	30minutes at room temp.1: 500 ,0.3%BSA in 1xPBS
F3165M Mouse Monoclonal (αFLAG)	SIGMA	2hours at room temp.1: 500 ,0.25%PBST Milk	ECL α-Mouse IgG (from sheep) horse reddish peroxidase linked	GE healthcare	1hour at room temperature, 1:10,000, ,0.25%PBST- Milk 0.02% SDS
5C5A7Mouse Monoclonal (αDpm1)	Molecular Probes	2hours at room temp.1: 500 ,0.25%PBST Milk	ECL α-Mouse IgG (from sheep) horse reddish peroxidase linked	GE healthcare	1hour at room temperature, 1:10,000, ,0.25%PBST- Milk 0.02% SDS
Rabbit polyclonal (αCdc28)	a gift from C. Mann	2hours at room temp.1: 500 ,0.25%PBST Milk	ECL α-Rabbit IgG (from donkey) horse reddish peroxidase linked	GE healthcare	1hour at room temperature, 1:10,000, ,0.25%PBST- Milk 0.02% SDS
Mouse Monoclonal (αGFP)	Roche	2hours at room temp.1: 500 ,0.25%PBST Milk	ECL α-Mouse IgG (from sheep) horse reddish peroxidase linked	GE healthcare	1hour at room temperature, 1:10,000, ,0.25%PBST- Milk 0.02% SDS
1G10.H8 Mouse Monoclonal (αYDJ1)	Abnova	2hours at room temp. 1: 1000 ,0.25%PBST Milk	ECL α-Mouse IgG (from sheep) horse reddish peroxidase linked	GE healthcare	1hour at room temperature, 1:10,000, ,0.25%PBST- Milk 0.02% SDS
Rabbit α -goat IgG Alexa Fluor® 568 labeled antibodies	Invitrogen	30minutes at room temp.1: 500 ,0.3%BSA in 1xPBS			
Rabbit α -GFP IgG polyclonal Alexa Fluor® 488 labeled antibodies	Molecular Probes	30minutes at room temp.1: 500 ,0.3%BSA in 1xPBS			
α -FLAG®M2 Affinity Gel agrose beads	Sigma	As described for IP of FLAG fusion proteins			
GST-p13^{suc1} agrose beads	Sigma	As described for IP of Cks1 protein			
Glutathione Sepharose beads	GE healthcare	As described for purification of GST fusion proteins			

Yeast strains used in this work

Strain	Construction details	Relevant Marker
CML128	Spore coming from CML123. Same ascus that CML125, 126 and 127. Originally called T2d	MATa, leu2-3,112, ura3-52, trp1, his4, canI.r
BY4741	A gift from Gemma Reverter	Mata his3-delta1, leu2-delta0, met15-delta0, ura3-delta0
CYC428	The Kan cassette in CML203 was replaced with the URA3 cassette with CMO91 & CMO92 primers and pCYC39.	CLN3-3HA::URA3
CYC430	WHI5-sGFP-KAN cassette amplified by PCR from pCYC86 using CYO612 and CYO1404 was inserted in CYC428 in WHI5 locus to obtain sGFP fusion.	CLN3-3HA::URA3 & WHI5-sGFP::KAN
CYC432	NAT-*GAL1p*-CDC28 cassette amplified by PCR from PYM-N23 using CYO1479 & CYO1480 was inserted in CYC430 in CDC28 locus to be under control of *GAL1p*-promoter.	CLN3-3HA::URA, WHI5-GFP::KAN& *GAL1p-CDC28*::NAT
CYC434	PCR-random mutagenesis of the CDC28 gene on a YCplac111 vector in CYC432	CLN3-3HA::URA, WHI5-GFP::KAN, *GAL1p-CDC28*::NAT & *CDC28* mutant pool::LEU2
CYC474	NAT-*GAL1p*-CDC28 cassette amplified by PCR from PYM-N23 using CYO1479 & CYO1480 was inserted in CYC421 in CDC28 locus under *GAL1p*-promoter. Checked by colony PCR using primers CYO1483&CYO1485 to obtain 270bp fragment	*Δcln3*::LEU,WHI5-GFP & *GAL1p-CDC28*::NAT
CYC484	NAT-*GAL1p*-CDC28 cassette amplified by PCR from PYM-N23 using CYO1479 & CYO1480 was inserted in CML128 in CDC28 locus to be under control of *GAL1p*-promoter.	*GAL1p-CDC28*::NAT
CYC484	NAT-*GAL1p*-CDC28 cassette amplified by PCR from PYM-N23 using CYO1479 & CYO1480 was inserted in CYC9 in CDC28 locus to be under control of *GAL1p*-promoter.	CLN3-3HA::KAN, *Δwhi3*::URA3MX & *GAL1p-CDC28*
713-Y	PCR fragment obtained from pFA6-KANmx4 using 261 and 262 was transformed into CML128 and checked by colony PCR	*Δsrl3*::KAN
246-Y	1.3Kb fragment obtained by PCR using O-260&O-261 using pYM22as a template transformed into CML128 and checked by colony PCR using O-263 &CYC1481 and western blot	SRL3-3HA::TRP
227-Y	1.3Kb fragment obtained by PCR using O-293 & O-294 using pYM22as a template transformed into CML128 and checked by colony PCR using O-298 & CYC1481 and western blot	YGR250c-3HA::TRP
244-Y	1.7Kb fragment obtained by PCR using O-261 & O-262 using PAG60 as a template was transformed into CML203 and checked by colony PCR using O-307 & CYC1481	CLN3-3HA::KAN & *Δsrl3*::URA
245-Y	1.7Kb fragment obtained by PCR using O-294&O-295 using PAG60 as a template was transformed into CML203 and checked by colony PCR using O-308&CYC1481	CLN3-3HA::KAN& *Δ*ygr*250c*::URA
253-Y	NAT-*GAL1p*-CDC28 cassette amplified by PCR from PYM-N23 using CYO1479 & CYO1480 was inserted in 227-Y in CDC28 locus to be under control of *GAL1p*-promoter	YGR250c-3HA::TRP& *GAL1p-CDC28*::NAT
254-Y	NAT-*GAL1p*-CDC28 cassette amplified by PCR from PYM-N23 using CYO1479 & CYO1480 was inserted in 247-Y in CDC28 locus to be under control of *GAL1p*-promoter	SRL3-3HA::TRP& *GAL1p-CDC28*::NAT
279-Y	Adh-Galactose-hER-Vp16 has been digested with NdeI to be integrated in URA gene of CML203	CLN3-3HA::KAN & Adh-Galactose-hER-Vp16::URA
282-Y	Adh-Galactose-hER-Vp16 has been digested with NdeI to be integrated in URA gene of 246Y	SRL3-3HA::TRP & Adh-Galactose-hER-Vp16::URA
284-Y	261 &262-O were used to amplify 1,3kb fragment by PCR using pAG25 as a template the PCR fragment was transformed to BY4171 WHI5GFP background to delete SRL3 and checked by colony PCR using 307-O & CYO1481	BY4171 WHI5-GFP& *Δsrl3*::NAT
286-Y	2Kb fragment obtained by PCR using 293 & 294-O using pCYC67as a template transformed into CML128 and checked by colony PCR using 298-O & CYC1481 and western blot	YGR250C-6FLAG::KAN

429-Y	261 &262-O were used to amplify 1,3kb fragment by PCR using pAG25 as a template the PCR fragment was transformed to 279-Y background to delete SRL3 and checked by colony PCR using 307-O & CYO1481	CLN3-3HA::KAN , Adh-Galactose-hER-Vp16::URA & *Δsrl3*::NAT
462-Y	A 2.6 Kb fragment was amplified with 294 & 295-O from pCYC86 corresponding to the sGFP-kanMX4 cassette, and was integrated in CML128 to tag the YGR250c protein at the C terminus. Checked by fluorescence microscopy	YGR250c-GFP::KAN
463-Y	1.9Kb fragment obtained by PCR using 294 & 295-O using pCM376 as a template was transformed into CYC9 and checked by colony PCR using O-308 & CYC1481	*Δwhi3*::URA,*ygr250c*::LEU & CLN3-3HA::KAN
464-Y	1.7Kb fragment obtained by PCR using 294 & 295-O using PAG60 as a template was transformed into CML211 and checked by colony PCR using 308-O & CYC1481	*Δcln3*::LEU & *Δygr250c*::URA
465-Y	1.3Kb fragment obtained by PCR using 293 & 294-O using pYM22as a template transformed into CYC243 and checked by colony PCR using 298-O & CYC1481 and western blot	OLE1-GFP::KAN & YGR250c-3HA::TRP
533-Y	A 2.6 Kb fragment was amplified with 294 & 293-O from pCYC86 corresponding to the sGFP-kanMX4 cassette, and was integrated in BY4741 to tag the YGR250c protein at the C terminus. Checked by fluorescence microscopy	YGR250c-GFP::KAN in BY4741
534-Y	1.6Kb fragment obtained by PCR using 294 & 295-O using pFA6a-kanMX4 as a template was transformed into BY4741 and checked by colony PCR using 308-O&CYC1481	*Δ*ygr*250c*::KAN
655-Y	PCR fragment obtained from pFA6-natNT2 using 294 & 295-O was transformed into BY4741 and checked by colony PCR	*Δ*ygr*250c*::NAT
656-Y	PCR fragment obtained from pFA6-natNT2 using 294 & 295-O was transformed into 280-Y and checked by colony PCR	CLN3-3HA::KAN & *Δ*ygr*250c*::NAT
657-Y	PCR fragment obtained from pFA6-natNT2 using 294 & 295-O was transformed into CYC9 and checked by colony PCR	*Δ*ygr*250c*::NAT & *Δwhi3*::URA
717-Y	PCR fragment using 856 & 857-O from PBS34 transformed to BY4741 and checked by fluorescent microscopy	BY4741 PUB1-mCHerry::KAN
720-Y	PCR fragment obtained from pFA6-NATmx4 using 873 & 874-O was transformed into BY4741 and checked by colony PCR	BY4741*Δ bcy1*::NAT
754-Y	PCR fragment obtained from pCYC67 using 928 & 929-O was transformed into BY4741 and checked by colony PCR & western blot	BY4741 PUB1-6FLAG::KAN
755-Y	PCR fragment obtained from pCYC67 using 928 & 929-O was transformed into 655-Y and checked by colony PCR & western blot	BY4741 PUB1-6FLAG::KAN & *Δ*ygr*250c*::NAT
756-Y	PCR fragment obtained fromPFA6hphMX4 by CMO160 & CMO161 old oligos was transformed to 755-Y to disrupt WHI3 locus and checked by colony PCR	BY4741 PUB1-6FLAG::KAN, *Δ*ygr*250c*::NAT & *Δwhi3*::HYG
841-Y	PCR fragment from pCYC86 using 1006 & 294-O was transformed to BY4741 and positive transformant checked by western blot and fluorescent microscopy	BY4741 *WHI8-1*-GFP::KAN
842-Y	PCR fragment from pCYC59 using 928 & 929-O transformed to BY4741 and positive transformant checked by western blot	BY4741 PUB1-3HA::KAN

Plasmids used in this work

Plasmid	Construction details	Relevant Marker
pCYC1103	First the whole CDC28 gene amplified from genomic DNA by PCR using CYO1495&CYO1496 then used as template for another PCR using CYO1497&CYO1498 the 1.8 fragment together with YCplac111 digested with Pst1 & Sal1 are transformed to yeast to religate the new plasmid which then amplified in E coli CDC28-wt	Amp &LEU2 CDC28^{wt} in YCplac111
pCYC1104	First the whole CDC28 gene amplified from genomic DNA by PCR using CYO1495&CYO1496 then used as template for another Mutagenic PCR using CYO1497&CYO1498. Mutant CDC28 allele with these sets of mutations A71G(K24R), G238A(D80N), A289G(R97G), A637G(S213G), A783G, A891G *CDC28-w4*	Amp &LEU2 *CDC28*^{w4} in YCplac111
pCYC1105	First the whole CDC28 gene amplified from genomic DNA by PCR using CYO1495&CYO1496 then used as template for another Mutagenic PCR using CYO1497&CYO1498 Mutant CDC28 allele with these sets of mutations A4G(S2G), A114T, A136G(S46G), A287C(K96T), A375T, A561C(K187N), A821G(K274R) *CDC28-w6*	Amp &LEU2 *CDC28*^{w6} in YCplac111
pCYC1106	First the whole CDC28 gene amplified from genomic DNA by PCR using CYO1495&CYO1496 then used as template for another Mutagenic PCR using CYO1497&CYO1498 Mutant CDC28 allele with these sets of mutations A136T(S46C), A287T(K96I), A752T(Q251L) *CDC28-w7*	Amp &LEU2 *CDC28*^{w7} in YCplac111
pCYC1107	First the whole CDC28 gene amplified from genomic DNA by PCR using CYO1495&CYO1496 then used as template for another Mutagenic PCR using CYO1497&CYO1498 Mutant CDC28 allele with these sets of mutations C642T, G669T (K223N), A862G(R288G) *CDC28-w8*	Amp &LEU2 *CDC28*^{w8} in YCplac111
pCYC1108	First the whole CDC28 gene amplified from genomic DNA by PCR using CYO1495&CYO1496 then used as template for another Mutagenic PCR using CYO1497&CYO1498 Mutant CDC28 allele with these sets of mutations A30G, T67C(Y23H), T181A(L61I), A375C, C388T(H130Y) *CDC28-w34*	Amp &LEU2 *CDC28*^{w34} in YCplac111
pCYC1109	First the whole CDC28 gene amplified from genomic DNA by PCR using CYO1495&CYO1496 then used as template for another Mutagenic PCR using CYO1497&CYO1498 Mutant CDC28 allele with these sets of mutations A166C(I56L), T522C, A558T, A625G(K209E), C825A *CDC28-w38*	Amp &LEU2 *CDC28*^{w38} in YCplac111
pCYC1110	pCYC1103 amplified by PCR using CYO1716 andCYO1717 and together with 550bp fragment of CDC28 carrying the 5 mutations Mutant CDC28 allele with these sets of mutations A289G(R97G), A637G(S213G), A287C(K96T),G669T (K223N) & A625G(K209E) transformed to yeast to religate the new vector which is then amplified in *E coli CDC28-wq*	Amp &LEU2 *CDC28*^{weet} in YCplac111
140P	A fragment of 12 amino acids and 3FLAG epitope and flanked with homology sequence of CDC28 was amplified by PCR using 40 & 41-O and pCYC1103 was opened by ExSite PCR using 42 & 43–O transformed to yeast to religate the new vector	Amp &LEU2 CDC28^{wt} -3FLAG in YCplac111
141P	A fragment of 12 amino acids and 3FLAG epitope and flanked with homology sequence of CDC28 was amplified by PCR using 40 & 41-O and pCYC1110 was opened by ExSite PCR using 42 & 43-O transformed to yeast to religate the new vector	Amp &LEU2 CDC28^{weet} -3FLAG in YCplac111
142P	pCM194 was opened by ExSite PCR using 32&33-O and also CDC28 ORF amplified by PCR using 34&35-O and the 2 PCR fragments treated with DpnI then transformed to CML211 to religate the CDC28-CLN3- 3HA CHIMERA .	Amp &URA CDC28-CLN3-3HA CHIMERA in YCplac33
174-P	YCpGAL digested with XbaI and HindIII and dephosphorylated then ligated with SRL3 PCR fragment digested with the same enzymes checked by EcoRI digestion and look for 1.4 fragment and 5kb fragmen	Amp & TRP SRL3 in YCpGAL
219-P	Adh-Galactose-hER-Vp16 allow expression of gal responsive genes upon addition of B-estradiol integrate in Ura by NdeI	Amp & URA Adh-Galactose-hER-Vp16
232-P	YGR250c was amplified by PCR using 296&297-O from genomic DNA then the fragment is digested with BamHI& SalI and cloned in YCpGAL digested with the same enzyme mixtures	Amp & TRP YGR250c in YCpGAL
266-P	396 &397-O were used to amplify the whole sequence of pCM194and deleting the 3HA tag by ExSite PCR and adding KpnI resstriction site then digested and ligated	Amp & URA CLN3 in YCplac33
267-P	396 &398-O were used to amplify the whole sequence of pCM194and deleting the NLS& 3HA tag by ExSite PCR and adding KpnI resstriction site then digested and ligated	Amp & URA *cln3ΔNLS* in YCplac33

276-P	439 &438-O were used to amplify CLN3 from 266-O by PCR then digested with XbaI & PstI and ligated with YCpGAL digested with the same restriction enzymes	Amp & Trp CLN3 in YCpGAL
277-P	439 &438-O were used to amplify CLN3-NLS from 267-O by PCR then digested with XbaI & PstI and ligated with YCpGAL digested with the same restriction enzymes	Amp & Trp *cln3ΔNLS* in YCpGAL
278-P	433 &434-O were used to amplify SRL3 from genomic DNA by PCR the the PCR fragment digested with XbaI & HindIII and ligated with YCplac22 digested with the same enzyme mix	Amp & Trp SRL3 in YCplac22
288-P	$SRL3^{NP}$ fragment obtained by digestion with SacI and KpnI from DNA obtained from Gene art recombined to YCplac22-SRL3 PCR fragmet obtained by ExSite pcr using 446&447-O then transformed to Ecoli	Amp & Trp $SRL3^{NP}$ in YCplac22
290-P	$SRL3^{NP}$ fragment obtained by PCR from 228-P using 259&448 –O and digested with XbaI and HindIII was ligated to YCpGAL digested with the same enzyme mix	Amp & Trp $SRL3^{NP}$ in YCpGAL
332-P	474 &475-O used for ExSite PCR of 278-P on the other hand 476 &477-O used to amplify 3HA-ADHt from pCM194 and the vector religated by recombination in yeast then transformed to E coli checked by WB and restriction by HindIII & PstI	Amp & Trp SRL3-3HA in YCplac22
333-P	474 &475-O used for ExSite pcr of 287-P on the other hand 476 &477-O used to amplify 3HA-ADHt from pCM194 and the vector religated by recombination in yeast then transformed to E coli checked by wb and restriction by HindIII & PstI	Amp & Trp $SRL3^{NP}$-3HA in YCplac22
334-P	474 &475-O used for ExSite pcr of 175-P on the other hand 476 &477-O used to amplify 3HA-ADHt from pCM194 and the vector religated by recombination in yeast then transformed to E coli checked by wb and restriction by HindIII & PstI	Amp & Trp SRL3-3HA in YCpGAL
335-P	474 &475-O used for ExSite PCR of 289-P on the other hand 476 &477-O used to amplify 3HA-ADHt from pCM194 and the vector religated by recombination in yeast then transformed to E coli checked by wb and restriction by HindIII & PstI	Amp & Trp $SRL3^{NP}$-3HA in YCpGAL
384-P	266-P was opened using 32&33-O (ExSite PCR). CDC28 was obtained from pCYC181 using 34&35-O. Then all PCR products were transformed in CML128 in order to recombine all of them.	Amp & URA CDC28-CLN3 CHIMERA in YCplac33
385-P	266-P was opened using 32 &33-O (ExSite PCR). Cdc28 was obtained from pCYC184 using 0034-O and 0035-O. Then all PCR products were transformed in CML128 in order to recombine all of them.	Amp & URA $CDC28^{KD}$ -CLN3 CHIMERA in YCplac33
386-P	267-P was opened using 32& 33-O (ExSite PCR). CDC28 was obtained from pCYC181 using 34 & 35-O. Then all PCR products were transformed in CML128 in order to recombine all of them.	Amp & URA CDC28- *cln3ΔNLS* CHIMERA in YCplac33
387-P	267-P was opened using 32& 33-O (ExSite PCR). CDC28 was obtained from pCYC184 using 34& 35-O. These primers anneal with the beginning and the end of Cdc28. Then all PCR products were transformed in CML128 in order to recombine all of them.	Amp & URA $CDC28^{KD}$ - *cln3ΔNLS* CHIMERA in YCplac33
470-P	GAL-YDJ1&GAL-SSA1 in YCplac111. 4PCR fragments of YDJ1,SSA1,GAL1 & opened YCplac111 fragments carrying flanking ends were recombined in CML128 to construct GAL-YDJ1&GAL-SSA1	Amp & LEU GAL1p-YDJ1&GAL10p-SSA1
545-P	YGR250c was amplified by PCR using 671&672-O from genomic DNA of BY4741 then the fragment is digested with SacI& SalI and cloned in YCplac111 digested with the same enzyme mixtures	Amp & LEU YGR250c in YCplac111
572-P	715&716-O were used to open 545-P by PCR and then digested with NotI then ligated to create *YGR250c AAA*	Amp & LEU *YGR250c AAA* in YCplac111
660-P	YCplac111-YGR250c was opened using 646&685-O by ExSite PCR and GFP fragment carrying homologous sequence of C-terminus of YGR250c was amplified by PCR using 644&685-O and the 2PCR fragments were recombined *in vivo* in CML128	Amp & LEU YGR250c-GFP in YCplac111
661-P	715&716-O were used to open 660-P by PCR and then digested with NotI then ligated to create YCplac111-*YGR250cAAA*-GFP	Amp & LEU *YGR250cAAA*-GFP in YCplac111
752-P	pG14-MS2-GFP vector was opend by 4 sets of primers 935&937-O and 936&938-O and mCHerry fragment with homology sequence to pG14-MS2 was amplified by 939&940-O and all the 3fragments recombined in BY4741 background checked by fluorescence	Amp & LEU pG14-MS2-mCHerry

Primers used in this work.

Primer	Sequence	Description
CYO1479	CATCAGCTACAGTGGAAAATAGCCCAGATCAAATAGAACT ATCCTTCGAACCGTACGCTGCAGGTCGAC	Forward primer to obtain a *GAL1p*-CDC28 fusion with pYM-N23
CYO1480	ACCTTCACCGACTTTCTCAAGTCTTTTGTAATTTGCTAAT TCACCGCTCATCGATGAATTCTCTGTCG	Reverse primer to obtain a *GAL1p*-CDC28 fusion with pYM-N23
CYO1481	GTCGACCTGCAGCGTACG	Universal diagnostic primer rS1/S3 to check for cassette insertions (Janke et al. 2004) (r1 for our tags)
CYO1495	TAAGAAGCGTTGGCAGACGCTG	Fw primer to amplify CDC28 (-551 from CDC28 ATG) with flanking sequences
CYO1496	ATACGGTCAGCGCTCCTTTGAG	Rv primer for CYO1495 (1466 from CDC28 ATG)
CYO1497	ACACAGGAAACAGCTATGACCATGATTACGCCAAGCTTGC ATGCCTGCAGGTCGACGAATTATCGTTCTCGAGATAG	Fw primer to amplify CDC28 (-349 from CDC28 ATG) with flanking sequences and homologous tails to YCplac111 polylinker
CYO1498	GTAAAACGACGGCCAGTGAATTCGAGCTCGGTACCCGGGG ATCCTCTAGAGTCGACGGTGACAAGTGAAACTCTTC	Rv primer for CYO1495 (1372 from CDC28 ATG)
CYO1501	CAAGCTTGCATGCCTGCAGG	Primers for CDC28 sequencing (-370 from CDC28 ATG) anneals in YCplac111
CYO1502	CAAGCTTGCATGCCTGCAGG	Primers for CDC28 sequencing (-136 from CDC28 ATG)
CYO1503	AGTGAAGACGAGGGTGTTCC	Primers for CDC28 sequencing (136 from CDC28 ATG)
CYO1504	CCACTCACACCGTATTCTGC	Primers for CDC28 sequencing (381 from CDC28 ATG)
CYO1505	CAGTGGCGATAGTGAGATCG	Primers for CDC28 sequencing (636 from CDC28 ATG)
CYO1506	CATCCACCCCTACTTCCAAG	Primers for CDC28 sequencing (870 from CDC28 ATG)
CYO1507	TCAGGGGTTAAAAGCTGGGC	Primers for CDC28 sequencing (1081 from CDC28 ATG)
CYO1716	TTCAGAGTATTGGGAACGCC	Fw primer to prepare a recombination recipient molecule from a YCplac111-CDC28 plasmid for CDC28 synthetic sequences 201-750
CYO1717	GGTCCAAATCGAGGAACTCA	Rv primer for CYO1716
CMO91	GTGGATTGTGATTTTAATGATAGTAGCAACCTCAAGAAAA CTCGCCGTACGCTGCAGGTCGAC	Fw primer to obtain CLN3-3HA.
CMO92	AAATTTTAATTTATTTGTTGTTAAATGCATTTTTTTTTTG TCGTTCATCGATGAATTCGAGCTCG	Rv primer for CMO91.
32-O	ATTAACCGGATTAGCGCCAGAAGAGCAGCCATCCACCCCT ACTTCCAAGAATCAATGGCCATATTGAAGGATACCA	Fw primer to create CDC28 -CLN3 CHIMERA using pCM194 vector containing CLN3-3HA fusion
33-O	TGTACCTTCACCGACTTTCTCAAGTCTTTTGTAATTTGCTA ATTCACCGCTCATCGTACAGAAAGCGTATCAAATC	Reverse primer for 32-O
40-O	TAGCGCCAGAAGAGCAGCCATCCACCCCTACTTCCAAGAA TCAAAGCTCAGCGAGAAAGCTCTCGAATCGGCAACGCTCA AGCTTATGGGATCACC AGGT	Fw primer to amplify a fragment of 12 amino acids alpha helix and 3FLAG epitope flanked with CDC28 homology sequence using pCDNA FLAG as a template
41-O	ATGACAGTGCAGTAGCATTTGTAATATAATAGCGAAATAG ATTATAATGCCGTTACTAGATGGATCCTT TGTC	Rv primer to 40-O flanked with homology sequence of YCplac111
42-O	GCATTATAATCTATTTCGCTAT	Fw primer to amplify the whole pCYC1103 or pCYC1110 (wt CDC28 and *wee CDC28* vectors) by ExSite PCR
43-O	TGATTCTTGGAAGTAGGGGT	Rv primer for 42-O
258-O	GCGTCTAGAGACGAATATAATGTTTCTTAAGA	Fw primer for cloning SRL3 in YCpGAL containing XbaI site
259-O	CGCAAGCTTAACCTGGTATATAGGTAATCG	Rv primer for cloning SRL3 in YCpGAL containing HindIII site
260-O	TAC AAGAAGTTGT TGCTATCGAT ACATTATTGA AGATGTCCTCATCGGAC CGTACGCTGCAGGTCGAC	Fw primer to tag SRL3 with 3HA epitope
261-O	ACCTAAAAGTAGCCAAAGCCATGTATATATGCGAAACCCG AATCATTAGTCATCGATGAATTCGAGCTCG	Rv primer for tagging SRL3 with 3HA or deleting SRL3
262-O	AAGGAAAGGCTAAGCAATGAAATGTTTCGTTATTTTATTG TATTTTCAAG CGTACGCTGCAGGTCGAC	Fw primer to delete SRL3
263-O	CAACGTTAACGTTTCGCC	Fw primer to check SRL3-3HA fusion
307-O	ACAGGAGCCTAAGAATAGAGA	Fw primer to check deletion of SRL3
293-O	GTAGTAATGAAGAGGAAGAATTTTCTAGTGGTGATTATTC TATGGACTAC CGTACGCTGCAGGTCGAC	Fw primer to tag YGR250c with 3HA epitope
294-O	AGTAATAAGAAAAGTTACCATAGGCTAGTTGAATGTCCAA GATCGTAAAG CATCGATGAATTCGAGCTCG	Rv primer to tag YGR250c with 3HA epitope or to delete

295-O	ATTACAAGGCACCCTGATTAAAAATCCAAAAATAAACCAT AAGTTTTATT CGTACGCTGCAGGTCGAC	Fw primer to delete YGR250c
296-O	GCGGGATCCGAAGTTTCGAGGATGAATATT	Fw primer for cloning YGR250c in YCpGAL with BamHI
297-O	CGCGTCGACTCATGTGAATTGTTTATCTATC	Rv primer for cloning YGR250c in YCpGAL with SalI
298-O	GCAGAATCCTGCAGCAAA	Fw primer to check tagging YGR250c
308-O	TTAGTTCGTTCAACGGTCTCA	Fw primer to check deletion of YGR250c
433-O	GCGAAGCTTTAGCACACATGTTTC ATAAC	Fw primer to clone SRL3 gene with HindIII site
434-O	GCGTCTAGATTCCAAGATTAAAAGAATAGG	Rv primer to clone SRL3 gene with XbaI site
438-O	GCG TCTAGA GCTTTCTGTA CGATGGCCAT	Fw primer to clone CLN3 or *cln3Δnls* with XbaI site in YCpGAL
439-O	GCG CTGCAG TCTTGCCGGT AGAGGTGTG	Rv primer to clone CLN3 or *cln3Δnls* with PstI site in YCpGAL
448-O	GCGTCTAGAGACGAATATAATGTTTCTTAAGG	Fw primer to clone $SRL3^{NP}$gene in YCpGAL with XbaI site
446-O	CGGGTTTCG CATATATACA T	Fw primer to amplify YCpLac22-SRL3 by ExSite pcr
447-O	ATATTCGTCTATTATTTATCCG	Rv primer of 446-O
474-O	TCGGGTTTCGCATATATACAT	Fw primer to amplify SRL3 containing vector by ExSite to delete the stop codon of SRL3 to allow in frame tagging with 3HA
475-O	GTCCGATGAGGACATCTTC	Rv primer to 474-O
476-O	TG TTGCTATCGA TACATTATTGA AGATGTCCT CATCGGAC CGTA CGCTGCAGGT CGAC	Fw primer to amplify 3HA-ADHt fragment with flanking sequence of C-terminus of SRL3
477-O	CCTAAAAGTAGCCAAAGCCATGTATATATGCGAAACCCGA TCTTGCCGGTAGAGGTGTG	Rv primer to 476-O
644-O	GAGGAAGAATTTTCTAGTGGTGATTATTCTATGGACTAC GGTTCTGGT ATGTCTAAAGGTGAAGAATTATTC	Fw primer to amplify GFP with homologous flanking sequence of YGR250c C-terminus
645-O	ATGACCATGATTACGCCAAGCTTGCATGCCTGCAGGTCGA CGTTGTGTGGAATTGTGAGCG	Rv primer to 644-O
646-O	GTAGTCCATAGAATAATCACCA	Fw primer to open vectors containing YGR250c
671-O	GCG GTCGAC GTGCCT TTTGTTCGAA GGA	Fw primer to clone the whole YGR250c gene with its own promotor from genomic DNA with SalI site
672-O	GCGGAGCTCTCATGTGAATTGTTTATCTATC	Rv primer to clone the whole YGR250c gene with its own terminator from genomic DNA with SacI site
673-O	GGTCT TCAACTGGAA CAATTG	Fw primer to ExSite the whole YGR250c gene in YCplac111 by PCR
674-O	TTCCTTTCAATTTTTATTGATTGG	Rv primer to ExSite the whole YGR250c gene in YCplac111 by PCR
685-O	GAGCTCGAATTCACTGGCC	Forward primer to add GFP at C-terminus of YGR250c in YCPlac22 or YCPlac111 by ExSite PCR
686-O	GTCACGACGTTGTAAAACGACGGCCAGTGAATTCGAGCTC GTTGTGTGGAATTGTGAGCG	Reverse primer to amplify GFP including CYC1 terminator with flanking sequence of YCplac22 or YCplac111
715-O	GTATGCGGCCGCTGGTCTTCAACTGGAA CAATTG	Fw primer to mutate STS of YGR250c to AAA with NotI site
716-O	GTATGCGGCCGCTTTCCTTTCAATTTTTATTGATTGG	Rv primer to 715-O
856-O	CCGGTTATGTCTGAGCAACAACAGCAACAGCAGCAACAGC AGCAACAACAAGGTGGATCTGGTTCCGGCTCTATGGTGAG CAAGGGCGAGG	Fw primer to tag PUB1 with mcherry at C-terminus
857-O	TTTGTAGGTTGCCTCTCTTTATTCTTTCTTTTTGTTTCATT CCACTTTTCTTCATAATATTCATCGATGAATTCGAGCTCG	Rv primer to 856-O
858-O	GAAACTTGAG AACCGGTTGG	Diagnostic primer to test correct tagging
873-O	TACAACAAGCAGATTATTTTCAAAAGACAACAGTAAGAAT AAACG CGTACGCTGCAGGTCGAC	Forward primer to delete BCY1
874-O	GAGAAAGGAAATTCATGTGGATTTAAGATCGCTTCCCCTT TTTACCATCGATGAATTCGAGCTCG	Reverse primer to delete BCY1
875-O	CTCGACTAAG TCAAGCGATC	Diagnostic primer for BCY1 deletion
928-O	CCGGTTATGTCTGAGCAACAACAGCAACAGCAGCAACAGC AGCAACAACAA CGTACGCTGCAGGTCGAC	Fw primer to tag PUB1 with 6FLAG
929-O	TTTGTAGGTTGCCTCTCTTTATTCTTTCTTTTTGTTTCATT CCACTTTTCTTCATAATATCATCGATGAATTCGAGCTCG	Rv primer to tag PUB1 with 6FLAG
997-O	CGCGGATCCAATATTGCAGAAGAACCATCAG	Fw primer to clone YGR250c from Amino acid no.2 to Amino acid no.100 in pGEX-KG with BamHI
998-O	CGCGTCGACTTCTGTATCAGAGTTGTTAACG	Rv primer to clone YGR250c from Amino acid no.2 to Amino acid no.100 in pGEX-KG with SalI
1009-O	GACGGGTATCAAGTGAGCAAAGATCAAGTGTTATCTGTTT CTTTCGCT CGTACGCTGCAGGTCGAC	Fw primer to delete the C-terminus of YGR250c from AA no.637

RT-qPCR primers and probes used in this work.

Gene	Sense primer	Anti-Sense primer	Dual labeled probe FAM-BHQ
CLN3	AACCCTAATCTCGTTAAAAG	GACAGTACATGATGAAGTC	ACATCACTCAGCGATCAGCGA
CDC28	GCAACTTTGTAAGGGTATTG	CCATCTTTGTTAATCAATAAGTTC	ACTGCCACTCACACCGTATTCT
CKS1	CTGACCAAGAAAGAGCAC	CTCTCCATTCGTCTTCTG	TTCAAGATTCCATTCACTATTCTCCGC
WHI3	GGAACATGAGCAAGTAGC	GGATGAATCTTCCAGAGAAC	TTGATTCCTCCACCTCCGACG
WHI7	CGATCCATTTTCCAATGA	CCTTGAGAAGATAACGGTA	TAAGCCAACAGCAATCTCAACAGC
WHI8	CCAACAAAGTATAATAAGAAA	GTTGGTATTAGGGTACTG	CTCAGAACCAATCGCAACAGCAA
HXK1	ACCACTCAATCCAAGTATA	GACCATAAAGTCCTTCAAA	AGAACCACTAAGCACCAAGAGGAG
RPL19s	GAACGATAATAACTAACATGAC	GAGGTTTCATTTGGATCTAA	TTCTCTTACCGACACCGACGAC

Top 20 candidates detected in the iTRAQ.

Accession	Q/S	P value
sp|P36167|SRL3_YEAST	-2.416	3.8E-19
sp|P19882|HSP60_YEAST	-2.018	4.7E-14
sp|P15180|SYKC_YEAST	-0.967	1.0E-04
sp|P07281|RS19B_YEAST	-0.851	4.9E-04
sp|P37263|YC16_YEAST	-0.806	8.6E-04
sp|P53316|YG5B_YEAST	-0.737	1.9E-03
sp|P47006|RPA34_YEAST	-0.672	3.9E-03
sp|P16521|EF3A_YEAST	-0.656	4.6E-03
sp|P39015|STM1_YEAST	-0.631	6.0E-03
sp|P27825|CALX_YEAST	-0.617	6.9E-03
sp|P34167|IF4B_YEAST	-0.538	1.5E-02
sp|Q12344|GYP5_YEAST	-0.498	2.1E-02
sp|P20486|CKS1_YEAST	-0.494	2.1E-02
sp|P46655|SYEC_YEAST	-0.450	3.1E-02
sp|Q01855|RS15_YEAST	-0.432	3.6E-02
sp|P38934|BFR1_YEAST	-0.429	3.6E-02
sp|P05747|RL29_YEAST	-0.408	4.3E-02
sp|P30771|NAM7_YEAST	-0.402	4.5E-02
sp|P38754|RL14B_YEAST	-0.401	4.5E-02
sp|P0CX28|RL44B_YEAST	-0.400	4.6E-02

List of Figures

List of Tables

Abbreviations

AMP	Ampicillin
APC	Anaphase promoting complex
ATP	Adenosine tri-phosphate
BSA	Bovine serum albumin
CDK	Cyclin dependent kinase
CAK	Cdk-activating kinase
cAMP	Cyclic adenosine monophosphate
DAPI	4',6-Diamidino-2-Phenylindole
DEPC	Diethylpyrocarbonate
DNA	Deoxyribonucleic acid
DMSO	Dimethyl sulfoxide
DOC	Deoxycholate
DTT	Dithiothreitol
EDTA	Ethylene diamine tetra acetic acid
ER	Endoplasmic reticulum
GFP	Green fluorescent protein
GST	Glutathione S-transferase
KAN	Kanamycin
I.P	Immunoprecipitation
IPTG	Isopropyl β-D-1-thiogalactopyranoside
ITRAQ	Isobaric tags for relative and absolute quantitation
IDD	Intrinsically disordered domain
KD	Kinase dead
LB	Luria Bertani
MEN	Mitotic exit network
mRNA	Messenger ribonucleic acid
MW.	Molecular weight
NAT	Nourseothricin
NLS	Nuclear localization signal
OD	Optical density
PBs	Processing bodies
PBS	Phosphate-buffered saline
PBST	Phosphate -buffered saline containing 0.05% tween-20
PCR	Polymerase chain reaction
PEG	Polyethylene glycol
PKA	Protein kinase A
PMSF	Phenylmethylsulfonyl fluoride
PRD	Prion related domain
PVDF	Polyvinylidene difluoride
RAS	Rat sarcoma
RIP	RNA immunoprecipitation
RNA	Ribonucleic acid
RT	Room temperature
RRM	RNA Recognition motif
SDC	Synthetic dextrose complete
SDS	Sodium dodecyl sulfate
SDS-PAGE	Sodium dodecyl sulfate polyacrylamide gel electrophoresis
SGs	Stress granules
ssDNA	Single stranded DNA
TAE	Tris-acetate-EDTA buffer
TCA	Trichloro acetic acid
TE	Tris- EDTA buffer
TEMED	Tetramethylethylenediamine
UV	Ultra violet
WT	Wild type
YNB	Yeast nitrogen base
YPD	Yeast peptone dextrose
YPG	Yeast peptone galactose
YPRAF	Yeast peptone raffinose

Bibliography

Afkarian, M., Bhasin, M., Dillon, S. T., Guerrero, M. C., Nelson, R. G., Knowler, W. C.,Thadhani, R., & Libermann, T. A. (2010). Optimizing a proteomics platform for urine biomarker discovery. *Molecular & Cellular Proteomics : MCP*, *9* (10), 2195–204.

Aldea, M. (2007). Control of Cell Cycle and Cell Growth by Molecular Chaperones. *Cell Cycle*, *6* (21), 2599–2603.

Angeli, D., Ferrell, J. E., & Sontag, E. D. (2004). Detection of multistability, bifurcations, and hysteresis in a large class of biological positive-feedback systems. *Proceedings of the National Academy of Sciences of the United States of America*, *101* (7), 1822–7.

Archambault, V., Chang, E. J., Drapkin, B. J., Cross, F. R., Chait, B. T., & Rout, M. P. (2004). Targeted proteomic study of the cyclin-Cdk module. *Molecular Cell*, *14* (6), 699–711.

Bai, C., Sen, P., Hofmann, K., Ma, L., Goebl, M., Harper, J. W., & Elledge, S. J. (1996). SKP1 connects cell cycle regulators to the ubiquitin proteolysis machinery through a novel motif, the F-box. *Cell*, *86* (2), 263–74.

Barberis, M., De Gioia, L., Ruzzene, M., Sarno, S., Coccetti, P., Fantucci, P., Vanoni, M., & Alberghina, L. (2005). The yeast cyclin-dependent kinase inhibitor Sic1 and mammalian p27Kip1 are functional homologues with a structurally conserved inhibitory domain. *The Biochemical Journal*, *387* (Pt 3), 639–647.

Bardwell, L., Cook, J. G., Zhu-Shimoni, J. X., Voora, D., & Thorner, J. (1998). Differential regulation of transcription: repression by unactivated mitogen-activated protein kinase Kss1 requires the Dig1 and Dig2 proteins. *Proceedings of the National Academy of Sciences of the United States of America*, *95* (26), 15400–5.

Baroni, M. D., Martegani, E., Monti, P., & Alberghina, L. (1989). Cell size modulation by CDC25 and RAS2 genes in Saccharomyces cerevisiae. *Molecular and Cellular Biology*, *9* (6), 2715–2723.

Barral, Y., Jentsch, S., & Mann, C. (1995). G1 cyclin turnover and nutrient uptake are controlled by a common pathway in yeast. *Genes & Development*, *9* (4), 399–409.

Baserga, R. (2007). Is cell size important? *Cell Cycle*, *6* (7):814-6.

Berry, D. B., & Gasch, A. P. (2008). Stress-activated genomic expression changes serve a preparative role for impending stress in yeast. *Molecular Biology of the Cell*, *19* (11), 4580–4587.

Bertoli, C., Skotheim, J. M., & de Bruin, R. a M. (2013). Control of cell cycle transcription during G1 and S phases. *Nature Reviews. Molecular Cell Biology*, *14* (8), 518–28.

Blondel, M., Galan, J. M., Chi, Y., Lafourcade, C., Longaretti, C., Deshaies, R. J., & Peter, M. (2000). Nuclear-specific degradation of Far1 is controlled by the localization of the F-box protein Cdc4. *The EMBO Journal*, *19* (22), 6085–97.

Booher, R. N., Deshaies, R. J., & Kirschner, M. W. (1993). Properties of Saccharomyces cerevisiae wee1 and its differential regulation of p34CDC28 in response to G1 and G2 cyclins. *The EMBO Journal*, *12* (9), 3417–26.

Booher, R. N., Holman, P. S., & Fattaey, A. (1997). Human Myt1 is a cell cycle-regulated kinase that inhibits Cdc2 but not Cdk2 activity. *The Journal of Biological Chemistry*, *272* (35), 22300–6.

Borg, M., Mittag, T., Pawson, T., Tyers, M., Forman-Kay, J. D., & Chan, H. S. (2007). Polyelectrostatic interactions of disordered ligands suggest a physical basis for ultrasensitivity. *Proceedings of the National Academy of Sciences of the United States of America*, *104* (23), 9650–5.

Boros, J., Lim, F.-L., Darieva, Z., Pic-Taylor, A., Harman, R., Morgan, B. A., & Sharrocks, A. D. (2003). Molecular determinants of the cell-cycle regulated Mcm1p-Fkh2p transcription factor complex. *Nucleic Acids Research*, *31* (9), 2279–88.

Bourne, Y., Watson, M. H., Hickey, M. J., Holmes, W., Rocque, W., Reed, S. I., & Tainer, J. A. (1996). Crystal structure and mutational analysis of the human CDK2 kinase complex with cell cycle-regulatory protein CksHs1. *Cell*, *84* (6), 863–874.

Breitkreutz, A., Boucher, L., Breitkreutz, B.-J., Sultan, M., Jurisica, I., & Tyers, M. (2003). Phenotypic and transcriptional plasticity directed by a yeast mitogen-activated protein kinase network. *Genetics*, *165* (3), 997–1015.

Breitkreutz, A., Choi, H., Sharom, J. R., Boucher, L., Neduva, V., Larsen, B., Lin, Z. Y., Breitkreutz, B. J., Stark, C., Liu G., Ahn, J., Dewar-Darch, D., Reguly, T., Tang, X., Almeida, R., Qin, Z.S., Pawson, T., Gingras, A.C., Nesvizhskii, A.I.,& Tyers, M. (2010). A global protein kinase and phosphatase interaction network in yeast. *Science (New York, N.Y.)*, *328* (5981), 1043–1046.

Brocca, S., Samalíková, M., Uversky, V. N., Lotti, M., Vanoni, M., Alberghina, L., & Grandori, R. (2009). Order propensity of an intrinsically disordered protein, the cyclin-dependent-kinase inhibitor Sic1. *Proteins*, *76* (3), 731–46.

Brown, N. R., Noble, M. E., Endicott, J. A., & Johnson, L. N. (1999). The structural basis for specificity of substrate and recruitment peptides for cyclin-dependent kinases. *Nature Cell Biology*, *1* (7), 438–443.

Buchan, J. R., Muhlrad, D., & Parker, R. (2008). P bodies promote stress granule assembly in Saccharomyces cerevisiae. *Journal of Cell Biology*, *183* (3), 441–455.

Buchan, J. R., & Parker, R. (2009). Eukaryotic Stress Granules : The Ins and Out of Translation. *Mol Cell*, *36* (6).

Byrne, K. P., & Wolfe, K. H. (2005). The Yeast Gene Order Browser: Combining curated homology and syntenic context reveals gene fate in polyploid species. *Genome Research*, *15* (10), 1456–1461.

Cai, Y., & Futcher, B. (2013). Effects of the yeast RNA-binding protein Whi3 on the half-life and abundance of CLN3 mRNA and other targets. *PLoS ONE*, *8* (12).

Cannon, J. F., & Tatchell, K. (1987). Characterization of Saccharomyces cerevisiae genes encoding subunits of cyclic AMP-dependent protein kinase. *Molecular and Cellular Biology*, *7* (8), 2653–63.

Caplan, A. J., Cyr, D. M., & Douglas, M. G. (1992). YDJ1p facilitates polypeptide translocation across different intracellular membranes by a conserved mechanism. *Cell*, *71* (7), 1143–1155.

Chan, F. K., Zhang, J., Cheng, L., Shapiro, D. N., & Winoto, A. (1995). Identification of human and mouse p19, a novel CDK4 and CDK6 inhibitor with homology to p16ink4. *Molecular and Cellular Biology*, *15* (5), 2682–8.

Charvin, G., Oikonomou, C., Siggia, E. D., & Cross, F. R. (2010). Origin of irreversibility of cell cycle start in budding yeast. *PLoS Biology*, *8* (1).

Chen, J., Jackson, P. K., Kirschner, M. W., & Dutta, A. (1995). Separate domains of p21 involved in the inhibition of Cdk kinase and PCNA. *Nature*, *374* (6520), 386–8.

Chen, J., Saha, P., Kornbluth, S., Dynlacht, B. D., & Dutta, A. (1996). Cyclin-binding motifs are essential for the function of p21CIP1. *Molecular and Cellular Biology*, *16* (9), 4673–82.

Cho, R. J., Campbell, M. J., Winzeler, E. A., Steinmetz, L., Conway, A., Wodicka, L., Wolfsberg, T. G., Gabrielian, A. E., Landsman, D., Lockhart, D.J., & Davis, R. W. (1998). A genome-wide transcriptional analysis of the mitotic cell cycle. *Molecular Cell*, *2* (1), 65–73.

Cohen-Fix, O., Peters, J. M., Kirschner, M. W., & Koshland, D. (1996). Anaphase initiation in Saccharomyces cerevisiae is controlled by the APC-dependent degradation of the anaphase inhibitor Pds1p. *Genes & Development*, *10* (24), 3081–93.

Collins, S. R., Kemmeren, P., Zhao, X.-C., Greenblatt, J. F., Spencer, F., Holstege, F. C. P., Weissman, J. S., & Krogan, N. J. (2007). Toward a comprehensive atlas of the physical interactome of Saccharomyces cerevisiae. *Molecular & Cellular Proteomics : MCP*, *6* (3), 439–50.

Colomina, N., Ferrezuelo, F., Wang, H., Aldea, M., & Garí, E. (2008). Whi3, a developmental regulator of budding yeast, binds a large set of mRNAs functionally related to the endoplasmic reticulum. *The Journal of Biological Chemistry*, *283* (42), 28670–28679.

Cook, M., & Tyers, M. (2007). Size control goes global. *Current Opinion in Biotechnology*, *18* (4):341-50.

Cooper, S. (2004). Control and maintenance of mammalian cell size. *BMC Cell Biology*, *5* (1), 35.

Costanzo, M., Nishikawa, J. L., Tang, X., Millman, J. S., Schub, O., Breitkreuz, K., Dewar, D., Rupes, I., Andrews, B., & Tyers, M. (2004). CDK activity antagonizes Whi5, an inhibitor of G1/S transcription in yeast. *Cell*, *117* (7), 899–913.

Coudreuse, D., & Nurse, P. (2010). Driving the cell cycle with a minimal CDK control network. *Nature*, *468* (7327), 1074–1079.

Craig, K. L., & Tyers, M. (1999). The F-box: A new motif for ubiquitin dependent proteolysis in cell cycle regulation and signal transduction. *Progress in Biophysics and Molecular Biology*.

Cross, F. R. (1988). DAF1, a mutant gene affecting size control, pheromone arrest, and cell cycle kinetics of Saccharomyces cerevisiae. *Molecular and Cellular Biology*, *8* (11), 4675–4684.

Cross, F. R., & Tinkelenberg, A. H. (1991). A potential positive feedback loop controlling CLN1 and CLN2 gene expression at the start of the yeast cell cycle. *Cell*, *65* (5), 875–883.

Darieva, Z., Bulmer, R., Pic-Taylor, A., Doris, K. S., Geymonat, M., Sedgwick, S. G., Morgan, B. A., & Sharrocks, A. D. (2006). Polo kinase controls cell-cycle-dependent transcription by targeting a coactivator protein. *Nature*, *444* (7118), 494–8.

Darieva, Z., Han, N., Warwood, S., Doris, K. S., Morgan, B. A., & Sharrocks, A. D. (2012). Protein kinase C regulates late cell cycle-dependent gene expression. *Molecular and Cellular Biology*, *32* (22), 4651–61.

De Bruin, R. A. M., McDonald, W. H., Kalashnikova, T. I., Yates, J., & Wittenberg, C. (2004). Cln3 activates G1-specific transcription via phosphorylation of the SBF bound repressor Whi5. *Cell*, *117* (7), 887–898.

DeSalle, L. M., & Pagano, M. (2001). Regulation of the G1 to S transition by the ubiquitin pathway. *FEBS Letters*, *490* (3), 179–89.

Desany, B. A., Alcasabas, A. A., Bachant, J. B., & Elledge, S. J. (1998). Recovery from DNA replicational stress is the essential function of the S-phase checkpoint pathway. *Genes and Development*, *12* (18), 2956–2970.

Deshaies, R. J. (1999). SCF and Cullin/Ring H2-based ubiquitin ligases. *Annual Review of Cell and Developmental Biology*, *15*, 435–67.

Deshaies, R. J., & Ferrell, J. E. (2001). Multisite phosphorylation and the countdown to S phase. *Cell*, *107* (7), 819–22.

Di Talia, S., Skotheim, J. M., Bean, J. M., Siggia, E. D., & Cross, F. R. (2007). The effects of molecular noise and size control on variability in the budding yeast cell cycle. *Nature*, *448* (7156), 947–951.

Diehl, J. A., Yang, W., Rimerman, R. A., Xiao, H., & Emili, A. (2003). Hsc70 regulates accumulation of cyclin D1 and cyclin D1-dependent protein kinase. *Molecular and Cellular Biology*, *23* (5), 1764–1774.

Dirick, L., Böhm, T., & Nasmyth, K. (1995). Roles and regulation of Cln-Cdc28 kinases at the start of the cell cycle of Saccharomyces cerevisiae. *The EMBO Journal*, *14* (19), 4803–4813.

Dirick, L., & Nasmyth, K. (1991). Positive feedback in the activation of G1 cyclins in yeast. *Nature*, *351* (6329), 754–757.

Dohrmann, P. R., Voth, W. P., & Stillman, D. J. (1996). Role of negative regulation in promoter specificity of the homologous transcriptional activators Ace2p and Swi5p. *Molecular and Cellular Biology*, *16* (4), 1746–58.

Donachie, W. D., & Blakely, G. W. (2003). Coupling the initiation of chromosome replication to cell size in *Escherichia coli*. *Current Opinion in Microbiology*, *6* (2):146-50.

Drury, L. S., Perkins, G., & Diffley, J. F. (1997). The Cdc4/34/53 pathway targets Cdc6p for proteolysis in budding yeast. *The EMBO Journal*, *16* (19), 5966–76.

Dulić, V., Kaufmann, W. K., Wilson, S. J., Tlsty, T. D., Lees, E., Harper, J. W., Elledge, S. J., & Reed, S. I. (1994). p53-dependent inhibition of cyclin-dependent kinase activities in human fibroblasts during radiation-induced G1 arrest. *Cell*, *76* (6), 1013–1023.

Dumont, J. N. (1972). Oogenesis in Xenopus laevis (Daudin). I. Stages of oocyte development in laboratory maintained animals. *Journal of Morphology*, *136* (2), 153–179.

Edgington, N. P., & Futcher, B. (2001). Relationship between the function and the location of G1 cyclins in S. cerevisiae. *Journal of Cell Science*, *114* (Pt 24), 4599–4611.

el-Deiry, W. S., Tokino, T., Velculescu, V. E., Levy, D. B., Parsons, R., Trent, J. M., Lin, D., Mercer, W. E., Kinzler, K. W., & Vogelstein, B. (1993). WAF1, a potential mediator of p53 tumor suppression. *Cell*, *75* (4), 817–25.

Espinoza, F. H., Farrell, A., Erdjument-Bromage, H., Tempst, P., & Morgan, D. O. (1996). A cyclin-dependent kinase-activating kinase (CAK) in budding yeast unrelated to vertebrate CAK. *Science (New York, N.Y.)*, *273* (5282), 1714–1717.

Fattaey, A., & Booher, R. N. (1997). Myt1: a Wee1-type kinase that phosphorylates Cdc2 on residue Thr14. *Progress in Cell Cycle Research*, *3*, 233–40.

Feldman, R. M., Correll, C. C., Kaplan, K. B., & Deshaies, R. J. (1997). A complex of Cdc4p, Skp1p, and Cdc53p/cullin catalyzes ubiquitination of the phosphorylated CDK inhibitor Sic1p. *Cell*, *91* (2), 221–30.

Ferrell, J. E. (2002). Self-perpetuating states in signal transduction: Positive feedback, double-negative feedback and bistability. *Current Opinion in Cell Biology*, *14* (2):140-8.

Ferrezuelo, F., Colomina, N., Palmisano, A., Garí, E., Gallego, C., Csikász-Nagy, A., & Aldea, M. (2012). The critical size is set at a single-cell level by growth rate to attain homeostasis and adaptation. *Nature Communications*.

Forsburg, S., & Nurse, P. (1991). Cell Cycle Regulation in the Yeasts Saccharomyces Cerevisiae and Schizosaccharomyces Pombe. *Annual Reviews in Cell Biology*.

Fujimura, K., Kano, F., & Murata, M. (2008). Identification of PCBP2, a facilitator of IRES-mediated translation, as a novel constituent of stress granules and processing bodies. *RNA (New York, N.Y.)*, *14* (3), 425–431.

Futcher, B. (2002). Transcriptional regulatory networks and the yeast cell cycle. *Current Opinion in Cell Biology*, 14 (6):676-83.

Gallego, C., Garí, E., Colomina, N., Herrero, E., & Aldea, M. (1997). The Cln3 cyclin is down-regulated by translational repression and degradation during the G1 arrest caused by nitrogen deprivation in budding yeast. *The EMBO Journal*, *16* (23), 7196–7206.

Garí, E., Volpe, T., Wang, H., Gallego, C., Futcher, B., & Aldea, M. (2001). Whi3 binds the mRNA of the G1 cyclin CLN3 to modulate cell fate in budding yeast. *Genes & Development*, *15* (21), 2803–2808.

Gasch, A. P., Spellman, P. T., Kao, C. M., Carmel-Harel, O., Eisen, M. B., Storz, G., Botstein, D., & Brown, P. O. (2000). Genomic expression programs in the response of yeast cells to environmental changes. *Molecular Biology of the Cell*, *11* (12), 4241–4257.

Gavin, A.-C., Aloy, P., Grandi, P., Krause, R., Boesche, M., Marzioch, M., Rau, C., Jensen, L. J., Bastuck, S., Dümpelfeld, B., Edelmann, A., Heurtier, M. A., Hoffman, V., Hoefert, C., Klein, K., Hudak, M., Michon, A. M., Schelder, M., Schirle, M., Remor, M., Rudi, T., Hooper, S., Bauer, A., Bouwmeester, T., Casari, G., Drewes, G., Neubauer, G., Rick, J. M., Kuster, B., Bork, P., Russell, R. B., & Superti-Furga, G. (2006). Proteome survey reveals modularity of the yeast cell machinery. *Nature*, *440* (7084), 631–6.

Gavin, A.-C., Bösche, M., Krause, R., Grandi, P., Marzioch, M., Bauer, A., Schultz, J., Rick, J. M., Michon, A. M., Cruciat, C. M., Remor, M., Höfert, C., Schelder, M., Brajenovic, M., Ruffner, H., Merino, A., Klein, K., Hudak, M., Dickson, D., Rudi, T., Gnau, V., Bauch, A., Bastuck, S., Huhse, B., Leutwein, C., Heurtier, M. A., Copley, R. R., Edelmann, A, Querfurth, E., Rybin, V., Drewes, G., Raida, M., Bouwmeester, T., Bork, P., Seraphin, B., Kuster, B., Neubauer, G., & Superti-Furga, G. (2002). Functional organization of the yeast proteome by systematic analysis of protein complexes. *Nature*, *415* (6868), 141–7.

Ghiara, J. B., Richardson, H. E., Sugimoto, K., Henze, M., Lew, D. J., Wittenberg, C., & Reed, S. I. (1991). A cyclin B homolog in S. cerevisiae: chronic activation of the Cdc28 protein kinase by cyclin prevents exit from mitosis. *Cell*, *65* (1), 163–74.

Gilks, N., Kedersha, N., Ayodele, M., Shen, L., Stoecklin, G., Dember, L. M., & Anderson, P. (2004). Stress granule assembly is mediated by prion-like aggregation of TIA-1. *Molecular Biology of the Cell*, *15* (12), 5383–5398.

Goebl, M. G., Yochem, J., Jentsch, S., McGrath, J. P., Varshavsky, A., & Byers, B. (1988). The yeast cell cycle gene CDC34 encodes a ubiquitin-conjugating enzyme. *Science (New York, N.Y.)*, *241* (4871), 1331–5.

Gordon, D. M., & Roof, D. M. (2001). Degradation of the kinesin Kip1p at anaphase onset is mediated by the anaphase-promoting complex and Cdc20p. *Proceedings of the National Academy of Sciences of the United States of America*, *98* (22), 12515–20.

Grebien, F., Dolznig, H., Beug, H., & Mullner, E. W. (2005). Cell size control: new evidence for a general mechanism. *Cell Cycle (Georgetown, Tex.)*, *4* (3), 418–421.

Gu, W., Deng, Y., Zenklusen, D., & Singer, R. H. (2004). A new yeast PUF family protein, Puf6p, represses ASH1 mRNA translation and is required for its localization. *Genes and Development*, *18* (12), 1452–1465.

Gu, Y., Turck, C. W., & Morgan, D. O. (1993). Inhibition of CDK2 activity in vivo by an associated 20K regulatory subunit. *Nature*, *366* (6456), 707–10.

Guan, K. L., Jenkins, C. W., Li, Y., Nichols, M. A., Wu, X., O'Keefe, C. L., Matera, A. G., & Xiong, Y. (1994). Growth suppression by p18, a p16INK4/MTS1- and p14INK4B/MTS2-related CDK6 inhibitor, correlates with wild-type pRb function. *Genes & Development*, *8* (24), 2939–52.

Haim, L., Zipor, G., Aronov, S., & Gerst, J. E. (2007). A genomic integration method to visualize localization of endogenous mRNAs in living yeast. *Nature Methods*, *4* (5), 409–412.

Hall, D. D., Markwardt, D. D., Parviz, F., & Heideman, W. (1998). Regulation of the Cln3-Cdc28 kinase by cAMP in Saccharomyces cerevisiae. *EMBO Journal*, *17* (15), 4370–4378.

Hannon, G. J., & Beach, D. (1994). p15INK4B is a potential effector of TGF-beta-induced cell cycle arrest. *Nature*, *371* (6494), 257–61.

Harper, J. W. (2001). Protein destruction: Adapting roles for Cks proteins. *Current Biology*, *11* (11).

Harper, J. W. (2002). A phosphorylation-driven ubiquitination switch for cell-cycle control. *Trends in Cell Biology*, *12* (3), 104–7.

Harper, J. W., Adami, G. R., Wei, N., Keyomarsi, K., & Elledge, S. J. (1993). The p21 Cdk-interacting protein Cip1 is a potent inhibitor of G1 cyclin-dependent kinases. *Cell*, *75* (4), 805–816.

Hartwell, L. H., Culotti, J., Pringle, J. R., & Reid, B. J. (1973). Genetic Control of the Cell Division Cycle in Yeast. *Science*, *183* (4120), 46–51.

Hartwell, L. H., & Unger, M. W. (1977). Unequal division in Saccharomyces cerevisiae and its implications for the control of cell division. *The Journal of Cell Biology*, *75* (2 Pt 1), 422–435.

Heald, R., McLoughlin, M., & McKeon, F. (1993). Human wee1 maintains mitotic timing by protecting the nucleus from cytoplasmically activated Cdc2 kinase. *Cell*, *74* (3), 463–74.

Henchoz, S., Chi, Y., Catarin, B., Herskowitz, I., Deshaies, R. J., & Peter, M. (1997). Phosphorylation- and ubiquitin-dependent degradation of the cyclin-dependent kinase inhibitor Far1p in budding yeast. *Genes & Development*, *11* (22), 3046–60.

Hershko, A., & Ciechanover, A. (1998). The ubiquitin system. *Annual Review of Biochemistry*, *67*, 425–79.

Hirai, H., Roussel, M. F., Kato, J. Y., Ashmun, R. A., & Sherr, C. J. (1995). Novel INK4 proteins, p19 and p18, are specific inhibitors of the cyclin D-dependent kinases CDK4 and CDK6. *Molecular and Cellular Biology*, *15* (5), 2672–81.

Ho, Y., Gruhler, A., Heilbut, A., Bader, G. D., Moore, L., Adams, S.-L., Millar, A., Taylor, P., Bennett, K., Boutilier, K., Yang, L., Wolting, C., Donaldson, I., Schandorff, S., Shewnarane, J., Vo, M., Taggart, J., Goudreault, M., Muskat, B., Alfarano, C., Dewar, D., Lin, Z., Michalickova, K., Willems, A. R., Sassi, H., Nielsen, P. A., Rasmussen, K. J., Andersen, J. R., Johansen, L. E., Hansen, L. H., Jespersen, H., Podtelejnikov, A., Nielsen, E., Crawford, J., Poulsen, V., Sørensen, B. D., Matthiesen, J., Hendrickson, R. C., Gleeson, F., Pawson, T., Moran, M. F., Durocher, D., Mann, M., Hogue, C. W., Figeys, D., & Tyers, M. (2002). Systematic identification of protein complexes in Saccharomyces cerevisiae by mass spectrometry. *Nature*, *415* (6868), 180–183.

Hoffmann, I., Clarke, P. R., Marcote, M. J., Karsenti, E., & Draetta, G. (1993). Phosphorylation and activation of human cdc25-C by cdc2--cyclin B and its involvement in the self-amplification of MPF at mitosis. *The EMBO Journal*, *12* (1), 53–63.

Hollenhorst, P. C., Pietz, G., & Fox, C. A. (2001). Mechanisms controlling differential promoter-occupancy by the yeast forkhead proteins Fkh1p and Fkh2p: implications for regulating the cell cycle and differentiation. *Genes & Development*, *15* (18), 2445–56.

Holmes, K. J., Klass, D. M., Guiney, E. L., & Cyert, M. S. (2013). Whi3, an S. cerevisiae RNA-binding protein, is a component of stress granules that regulates levels of its target mRNAS. *PLoS ONE*, *8* (12).

Horak, C. E., Luscombe, N. M., Qian, J., Bertone, P., Piccirrillo, S., Gerstein, M., & Snyder, M. (2002). Complex transcriptional circuitry at the G1/S transition in Saccharomyces cerevisiae. *Genes & Development*, *16* (23), 3017–33.

Huang, J., Zhu, H., Haggarty, S. J., Spring, D. R., Hwang, H., Jin, F., Snyder, M., & Schreiber, S. L. (2004). Finding new components of the target of rapamycin (TOR) signaling network through chemical genetics and proteome chips. *Proceedings of the National Academy of Sciences of the United States of America*, *101* (47), 16594–16599.

Jackson, L. P., Reed, S. I., & Haase, S. B. (2006). Distinct mechanisms control the stability of the related S-phase cyclins Clb5 and Clb6. *Molecular and Cellular Biology*, *26* (6), 2456–66.

Janke, C., Magiera, M. M., Rathfelder, N., Taxis, C., Reber, S., Maekawa, H., Moreno-Borchart, A., Doenges, G., Schwob, E., Schiebel, E., & Knop, M. (2004). A versatile toolbox for PCR-based tagging of yeast genes: New fluorescent proteins, more markers and promoter substitution cassettes. *Yeast*, *21* (11), 947–962.

Jaspersen, S. L., Charles, J. F., & Morgan, D. O. (1999). Inhibitory phosphorylation of the APC regulator Hct1 is controlled by the kinase Cdc28 and the phosphatase Cdc14. *Current Biology : CB*, *9* (5), 227–36.

Johnson, L. N., De Moliner, E., Brown, N. R., Song, H., Barford, D., Endicott, J. A., & Noble, M. E. M. (2002). Structural studies with inhibitors of the cell cycle regulatory kinase cyclin-dependent protein kinase 2. In *Pharmacology and Therapeutics* (Vol. 93, pp. 113–124).

Johnston, G. C., Pringle, J. R., & Hartwell, L. H. (1977). Coordination of growth with cell division in the yeast Saccharomyces cerevisiae. *Experimental Cell Research*, *105* (1), 79–98.

Jorgensen, P., Nishikawa, J. L., Breitkreutz, B.-J., & Tyers, M. (2002). Systematic identification of pathways that couple cell growth and division in yeast. *Science*, *297* (5580), 395–400.

Jorgensen, P., Rupes, I., Sharom, J. R., Schneper, L., Broach, J. R., & Tyers, M. (2004). A dynamic transcriptional network communicates growth potential to ribosome synthesis and critical cell size. *Genes & Development*, *18* (20), 2491–2505.

Jorgensen, P., & Tyers, M. (2004). How cells coordinate growth and division. *Current Biology*, 14 (23):R1014-27.

Juang, Y. L., Huang, J., Peters, J. M., McLaughlin, M. E., Tai, C. Y., & Pellman, D. (1997). APC-mediated proteolysis of Ase1 and the morphogenesis of the mitotic spindle. *Science (New York, N.Y.)*, *275* (5304), 1311–4.

Kaiser, P., Sia, R. A., Bardes, E. G., Lew, D. J., & Reed, S. I. (1998). Cdc34 and the F-box protein Met30 are required for degradation of the Cdk-inhibitory kinase Swe1. *Genes & Development*, *12* (16), 2587–97.

Kaldis, P. (1999). The cdk-activating kinase (CAK): From yeast to mammals. *Cellular and Molecular Life Sciences*, 55 (2):284-96.

Kaldis, P., Pitluk, Z. W., Bany, I. A., Enke, D. A., Wagner, M., Winter, E., & Solomon, M. J. (1998). Localization and regulation of the cdk-activating kinase (Cak1p) from budding yeast. *Journal of Cell Science*, 111 (Pt 24):3585-96.

Kim, S. Y., & Ferrell, J. E. (2007). Substrate competition as a source of µltrasensitivity in the inactivation of Wee1. *Cell*, *128* (6), 1133–45.

King, K., Kang, H., Jin, M., & Lew, D. J. (2013). Feedback control of Swe1p degradation in the yeast morphogenesis checkpoint. *Molecular Biology of the Cell*, *24* (7), 914–22.

Koch, C., Moll, T., Neuberg, M., Ahorn, H., & Nasmyth, K. (1993). A role for the transcription factors Mbp1 and Swi4 in progression from G1 to S phase. *Science (New York, N.Y.)*, *261* (5128), 1551–7.

Koepp, D. M., Harper, J. W., & Elledge, S. J. (1999). How the cyclin became a cyclin: regulated proteolysis in the cell cycle. *Cell*, *97* (4), 431–4.

Kõivomägi, M., Örd, M., Iofik, A., Valk, E., Venta, R., Faustova, I., Kivi, R., Balog, E. R. M., Rubin, S. M., & Loog, M. (2013). Multisite phosphorylation networks as signal processors for Cdk1. *Nature Structural & Molecular Biology*, *20* (12), 1415–1424.

Kõivomägi, M., Valk, E., Venta, R., Iofik, A., Lepiku, M., Balog, E. R. M., Rubin, S. M., Morgan, D. O., & Loog, M. (2011). Cascades of multisite phosphorylation control Sic1 destruction at the onset of S phase. *Nature*. 480 (7375):128-31.

Koranda, M., Schleiffer, A., Endler, L., & Ammerer, G. (2000). Forkhead-like transcription factors recruit Ndd1 to the chromatin of G2/M-specific promoters. *Nature*, *406* (6791), 94–8.

Kreegipuu, A., Blom, N., & Brunak, S. (1999). PhosphoBase, a database of phosphorylation sites: Release 2.0. *Nucleic Acids Research*, 27 (1):237-9.

Kumagai, A., & Dunphy, W. G. (1992). Regulation of the cdc25 protein during the cell cycle in Xenopus extracts. *Cell*, *70* (1), 139–51.

Kumar, A., Agarwal, S., Heyman, J. A., Matson, S., Heidtman, M., Piccirillo, S., Umansky, L., Drawid, A., Jansen, R., Liu, Y., Cheung, K. H., Miller, P., Gerstein, M., Roeder, G. S., & Snyder, M. (2002). Subcellular localization of the yeast proteome. *Genes and Development*, *16* (6), 707–719.

Kumar, R., Reynolds, D. M., Shevchenko, A., Goldstone, S. D., & Dalton, S. (2000). Forkhead transcription factors, Fkh1p and Fkh2p, collaborate with Mcm1p to control transcription required for M-phase. *Current Biology : CB*, *10* (15), 896–906.

Kusari, A. B., Molina, D. M., Sabbagh, W., Lau, C. S., & Bardwell, L. (2004). A conserved protein interaction network involving the yeast MAP kinases Fus3 and Kss1. *The Journal of Cell Biology*, *164* (2), 267–77.

Kwon, S., Zhang, Y., & Matthias, P. (2007). The deacetylase HDAC6 is a novel critical component of stress granules involved in the stress response. *Genes and Development*, *21* (24), 3381–3394.

Labib, K., & Moreno, S. (1996). rum1: a CDK inhibitor regulating G1 progression in fission yeast. *Trends in Cell Biology*, *6* (2), 62–6.

Lee, M. H., Reynisdóttir, I., & Massagué, J. (1995). Cloning of p57KIP2, a cyclin-dependent kinase inhibitor with unique domain structure and tissue distribution. *Genes & Development*, *9* (6), 639–49.

Lim, H. H., Goh, P. Y., & Surana, U. (1996). Spindle pole body separation in Saccharomyces cerevisiae requires dephosphorylation of the tyrosine 19 residue of Cdc28. *Molecular and Cellular Biology*, *16* (11), 6385–97.

Lin, J., Reichner, C., Wu, X., & Levine, A. J. (1996). Analysis of wild-type and mutant p21WAF-1 gene activities. *Molecular and Cellular Biology*, *16* (4), 1786–93.

Linding, R., Russell, R. B., Neduva, V., & Gibson, T. J. (2003). GlobPlot: Exploring protein sequences for globularity and disorder. *Nucleic Acids Research*, *31* (13), 3701–3708.

Liu, F., Stanton, J. J., Wu, Z., & Piwnica-Worms, H. (1997). The human Myt1 kinase preferentially phosphorylates Cdc2 on threonine 14 and localizes to the endoplasmic reticulum and Golgi complex. *Molecular and Cellular Biology*, *17* (2), 571–83.

Lolli, G., & Johnson, L. N. (2005). CAK-Cyclin-dependent Activating Kinase: a key kinase in cell cycle control and a target for drugs? *Cell Cycle (Georgetown, Tex.)*, *4* (4), 572–7.

Lord, P. G., & Wheals, A. E. (1981). Variability in individual cell cycles of Saccharomyces cerevisiae. *Journal of Cell Science*, *50*, 361–376.

Loschi, M., Leishman, C. C., Berardone, N., & Boccaccio, G. L. (2009). Dynein and kinesin regulate stress-granule and P-body dynamics. *Journal of Cell Science*, *122* (Pt 21), 3973–3982.

Louvion, J. F., Havaux-Copf, B., & Picard, D. (1993). Fusion of GAL4-VP16 to a steroid-binding domain provides a tool for gratuitous induction of galactose-responsive genes in yeast. *Gene, 131* (1), 129-34.

Loy, C. J., Lydall, D., & Surana, U. (1999). NDD1, a high-dosage suppressor of cdc28-1N, is essential for expression of a subset of late-S-phase-specific genes in Saccharomyces cerevisiae. *Molecular and Cellular Biology*, *19* (5), 3312–27.

Lydall, D., Ammerer, G., & Nasmyth, K. (1991). A new role for MCM1 in yeast: cell cycle regulation of SW15 transcription. *Genes & Development*, *5* (12B), 2405–19.

Mathias, N., Johnson, S. L., Winey, M., Adams, A. E., Goetsch, L., Pringle, J. R., Byers, B., & Goebl, M. G. (1996). Cdc53p acts in concert with Cdc4p and Cdc34p to control the G1-to-S-phase transition and identifies a conserved family of proteins. *Molecular and Cellular Biology*, *16* (12), 6634–43.

Matsuoka, S., Edwards, M. C., Bai, C., Parker, S., Zhang, P., Baldini, A., Harper, J. W., & Elledge, S. J. (1995). p57KIP2, a structurally distinct member of the p21CIP1 Cdk inhibitor family, is a candidate tumor suppressor gene. *Genes & Development*, *9* (6), 650–62.

McBride, H. J., Yu, Y., & Stillman, D. J. (1999). Distinct regions of the Swi5 and Ace2 transcription factors are required for specific gene activation. *The Journal of Biological Chemistry*, *274* (30), 21029–36.

McGowan, C. H., & Russell, P. (1993). Human Wee1 kinase inhibits cell division by phosphorylating p34cdc2 exclusively on Tyr15. *The EMBO Journal*, *12* (1), 75–85.

McGowan, C. H., & Russell, P. (1995). Cell cycle regulation of human WEE1. *The EMBO Journal*, *14* (10), 2166–75.

McInerny, C. J., Partridge, J. F., Mikesell, G. E., Creemer, D. P., & Breeden, L. L. (1997). A novel Mcm1-dependent element in the SWI4, CLN3, CDC6, and CDC47 promoters activates M/G1-specific transcription. *Genes & Development*, *11* (10), 1277–88.

Mendenhall, M. D. (1993). An inhibitor of p34CDC28 protein kinase activity from Saccharomyces cerevisiae. *Science (New York, N.Y.)*, *259* (5092), 216–9.

Mendenhall, M. D., al-Jumaily, W., & Nugroho, T. T. (1995). The Cdc28 inhibitor p40SIC1. *Progress in Cell Cycle Research*, *1*, 173–85.

Mendenhall, M. D., & Hodge, A. E. (1998). Regulation of Cdc28 cyclin-dependent protein kinase activity during the cell cycle of the yeast Saccharomyces cerevisiae. *Microbiology and Molecular Biology Reviews : MMBR*, *62* (4), 1191–1243.

Millar, J. B., McGowan, C. H., Lenaers, G., Jones, R., & Russell, P. (1991). p80cdc25 mitotic inducer is the tyrosine phosphatase that activates p34cdc2 kinase in fission yeast. *The EMBO Journal*, *10* (13), 4301–9.

Miller, M. E., & Cross, F. R. (2001). Mechanisms controlling subcellular localization of the G (1) cyclins Cln2p and Cln3p in budding yeast. *Molecular and Cellular Biology*, *21* (18), 6292–6311.

Mitchison, J. M. (2003). Growth during the cell cycle. *International Review of Cytology*, 226:165-258.

Mizunuma, M., Tsubakiyama, R., Ogawa, T., Shitamukai, A., Kobayashi, Y., Inai, T., Kume, K., & Hirata, D. (2013). Ras/cAMP-dependent protein kinase (PKA) regulates multiple aspects of cellular events by phosphorylating the Whi3 cell cycle regulator in budding yeast. *The Journal of Biological Chemistry*, *288* (15), 10558–66.

Mokas, S., Mills, J. R., Garreau, C., Fournier, M.-J., Robert, F., Arya, P., Kaufman, R. J., Pelletier, J., & Mazroui, R. (2009). Uncoupling stress granule assembly and translation initiation inhibition. *Molecular Biology of the Cell*, *20* (11), 2673–2683.

Moreno, S., Labib, K., Correa, J., & Nurse, P. (1994). Regulation of the cell cycle timing of Start in fission yeast by the rum1+ gene. *Journal of Cell Science. Supplement*, *18*, 63–8.

Morgan, D. O. (1997). Cyclin-dependent kinases: engines, clocks, and microprocessors. *Annual Review of Cell and Developmental Biology*, *13*, 261–291.

Morgan, D. O. (2007). *The Cell Cycle Principles and Control* (1st ed.). London: New Science Press Ltd.

MORTIMER, R. K. (1958). Radiobiological and genetic studies on a polyploid series (haploid to hexaploid) of Saccharomyces cerevisiae. *Radiation Research*, *9* (3), 312–326.

Mueller, P. R., Coleman, T. R., & Dunphy, W. G. (1995). Cell cycle regulation of a Xenopus Wee1-like kinase. *Molecular Biology of the Cell*, *6* (1), 119–34.

Mueller, P. R., Coleman, T. R., Kumagai, A., & Dunphy, W. G. (1995). Myt1: a membrane-associated inhibitory kinase that phosphorylates Cdc2 on both threonine-14 and tyrosine-15. *Science (New York, N.Y.)*, *270* (5233), 86–90.

Murakami, H., Aiba, H., Nakanishi, M., & Murakami-Tonami, Y. (2010). Regulation of yeast forkhead transcription factors and FoxM1 by cyclin-dependent and polo-like kinases. *Cell Cycle (Georgetown, Tex.)*, *9* (16), 3233–42.

Nakanishi, M., Robetorye, R. S., Adami, G. R., Pereira-Smith, O. M., & Smith, J. R. (1995). Identification of the active region of the DNA synthesis inhibitory gene p21Sdi1/CIP1/WAF1. *The EMBO Journal*, *14* (3), 555–63.

Nash, P., Tang, X., Orlicky, S., Chen, Q., Gertler, F. B., Mendenhall, M. D., Sicheri, F., Pawson, T., & Tyers, M. (2001). Multisite phosphorylation of a CDK inhibitor sets a threshold for the onset of DNA replication. *Nature*, *414* (6863), 514–521.

Nash, R. S., Volpe, T., & Futcher, B. (2001). Isolation and characterization of WHI3, a size-control gene of Saccharomyces cerevisiae. *Genetics*, *157* (4), 1469–1480.

Nash, R., Tokiwa, G., Anand, S., Erickson, K., & Futcher, A. B. (1988). The WHI1+ gene of Saccharomyces cerevisiae tethers cell division to cell size and is a cyclin homolog. *The EMBO Journal*, *7* (13), 4335–4346.

Nasmyth, K. (1996). At the heart of the budding yeast cell cycle. *Trends in Genetics : TIG*, *12* (10), 405–412.

Nasmyth, K., & Dirick, L. (1991). The role of SWI4 and SWI6 in the activity of G1 cyclins in yeast. *Cell*, *66* (5), 995–1013.

Nasmyth, K., Seddon, A., & Ammerer, G. (1987). Cell cycle regulation of SW15 is required for mother-cell-specific HO transcription in yeast. *Cell*, *49* (4), 549–58.

Noda, A., Ning, Y., Venable, S. F., Pereira-Smith, O. M., & Smith, J. R. (1994). Cloning of senescent cell-derived inhibitors of DNA synthesis using an expression screen. *Experimental Cell Research*, *211* (1), 90–8.

Novak, B., Kapuy, O., Domingo-Sananes, M. R., & Tyson, J. J. (2010). Regulated protein kinases and phosphatases in cell cycle decisions. *Current Opinion in Cell Biology*, 22 (6):801-8.

Nurrish, S. J., & Treisman, R. (1995). DNA binding specificity determinants in MADS-box transcription factors. *Molecular and Cellular Biology*, *15* (8), 4076–85.

Nurse, P. (1975). Genetic control of cell size at cell division in yeast. *Nature*, *256* (5518), 547–551.

Nurse, P. (1990). Universal control mechanism regulating onset of M-phase. *Nature*, *344* (6266), 503–508.

Oehlen, L. J., McKinney, J. D., & Cross, F. R. (1996). Ste12 and Mcm1 regulate cell cycle-dependent transcription of FAR1. *Molecular and Cellular Biology*, *16* (6), 2830–7.

Ohn, T., Kedersha, N., Hickman, T., Tisdale, S., & Anderson, P. (2008). A functional RNAi screen links O-GlcNAc modification of ribosomal proteins to stress granule and processing body assembly. *Nature Cell Biology*, *10* (10), 1224–1231.

Ohta, T., Michel, J. J., Schottelius, A. J., & Xiong, Y. (1999). ROC1, a homolog of APC11, represents a family of cullin partners with an associated ubiquitin ligase activity. *Molecular Cell*, *3* (4), 535–41.

Orlando, D. A., Lin, C. Y., Bernard, A., Wang, J. Y., Socolar, J. E. S., Iversen, E. S., Hartemink, A. J., & Haase, S. B. (2008). Global control of cell-cycle transcription by coupled CDK and network oscillators. *Nature*, *453* (7197), 944–7.

Palmer, A., Gavin, A. C., & Nebreda, A. R. (1998). A link between MAP kinase and p34 (cdc2)/cyclin B during oocyte maturation: p90 (rsk) phosphorylates and inactivates the p34 (cdc2) inhibitory kinase Myt1. *The EMBO Journal*, *17* (17), 5037–47.

Parker, L. L., & Piwnica-Worms, H. (1992). Inactivation of the p34cdc2-cyclin B complex by the human WEE1 tyrosine kinase. *Science (New York, N.Y.)*, *257* (5078), 1955–7.

Parviz, F., & Heideman, W. (1998). Growth-independent regulation of CLN3 mRNA levels by nutrients in Saccharomyces cerevisiae. *Journal of Bacteriology*, *180* (2), 225–230.

Patton, E. E., Willems, A. R., Sa, D., Kuras, L., Thomas, D., Craig, K. L., & Tyers, M. (1998). Cdc53 is a scaffold protein for multiple Cdc34/Skp1/F-box proteincomplexes that regulate cell division and methionine biosynthesis in yeast. *Genes & Development*, *12* (5), 692–705.

Patton, E. E., Willems, A. R., & Tyers, M. (1998). Combinatorial control in ubiquitin-dependent proteolysis: don't Skp the F-box hypothesis. *Trends in Genetics : TIG*, *14* (6), 236–43.

Pesin, J. A., & Orr-Weaver, T. L. (2008). Regulation of APC/C activators in mitosis and meiosis. *Annual Review of Cell and Developmental Biology*, *24*, 475–99.

Peter, M., Gartner, A., Horecka, J., Ammerer, G., & Herskowitz, I. (1993). FAR1 links the signal transduction pathway to the cell cycle machinery in yeast. *Cell*, *73* (4), 747–60.

Peter, M., & Herskowitz, I. (1994). Direct inhibition of the yeast cyclin-dependent kinase Cdc28-Cln by Far1. *Science (New York, N.Y.)*, *265* (5176), 1228–31.

Peters, J.-M. (2006). The anaphase promoting complex/cyclosome: a machine designed to destroy. *Nature Reviews. Molecular Cell Biology*, *7* (9), 644–656.

Petroski, M. D., & Deshaies, R. J. (2003). Context of multiubiquitin chain attachment influences the rate of Sic1 degradation. *Molecular Cell*, *11* (6), 1435–44.

Pic, A., Lim, F. L., Ross, S. J., Veal, E. A., Johnson, A. L., Sultan, M. R., West, A. G., Johnston, L. H., Sharrocks, A. D., & Morgan, B. A. (2000). The forkhead protein Fkh2 is a component of the yeast cell cycle transcription factor SFF. *The EMBO Journal*, *19* (14), 3750–61.

Pic-Taylor, A., Darieva, Z., Morgan, B. A., & Sharrocks, A. D. (2004). Regulation of cell cycle-specific gene expression through cyclin-dependent kinase-mediated phosphorylation of the forkhead transcription factor Fkh2p. *Molecular and Cellular Biology*, *24* (22), 10036–46.

Polyak, K., Kato, J. Y., Solomon, M. J., Sherr, C. J., Massague, J., Roberts, J. M., & Koff, A. (1994a). p27Kip1, a cyclin-Cdk inhibitor, links transforming growth factor-beta and contact inhibition to cell cycle arrest. *Genes & Development*, *8* (1), 9–22.

Polyak, K., Lee, M. H., Erdjument-Bromage, H., Koff, A., Roberts, J. M., Tempst, P., & Massagué, J. (1994b). Cloning of p27Kip1, a cyclin-dependent kinase inhibitor and a potential mediator of extracellular antimitogenic signals. *Cell*, *78* (1), 59–66.

Pramila, T., Miles, S., GuhaThakurta, D., Jemiolo, D., & Breeden, L. L. (2002). Conserved homeodomain proteins interact with MADS box protein Mcm1 to restrict ECB-dependent transcription to the M/G1 phase of the cell cycle. *Genes & Development*, *16* (23), 3034–45.

Pramila, T., Wu, W., Miles, S., Noble, W. S., & Breeden, L. L. (2006). The Forkhead transcription factor Hcm1 regulates chromosome segregation genes and fills the S-phase gap in the transcriptional circuitry of the cell cycle. *Genes & Development*, *20* (16), 2266–2278.

Prinz, S., Hwang, E. S., Visintin, R., & Amon, A. (1998). The regulation of Cdc20 proteolysis reveals a role for APC components Cdc23 and Cdc27 during S phase and early mitosis. *Current Biology : CB*, *8* (13), 750–60.

Ptacek, J., Devgan, G., Michaud, G., Zhu, H., Zhu, X., Fasolo, J., Guo, H., Jona, G., Breitkreutz, A., Sopko, R., McCartney, R. R., Schmidt, M. C., Rachidi, N., Lee, S. J., Mah, A. S., Meng, L., Stark, M. J., Stern, D. F., De Virgilio, C., Tyers, M., Andrews, B., Gerstein, M., Schweitzer, B., Predki, P. F., & Snyder, M. (2005). Global analysis of protein phosphorylation in yeast. *Nature*, *438* (7068), 679–684.

Ramachandran, V., Shah, K. H., & Herman, P. K. (2011). The cAMP-Dependent Protein Kinase Signaling Pathway Is a Key Regulator of P Body Foci Formation. *Molecular Cell*, *43* (6), 973–981.

Reynard, G. J., Reynolds, W., Verma, R., & Deshaies, R. J. (2000). Cks1 is required for G (1) cyclin-cyclin-dependent kinase activity in budding yeast. *Molecular and Cellular Biology*, *20* (16), 5858–5864.

Reynolds, D., Shi, B. J., McLean, C., Katsis, F., Kemp, B., & Dalton, S. (2003). Recruitment of Thr 319-phosphorylated Ndd1p to the FHA domain of Fkh2p requires Clb kinase activity: a mechanism for CLB cluster gene activation. *Genes & Development*, *17* (14), 1789–802.

Rhind, N., & Russell, P. (2001). Roles of the mitotic inhibitors Wee1 and Mik1 in the G (2) DNA damage and replication checkpoints. *Molecular and Cellular Biology*, *21* (5), 1499–508.

Roberts, C. J., Nelson, B., Marton, M. J., Stoughton, R., Meyer, M. R., Bennett, H. A., He, Y. D., Dai, H., Walker, W. L., Hughes, T. R., Tyers, M., Boone, C., & Friend, S. H. (2000). Signaling and circuitry of multiple MAPK pathways revealed by a matrix of global gene expression profiles. *Science (New York, N.Y.)*, *287* (5454), 873–880.

Ross, K. E., Kaldis, P., & Solomon, M. J. (2000). Activating phosphorylation of the Saccharomyces cerevisiae cyclin-dependent kinase, cdc28p, precedes cyclin binding. *Molecular Biology of the Cell*, *11* (5), 1597–609.

Rudner, A. D., & Murray, A. W. (2000). Phosphorylation by Cdc28 activates the Cdc20-dependent activity of the anaphase-promoting complex. *The Journal of Cell Biology*, *149* (7), 1377–90.

Russell, P., Moreno, S., & Reed, S. I. (1989). Conservation of mitotic controls in fission and budding yeasts. *Cell*, *57* (2), 295–303.

Russo, A. A., Jeffrey, P. D., Patten, A. K., Massagué, J., & Pavletich, N. P. (1996). Crystal structure of the p27Kip1 cyclin-dependent-kinase inhibitor bound to the cyclin A-Cdk2 complex. *Nature*, *382* (6589), 325–331.

Russo, A. A., Jeffrey, P. D., & Pavletich, N. P. (1996). Structural basis of cyclin-dependent kinase activation by phosphorylation. *Nature Structural Biology*, *3* (8), 696–700.

Russo, G. L., Van Den Bos, C., & Marshak, D. R. (2001). Mutation at the CK2 phosphorylation site on Cdc28 affects kinase activity and cell size in Saccharomyces cerevisiae. *Molecular and Cellular Biochemistry*, *227* (1-2), 113–117.

Sadowski, M., Suryadinata, R., Lai, X., Heierhorst, J., & Sarcevic, B. (2010). Molecular basis for lysine specificity in the yeast ubiquitin-conjugating enzyme Cdc34. *Molecular and Cellular Biology*, *30* (10), 2316–29.

Sambrook, J., Fritsch, E. F., & Maniatis, T. (1989). *Molecular Cloning: A Laboratory Manual. Cold Spring Harbor laboratory press*. *New York* (pp. 931–957).

Sánchez, M., Calzada, A., & Bueno, A. (1999). The Cdc6 protein is ubiquitinated in vivo for proteolysis in Saccharomyces cerevisiae. *The Journal of Biological Chemistry*, *274* (13), 9092–7.

Santangelo, G. M. (2006). Glucose signaling in Saccharomyces cerevisiae. *Microbiology and Molecular Biology Reviews : MMBR*, *70* (1), 253–282.

Schwob, E., Böhm, T., Mendenhall, M. D., & Nasmyth, K. (1994). The B-type cyclin kinase inhibitor p40SIC1 controls the G1 to S transition in S. cerevisiae. *Cell*, *79* (2), 233–44.

Seol, J. H., Feldman, R. M., Zachariae, W., Shevchenko, A., Correll, C. C., Lyapina, S., … Deshaies, R. J. (1999). Cdc53/cullin and the essential Hrt1 RING-H2 subunit of SCF define a ubiquitin ligase module that activates the E2 enzyme Cdc34. *Genes & Development*, *13* (12), 1614–26.

Serrano, M., Hannon, G. J., & Beach, D. (1993). A new regulatory motif in cell-cycle control causing specific inhibition of cyclin D/CDK4. *Nature*, *366* (6456), 704–7.

Shah, K. H., Zhang, B., Ramachandran, V., & Herman, P. K. (2013). Processing body and stress granule assembly occur by independent and Differentially regulated pathways in Saccharomyces cerevisiae. *Genetics*, *193* (1), 109–123.

Sherr, C. J., & Roberts, J. M. (1999). CDK inhibitors: positive and negative regulators of G1-phase progression. *Genes & Development*, *13* (12), 1501–1512.

Shirayama, M., Zachariae, W., Ciosk, R., & Nasmyth, K. (1998). The Polo-like kinase Cdc5p and the WD-repeat protein Cdc20p/fizzy are regulators and substrates of the anaphase promoting complex in Saccharomyces cerevisiae. *The EMBO Journal*, *17* (5), 1336–49.

Shore, P., & Sharrocks, A. D. (1995). The MADS-box family of transcription factors. *European Journal of Biochemistry / FEBS*, *229* (1), 1–13.

Simpson, D. P. (1977). *Cassell's Latin Dictionary: Latin-English, English-Latin.* MacMillan, pp. 840.

Skotheim, J. M., Di Talia, S., Siggia, E. D., & Cross, F. R. (2008). Positive feedback of G1 cyclins ensures coherent cell cycle entry. *Nature*, *454* (7202), 291–296.

Skowyra, D., Craig, K. L., Tyers, M., Elledge, S. J., & Harper, J. W. (1997). F-box proteins are receptors that recruit phosphorylated substrates to the SCF ubiquitin-ligase complex. *Cell*, *91* (2), 209–19.

Slansky, J. E., & Farnham, P. J. (1996). Introduction to the E2F family: protein structure and gene regulation. *Current Topics in Microbiology and Immunology*, *208*:1–30.

Solomon, M. J., Glotzer, M., Lee, T. H., Philippe, M., & Kirschner, M. W. (1990). Cyclin activation of p34cdc2. *Cell*, *63* (5), 1013–24.

Spellman, P. T., Sherlock, G., Zhang, M. Q., Iyer, V. R., Anders, K., Eisen, M. B., Brown, P. O., Botstein, D., & Futcher, B. (1998). Comprehensive identification of cell cycle-regulated genes of the yeast Saccharomyces cerevisiae by microarray hybridization. *Molecular Biology of the Cell*, *9* (12), 3273–3297.

Strausfeld, U., Labbé, J. C., Fesquet, D., Cavadore, J. C., Picard, A., Sadhu, K., Russell, B., & Dorée, M. (1991). Dephosphorylation and activation of a p34cdc2/cyclin B complex in vitro by human CDC25 protein. *Nature*, *351* (6323), 242–5.

Stuart, D., & Wittenberg, C. (1995). CLN3, not positive feedback, determines the timing of CLN2 transcription in cycling cells. *Genes and Development*, *9* (22), 2780–2794.

Sudbery, P. E., Goodey, A. R., & Carter, B. L. (1980). Genes which control cell proliferation in the yeast Saccharomyces cerevisiae. *Nature*, *288* (5789), 401–404.

Sun, T. T., & Green, H. (1976). Differentiation of the epidermal keratinocyte in cell culture: formation of the cornified envelope. *Cell*, *9* (4 Pt 1), 511–521.

Surana, U., Robitsch, H., Price, C., Schuster, T., Fitch, I., Futcher, A. B., & Nasmyth, K. (1991). The role of CDC28 and cyclins during mitosis in the budding yeast S. cerevisiae. *Cell*, *65* (1), 145–61.

Sutton, A., & Freiman, R. (1997). The Cak1p protein kinase is required at G1/S and G2/M in the budding yeast cell cycle. *Genetics*, *147* (1), 57–71.

Taberner, F. J., Quilis, I., & Igual, J. C. (2009). Spatial regulation of the start repressor Whi5. *Cell Cycle (Georgetown, Tex.)*, *8* (18), 3010–3018.

Takaki, T., Echalier, A., Brown, N. R., Hunt, T., Endicott, J. A., & Noble, M. E. M. (2009). The structure of CDK4/cyclin D3 has implications for models of CDK activation. *Proceedings of the National Academy of Sciences of the United States of America*, *106* (11), 4171–4176.

Tamaki, H. (2007). Glucose-stimulated cAMP-protein kinase A pathway in yeast Saccharomyces cerevisiae. *Journal of Bioscience and Bioengineering*, *104* (4), 245–250.

Thevelein, J. M., & De Winde, J. H. (1999). Novel sensing mechanisms and targets for the cAMP-protein kinase A pathway in the yeast Saccharomyces cerevisiae. *Molecular Microbiology*, *33* (5):904-18.

Tkach, J. M., Yimit, A., Lee, A. Y., Riffle, M., Costanzo, M., Jaschob, D., Hendry, J. A., Ou, J., Moffat, J., Boone, C., Davis, T. N., Nislow, C., & Brown, G. W. (2012). Dissecting DNA damage response pathways by analysing protein localization and abundance changes during DNA replication stress. *Nature Cell Biology*, *14* (9):966-76.

Toda, T., Cameron, S., Sass, P., Zoller, M., Scott, J. D., McMullen, B., Hurwitz, M., Krebs, E.G., & Wigler, M. (1987). Cloning and characterization of BCY1, a locus encoding a regulatory subunit of the cyclic AMP-dependent protein kinase in Saccharomyces cerevisiae. *Molecular and Cellular Biology*, *7* (4), 1371–7.

Tokiwa, G., Tyers, M., Volpe, T., & Futcher, B. (1994). Inhibition of G1 cyclin activity by the Ras/cAMP pathway in yeast. *Nature*, *371* (6495), 342–345.

Toyoshima, H., & Hunter, T. (1994). p27, a novel inhibitor of G1 cyclin-Cdk protein kinase activity, is related to p21. *Cell*, *78* (1), 67–74.

Traven, A., Huang, D. C. S., & Lithgow, T. (2004). Protein hijacking: Key proteins held captive against their will. *Cancer Cell*, *5* (2):107-8.

Trunnell, N. B., Poon, A. C., Kim, S. Y., & Ferrell, J. E. (2011). Ultrasensitivity in the Regulation of Cdc25C by Cdk1. *Molecular Cell*, *41* (3), 263–74.

Tyers, M., Tokiwa, G., & Futcher, B. (1993). Comparison of the Saccharomyces cerevisiae G1 cyclins: Cln3 may be an upstream activator of Cln1, Cln2 and other cyclins. *The EMBO Journal*, *12* (5), 1955–1968.

Ubersax, J. A., Woodbury, E. L., Quang, P. N., Paraz, M., Blethrow, J. D., Shah, K., Shokat, K. M., & Morgan, D. O. (2003). Targets of the cyclin-dependent kinase Cdk1. *Nature*, *425* (6960), 859–864.

Van Drogen, F., Stucke, V. M., Jorritsma, G., & Peter, M. (2001). MAP kinase dynamics in response to pheromones in budding yeast. *Nature Cell Biology*, *3* (12), 1051–9.

Vergés, E., Colomina, N., Garí, E., Gallego, C., & Aldea, M. (2007). Cyclin Cln3 is retained at the ER and released by the J chaperone Ydj1 in late G1 to trigger cell cycle entry. *Molecular Cell*, *26* (5), 649–62.

Verma, R., Annan, R. S., Huddleston, M. J., Carr, S. A., Reynard, G., & Deshaies, R. J. (1997). Phosphorylation of Sic1p by G1 Cdk required for its degradation and entry into S phase. *Science (New York, N.Y.)*, *278* (5337), 455–460.

Verma, R., Feldman, R. M., & Deshaies, R. J. (1997). SIC1 is ubiquitinated in vitro by a pathway that requires CDC4, CDC34, and cyclin/CDK activities. *Molecular Biology of the Cell*, *8* (8), 1427–1437.

Verma, R., McDonald, H., Yates, J. R., & Deshaies, R. J. (2001). Selective degradation of ubiquitinated Sic1 by purified 26S proteasome yields active S phase cyclin-Cdk. *Molecular Cell*, *8* (2), 439–448.

Visintin, R., Prinz, S., & Amon, A. (1997). CDC20 and CDH1: a family of substrate-specific activators of APC-dependent proteolysis. *Science (New York, N.Y.)*, *278* (5337), 460–3.

Wagner, M. V., Smolka, M. B., de Bruin, R. A. M., Zhou, H., Wittenberg, C., & Dowdy, S. F. (2009). Whi5 regulation by site specific CDK-phosphorylation in Saccharomyces cerevisiae. *PLoS ONE*, *4* (1).

Wang, H., Carey, L. B., Cai, Y., Wijnen, H., & Futcher, B. (2009). Recruitment of Cln3 cyclin to promoters controls cell cycle entry via histone deacetylase and other targets. *PLoS Biology*, *7* (9).

Wang, H., Garí, E., Vergés, E., Gallego, C., & Aldea, M. (2004). Recruitment of Cdc28 by Whi3 restricts nuclear accumulation of the G1 cyclin-Cdk complex to late G1. *The EMBO Journal*, *23* (1), 180–190.

Warbrick, E., Lane, D. P., Glover, D. M., & Cox, L. S. (1995). A small peptide inhibitor of DNA replication defines the site of interaction between the cyclin-dependent kinase inhibitor p21WAF1 and proliferating cell nuclear antigen. *Current Biology : CB*, *5* (3), 275–82.

Watanabe, N., Arai, H., Nishihara, Y., Taniguchi, M., Watanabe, N., Hunter, T., & Osada, H. (2004). M-phase kinases induce phospho-dependent ubiquitination of somatic Wee1 by SCFbeta-TrCP. *Proceedings of the National Academy of Sciences of the United States of America*, *101* (13), 4419–24.

Weinreich, M., Liang, C., Chen, H. H., & Stillman, B. (2001). Binding of cyclin-dependent kinases to ORC and Cdc6p regulates the chromosome replication cycle. *Proceedings of the National Academy of Sciences of the United States of America*, *98* (20), 11211–7.

Wijnen, H., Landman, A., & Futcher, B. (2002). The G (1) cyclin Cln3 promotes cell cycle entry via the transcription factor Swi6. *Molecular and Cellular Biology*, *22* (12), 4402–4418.

Willems, A. R., Goh, T., Taylor, L., Chernushevich, I., Shevchenko, A., & Tyers, M. (1999). SCF ubiquitin protein ligases and phosphorylation-dependent proteolysis. *Philosophical Transactions of the Royal Society of London. Series B, Biological Sciences*, *354* (1389), 1533–50.

Willems, A. R., Lanker, S., Patton, E. E., Craig, K. L., Nason, T. F., Mathias, N., Kobayashi, R., Wittenberg, C., & Tyers, M. (1996). Cdc53 targets phosphorylated G1 cyclins for degradation by the ubiquitin proteolytic pathway. *Cell*, *86* (3), 453–63.

Wilson, E.B. (1925). *The Cell in Development and Heredity***.** MacMillan, New York.

Wittenberg, C., & Reed, S. I. (2005). Cell cycle-dependent transcription in yeast: promoters, transcription factors, and transcriptomes. *Oncogene*, *24* (17), 2746–2755.

Wittenberg, C., Richardson, S. L., & Reed, S. I. (1987). Subcellular localization of a protein kinase required for cell cycle initiation in Saccharomyces cerevisiae: evidence for an association between the CDC28 gene product and the insoluble cytoplasmic matrix. *Journal of Cell Biology*, *105* (4), 1527–1538.

Woodbury, E. L., & Morgan, D. O. (2007). Cdk and APC activities limit the spindle-stabilizing function of Fin1 to anaphase. *Nature Cell Biology*, *9* (1), 106–112.

Wout, P. K., Sattlegger, E., Sullivan, S. M., & Maddock, J. R. (2009). Saccharomyces cerevisiae Rbg1 protein and its binding partner gir2 interact on polyribosomes with Gcn1. *Eukaryotic Cell*, *8* (7), 1061–1071.

Xiong, Y., Hannon, G. J., Zhang, H., Casso, D., Kobayashi, R., & Beach, D. (1993). p21 is a universal inhibitor of cyclin kinases. *Nature*, *366* (6456), 701–4.

Yahya, G., Parisi, E., Flores, A., Gallego, C., & Aldea, M. (2014). A Whi7-Anchored Loop Controls the G1 Cdk-Cyclin Complex at Start. *Molecular Cell*, *53* (1), 115–126.

Zachariae, W., & Nasmyth, K. (1999). Whose end is destruction: cell division and the anaphase-promoting complex. *Genes & Development*, *13* (16), 2039–58.

Zaritsky, A., Vischer, N., & Rabinovitch, A. (2007). Changes of initiation mass and cell dimensions by the "eclipse." *Molecular Microbiology*, *63* (1):15-21.

Zhu, G., Spellman, P. T., Volpe, T., Brown, P. O., Botstein, D., Davis, T. N., & Futcher, B. (2000). Two yeast forkhead genes regulate the cell cycle and pseudohyphal growth. *Nature*, *406* (6791), 90–4.

Zhu, H., Klemic, J. F., Chang, S., Bertone, P., Casamayor, A., Klemic, K. G., Smith, D., Gerstein, M., Reed, M. A., & Snyder, M. (2000). Analysis of yeast protein kinases using protein chips. *Nature Genetics*, *26* (3), 283–289.

Publications

A Whi7-anchored loop controls the G1 Cdk-Cyclin complex at Start

Yahya G, Parisi E, Flores A, Gallego C, Aldea M.

Molecular Cell 53(1):115-126 (2014)

Inntags: small self-structured epitopes for innocuous protein tagging

Georgieva MV*, Yahya G*, Codó L, Ortiz R, Teixidó L, Claros J, Jara R, Jara M, Iborra A, Gelpí JL, Gallego C, Orozco M, Aldea M.

Nature Methods. doi:10.1038/nmeth.3556 (2015)

* First co-authors